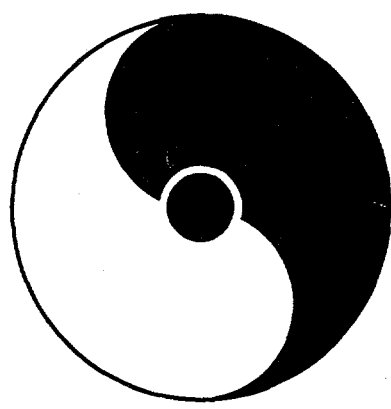


CONF-980451--Proc

RHIC SPIN PHYSICS

April 27-29, 1998



Organizers

Gerry Bunce, Yousef Makdisi, Naohito Saito,
Mike Tannenbaum, Larry Trueman and Aki Yokosawa

MASTER

DISTRIBUTION OF THIS DOCUMENT IS UNLIMITED

A small, handwritten mark or signature, possibly initials, located below the distribution statement.

RIKEN BNL Research Center

Building 510, Brookhaven National Laboratory, Upton, NY 11973, USA

Other RIKEN BNL Research Center Proceedings Volumes:

- Volume 8 - Fermion Frontiers in Vector
Lattice Gauge Theories - BNL-65634
May 6-9, 1998 - Organizers: Robert Mawhinney and Shigemi Ohta
- Volume 7 - RHIC Spin Physics - BNL-65615
April 27-29, 1998 - Organizers: Gerry Bunce,
Yousef Makdisi, Naohito Saito, Mike Tannenbaum and Aki Yokosawa
- Volume 6 - Quarks and Gluons in the Nucleon - BNL-65234
November 28-29, 1997, Saitama, Japan
Organizers: Tashiaki Shibata and Koichi Yazaki
- Volume 5 - Color Superconductivity, Instantons and Parity (Non?)-Conservation at
High Baryon Density - BNL-65105
November 11, 1997 - Organizer - Miklos Gyulassy
- Volume 4 - Inauguration Ceremony, September 22 and
Non-Equilibrium Many Body Dynamics - BNL- 64912
September 23-25, 1997 - Organizer - Miklos Gyulassy
- Volume 3 - Hadron Spin-Flip at RHIC Energies - BNL-64724
July 21 - August 22, 1997 - Organizers: T.L. Trueman and Elliot Leader
- Volume 2 - Perturbative QCD as a Probe of Hadron Structure - BNL-64723
July 14-25, 1997 - Organizers: Robert Jaffe and George Sterman
- Volume 1 - Open Standards for Cascade Models for RHIC - BNL-64722
June 23-27, 1997 - Organizer - Miklos Gyulassy

Isabel Harrity
RIKEN BNL Research Center
Bldg. 510A
Brookhaven National Laboratory
Upton, NY 11793
E-mail: isabel@bnl.gov
Phone: 516 344-2524

DISCLAIMER

This report was prepared as an account of work sponsored by an agency of the United States Government. Neither the United States Government nor any agency thereof, nor any of their employees, makes any warranty, express or implied, or assumes any legal liability or responsibility for the accuracy, completeness, or usefulness of any information, apparatus, product, or process disclosed, or represents that its use would not infringe privately owned rights. Reference herein to any specific commercial product, process, or service by trade name, trademark, manufacturer, or otherwise does not necessarily constitute or imply its endorsement, recommendation, or favoring by the United States Government or any agency thereof. The views and opinions of authors expressed herein do not necessarily state or reflect those of the United States Government or any agency thereof.

DISCLAIMER

Portions of this document may be illegible in electronic image products. Images are produced from the best available original document.

Preface to the Series

The RIKEN BNL Research Center was established this April at Brookhaven National Laboratory. It is funded by the "Rikagaku Kenkyusho" (Institute of Physical and Chemical Research) of Japan. The Center is dedicated to the study of strong interactions, including hard QCD/spin physics, lattice QCD and RHIC physics through nurturing of a new generation of young physicists.

For the first year, the Center will have only a Theory Group, with an Experimental Group to be structured later. The Theory Group will consist of about 12-15 Postdocs and Fellows, and plans to have an active Visiting Scientist program. A 0.6 teraflop parallel processor will be completed at the Center by the end of this year. In addition, the Center organizes workshops centered on specific problems in strong interactions.

Each workshop speaker is encouraged to select a few of the most important transparencies from his or her presentation, accompanied by a page of explanation. This material is collected at the end of the workshop by the organizer to form a proceedings, which can therefore be available within a short time.

T.D. Lee
July 4, 1997

CONTENTS

Preface to the Series	i
Introduction	
<i>Gerry Bunce</i>	1
Workshop Agenda	3
Spin of the Proton: Hard QCD Probes of Hadron Structure	
<i>Bob Jaffe</i>	7
Physics of Accelerating Polarized Protons and Plans	
<i>Thomas Roser</i>	43
RHIC Progress and Schedule	
<i>Mike Harrison</i>	51
Introduction to Mini-Workshop on Gluons at RHIC	
<i>Naohito Saito</i>	59
Unpolarized Gluon Uncertainties and Direct Photon Measurements	
<i>Steve Kuhlmann</i>	65
An Introduction to Resummation and Intrinsic p_T	
<i>George Sterman</i>	71
On Possibility to determine sign of ΔG from Asymmetry of Jet Production in Polarised pp Collisions at RHIC	
<i>M. V. Tokarev</i>	79
Experimental Information for DIS	
<i>Toshiaki Shibata</i>	85
Bremsstrahlung Model of Gluon Polarization	
<i>Denis Sivers</i>	91
How to Extract Gluon Polarization Using RHIC Probes - A Critical Analysis	
<i>Jacques Soffer</i>	99
x-Dependent Polarized Parton Distributions for RHIC	
<i>Gordon Ramsey</i>	105
Direct Photon at STAR	
<i>Steve Vigdor</i>	113
Prompt Photon at Phenix	
<i>Yuji Goto</i>	119

Measuring ΔG with Jets - STAR	
<i>Steve Heppelmann</i>	125
Gluon Polarization and Dihadron Production at RHIC	
<i>Guanghua Xu</i>	131
Determination of ΔG from Open Heavy-Flavor Production	
<i>Melynda Brooks</i>	137
J/ψ Production in pp Collisions at Phenix	
<i>Naoki Hayashi</i>	145
Introduction - Polarimetry at RHIC	
<i>Yousef Makdisi</i>	151
RHIC Pion Polarimeter	
<i>Hal Spinka</i>	157
Ion Polarimetry Issues	
<i>Igor Alekseev</i>	163
Notes on Elastic pp Polarimetry at High t for RHIC	
<i>Vadim Kanavets</i>	167
A CNI Polarimeter for RHIC	
<i>Kenichi Imai</i>	175
A Proposal for a $p + C$ CNI Polarimeter for RHIC	
<i>Douglas Fields</i>	183
Luminosity Monitor	
<i>Dave Underwood</i>	189
Polarized Target Proposal and Status	
<i>Aldo Penzo</i>	195
Gauge Invariant Quark and Gluon Spin and Orbital Angular Momentum Distributions	
<i>Sergei Bashinsky</i>	203
Detector Limitations, STAR	
<i>Dave Underwood</i>	211
Uncertainties in ΔG Measurements at PHENIX	
<i>Akio Ogawa/Yuji Goto</i>	217
Next-to-Leading Order Issues in Spin Pdf Determinations	
<i>Basim Kamal</i>	223
Determinations of the Polarized Gluon Distribution	
<i>Andy Contogouris</i>	229
ep Spin Physics Future - HERA	
<i>Albert de Roeck</i>	235
Polarized Protons Project Status and Plans	
<i>Mike Syphers</i>	245
AGS RF Dipole Experiment	
<i>Mei Bai</i>	251
How Do We Reach 70% Polarization at the AGS	
<i>Haijin Huang</i>	259

Helical Magnets <i>Eric Willen</i>	265
Polarized Protons Acceleration in HERA <i>Vladimir Anferov</i>	271
Polarized Neutrons at RHIC <i>Ernest Courant</i>	275
Parity-violating Asymmetries in W^\pm Production with STAR <i>Leslie Bland</i>	281
Measurements of Anti-Quark Polarization at Phenix <i>Naohito Saito</i>	287
Sensitivity to New Physics in Parity Violating Asymmetries at RHIC <i>Jean-Marc Virey</i>	293
STAR Parity Violation Search with Jets <i>Geary Eppley</i>	301
Could Large CP-violation be Detected in Polarized Proton Collisions at RHIC? <i>Vladimir Rykov</i>	307
The Usefulness of Positivity in Spin Physics <i>Jacques Soffer</i>	313
Transversity and Polarized Drell-Yan at RHIC <i>Verner Vogelsang</i>	321
Studies of Transversity Distributions at RHIC <i>Shunzo Kumano</i>	327
Probing the Nucleon's Transversity with Two-Pion Production at RHIC <i>Jian Tang</i>	333
Polarized Λ -Baryon Production in pp <i>Daniel de Florian</i>	343
Single Spin Asymmetries and Higher Twist <i>George Sterman</i>	351
Possibilities for Spin Measurements in Brahm's <i>Fleming Videbaek</i>	359
Bounds on Helicity Amplitudes at Low Momentum Transfer <i>Nigel Buttimore</i>	365
The Odderon and Spin-dependence of Elastic Proton-Proton Scatter- ing <i>Larry Trueman</i>	373
Experiment to Measure Total Cross Sections, Differential Cross Sections and Polarization Effects in pp Elastic Scattering at RHIC <i>Wlodek Guryń</i>	385

Feasibility of DIS (Polarized e-p Collider) at RHIC	
<i>George Igo</i>	393
Participant List	
.	401
Photographs	
.	407

INTRODUCTION

Welcome! This workshop follows in a series of RHIC Spin Collaboration annual meetings: Marseille in 1996, MIT in 1995, Argonne 1994, Tuscon in 1991, and the Polarized Collider Workshop at Penn State in 1990.

For the first time, we have a sponsor! The RIKEN-BNL Research Center has a thriving theory group already, and also sponsors a long-running spin discussion group which meets Tuesdays at 10. There is so much work going on in spin now that this workshop has little time for questions and discussion. You are encouraged to come to BNL and lead a Tuesday discussion on your topic. The spin discussion schedule and material from the discussions are posted on <http://riksg01.rhic.bnl.gov/rsc>.

The RIKEN BNL Research Center is starting a new Spin Physics Experimental Division and there are openings for Fellow and Research Associate positions. Professor Masayasu Ishihara of RIKEN is the Group Leader for the Division and Dr. Gerry Bunce is Deputy Group Leader. The ad for the positions is posted on the Center web site: <http://penguin.phy.bnl.gov/www/riken>.

The Center is providing a home for the role we in RSC have played— combining work and ideas of theorists, experimenters, and accelerator physicists to develop and carry out the spin program at RHIC.

This Proceedings compiles one-page summaries and five transparencies for each talk, with the intention that the speaker should include a web location for additional information in the summary. Also, email addresses are given with the participant list. The order follows the agenda: gluon, polarimetry, accelerator, W production and quark/antiquark polarization, parity violation searches, transversity, single transverse spin, small angle elastic scattering, and the final talk on ep collisions at RHIC. We begin the Proceedings with the full set of transparencies from Bob Jaffe's colloquium on spin, by popular request!

This workshop has been planned by a "local" committee and by the RIKEN Center secretaries, Pam Esposito and Isabel Harrity. We would like to thank them for their advice, planning and support! We also thank Brookhaven National Laboratory and the U.S. Department of Energy for providing facilities.

Gerry Bunce

RIKEN BNL RESEARCH CENTER

WORKSHOP ON RHIC SPIN PHYSICS PHYSICS DEPARTMENT - LARGE SEMINAR ROOM APRIL 27 - 29, 1998

AGENDA

Monday Morning, April 27

[Chair - Aki Yokosawa]

- 09:00 Welcome from the RIKEN BNL Center (Larry Trueman)
Workshop Introduction from Organizing Committee (Gerry Bunce)
09:15 RHIC Spin Collider – Physics of Accelerating Polarized Protons and Plans (Thomas Roser)
09:45 RHIC Progress and Schedule (Mike Harrison)

Beginning of 1.5 Day Mini-Workshop on Gluons at RHIC

- 10:30 Introduction to Mini-Workshop on Gluons (Naohito Saito)

Unpolarized Gluons – What Do We Know?

- 10:45 Unpolarized Gluon Distribution Uncertainties and Direct Photon Measurements (Steve Kuhlmann)
11:30 Resummation and Intrinsic p_T (George Sterman)

Monday Afternoon, April 27

[Chair - Naohito Saito]

Polarized Gluons

- 02:00 Experimental Information from DIS (Toshiaki Shibata)
02:30 Bremsstrahlung Model of Gluon Polarization (Dennis Sivers)
03:00 How to Extract Gluon Polarization Using RHIC Probes – A Critical Analysis (Jacques Soffer)

RHIC Probes of the Gluon

- 04:00 Direct Photon at STAR (Steve Vigdor)
04:20 Direct Photon at Phenix (Yuji Goto)
04:40 Jets – STAR (Steve Heppelmann)
05:00 Jets – Phenix (Guanghua Xu)
05:20 Open Charm – PHENIX (Melynda Brooks)
05:40 J/ψ – Phenix (Naoki Hayashi)

Monday Evening, April 27**[Chair - George Igo]*****Polarimetry at RHIC***

- 07:30 Introduction (Yousef Makdisi)
- 08:00 RHIC Pion Polarimeter (Hal Spinka)
- 08:20 Ion Polarimetry Issues (Igor Alekseev)
- 08:40 Polarimetry with pp Elastic Scattering at $t=1$ (Vadim Kanavets)
- 09:00 A CNI Polarimeter for RHIC (Kenichi Imai)
- 09:20 p+C CNI Polarimeter (Douglas Fields)
- 09:40 Luminosity Issues (Dave Underwood)
- 10:00 Polarized Target Proposal and Status (Aldo Penzo)

Tuesday Morning, April 28**[Chair - Bob Jaffe]*****Mini-Workshop on Gluons, continued***

- 09:00 Gauge Invariant Quark and Gluon Angular Momentum Distributions (Sergei Bashinsky)
- 09:30 Physics Limitations from the Detector – STAR (Dave Underwood)
- 10:00 Uncertainties in Measurement (Akio Ogawa and Yuji Goto)

Uncertainties in Interpretation

- 11:00 Next to Leading Order and Parton Spin Distributions (Basim Kamal)
- 11:30 Heavy Flavor (Andy Contogouris)
- 12:00 ep Spin Physics Future – HERA (Albert de Roeck)
- 12:30 Discussion – Open Questions for Gluon Measurements at RHIC (Naohito Saito)

End of 1.5 Day Mini-Workshop on Gluons at RHIC

Tuesday Afternoon, April 28**[Chair - Thomas Roser]*****Accelerator Spin Issues and Preparation***

- 02:00 Introduction – Plans and Schedule (Mike Syphers, Project Manager)
- 02:20 AGS rf Dipole Experiment (Mei Bai)
- 02:40 How Do We Reach 70% Polarization? (Haixin Huang)
- 03:00 Siberian Snake Magnet Construction (Eric Willen)
- 03:30 Physics Colloquium — Spin of the Proton: Hard QCD Probes of Hadron Structure (Bob Jaffe)
- 05:00 Tour of RHIC, Star and Phenix
- 07:30 *Dinner — Paula Jean's Supper Club, East Setauket — Eli Yamin Jazz Trio*

Wednesday Morning, April 29

[Chair - Mike Tannenbaum]

- 09:00 Polarized Neutrons at RHIC (Ernest Courant)
09:15 End of Accelerator Session

Quark and Anti-Quark Polarization at RHIC – W Production

- 09:20 STAR (Leslie Bland)
09:40 Phenix (Naohito Saito)

Parity Violation Searches at RHIC

- 10:00 Sensitivity to New Physics (Jean-Marc Virey)
10:30 STAR Parity Violation Search with Jets (Geary Eppley)
11:00 Could Large CP and/or T-violating Asymmetries be Detected in Polarized Proton Collisions at RHIC?
(Vladimir Rykov)
11:15 The Usefulness of Positivity in Spin Physics (Jacques Soffer)

Transversity

- 11:30 Drell-Yan at RHIC (Werner Vogelsang)
12:00 Studies of Transversity Distribution at RHIC (Shunzo Kumano)
12:30 Probing Transversity with 2 Pions at RHIC (Jian Tang)

Wednesday Afternoon, April 29

[Chair - Jacques Soffer]

- 02:00 Polarized Lambda Production in pp, Measurement of Polarized Fragmentation Functions (Daniel de Florian)

Single Transverse Spin – high p_T – at RHIC

- 02:30 Single Spin Asymmetries and Higher Twist (George Sterman)
03:00 The Brahm's Experiment and Spin (Flemming Videbaek)

Small Angle Scattering and Transverse Spin

- 03:30 Bounds on Helicity Amplitudes at Low Momentum Transfer (Nigel Buttimore)
04:00 The Odderon and Spin Dependence of pp Elastic Scattering (Larry Trueman)
04:20 The pp2pp Experiment (Wlodek Guryan)
04:45 Feasibility of DIS (Polarized ep Collider) at RHIC (George Igo)
05:15 Workshop Ends

Bob JAFFE

M.I.T.

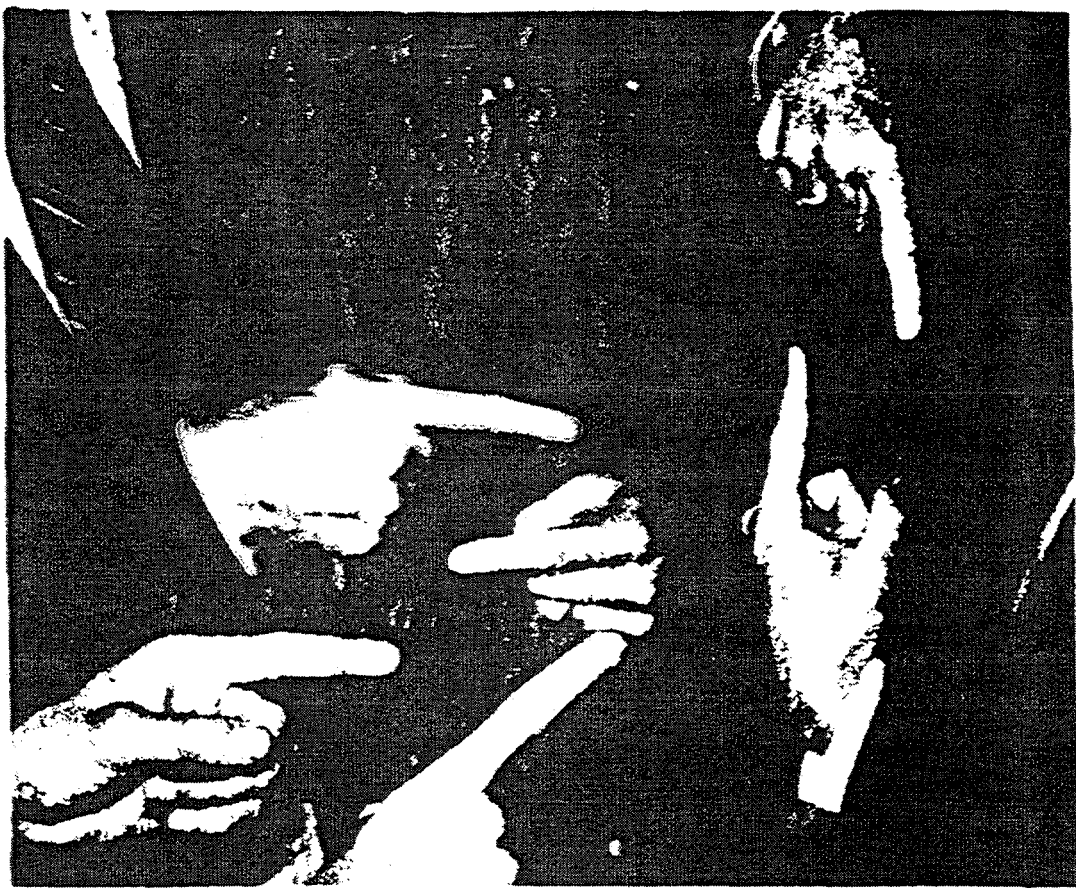
COLLOQUIUM

THE SPIN OF THE PROTON

HARD QCD PROBES OF HADRON STRUCTURE

– OR –

WHAT IS THE COMPOSITION OF MATTER?



$$\mathcal{L}_{\text{QED}} = -\frac{1}{4} \text{Tr} F_{\mu\nu} F^{\mu\nu} + \bar{q}(i\not{D} + m)q$$

A QCD PRIMER

- QUARKS: 3 LIGHT FLAVORS, 3 HEAVY FLAVORS

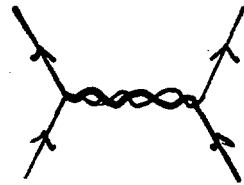
FLAVOR	CHARGE	MASS
u	$2/3$	$\sim 5 \text{ MeV}$
d	$-1/3$	$\sim 10 \text{ MeV}$
s	$-1/3$	$\sim 150 \text{ MeV}$
$\Lambda_{\text{QCD}} \approx 150 - 250 \text{ MeV}$		
c	$2/3$	$\sim 1.5 \text{ GeV}$
b	$-1/3$	$\sim 4.5 \text{ GeV}$
t	$2/3$	$\sim 170 \text{ GeV}$

← "NATURAL" SCALE OF STRONG FORCE

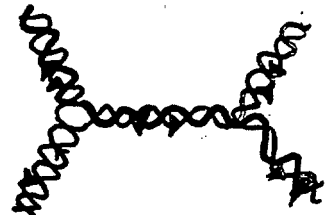
• COLOR AND QUANTUM CHROMODYNAMICS

- QUARKS COME IN 3-COLORS 
- COLOR IS A CHARGE COUPLED TO EIGHT GENERALIZED "PHOTONS" CALLED GLUONS

SPIN-ONE 



QUARK-QUARK FORCE



GLUON-GLUON FORCE

• COLOR CONFINEMENT

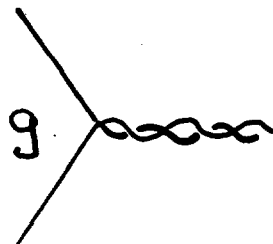
QUARKS ARE CONFINED IN BAGS OF "NORMAL VACUUM" SURROUNDED BY SOME (POORLY UNDERSTOOD) COMPLEX PHASE OF GLUON CONDENSATE



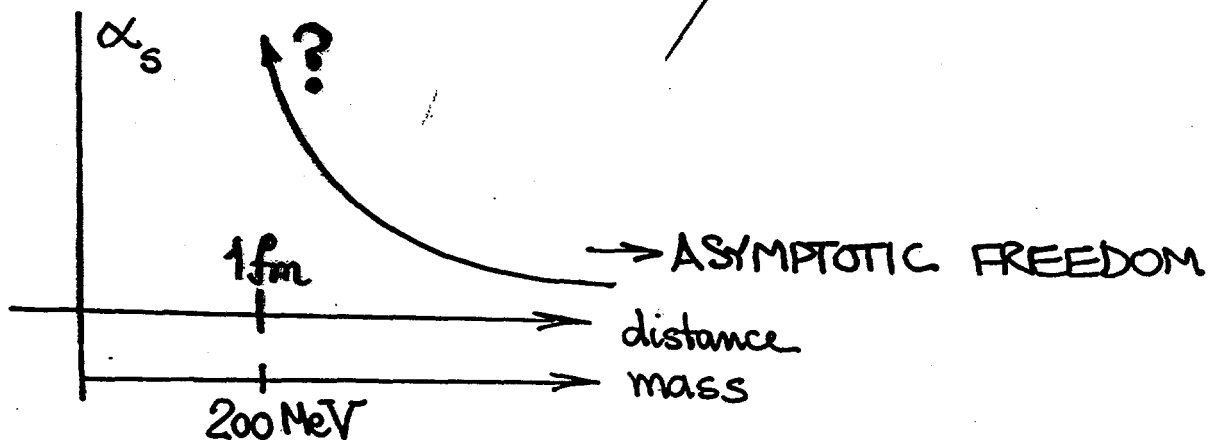
WHY IS QCD SO HARD?

- NO SCALE
- NO PARAMETER

WAIT - WHAT ABOUT α_s



$$\alpha_s \equiv \frac{g^2}{4\pi}$$



- HADRONS FORM @ THE SCALE WHERE α_s GROWS LARGE.
- THAT SCALE — Λ_{QCD} — DEFINES BASIC UNIT OF MASS FOR HADRONS

WHAT ABOUT QUARK MASSES?

$$m_u, m_d \ll \Lambda_{\text{QCD}}$$

$$m_s \approx \Lambda_{\text{QCD}}$$

$$m_c, m_b \gg \Lambda_{\text{QCD}}$$

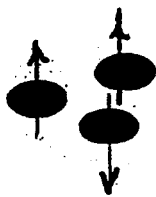
NEGLECTIBLE

NON-TRIVIAL

SIMPLIFYING

THE [ULTRA] NAIVE QUARK MODEL

THE NUCLEON:



SYMMETRIC, NON-RELATIVISTIC
S-WAVE

$$|p^\uparrow\rangle = \frac{1}{\sqrt{6}} [2|u^\uparrow u^\uparrow d^\downarrow\rangle - |u^\uparrow u^\downarrow d^\uparrow\rangle - |u^\downarrow u^\uparrow d^\uparrow\rangle]$$

(likewise for neutron)

$$\vec{\mu}_u = \frac{2}{3} \mu_0 \vec{\sigma}$$

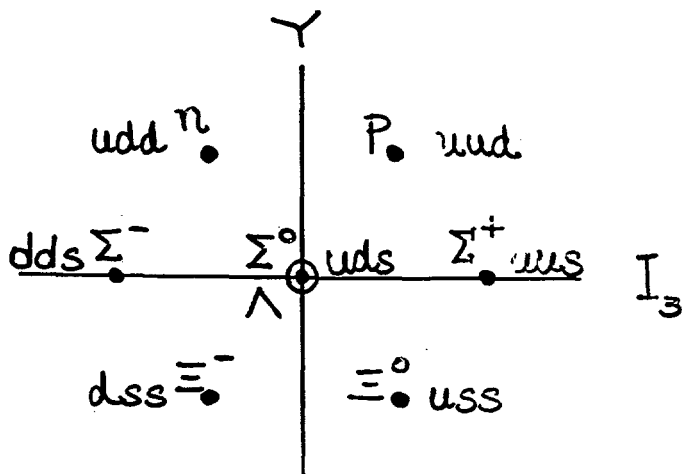
$$\vec{\mu}_d = -\frac{1}{3} \mu_0 \vec{\sigma}$$

A CLASSIC TEXTBOOK CALCULATION

$$\frac{\mu_p}{\mu_n} = -\frac{3}{2} \quad (\text{EXPT} \rightarrow -1.460\dots)$$

HYPERONS \neq BARYON OCTET

$$\vec{\mu} = \begin{pmatrix} \frac{2}{3} \\ -\frac{1}{3} \\ -\frac{1}{3} \frac{\mu_s}{\mu_0} \end{pmatrix}$$



$\frac{\mu_s}{\mu_0} \neq 1$ allows for $s \leftrightarrow (u,d)$ distinction.

SUMMARIZES SIMPLICITY OF QUARK MODEL STATES

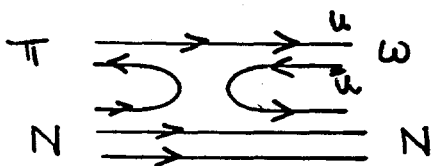
- HADRONS CONTAIN ONLY THOSE QUARKS REQUIRED BY THEIR QUANTUM NUMBERS
- PAIR CREATION* IS SUPPRESSED

* IN A SINGLE HADRONS

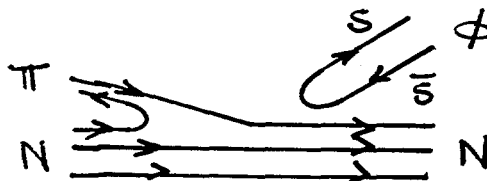
* MOTIVATION:

- SIMPLE STATIC QUARK MODEL CALCULATIONS
- REACTIONS AND DECAYS (QUALITATIVE)

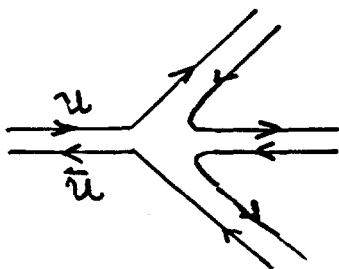
• $\pi N \rightarrow \omega N$



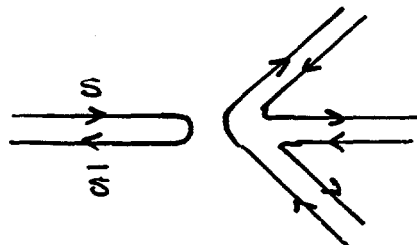
$\gg \pi N \rightarrow \phi N$



• $\omega \rightarrow 3\pi$



$\gg \phi \rightarrow 3\pi$



I. INTRODUCTION - INFORMATION ABOUT THE NUCLEON

TRADITIONAL TOOLS (ATOMIC, NUCLEAR...)

- FORM FACTORS *
- EXCITATION SPECTRA **
- QUASI-ELASTIC SCATTERING ****

• FORM FACTORS

LEARN $g_A, \mu, \langle r^2 \rangle$

LIMITATION

LINK BETWEEN $F(q^2) \neq \rho(r^2)$ FAILS FOR "SMALL" SYSTEMS. CRITERION

$$\langle r^2 \rangle^{1/2} \gg \frac{1}{M}$$

EXCELLENT FOR ATOMIC \neq NUCLEAR PHYSICS
FOR NUCLEON $0.8 \text{ fm} \leftrightarrow 0.2 \text{ fm}$

RULE OF THUMB: ONLY $\langle r^2 \rangle$ HAS
RELIABLE CONNECTION TO $F(q^2)$.

• EXCITATION SPECTRA

LEARN FLAVOR SYMMETRIES $SU(2), SU(3)$
DYNAMICAL SYMMETRIES $SU(6)$

LIMITATION

15

EXCITED STATES ARE ABOVE PARTICLE
(HADRON) THRESHOLDS $\Delta \rightarrow N\pi$, ETC.
AND FUNDAMENTAL QUANTA ARE VERY LIGHT

$$N = q\bar{q}q + (q\bar{q}) + g + \dots$$

QUASIPARTICLES

SPECTROSCOPY BECOMES UNINTERPRETABLE
BEYOND FIRST FEW STATES

- QUASI-ELASTIC SCATTERING \equiv DEEP INELASTIC SCATTERING

LEARN

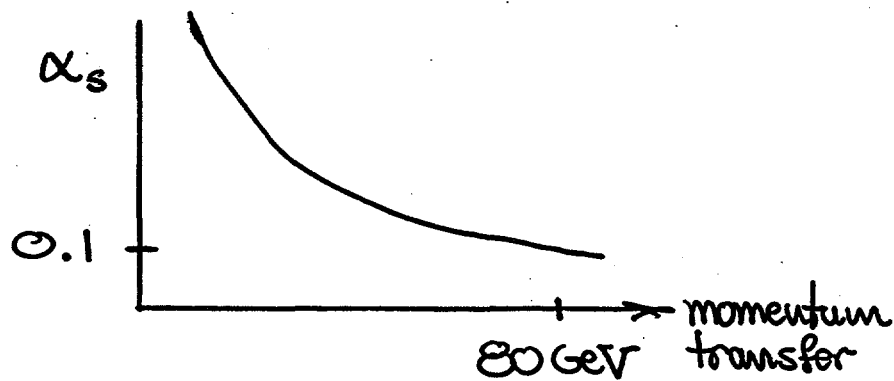
QUARK, ANTIQUARK & GLUON DISTRIBUTIONS
SPIN-DEPENDENT DISTRIBUTIONS
"MOMENTUM"
QUARK-GLUON CORRELATIONS (HIGHER TWIST)
FRAGMENTATION FUNCTIONS

LIMITATIONS ?

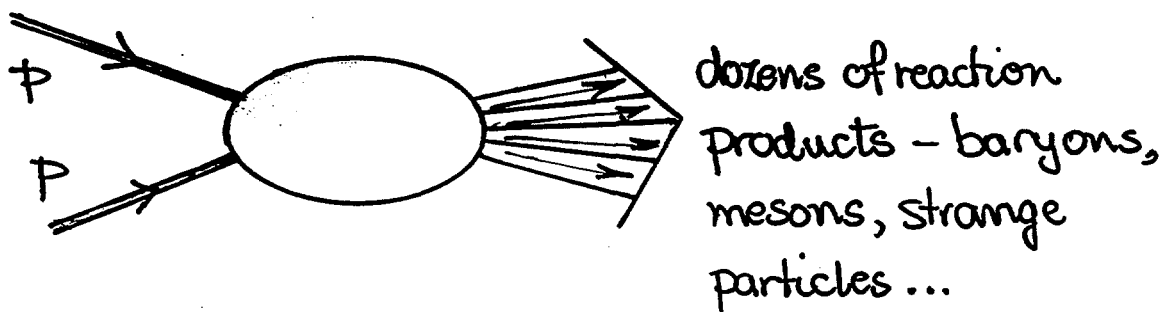
BY FAR THE BEST SOURCE OF DETAILED
INFORMATION ON HADRON STRUCTURE

TURN PQCD TO OUR PURPOSES: USE WELL-
UNDERSTOOD PQCD AS A PROBE OF HADRON
STRUCTURE.

"HARD" MOMENTUM TRANSFER MAKES QCD EASY!

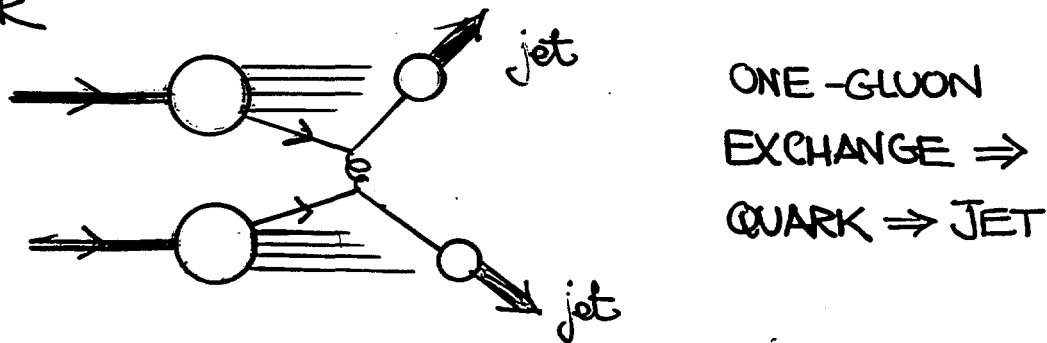


- HADRON-HADRON SCATTERING AT LOW-MOMENTUM TRANSFER (SWISS-WATCHES!)



NEARLY UNINTERPRETABLE

- HADRON-HADRON SCATTERING AT HIGH-MOMENTUM TRANSFER



- TURN QCD ON ITSELF!

REMINDER OF SURPRISES OF THE PAST

17

- MOMENTUM FRACTION: $\langle E_Q \rangle \approx \langle E_G \rangle \approx \frac{1}{2}$
- ISOSPIN STRUCTURE OF THE SEA

$$\bar{u}(x) \neq \bar{d}(x)$$

- SPIN FRACTION OF QUARKS

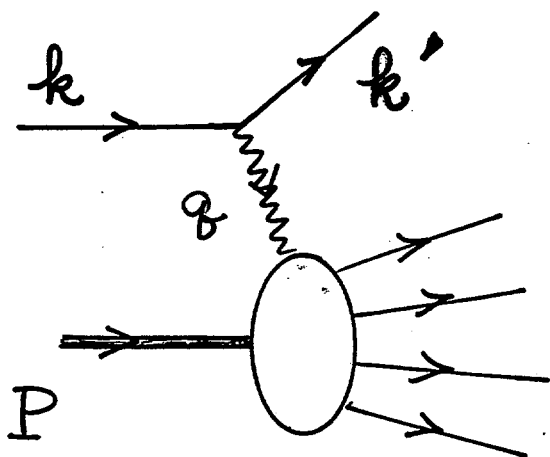
$$\Sigma \approx \frac{1}{3} \quad (\text{SEE BRIEF REVIEW})$$

- IMPORTANCE OF STRANGE QUARKS

$$\begin{array}{ll} \text{MOMENTUM} & \langle S + \bar{S} \rangle = 4.1 \pm 0.4\% \\ \text{SPIN} & \Delta S = -10\% \pm 3\% \end{array}$$

SURPRISES OF THE FUTURE ?

DEEP INELASTIC SCATTERING



$$q = k - k' \quad \text{FOUR-MOMENTUM}$$

$$q^2 = -Q^2 < 0$$

$$P \cdot q = ME_{\gamma}^{\text{LAB}} \equiv \nu$$

ELECTROPRODUCTION



NEUTRINO PRODUCTION



DEEP INELASTIC OR BJORKEN LIMIT

$Q^2 \rightarrow \infty$ $\nu \rightarrow \infty$	$x \equiv \frac{Q^2}{2\nu} \text{ FIXED}$
--	---

$\nu \rightarrow \infty$ LARGE ENERGY LOSS - MULTIHADRON PROD.

$Q^2 \rightarrow \infty$ LARGE MOMENTUM TRANSFER - SHORT DISTANCE PROBE.

KINEMATICS

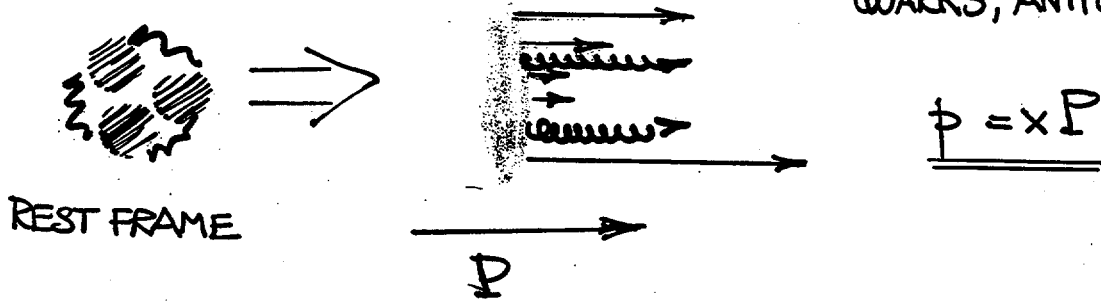
$$0 < x \leq 1$$

OBSERVABLES

$$\Theta(x, Q^2)$$

PARTON MODEL

QUARKS, ANTIQUARKS, GLUONS



- "INFINITE MOMENTUM FRAME" $P \rightarrow \infty$
- PROBABILITY DISTRIBUTIONS $u(x), \bar{u}(x), d(x), \dots$
 $G(x)$
- BJORKEN $x \Leftrightarrow$ LONGITUDINAL MOMENTUM FRACTION
- QUASIELASTIC : AS $Q^2 \rightarrow \infty$, ELECTRON SCATTERS ELASTICALLY FROM QUARKS

$$2F_1(x) = \frac{4}{9} (u(x) + \bar{u}(x)) + \frac{1}{9} (d(x) + \bar{d}(x) + s(x) + \bar{s}(x))$$

- SPIN DEPENDENT $e^\uparrow p^\uparrow \rightarrow e' X$

$U^\uparrow(x)$ QUARK SPIN PARALLEL TO NUCLEON SPIN

$U^\downarrow(x)$ ANTI PARALLEL

$$2g_1^p(x) = \frac{4}{9} (\Delta u(x) + \Delta \bar{u}(x)) + \frac{1}{9} (\Delta d(x) + \Delta \bar{d}(x)) + \frac{1}{9} (\Delta s(x) + \Delta \bar{s}(x))$$

$$2g_1^n(x) = \frac{1}{9} (\Delta u(x) + \Delta \bar{u}(x)) + \frac{4}{9} (\Delta d(x) + \Delta \bar{d}(x)) + \frac{1}{9} (\Delta s(x) + \Delta \bar{s}(x))$$

$$\Delta u(x) \equiv U^\uparrow(x) - U^\downarrow(x)$$

CONCENTRATE ON SPIN

- WHO DISCOVERED THE SPIN OF THE PROTON ?
 - HINT NOT UHLENBECK & GOUDSMIT
 - HINT HE WON THE 1932 NOBEL PRIZE FOR THIS DISCOVERY
 - HINT HE WAS A THEORIST
 - HINT HE WORE AN $\frac{p}{h}$ TIE PIN (!)
 - WERNER HEISENBERG

"FOR THE CREATION OF QUANTUM MECHANICS,
THE APPLICATION OF WHICH HAS LED,
INTER ALIA, TO THE DISCOVERY OF THE
ALLOTROPIC FORMS OF HYDROGEN"

Nobel Laureates in Physics 1901 - 1997

Physics 1932

The prize was reserved and awarded in 1933 to:

Heisenberg, Werner

b. 1901, d. 1976

Leipzig University

"for the creation of quantum mechanics, the application of which has, inter alia, led to the discovery of the allotropic forms of hydrogen".

PARAHYDROGEN



$$S = 0$$

$$k = 0, 2, 4$$

ORTHOHYDROGEN



$$S = 1$$

$$k = 1, 3, 5, \dots$$

Nobel Laureates in Physics 1901 - 1997

Physics 1932

The prize was reserved and awarded in 1933 to:

Heisenberg, Werner /

b. 1901, d. 1976

Leipzig University

"for the creation of quantum mechanics, the application of which has, inter alia, led to the discovery of the allotropic forms of hydrogen".

CONTRIBUTIONS TO PROTON SPIN

$$\frac{1}{2} = \frac{1}{2} \Delta\Sigma + \Delta g + L_q + L_g$$

$\Delta\Sigma$ QUARK SPIN MEASURABLE IN D.I.S. + β -DECAY

- ARCHAIC EXPECTATION $\Delta\Sigma = 1$
- CLASSIC EXPECTATION $\Delta\Sigma = 0.58 \pm 0.02$
- EXISTING MEASUREMENT $\Delta\Sigma = 0.29 \pm 0.06$

Δg GLUON SPIN

- COULD BE LARGE
- PRESENT INDICATIONS $\Delta g \neq 0$
- PRIME TARGET FOR POLARIZED RHIC COLLIDER

$L_q \neq L_g$ QUARK \neq GLUON ORBITAL ANGULAR MOMENTUM

- VARIOUS DEFINITIONS
- NOW A GOOD CANDIDATE FOR SIGNIFICANT CONTRIBUTION
- MEASURE ??

HISTORY

BJORKEN (1966) - SPECULATION - HADRONIC CURRENT
COMMUTATORS FROM FREE FIELD \mathcal{O}_y ?

DO HADRON CONSTITUENTS BEHAVE LIKE FREE
PARTICLES AT SMALL DISTANCES

$$[J_\mu(\vec{x}), J_\nu(\vec{y})] = \dots \underbrace{\delta^3(\vec{x}-\vec{y})}_{\text{underlined}} \mathcal{O}(\vec{x})$$

- BJORKEN YES
- THEN NO
- NOW ALMOST!

BJ. DERIVED A SET OF POWERFUL RESULTS
ROADMAP FOR 3-DECADES WORK

$(Q^2 \rightarrow \infty)$

$$\int_0^\infty \frac{Q^2 du}{u^2} \{ g_1^p(Q^2, u) - g_1^n(Q^2, u) \} = \frac{1}{3} \frac{g_A}{g_V}$$

$$\int_0^1 dx g_1^{p-n}(x, Q^2) = \frac{1}{6} \frac{g_A}{g_V}$$

$$\frac{g_A}{g_V} = 1.2573 \pm 0.0028$$

$$Z_p - Z_n = \frac{1}{3} \left(\frac{G_A}{G_V} \right). \quad (6.17)$$

Thus,

$$\int_0^\infty \frac{d\nu'}{\nu'} \frac{d}{dq^2 d\nu'} \times [\sigma_p^{\uparrow\uparrow} - \sigma_p^{\downarrow\downarrow} - \sigma_n^{\uparrow\uparrow} + \sigma_n^{\downarrow\downarrow}] \rightarrow \frac{-8\pi\alpha^2}{3q^4 E} \left(\frac{G_A}{G_V} \right). \quad (6.18)$$

Something may ~~be salvaged~~ from this worthless equation by constructing an inequality¹⁸:

$$\lim_{q^2 \rightarrow -\infty} \lim_{E \rightarrow \infty} q^4 E \int_0^\infty \frac{d\nu'}{\nu'} \left[\frac{d\sigma_p}{dq^2 d\nu'} + \frac{d\sigma_n}{dq^2 d\nu'} \right] > \frac{8\pi\alpha^2}{3} \left| \frac{G_A}{G_V} \right|. \quad (6.19)$$

¹⁷ Compare Eqs. (5.7)-(5.9).

¹⁸ $\sigma_p = \sigma_p^{\uparrow\uparrow} + \sigma_p^{\downarrow\downarrow}$.

$$\int_0^1 dx (\Delta u(x) + \Delta \bar{u}(x) - \Delta d(x) - \Delta \bar{d}(x)) = g_A/g_V$$

$$\int_0^1 dx (\Delta u(x) + \Delta \bar{u}(x)) \equiv \Delta U \quad \text{FRACTION OF PROTON SPIN CARRIED BY U-QUARK}$$

BJORKEN $\Delta U - \Delta d = \frac{g_A}{g_V} = F + D$

SCURDIN (1972) $\Delta U - \Delta s = 2F$

KNOWING THE TWO COMBINATIONS $\Delta U - \Delta d$ AND $\Delta U - \Delta s$ IS NOT SUFFICIENT TO PREDICT $\int g_i^p$ OR $\int g_i^n$

SU(3) SYMMETRY \nexists BETA DECAY	
$n \rightarrow p e \bar{\nu}$	} SU(3) INV. ↓ F \neq D REMARKABLE SUCCESS
$\Lambda^0 \rightarrow p e \bar{\nu}$	
$\Xi^- \rightarrow n e \bar{\nu}$	
\vdots	
F + D = 1.257 ± 0.003	
3F - D = 0.575 ± 0.016	

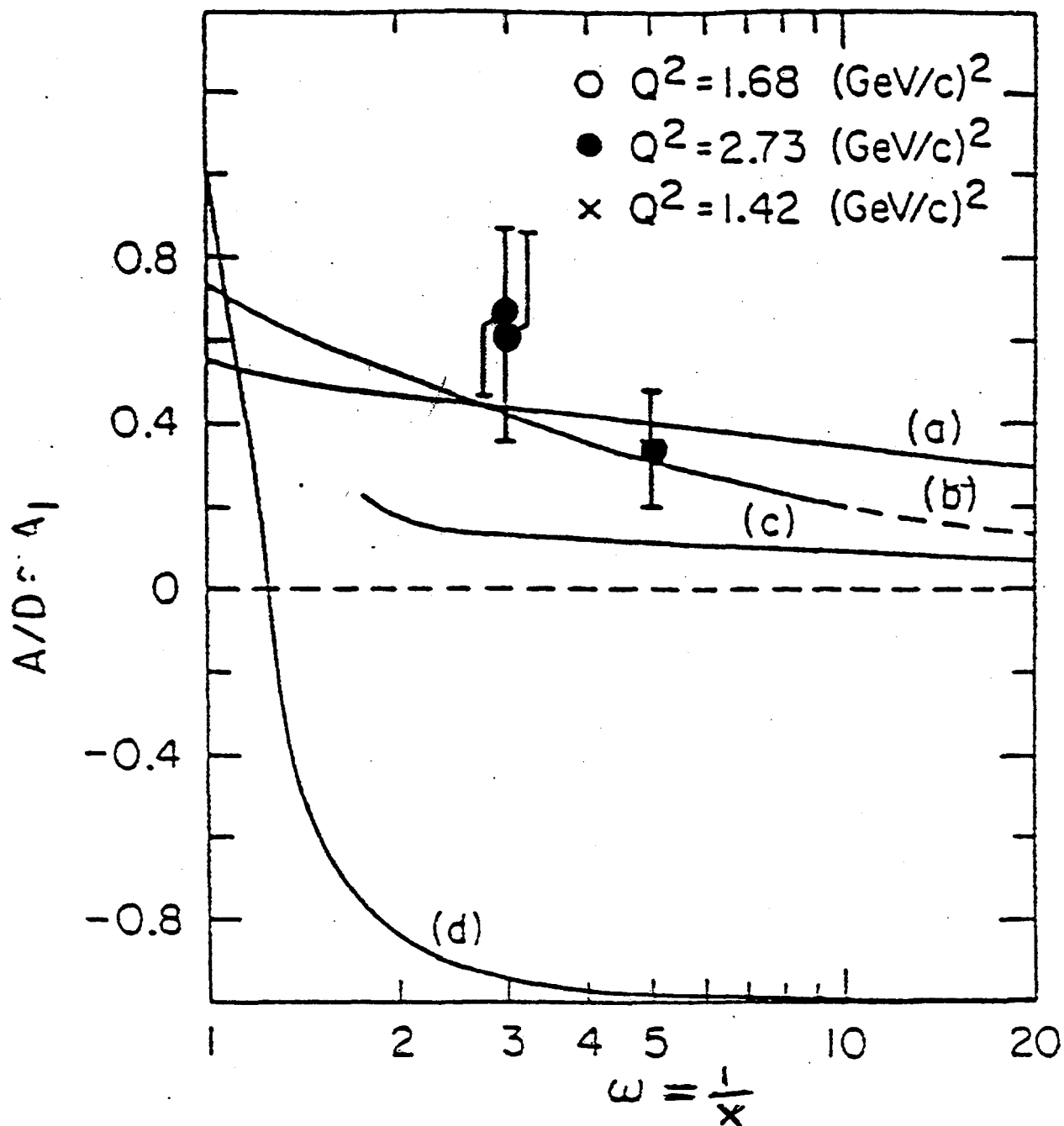
$$\int_0^1 dx g_i^p(x) = \frac{1}{18} (9F - D + 6\Delta s) = \frac{1}{18} (3F + D + 2\Sigma)$$

$$\int_0^1 dx g_i^n(x) = \frac{1}{18} (6F - 4D + 6\Delta s) = \frac{1}{18} (-2D + 2\Sigma)$$

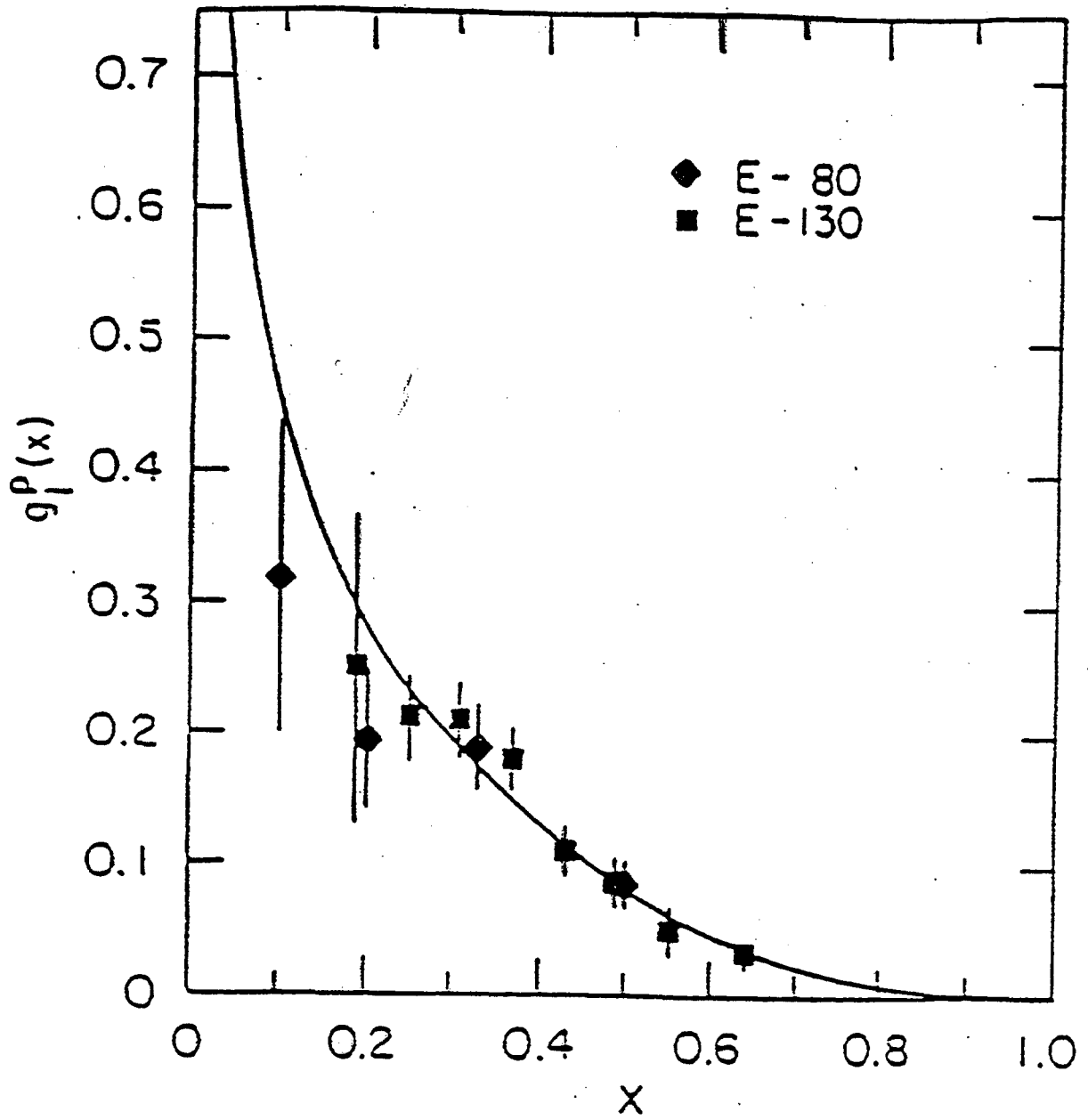
WHERE

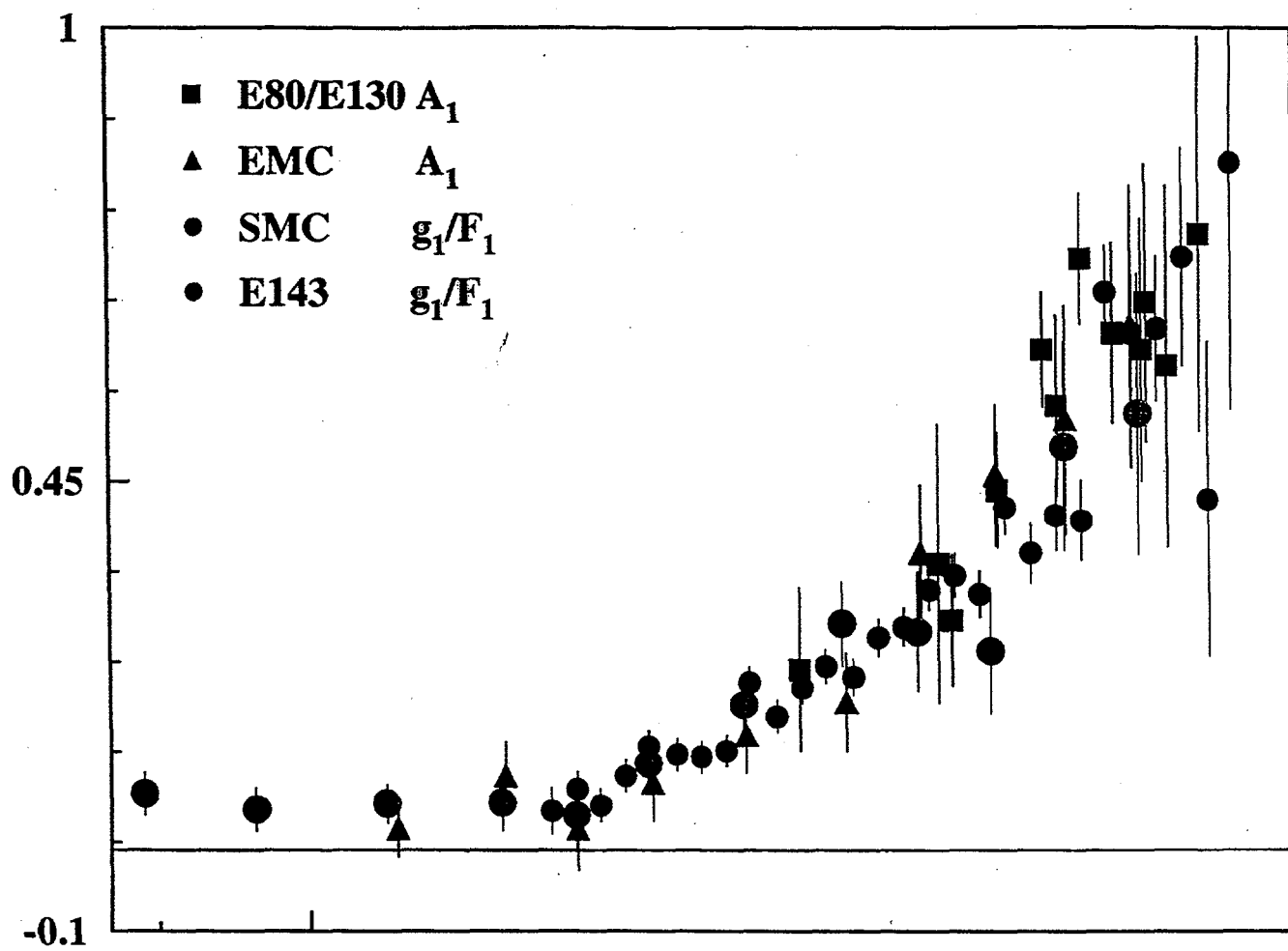
$$\Sigma = \Delta U + \Delta d + \Delta s$$

FRACTION OF NUCLEON SPIN ON QUARK SPIN

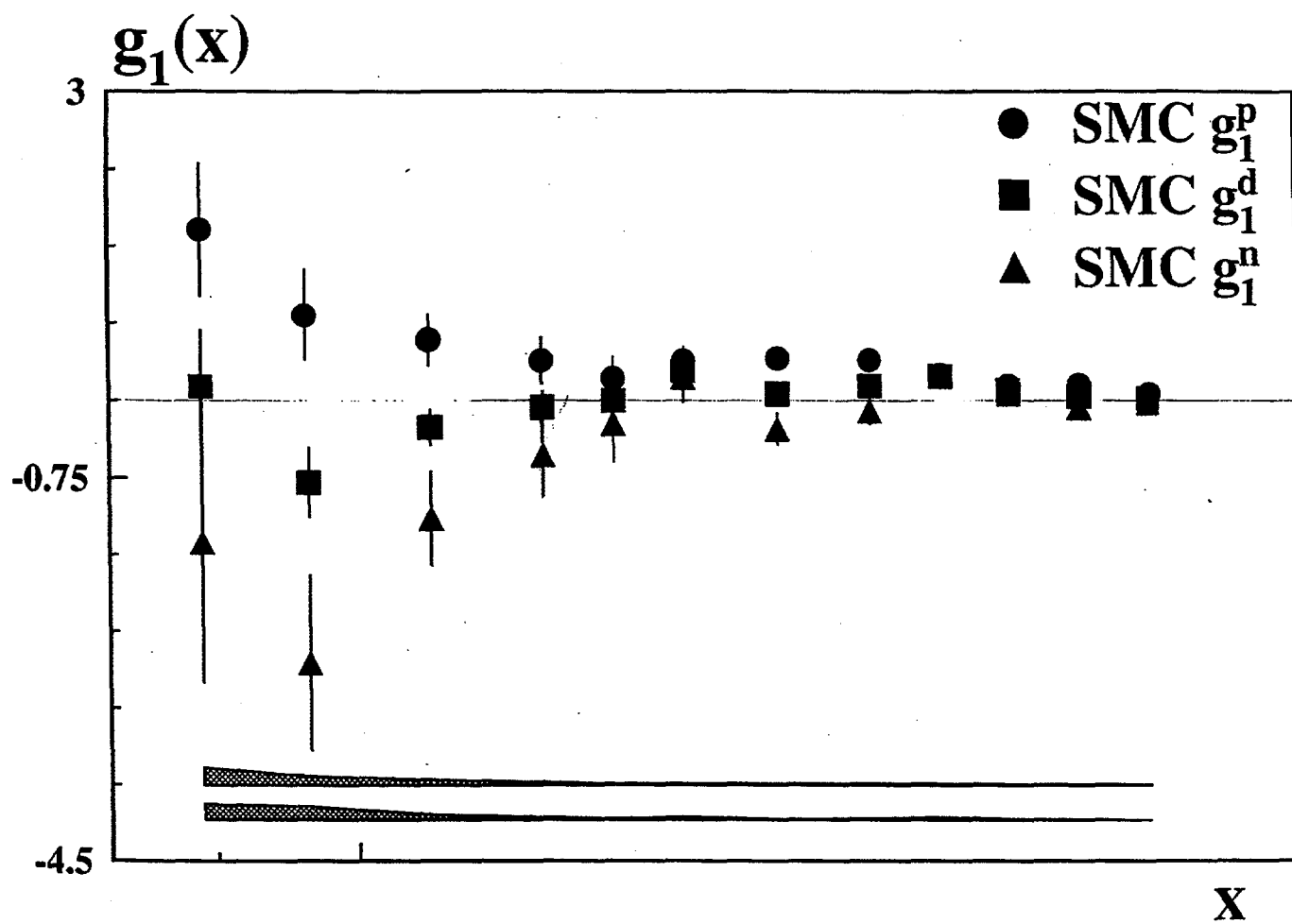


VERNON HUGHES & COLLABORATORS
(SLAC-YALE)

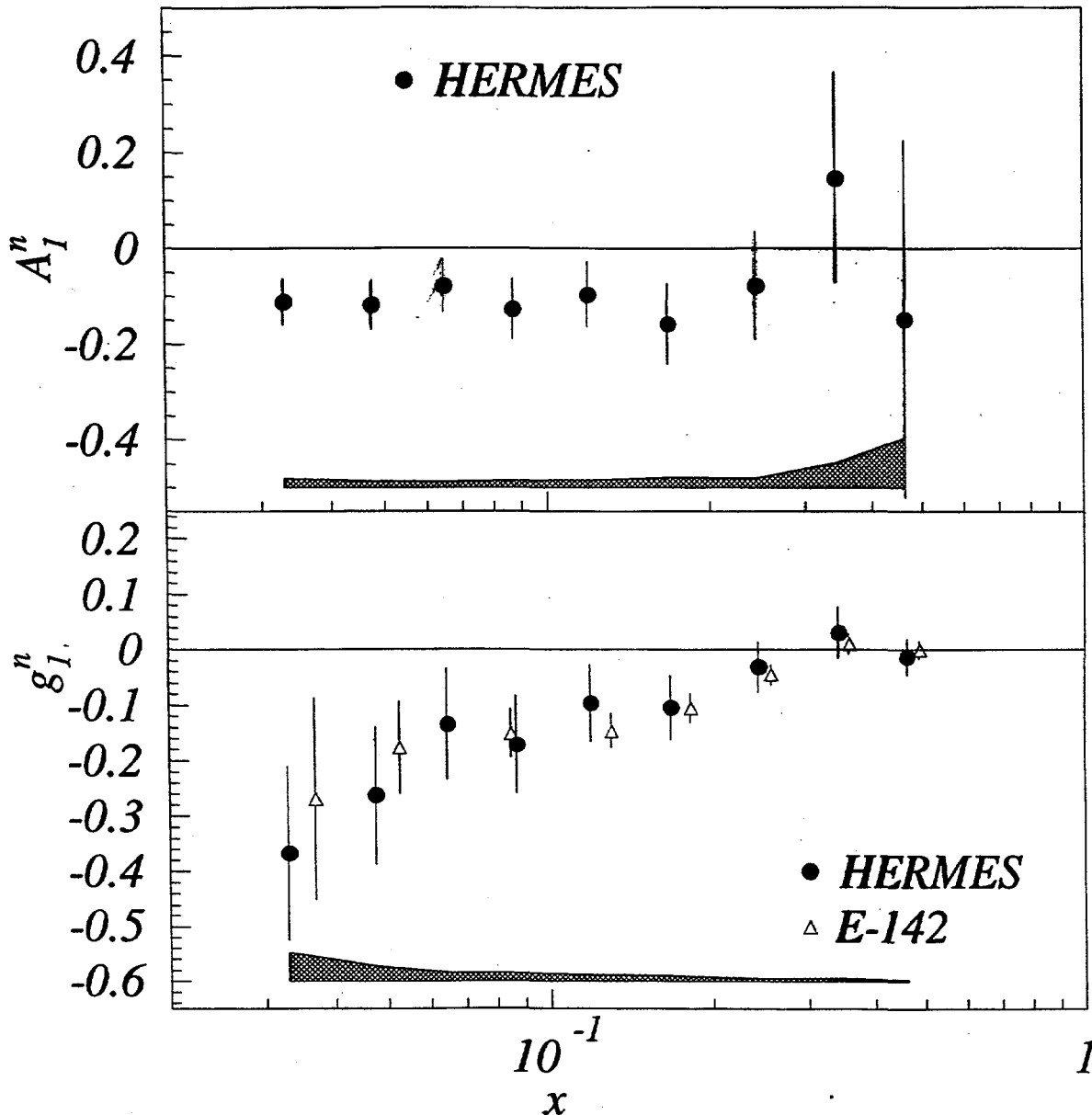




X



Spin Asymmetry $A_1^n(x)$ and Spin Structure Function $g_1^n(x)$ of the Neutron:

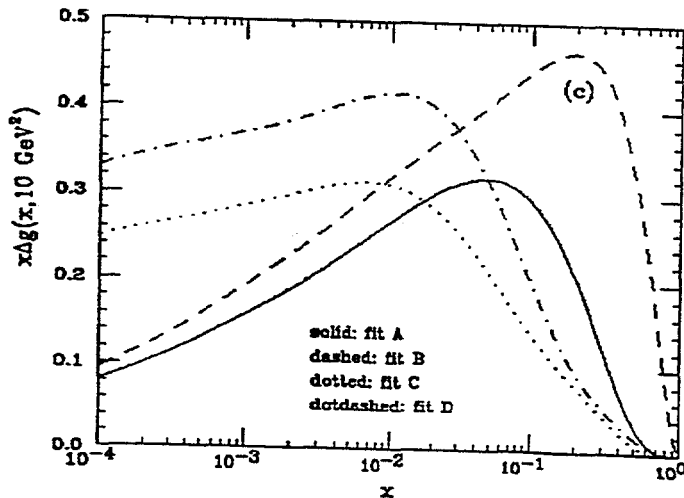
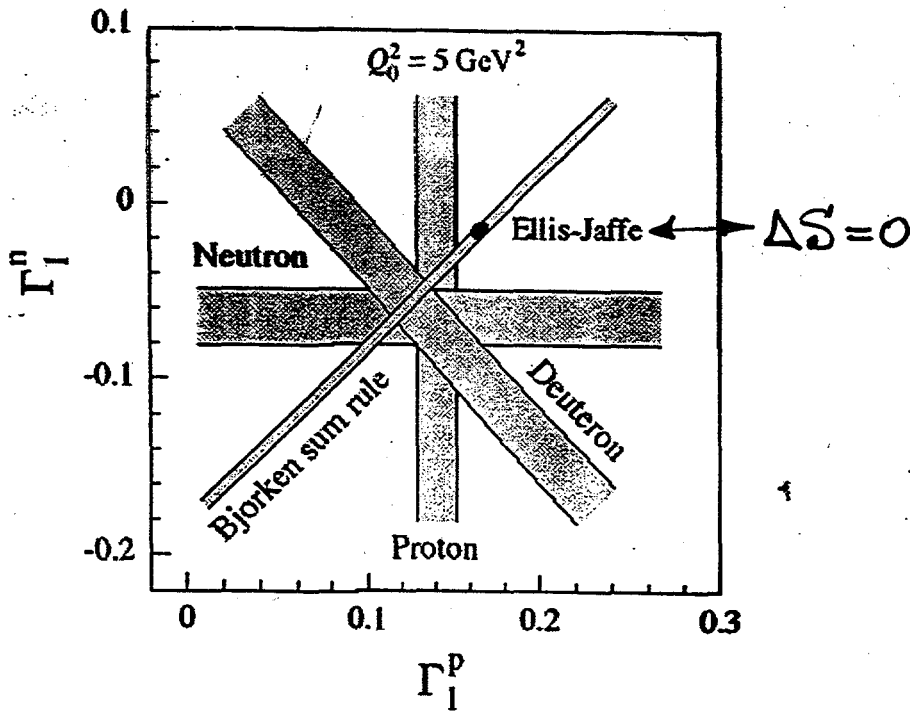


Ellis-Jaffe Sum (HERMES at $Q^2 = 2.5 \text{ (GeV/c)}^2$):

$$\int_0^1 g_1^n(x) dx = -0.037 \pm 0.013_{stat.} \pm 0.005_{syst.} \pm 0.006_{extrapol.}$$

ELECTRON/MUON SCATTERING DATA SUMMARY

$Q_0^2 = 5 \text{ GeV}^2$ $\Delta U = \Delta u + \Delta \bar{u} = 0.82 \pm 0.02$ 1997 SMC REVIEW
 $\Delta D = \Delta d + \Delta \bar{d} = -0.43 \pm 0.02$
 $\Delta S = \Delta s + \Delta \bar{s} = -0.10 \pm 0.02$
 $\Sigma = \sum_a \Delta Q_a = 0.29 \pm 0.06$



ATTEMPTS TO EXTRACT
 $\Delta g(x, Q^2)$ FROM QCD
 EVOLUTION OF $g_i(x, Q^2)$

(AB SCHEME)

$\Delta g > 0$ $\Delta g \sim 1$

ALTARELLI, BALL,
 FORTE, RUDOLFI

PREVIEW OF CONING ATTRACTIONS

• SEPARATE QUARK & ANTIQUARK SPINS BY FLAVOR

$$\begin{matrix} \Delta u(x, Q^2) & \Delta \bar{u}(x, Q^2) \\ \Delta d(x, Q^2) & \Delta \bar{d}(x, Q^2) \end{matrix}$$

- $\vec{p}p \rightarrow W^\pm X$ AT RHIC
- FLAVOR TAGGING IN $\vec{e}p \rightarrow ehX$

• POLARIZED GLUE

$$\Delta g(x, Q^2)$$

- $\vec{p}p \rightarrow \gamma \text{ jet} / c\bar{c} \text{ jets}$ AT RHIC
- $\vec{p}p \rightarrow \text{jets}$ AT RHIC
- $\vec{p}p \rightarrow \chi_2 X$ AT RHIC
- $\vec{e}p \rightarrow c\bar{c} + X$
- EVOLUTION OF $g_i(x, Q^2)$

• QUARK TRANSVERSE SPIN

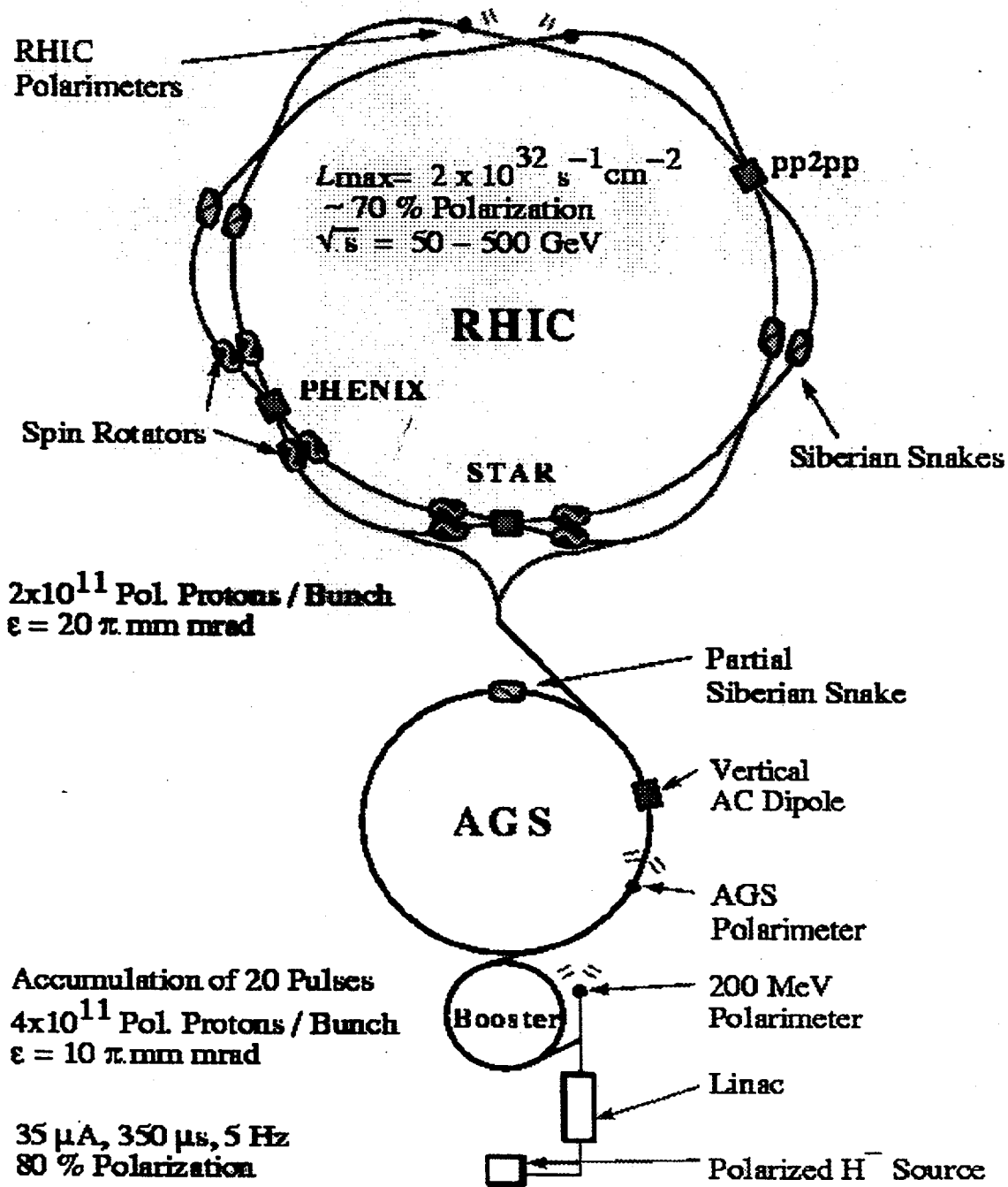
A "SPIN OFF" OF THE SPIN CRISIS WAS THE REALIZATION THAT QUARK SPIN TRANSVERSE TO MOMENTUM - TRANSVERSITY - IS DIFFERENT THAN HELICITY - A CONSEQUENCE OF RELATIVITY

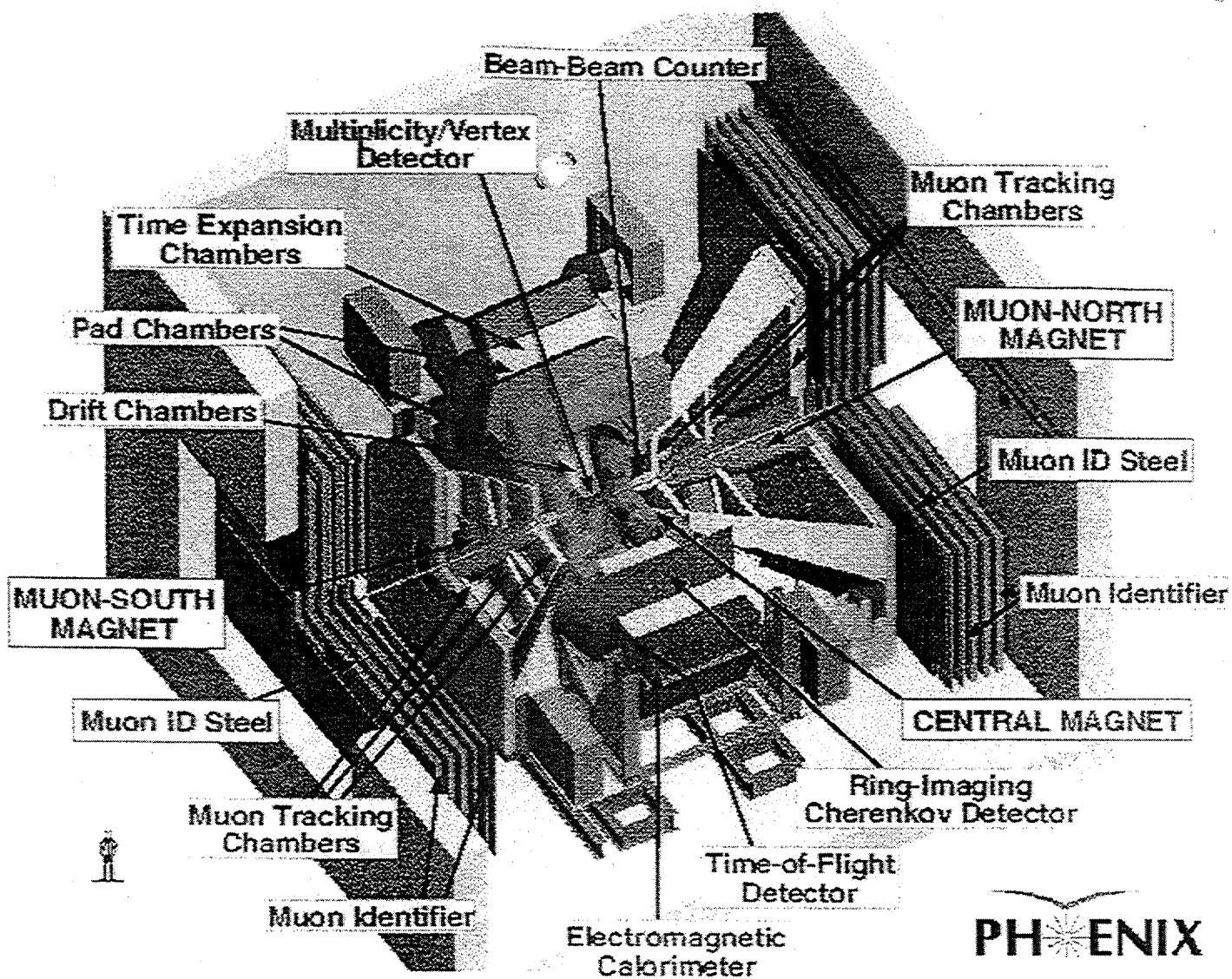
- $\vec{p}_\perp p_\perp \rightarrow \mu^+ \mu^- X$ RHIC
- $\vec{p}_\perp p \rightarrow \pi^+ X \pi^- X$ RHIC
- $e \vec{p} \rightarrow \pi^+ X \pi^- X$
- $e \vec{p}_\perp \rightarrow \Lambda X$

$\delta g(x, Q^2)$ FOR EACH FLAVOR
NO GLUON TRANSVERSITY

$$\left[\begin{matrix} \vec{p}p \rightarrow \text{jets} \\ \vec{p}_\perp p_\perp \rightarrow \text{jets} \end{matrix} \right] \text{ AT RHIC}$$

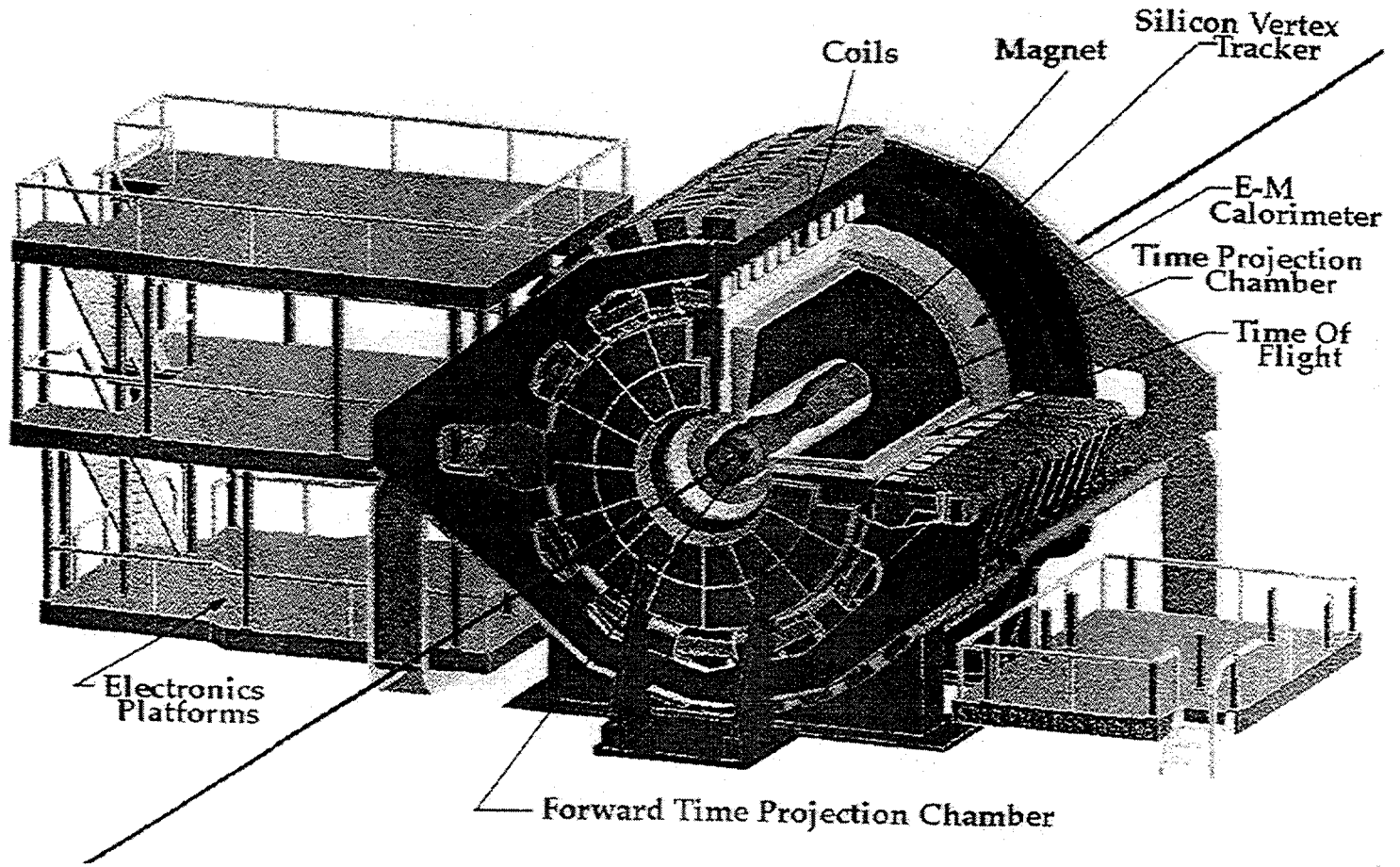
Polarized Proton Collisions at BNL





PHENIX

STAR Detector



POLARIZED ANTIQUARKS IN DREULYAN

- WHY? $\Delta\bar{u} \neq \Delta\bar{d}$ PLAY A CENTRAL ROLE IN SPIN DEVIATION FROM NAIVE EXPECTATIONS

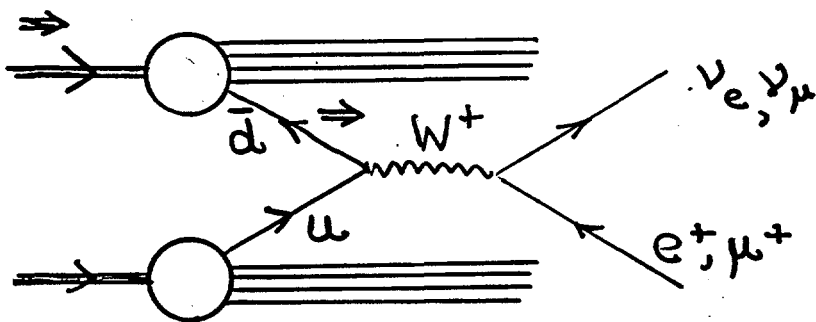
$$\Delta S = \Delta s + \Delta\bar{s} \quad \& \quad \text{EXPECT } \Delta s \cong \Delta\bar{s} \cong \Delta\bar{u}, \Delta\bar{d}$$

- HOW?

$$\vec{PP} \rightarrow W^\pm X$$

$$A_L = \frac{N^\uparrow - N^\downarrow}{N^\uparrow + N^\downarrow}$$

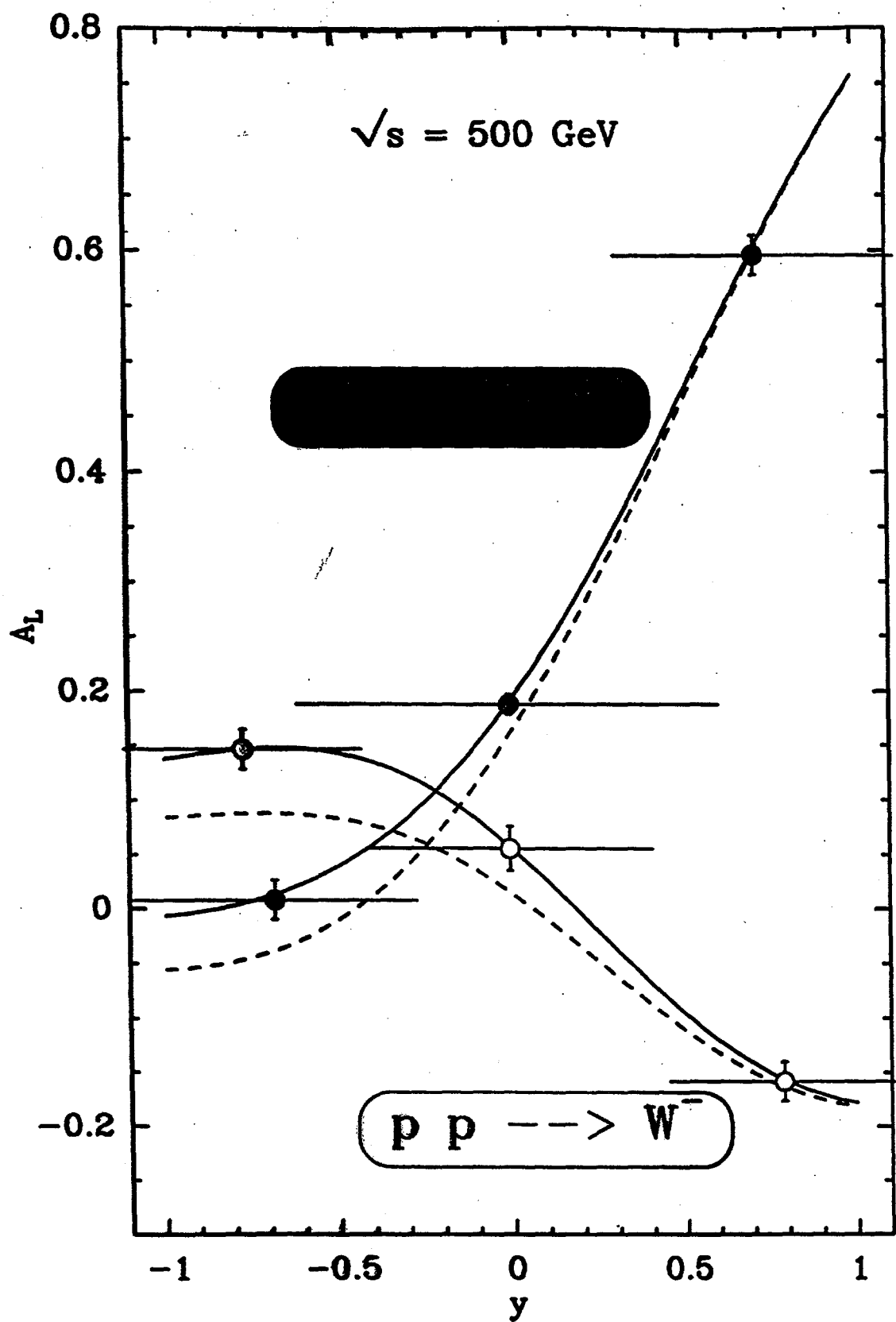
[TWO SPIN ASYMMETRY
 A_L YIELDS NO NEW INFO]



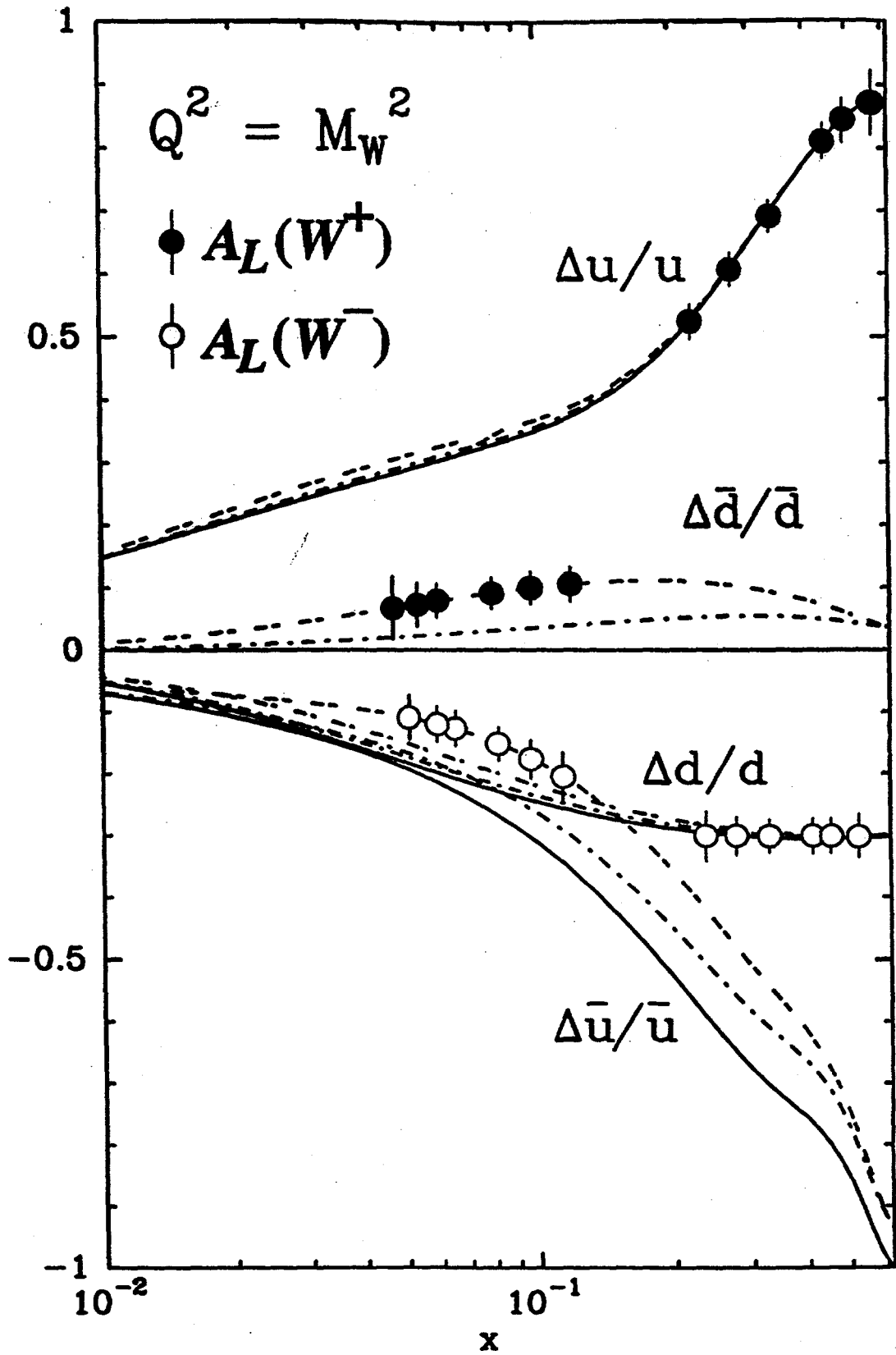
$$A_L^+ \sim \frac{\Delta u(x_1) \bar{d}(x_2) - \Delta \bar{d}(x_1) u(x_2)}{u(x_1) \bar{d}(x_2) + \bar{d}(x_1) u(x_2)}$$

$$\xrightarrow{x_2 \rightarrow 1} \frac{\Delta \bar{d}(x_1)}{\bar{d}(x_1)}$$

$$A_L^- \xrightarrow{x_2 \rightarrow 1} \frac{\Delta \bar{u}(x_1)}{\bar{u}(x_1)}$$



courtesy of Jacques Soffer & Claude Bourrely



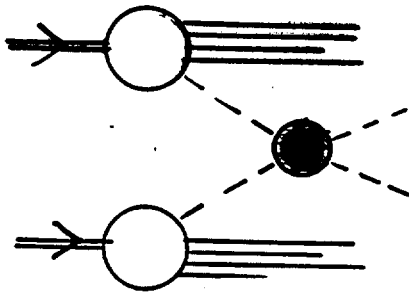
courtesy of Jacques Soffer & Claude Bourrely

POLARIZED GLUON DISTRIBUTION

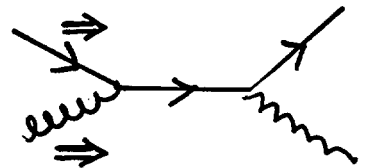
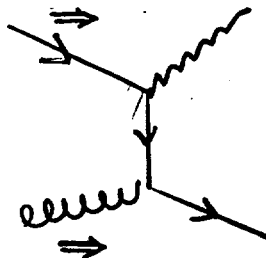
• WHY? Δg LIKELY LARGE IF Σ IS NOT CANONICAL

• HOW?

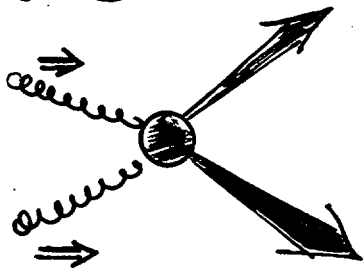
- $\vec{p} \vec{p} \rightarrow \gamma + X$
- $\vec{p} \vec{p} \rightarrow \text{jets}$
- $\vec{p} \vec{p} \rightarrow \chi_2 (c\bar{c}) X$



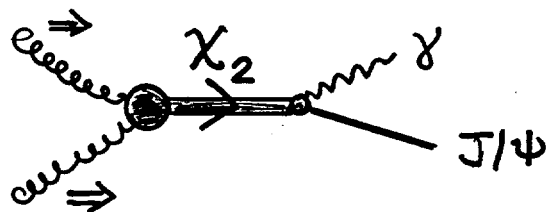
• $\gamma + X$ QCD COMPTON



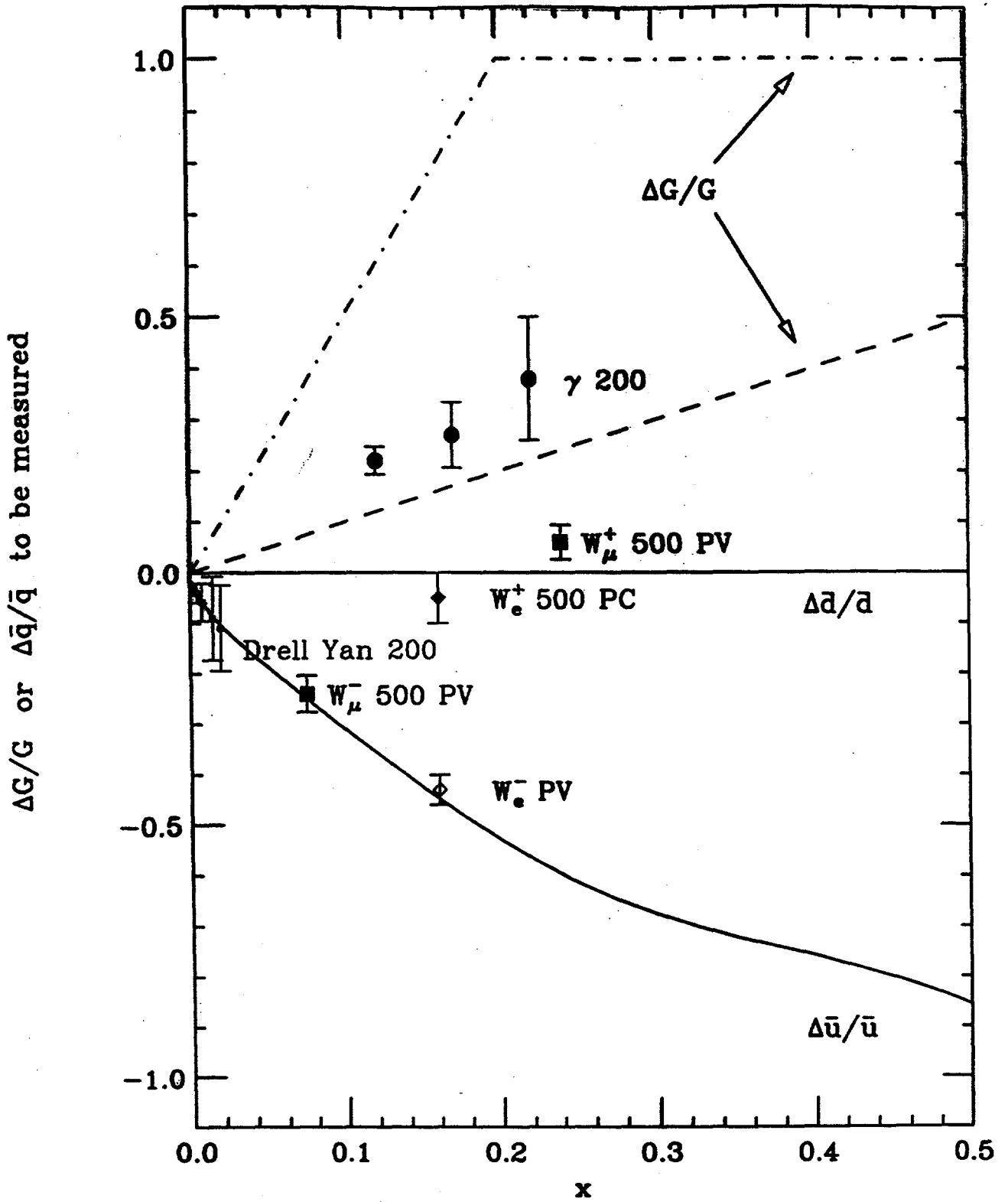
• JETS



• ONIUM $gg \rightarrow \chi_2^{2++} \rightarrow J/\psi + \gamma$

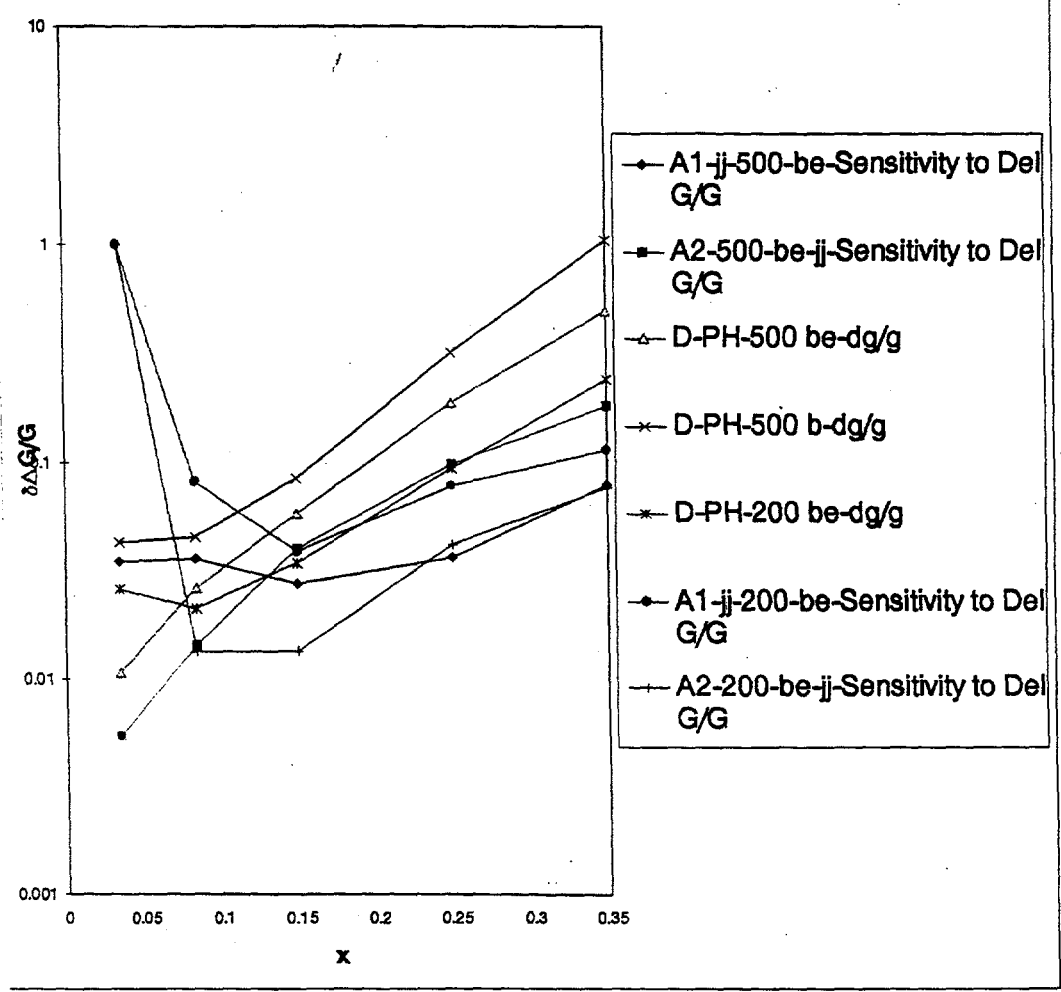


Bourenly---Soffer Predictions



Error in $\Delta G(x)/G(x)$ For Various Measurements

Error in Gluon Polarization Measurement



RHIC Spin Collider – Physics of Accelerating Polarized Protons and Plans

Thomas Roser

The evolution of the polarization \vec{P} of protons in a circular accelerator is governed by the Thomas-BMT precession equation

$$\frac{d\vec{P}}{dt} = -\left(\frac{e}{\gamma m}\right) \left[G\gamma \vec{B}_{trans.} + (1+G)\vec{B}_{long.} \right] \times \vec{P} \quad ; \quad G = 1.7928$$

This is to be compared with the Lorentz equation that governs the orbital motion:

$$\frac{d\vec{v}}{dt} = -\left(\frac{e}{\gamma m}\right) \left[\vec{B}_{trans.} \right] \times \vec{v}$$

For a pure vertical field the number of spin precesses per orbit revolution, also called ‘spin tune’, is $G\gamma$. To manipulate the spin direction at low energy a longitudinal magnetic field can be used. For example the 9 degree spin rotator used in the AGS is simply a large solenoid. However, at high energy a sequence of alternating horizontal and vertical fields has to be used. In such a wiggler-like structure the relative small orbit deflections are cancelled whereas for the much larger spin precessions the non-commutative character of rotations can not be ignored. Structures for which the total residual spin rotation adds up to 180 degrees are called Siberian Snakes. In RHIC the Snakes and the spin rotators to produce the longitudinal polarization at the interaction regions each consist of four 2.4 m long full-twist helical dipole magnets.

In a circular particle accelerator the polarization direction of the beam that is the same every turn is called the ‘stable spin direction’. Other names are ‘invariant spin direction’ or ‘spin closed orbit’. Although for a pure vertical field this direction is vertical everywhere, in general it will depend on the ring rigidity, location around the ring and the ring lattice. It does, however, not depend on the initial beam parameters or any dynamic quantities such as the acceleration rate. The stable spin direction of the AGS with the 9 degree spin rotator (Partial Snake) is mostly vertical but reverses sign whenever $G\gamma$ crosses an integer value. In RHIC two Siberian Snakes will be installed in each of the two rings separating each ring into two exactly equally long halves. In one half the stable spin direction points up and the other down. In this case the spin tune is a half-integer independent of energy.

Depolarization occurs when the stable spin direction changes so fast during acceleration that the beam polarization can't adiabatically follow it. This condition is avoided in the AGS with the 9 degree Partial Snake and in RHIC with the two full Snakes. Particles on the edge of the beam will sample the focusing fields of the ring quadrupoles and their stable spin direction becomes very sensitive to these fields when the betatron frequency is equal to the spin precession frequency (intrinsic spin resonance). This condition cannot arise in RHIC since the spin tune is a half-integer. To avoid depolarization in the AGS we excited coherent betatron oscillations of all particles while accelerating through the resonance condition. All particles then experience strong enough focusing fields that the stable spin direction moves slow enough from up to down that the beam polarization can follow it adiabatically. A maximum polarization of about 51 % has been reached in the AGS at 22 GeV.

By summer of 1999 two Snakes and one high energy polarimeter will be installed in one of the rings of RHIC. This will allow for the commissioning of polarized beam acceleration in this ring during the first year of RHIC operation starting in October 1999. The goal is to accelerate polarized beam to at least 100 GeV in preparation for a spin physics run at $\sqrt{s} = 200 \text{ GeV}$ in the second RHIC year starting in October 2000.

Precession Equation in Laboratory Frame :
 (Thomas [1927], Bargmann, Michel, Telegdi [1959])

$$d\mathbf{P}/dt = -(e/\gamma m) [G\gamma \mathbf{B}_{\perp} + (1+G) \mathbf{B}_{\parallel}] \times \mathbf{P}$$

Lorentz Force equation:

$$d\mathbf{v}/dt = -(e/\gamma m) [\mathbf{B}_{\perp}] \times \mathbf{v}$$

$$\gamma = E/m$$

- **For Pure Vertical Field:**
Spin Rotates $G\gamma$ Times Faster than Motion
SPIN TUNE $\nu_{sp} = G\gamma$
- **For Spin Manipulations:**
At Low Energy, use Longitudinal Fields
At High Energy, use Transverse Fields

Spin Resonances and Siberian Snakes

Spin Tune ν_{sp} : Number of 360° Spin Rotations per Turn

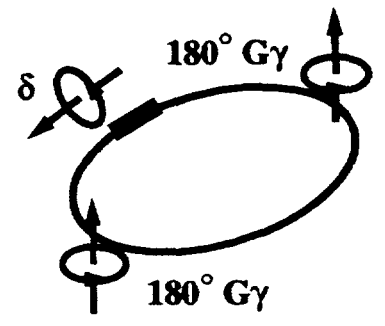
Depolarizing Resonance Condition:

Number of Spin Rotations per Turn
 = Number of Spin Kicks per Turn

Only Vertical Field

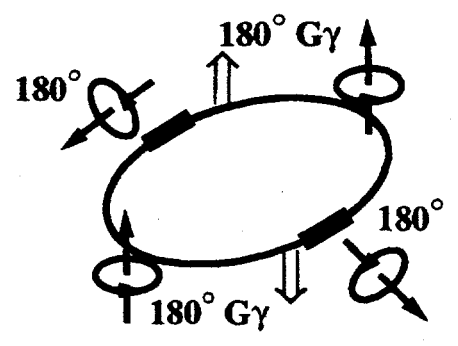
$$\left(\begin{matrix} G\gamma = 1.79 \\ \gamma = E/m \end{matrix} \right) \begin{matrix} G\gamma = \nu_{sp} = n & \text{Imperfection} \\ G\gamma = \nu_{sp} = n \pm \nu_y & \text{Intrinsic} \end{matrix}$$

Local Spin Rotators (Siberian Snakes)



$$\cos(180^\circ \nu_{sp}) = \cos(\delta/2) \cdot \cos(180^\circ G\gamma)$$

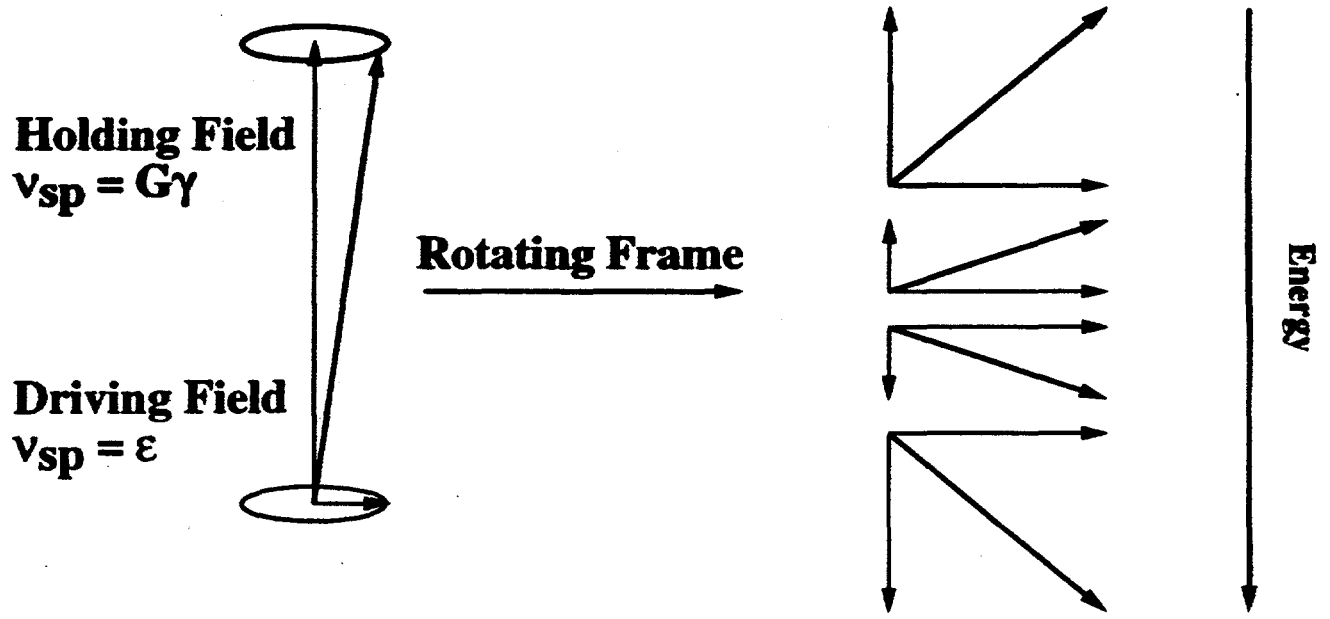
- $\delta \neq 0^\circ \rightarrow \nu_{sp} \neq n \Rightarrow$ **No Imperfection Resonances...**
Partial Siberian Snake (AGS)
- $\delta = 180^\circ \rightarrow \nu_{sp} = 1/2 \Rightarrow$ **No Imperfection and No Intrinsic Resonances...**
Full Siberian Snake



Two Siberian Snakes (RHIC)

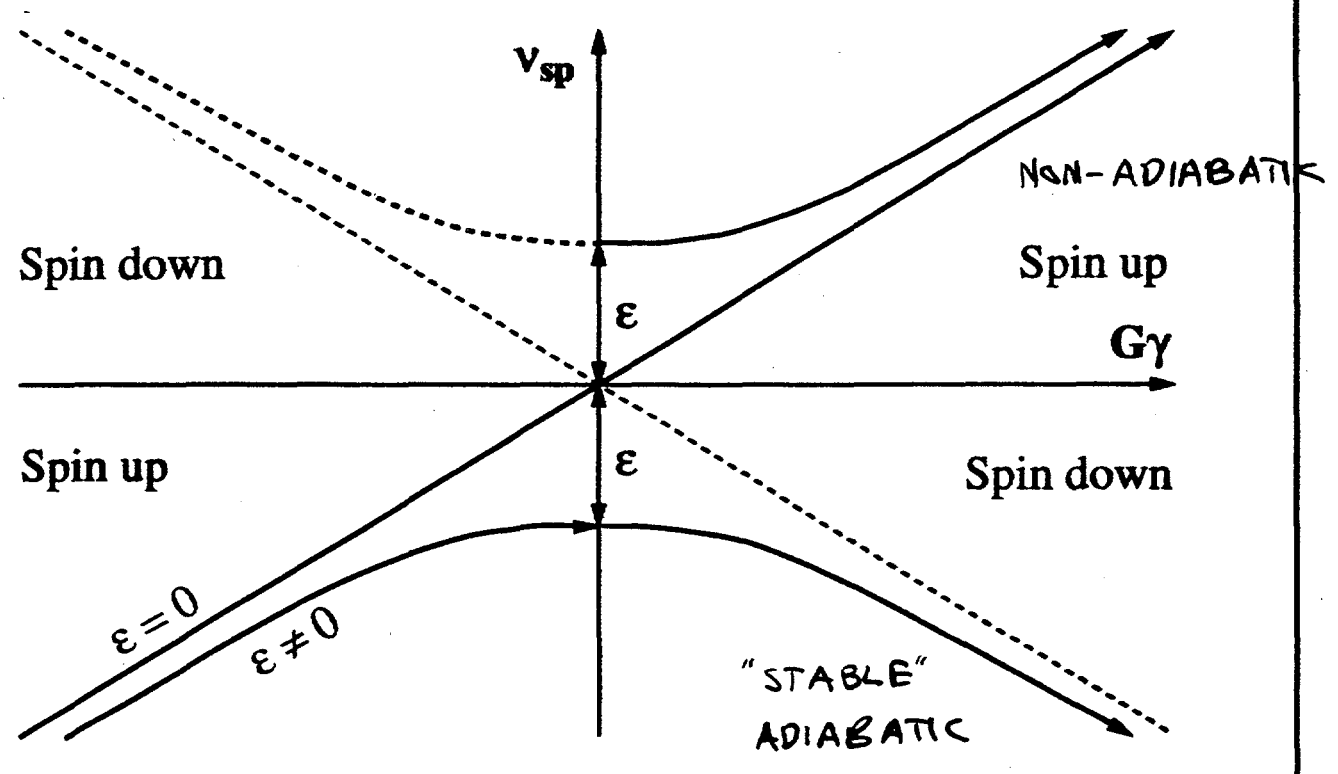
- $\nu_{sp} = 1/2$, Stable Vertical Polarization

Spin Resonances

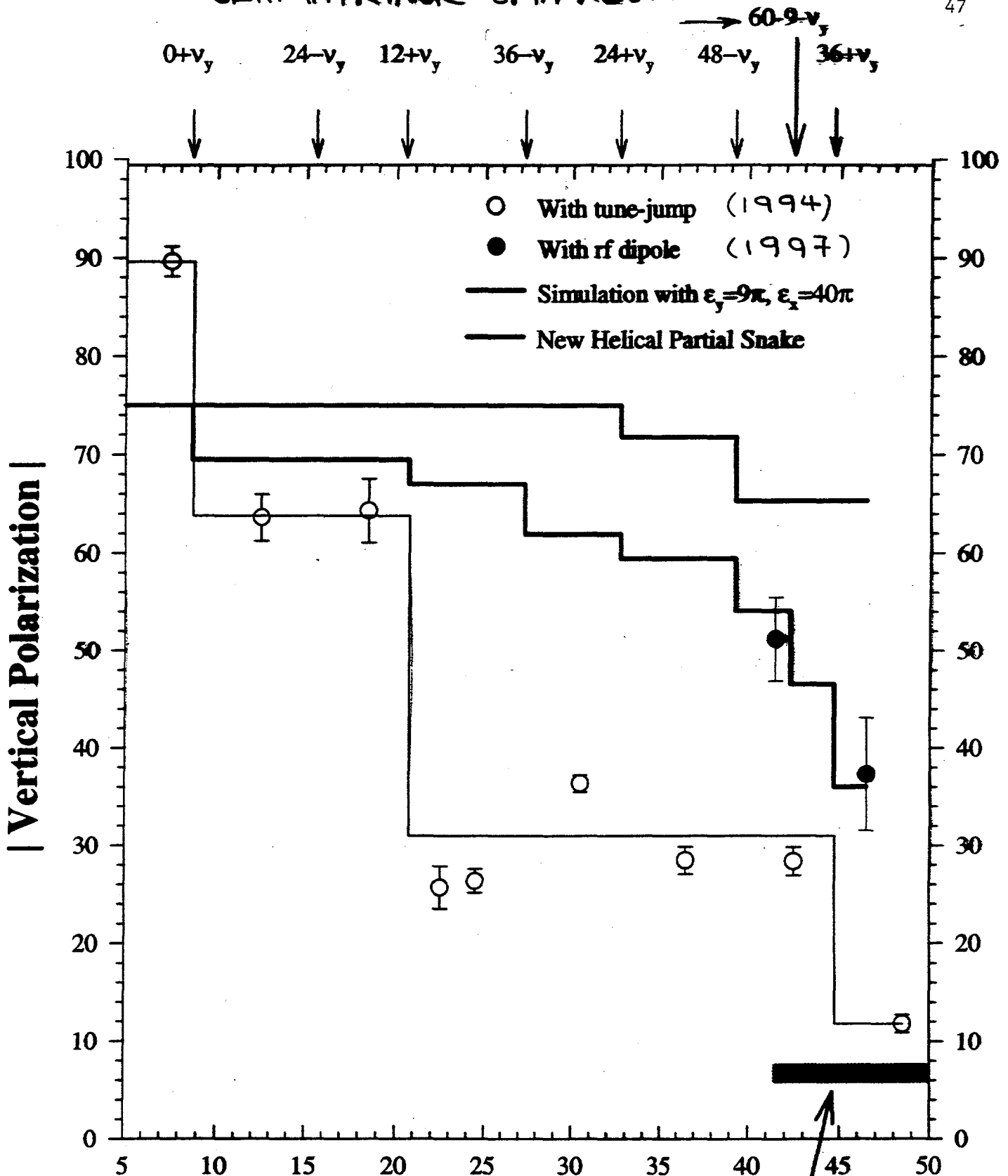


Froissart-Stora(1960): $P_{Final} / P_{Initial} = 2 \exp(\pi\epsilon^2 / 2\alpha) - 1$

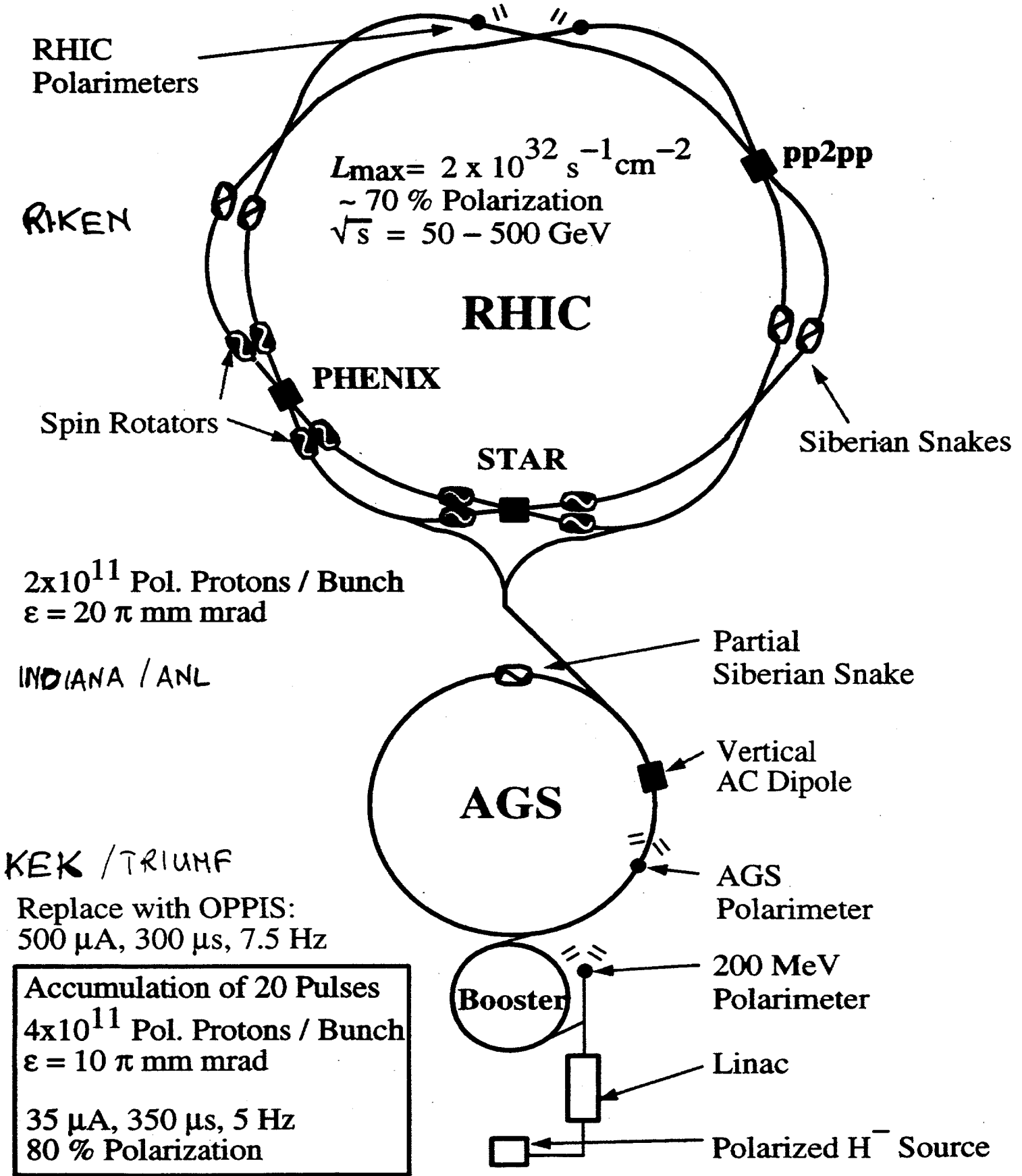
ϵ : Driving Field
 α : Crossing Speed



SEMI-INTRINSIC SPIN RESONANCE



Polarized Proton Collisions at BNL



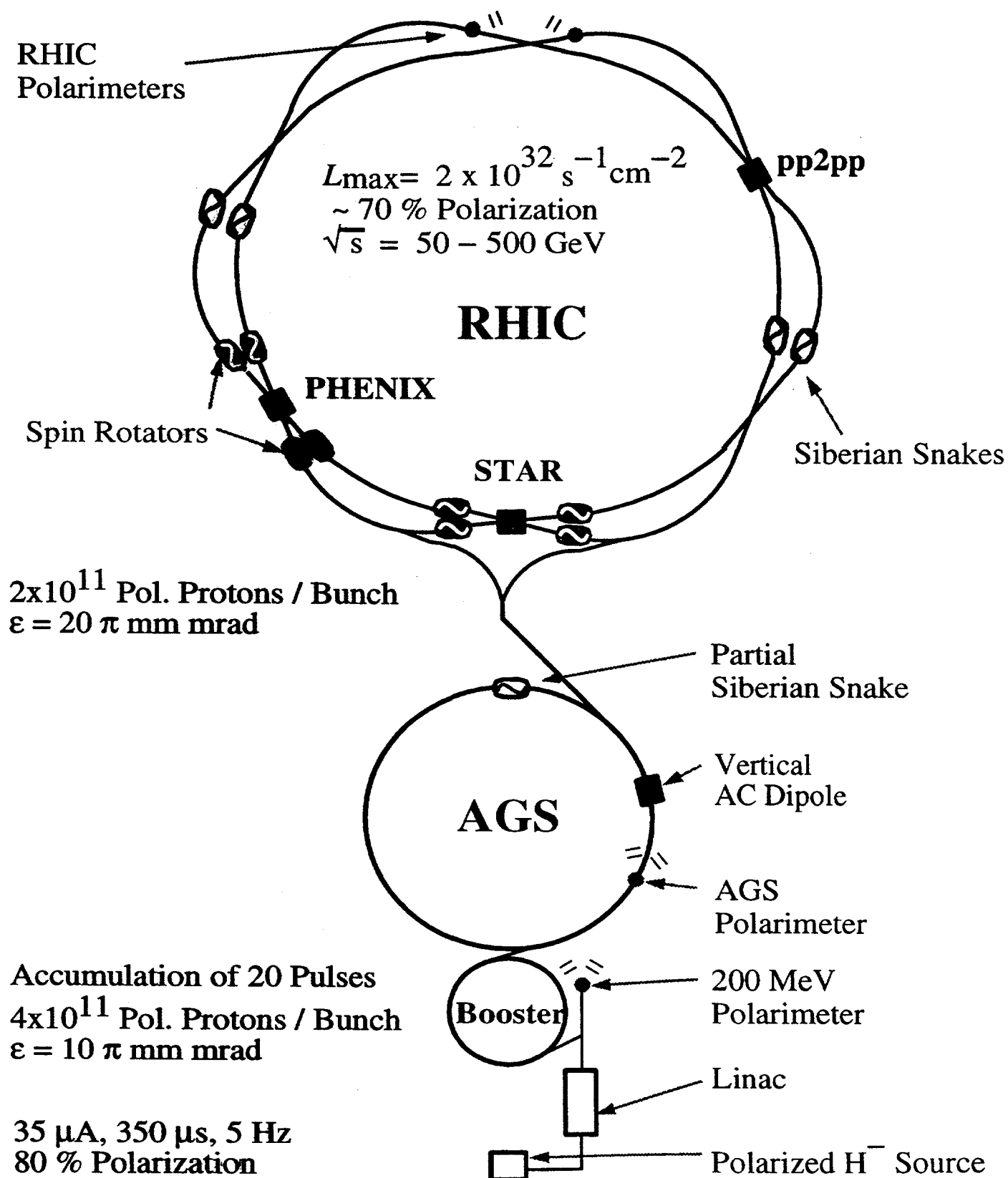
Important Dates and Schedule

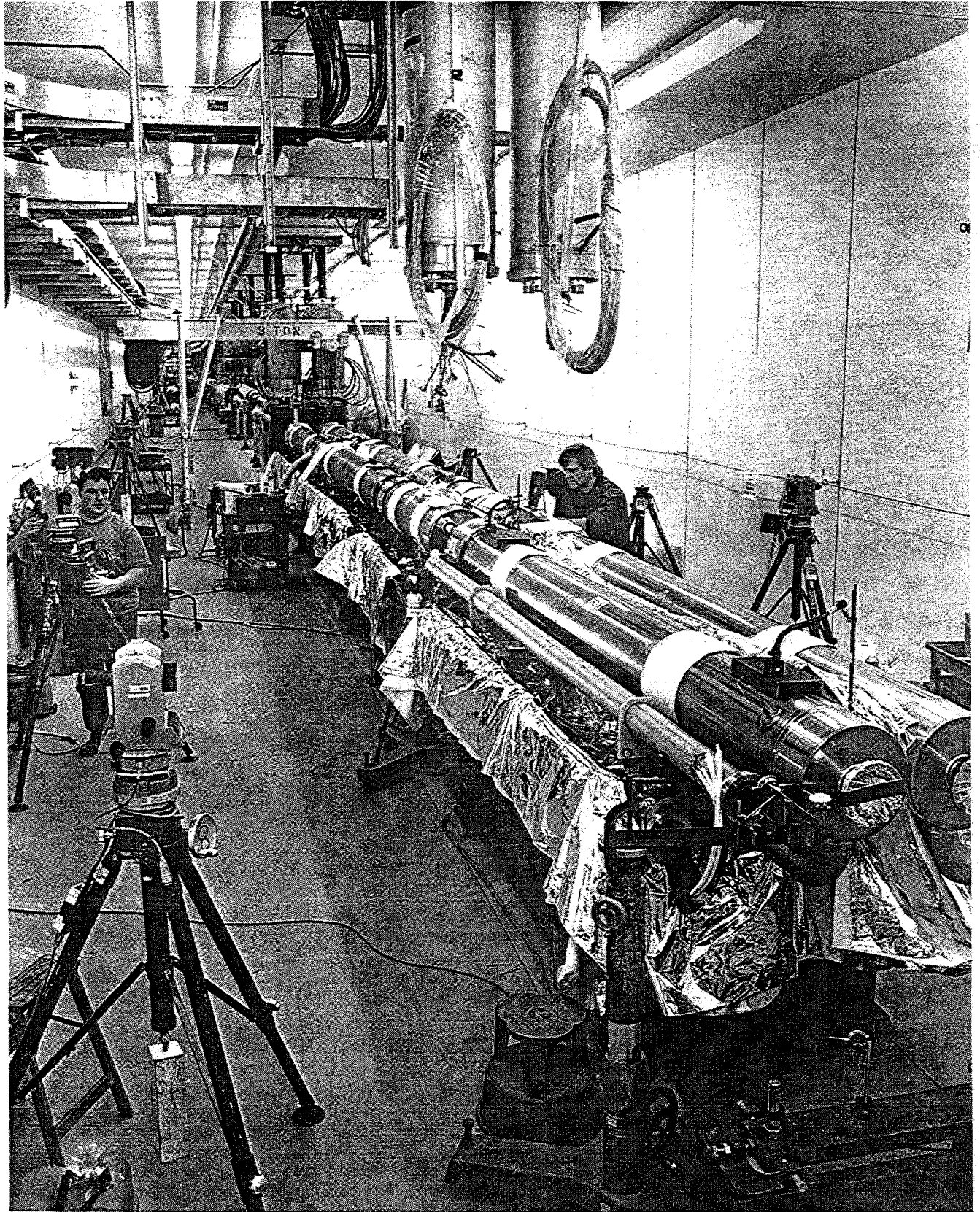
RHIC Spin Collaboration (RSC) Proposal	September 1992
1. Review of Pol. Proton Accel., Feasibility	February 1993
AGS Partial Snake Test (E-880)	April/ Dec. 1994
2. Review of Pol. Proton Accel., Progress	March 1995
RHIC Spin Physics Review	June 1995
RIKEN/BNL MoU signed	Sept. 25, 1995
RIKEN Japan Funding for Accel. (10M\$) and PHENIX Detector (10M\$)	1995 – 1999
Final Report of Polarization Measurement Working Group	July 31, 1996
First Helical Dipole Prototype Complete	October 1996
Second Helical Dipole Prototype Complete	January 1997
3. Review of Pol. Proton Accel., Progress	February 1997
First Full Helical Dipole Complete	May 1998
RHIC Completion	June 1999
2 Snakes and one Polarimeter Installed	September 1999
First Polarized Beam in RHIC	> October 1999
All Spin Rot./Snakes and Polarimeters Inst.	September 2000
First Spin Physics Run in RHIC	> October 2000

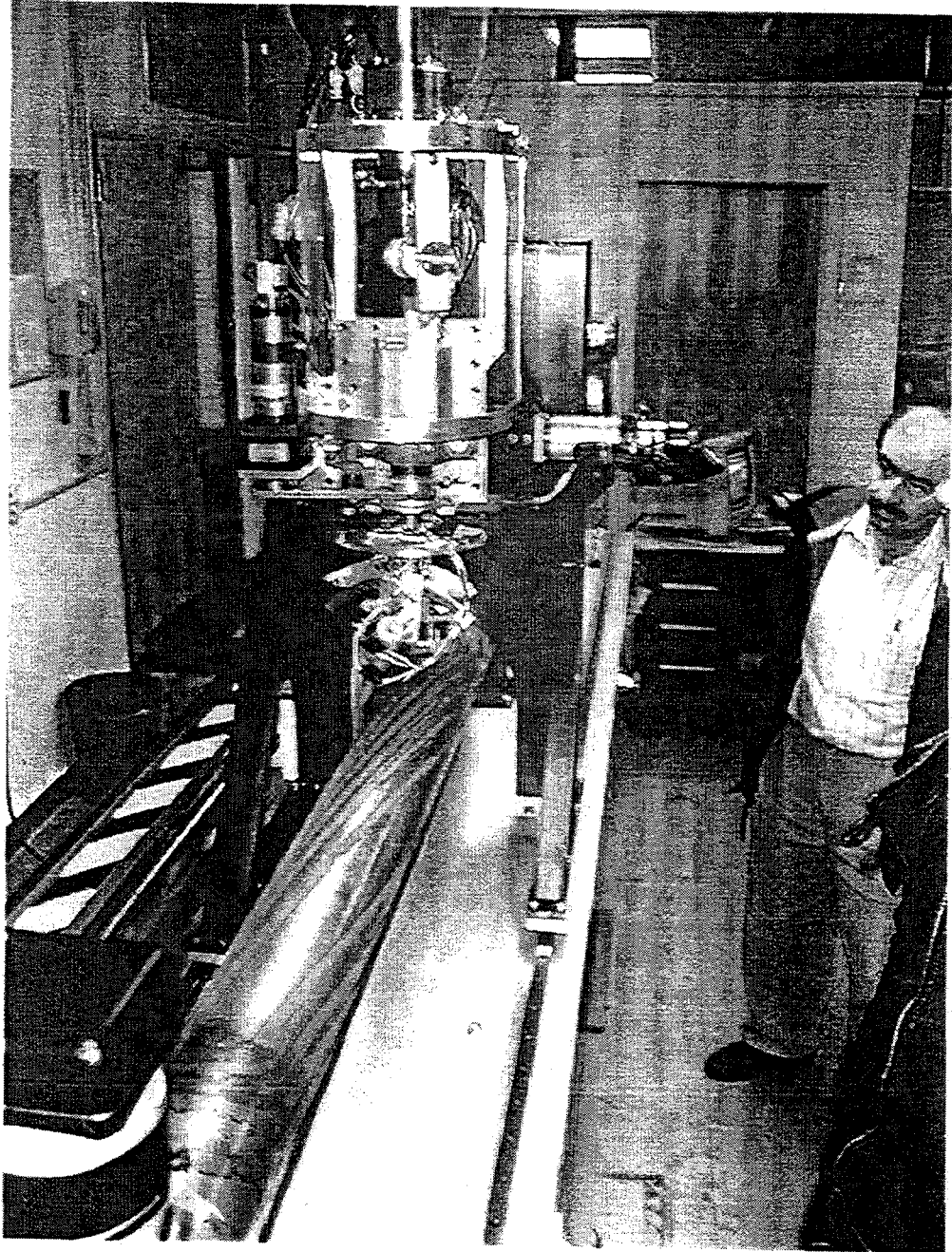
Michael HARRISON

Brookhaven National Laboratory
Upton, New York 11973

Polarized Proton Collisions at BNL







Status

Final focus triplet magnets in production, CQ1, CQ2, D0's completed. All CQ3's are in production, 62 out of 78 elements completed as of the end of March, last magnet scheduled for mid June

Large aperture dipole (DX) prototype fabricated and tested successfully. Production started magnet #1 approaching cold test. (~3 weeks behind schedule)

28Mhz RF cavities 2, 3, & 4 have been accepted and are in transit

All major power supply orders placed

Beam dump & kicker fabrication in progress

Final tunnel mechanical hardware (DX cryostats & transfer line) starts to arrive in May

Installation Status

All 8cm magnets installed, final interconnects in progress. Completion by end of April (on schedule)

Triplet lower cryostats assembled in the tunnel. Interring cold masses has started at sector 2, the first triplet.

Warm/cold transitions have started

DX lower cryostats by the end of April

External cryogenic piping in place at 2,4, 6 & 12. 8&10 start in June. Inside piping installed, interring in progress. Valve box piping complete, internal wiring started

Tunnel infrastructure:- final 2 sextants rewiring in progress, exhaust fans completed in half ring second half just starting

Security system in sectors 11 thru 5.

50A power supplies are showing up in the alcoves

Electrical work in RF, Instrumentation & beam dump areas. Generic tunnel complete

Issues

Need to demonstrate 2nd DX magnet

Cryogenic's has ~\$900K FY98 problem. Will exhaust this year's contingency. RF water system \$200K more than estimate.

Power supply procurement schedule remains only marginally consistent with Project. Limited initial impact - affects beam rather than hardware check-out.

Chronic inability to hire job shoppers (15 techs short at this time)

**Schedule items I'm watching: -
RF cooling water, safety system installation, liquid helium storage system, valve box wiring, BPM's.**

Introduction to the 1.5 days mini-workshop on Gluons at RHIC

Naohito Saito

Radiation Laboratory

RIKEN (The Institute of Physical and Chemical Research)

Saitama 351-0198, Japan

(<http://www.rhic.bnl.gov/phenix/WWW/publish/saito/>)

The gluons are abundant in the proton. Because of this, gluons play a very important role in the interaction of the protons. The reaction is dominated by gluon related sub processes such as $gg \rightarrow gg$ or $gq \rightarrow gq$. The dominance of gluon contribution is especially true for the higher energy hadron collisions, such as RHIC, Tevatron, and LHC.

The behavior of the gluon in the proton is less known than the quarks in the proton, since a major probe to investigate the internal structure of the proton, the deep inelastic scattering of leptons off the proton target, is not sensitive to the gluon distribution. Therefore, the behavior of the gluons in the protons has been studied in the pp or $p\bar{p}$ interactions.

The RHIC at Brookhaven National Laboratory will provide a completely new domain of the gluon study for the following reasons:

- 1) study of polarized gluons has become possible,
- 2) pp collision will reach its high energy frontier, and
- 3) pA and AA collisions will elucidate the gluons in nuclei, which is crucial information for the exotic search in AA collisions.

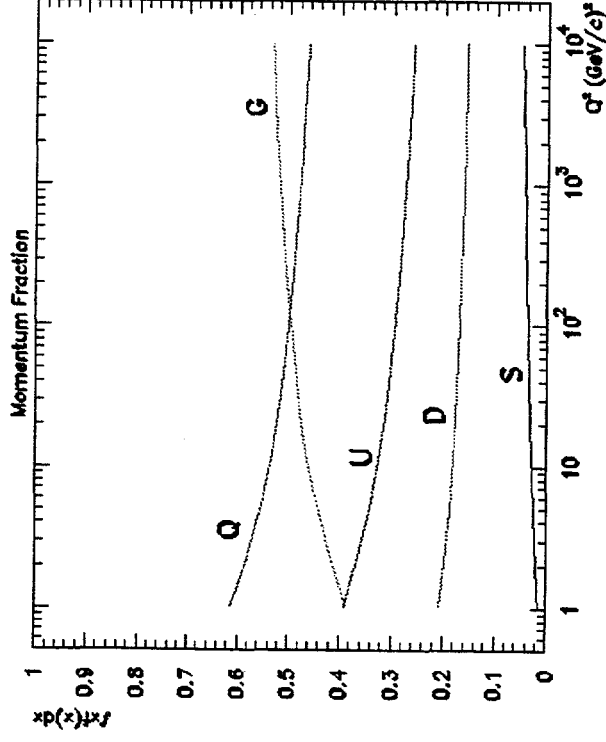
The goal of this workshop is to summarize the current status of the knowledge on the gluons in the unpolarized and the polarized proton and to discuss how we can improve our knowledge using the RHIC. A special emphasis is put on the measurements of gluon polarization in the proton at RHIC from three aspects:

- 1) theoretical definition of gluon polarization and its gauge-invariance,
- 2) experimental method to extract the gluon polarization from polarized pp reaction, and
- 3) theoretical and experimental uncertainties involved in the determination of the gluon polarization.

Finally the sensitivity of the proposed RHIC measurements will be compared with other possible measurements, such as COMPASS and polarized-HERA. The summary table will follow soon.

Gluon Studies in pp Collisions

- Gluons are abundant in the proton
 - gluon related processes dominate the reaction
 - $gg \rightarrow gg, gq \rightarrow gq$
 - This is true in extremely high energy
 - RHIC, (Tevatron), LHC
- Less known for gluon
 - sensitivity of DIS limited
 - extraction of structure fn's from hadron collisions more complicated than DIS



Gluons at RHIC

- Completely new domain of studies
 - polarized gluon, $\Delta G(x)$
 - one of the major interests in RHIC Spin physics
 - even unpolarized gluon $G(x)$
 - highest energy in pp collisions; any energy dependent systematic uncertainty?
 - “*EMC effect*” in gluon
 - pA and AA ; how gluons behave in nuclei?
 - provide a basis of “exotic search” in AA
 - J/ψ suppression ; open heavy flavor production
 - nuclear shadowing effect

Naohito Saito, RIKEN

Unpolarized Gluon Distribution

→ Steve Kuhlmann's Talk

• Comparison of the most recent analysis

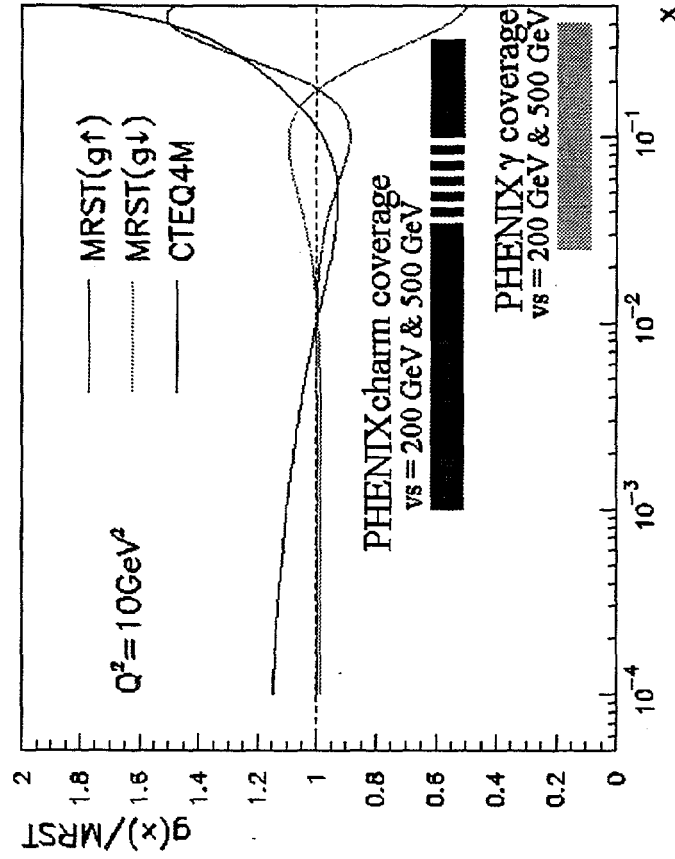
normalized to MRST central

– MRST distribution

- hep-ph/9803445
- 3 versions of $g(x)$
 - $\langle k_T \rangle = 0.0, 0.4, 0.64 \text{ GeV}$
 - MRST($g \uparrow$) high gluon
 - MRST central
 - MRST($g \downarrow$) low gluon

– CTEQ4M

- PR D55 (97) 1280



Naohito Saito, RIKEN

Partonic Kinematics

prompt photon example

- Simple minded reconstruction

of partonic kinematics

pp CMS = parton CMS

- What is Q^2 ?

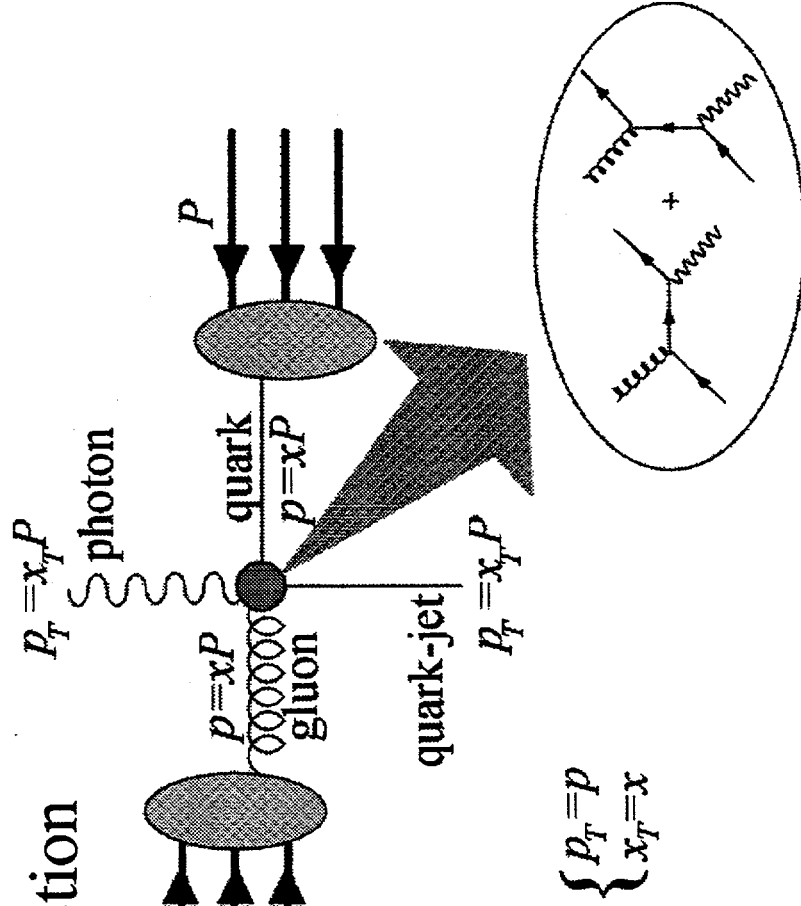
- $Q^2 = p_T^2$?

- $Q^2 = (p_T/2)^2$?

- $Q^2 = (2 p_T)^2$?

- How NLO changes

this view?



$$\begin{cases} p_T = p \\ x_T = x \end{cases}$$

温故知新

- 温故知新

revisit the past to learn something new

— 温_(vt.) (1) to warm up (2) to revisit or even
reincarnate

- 温糊知新

— 糊_(n) (1) glue

— 温糊知新 = RHIC Spin and HI!

(1) revisit gluon to learn something new

(2) warm up gluon to learn something new

Unpolarized Gluon Uncertainties and Direct Photon Measurements

S. Kuhlmann, Argonne National Laboratory

This talk described three topics: 1) the uncertainty on unpolarized gluons using just deep-inelastic scattering and Drell-Yan data, 2) the soft gluon effects in direct photon measurements, and 3) the details of the CDF direct photon measurement.

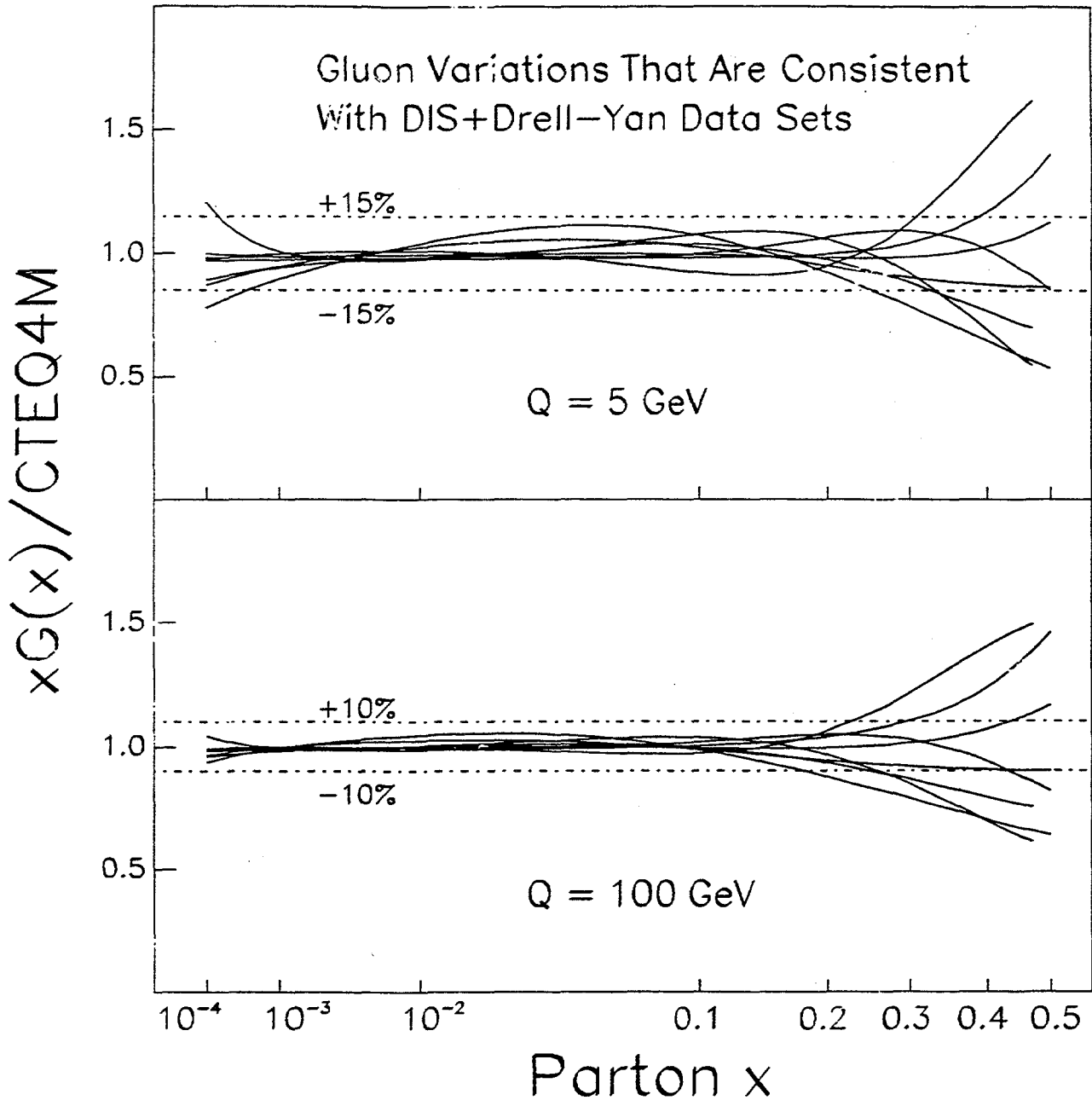
In reference [1], the uncertainty of the gluon distribution was studied using only deep-inelastic and Drell-Yan data sets. The parameters of the gluon distribution were varied systematically, and all of the other quark and gluon parameters were refit. Each variation was studied in detail, and the resulting band of acceptable gluon distributions provided an uncertainty estimate. The range of gluons was a relatively small 10% below $x < 0.1$, but grows to $\approx 50\%$ at larger values of x .

Direct photon data, in principle, could be used to reduce this uncertainty. But the release of the final E706 data [2] shows a deviation from NLO QCD of up to $\times 4$, much larger than the uncertainty of the gluon. This is attributed to the soft-gluon effects that are seen in heavy flavor and Drell-Yan data sets.

Finally, the CDF direct photon measurements [3] were described in detail. The detector is very similar to the STAR detector. The measurements used two independent methods of subtracting backgrounds, one which utilized transverse shower shapes, and the other which used photon conversion probabilities. The two methods agreed. Three main problems in performing the analysis were described: 1) GEANT did not provide an adequate simulation for either method, 2) the need to reconstruct mesons and compare to simulations, and 3) backgrounds that could not be attributed to the normal meson decays into photons. The CDF solutions to these three problems was described.

References

- [1] J. Huston et al., hep-ph/9801444
- [2] E706 Collaboration, hep-ex/9711017
- [3] CDF Collaboration, PRL73:2662, PRD48:2998



Bottom Line on K_t Effect

Most Recent MRS Analysis Applies K_t
Corrections For Direct Photons

Range of Gluons Provided Varying K_t Amount

Range is as Large as the CTEQ Band,
Which Only Used DIS+DY Data

Need Direct Photon P_t Resummation

For $\sqrt{s} = 200 - 500$, Expect All NLO QCD
Predictions to Need an Additional 2-3 GeV of K_t

Ask Yourself, Does it Matter?

Details of the CDF Direct Photon Measurements

Refs: PRL73:2662 and PRD48:2998

Data at Both $\sqrt{s} = 1800$ and 630 GeV

Detector Very Similar to STAR

Two Independent π^0 Subtraction Methods

Electromagnetic Shower Shape γ vs π^0

Count $\gamma \rightarrow e^+e^-$ Conversions In Preshower Det.

CDF Direct Photon Conclusions

Simulations Can Be Non-Trivial to Develop

Early (Online?) Comparison With
Reconstructed Mesons Is Useful

Isolation Useful to Check Background Mix

An Introduction to Resummation and Intrinsic p_T

George Sterman, *Institute for Theoretical Physics, SUNY Stony Brook*

The influence of partonic transverse momentum on single-particle inclusive cross sections has been a subject of interest for some time. The standard factorized cross section for $A + B \rightarrow C + X$ is a convolution in momentum fractions only,

$$E_C \frac{d\sigma_{AB \rightarrow C+X}}{d^3 p_C} = \sum_{abc} f_{a/A}(x_a, \mu^2) \otimes f_{b/B}(x_b, \mu^2) \otimes D_{C/c}(z, \mu^2) \otimes \hat{\sigma}(x_a p_A, x_b p_B, p_C/z, \mu). \quad (1)$$

Transverse momenta $k_T < \mu$ (relative to the incoming and outgoing directions) are absorbed into parton distributions f and fragmentation functions D , while larger transverse momenta are included in the partonic hard scattering $\hat{\sigma}$. Corrections associated with this organization of states appear systematically in higher-order corrections to $\hat{\sigma}$. An important example is direct photon production, which is of special relevance to the determination of the gluon distribution. Data on direct, or prompt, photons is available over a wide range of \sqrt{s} and p_T , generally with isolation cuts at collider energies. For some time, many, although not all [1], calculations of direct photon production based on Eq. (1) have fallen significantly below the data at low p_T , suggesting the need for a “ k_T -smearing”, perhaps reflecting the intrinsic transverse momentum of partons in hadrons [2].

An alternative factorization including transverse momenta is [3]

$$E_\ell \frac{d\sigma_{AB \rightarrow \gamma(\ell)+X}}{d^3 \ell} = \frac{1}{S^2} \sum_{ab} \int dx dy d^2 \mathbf{q} d^2 \mathbf{q}' \mathcal{P}_{a/A}(x, p_A \cdot n, \mathbf{q}) \mathcal{P}_{b/B}(y, p_B \cdot n, \mathbf{q}') \times \Omega_{ab\gamma} \left(\frac{s'}{\mu^2}, \frac{t'}{\mu^2}, \frac{u'}{\mu^2}, \alpha_s(\mu^2) \right), \quad (2)$$

with a modified hard-scattering function Ω , which depends on kinematic variables s', t', u' that include parton transverse momenta. The wave functions \mathcal{P} are related to the light-cone wave functions f in Eq. (1) by

$$\mathcal{P}_{a/A}(x, p \cdot n, \mathbf{q}) = \sum_c \int d\lambda f_{c/A}(\lambda, \mu^2) \int d^2 \mathbf{b} e^{-i\mathbf{q} \cdot \mathbf{b}} C_{a/c} \left(\frac{x}{\lambda}, |\mathbf{b}| \mu, \alpha_s(\mu^2) \right) e^{-S_c(|\mathbf{b}|, p \cdot n)}, \quad (3)$$

where the b -dependent exponent, which matches perturbative and nonperturbative contributions [4], has the effect of introducing a Gaussian k_T -smearing into the cross section (2). n^μ is an arbitrary gauge-fixing vector, so that $p \cdot n$ increases with the center-of-mass energy. The exponent S produces a k_T -smearing with a width that increases like the logarithm of s , as suggested by the analyses of [2].

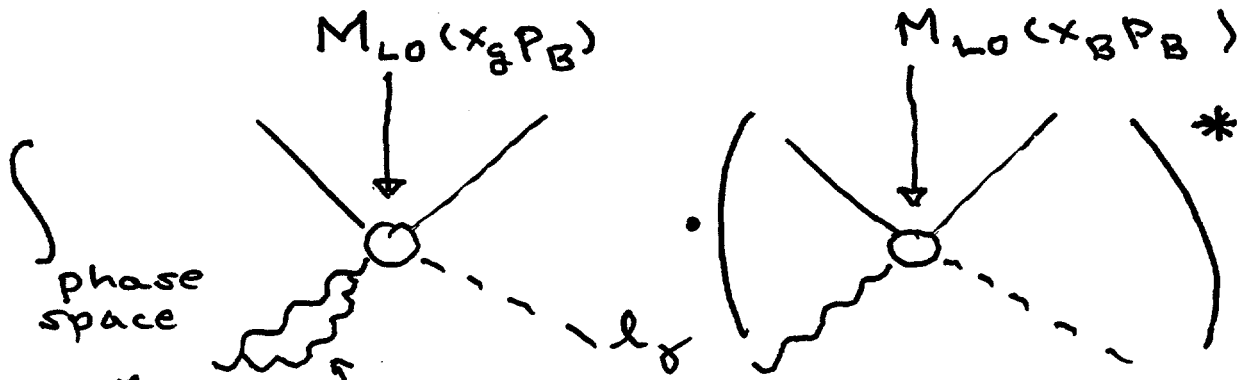
References

- [1] P. Aurenche *et al.*, Phys. Rev. D39, 3275 (1989).
- [2] J.F. Owens, Rev. Mod. Phys. 59, 465 (1987); J. Huston *et al.*, Phys. Rev. D51, 6139 (1995); H. Baer and M.H. Reno, Phys., Rev. D54, 2017 (1996); A.D. Martin *et al.*, hep-ph/9803445.
- [3] H.-L. Lai and H.-n. Li, hep-ph/9802414; E. Laenen, G. Oderda and G. Sterman, in preparation.
- [4] J.C. Collins and D.E. Soper, Nucl. Phys. B193, 381 (1981). J.C. Collins, D.E. Soper and G. Sterman, Nucl. Phys. B250, 199 (1985).

Can PT help account for these effects?
 Yes, take...

A closer look at higher orders:
 'hidden logs of k_T '

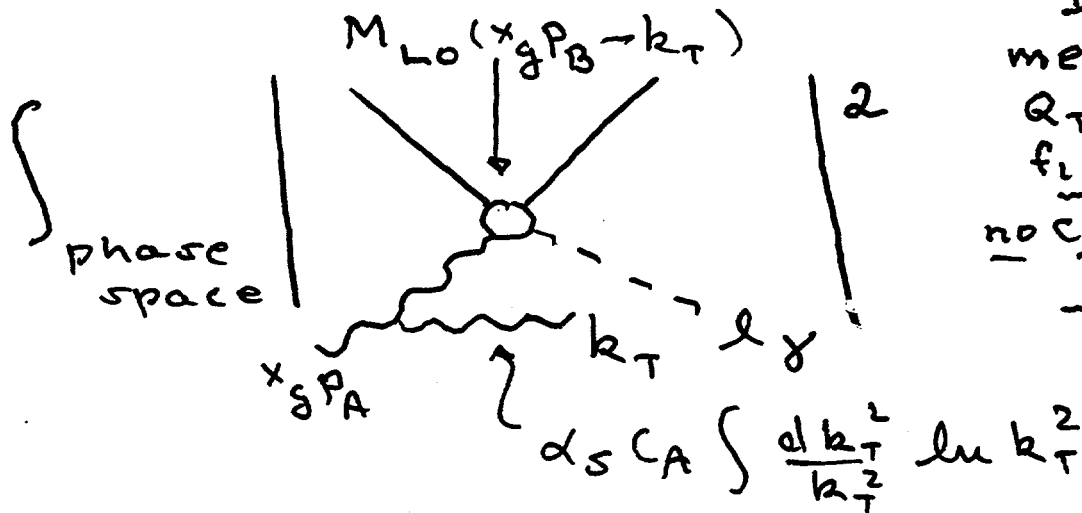
At NLO: soft glue in $\hat{\sigma}_{qg+\delta X}$



$C_A = N_C = 3$

$$- \alpha_s C_A \int \frac{dk_T'^2}{k_T'^2} \ln k_T'^2$$

soft



DY: if measure $Q_T = k_T \sim \dots$
 fixed, and
no cancellation
 $\rightarrow \frac{1}{k_T^2} \times \log s$

Sum:

$$- \alpha_s C_A |M_{LO}(x_g P_A)|^2 \int \frac{dk_T'^2}{k_T'^2} \ln k_T'^2$$

$$+ \alpha_s C_A \int \frac{dk_T^2}{k_T^2} \ln k_T^2 |M_{LO}(x_g P_A - k_T)|^2$$

cancellation of divergences at $k_T \rightarrow 0$

$k_T \rightarrow 0$ behavior approximately:

$$\alpha_S C_A \int dk_T^2 \ln k_T^2 \frac{\partial}{\partial k_T^2} |M_{LO}(x_S p_A - k_T)|^2$$

\uparrow finite integral $k_T^2 = 0$ \uparrow finite as $k_T \rightarrow 0$

- emission: redistribution of partonic 'beam'
- virtual correction: depletion of forward 'beam'
- unitarity: \rightarrow sum is finite
- in NLO: calculation the k_T^2 integral is done exactly
- beyond NLO: form of $k_T^2 \rightarrow 0$ behavior known to all orders

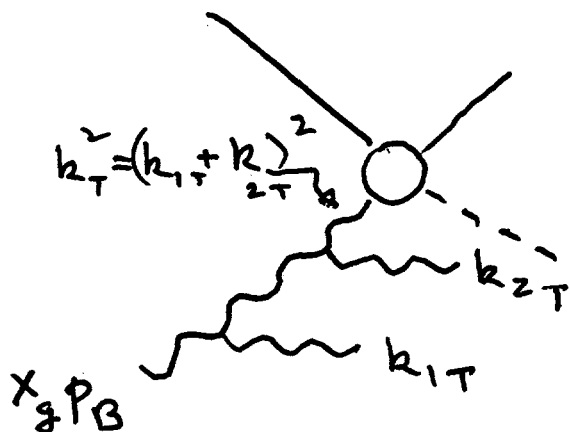
' k_T -resummation'

leading logs: $\alpha_S C_A \ln k_T^2$

$\rightarrow \alpha_S C_A \ln k_T^2 e$

$-\alpha_S C_A \frac{1}{2} \ln \frac{k_T^2}{Q^2}$
 \uparrow
 $Q \sim k_T$

Why exponentiation?



- $k_{1T} \ll k_{2T} \rightarrow$ second emission independent of first

- independence \rightarrow

$$(\text{change in}) |M|^2 \propto |M|^2$$

change with k_T scale
 $\sim d/d \ln k_T^2$

Effect of running coupling

$$\frac{1}{2} \alpha_s C_A \ln^2 k_T^2 / Q^2 \quad \begin{array}{c} \text{wavy line} \\ \text{---} k_T \end{array} \Rightarrow \int \alpha_s(k_T)$$

$$\rightarrow C_A \int_{k_T^2}^{\mu^2} \frac{d\mu^2}{\mu^2} \alpha_s(\mu^2) \ln \mu^2 / Q^2$$

in QCD: $\alpha_s(\mu^2)$ suppresses larger transverse momentum scales

K_T Resummation

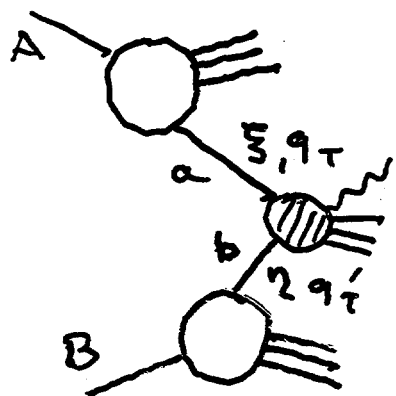
In NLO:

$$\int \frac{dk_T^2}{k_T^2} \rightarrow \ln(1-w) \quad \begin{array}{l} w \rightarrow 1 \\ \text{for exact} \\ qg \rightarrow qg \\ \text{elastic} \\ \text{scattering} \end{array}$$

It is possible to resum in k_T (organize all $\alpha_s^m \ln^m k_T^2$)

- higher order corrections to recoil of observed particle to soft radiation

Need alternative factorization



$\delta(\omega)$, for example
(but also $P_Q, P_{\bar{Q}}$)

$$\bar{E}_L \frac{d^3 \sigma_{AB}}{d^3 \ell} = \frac{1}{S^2} \sum_{ab} \int d\xi d\eta d^2 q d^2 q'$$

$$\cdot P_{a/A}(\xi, q_T) P_{b/B}(\eta, q_T')$$

$$\cdot \Omega_{ab} \left(\frac{s'}{\mu^2}, \frac{t'}{\mu^2}, \frac{u'}{\mu^2}, \alpha_s(\mu^2) \right)$$

s', t', u' : full on-shell kinematics with q_T, q_T'

E. Laenen, G. Odenda, J. Li, Lai

$$\Omega_{ab} = \frac{s^2}{2s'} |M_{\text{Born}}(s', t', u')|^2 (\delta(s'+t'+u') + \delta(\alpha_s))$$

$$x = \frac{1}{y_{s+T}} [y(-u) - 2(q+q') \cdot l_T + \dots]$$

hadronic

\mathcal{P} 's include evolution (Collins - Soper 81)

$$\mathcal{P}(x, q) = \int d\lambda \phi(\lambda, \mu^2)$$

$$\cdot \int d^2b e^{-iq \cdot b} C(\frac{v}{x}, b, \mu)$$

$$\cdot \exp[-S(b, Q)]$$

• expand S in α_s , do b integral
 → recover normal factorization order-by-order, or:

• possibility of incorporating NP q_T via Collins-Soper exponent (NP B193, 381 (1980))

$$S(b) \approx - \int_{c_1 b / \sqrt{(1+b^2/b_0^2)}}^{c_2 M} \frac{d\bar{\mu}}{\bar{\mu}} \left[\ln \frac{c_2 M^2}{\bar{\mu}^2} A(\alpha_s(\bar{\mu})) \right]$$

$$+ B(\alpha_s(\mu)) + b^2 (\ln Q) F(b) + b^2 F_1(b, x)$$

underlines
 match resummed series with power connection

Schematic results:

$S(b, Q) =$ perturbation theory (PT)
+ non-perturbative (NP)

PT: sums $\ln^2 k_T^2 / Q^2$
cutoff in IR (b_0 above)
'parton shower'

NP: induced by PT
also b_0 -dependent

Gaussian smearing!

$$e^{-b^2 \ln Q F_2 + b^2 F_1}$$

$$\rightarrow e^{-q_T^2 / 4 (F_2 \ln Q + F_1)}$$

Fourier transform

Q-dependent width

$$\langle q_T^2 \rangle \sim F_2 \ln Q + F_1 + \text{corrections}$$

Full result: convolution of resummed PT, NP with LO + modified NLO + ...

Gaussian, dominates at low E and grows with PT

On possibility to determine sign of ΔG from asymmetry of jet production in polarised pp collisions at RHIC

G.P.Škoro¹, M.V.Tokarev²

¹*Institute of Nuclear Sciences "Vinča", Belgrade, Yugoslavia*

²*Joint Institute for Nuclear Research, Dubna, Russia*

Abstract

The jet production in \bar{p} - \bar{p} collisions at high energies is studied. Double-spin asymmetry A_{LL} of the process is calculated by using Monte Carlo code SPHINX. A possibility to discriminate the spin-dependent gluon distributions and to determine sign of ΔG is discussed. The predictions for the longitudinal asymmetry A_{LL} of the jet and dijet production in the \bar{p} - \bar{p} collisions at RHIC energies have been made.

1 – Introduction

Both spin-dependent and spin-independent parton distributions in the nucleon are of universal nature, hence the direct measure of them is one of the actual problem of the high energy spin physics. Deep inelastic lepton-nucleon scattering allows us to obtain information on quark distributions but such information is not sufficient to resolve 'spin crisis' (see [1] and references therein). It is necessary to know a gluon contribution to proton spin. Therefore future research programs at the RHIC [2], HERA [3] and LHC (see [4] and references therein) colliders plan to perform experiments with polarized proton beams to study the spin-dependent gluon-distributions $\Delta G(x, Q^2)$.

In the framework of the parton model the basic subprocesses for jet production in the pp collision are $qq \rightarrow qq$, $qg \rightarrow qg$, $gg \rightarrow gg$. Their contributions to asymmetry A_{LL} depend on a chosen kinematical region. Therefore the main question is to find the kinematical region more suitable for measuring of $\Delta G(x, Q^2)$. For the direct photon production a main subprocess is the Compton $qg \rightarrow \gamma q$ scattering.

Up to now, there exists neither a running experiment to directly measure the polarized gluon distribution nor does the variety of indirect analyses give a unique result. Hence there is no completely convincing argument on the shape and sign of $\Delta G(x, Q^2)$ yet, although a recent NLO analysis [5] clearly favors a positive sign. However, recent calculations in the context of a non-relativistic quark model and the bag model, respectively, [6] indicate that the integral over $\Delta G(x, Q^2)$ might be negative too. Both positive and negative values of the sign of $\Delta G(x, Q^2)$ over a wide kinematical range $10^{-3} < x < 1$ were considered in [7]. The possibility to draw conclusions on the sign of the spin-dependent gluon distribution, $\Delta G(x, Q^2)$, from existing polarized DIS data have been studied in [8]. The result of the DIS data analysis [8] on g_1^p strongly supports the conclusion that the sign of $\Delta G(x, Q^2)$ should be positive. Nevertheless the additional confirmations on sign of ΔG are required and the experiments for direct measuring of the $\Delta G/G$ are necessary.

The aim of the present paper is to study the dependence of asymmetry of jet and dijet production in \bar{p} - \bar{p} collisions on different gluon distributions ΔG , and especially as a function of sign of ΔG , and made predictions of A_{LL} for the future experiment planed at RHIC [9].

¹goran@rudjer.ff.bg.ac.yu

²tokarev@sunhe.jinr.ru

2 – Spin-Dependent Gluon Distribution

The 3 sets of spin-dependent parton distributions [7] and [10] are used to calculate the jet asymmetry A_{LL} . First set is based on work of Altarelli and Stirling [10] and include a scenario with large gluon polarization ΔG . Second and third ones have been obtained by the phenomenological method [7] including some constraints on the signs of valence and sea quark distributions, taking into account the axial gluon anomaly and utilizes results on integral quark contributions to the nucleon spin. Based on the analysis of experimental data on deep inelastic data on structure function g_1 the parametrization of spin-dependent parton distributions for both positive and negative sign of ΔG have been constructed. We would like to note the both sets of distributions describe experimental data very well. We shall denote $\Delta G^{>0}$ and $\Delta G^{<0}$ sets of spin-dependent parton distributions obtained in [7] with positive and negative sign of ΔG , respectively. It was shown in [11] that phenomenological method reproduces the main features of the NLO QCD Q^2 -evolution of proton, deuteron and neutron structure function g_1 . Therefore the constructed spin-dependent quark and gluon distributions can be reasonably used to study a asymmetry of jet production in $\vec{p} - \vec{p}$ collisions too.

F We would like to note that integral contributions of gluons to the proton's spin is practically the same in all the parameterizations ($\Delta g \simeq 2$) so the difference in asymmetry should reflect the difference in shape of distributions (and sign of ΔG) used.

3 – Asymmetry of Jet Production

The cross-section for jet production in polarized $p - p$ collisions is given by a convolution of the partonic cross-section and the polarized parton distributions, summed over all partonic subprocesses contributing to the reaction $p+p \rightarrow jet + X$. Then, the double spin asymmetry is defined through the difference of cross-sections (numbers of jets) for antiparallel ($\uparrow\downarrow$) and parallel ($\uparrow\uparrow$) spins of colliding protons:

$$A_{LL} = \frac{\sigma^{\uparrow\downarrow} - \sigma^{\uparrow\uparrow}}{\sigma^{\uparrow\downarrow} + \sigma^{\uparrow\uparrow}} = \frac{N_{jet}^{\uparrow\downarrow} - N_{jet}^{\uparrow\uparrow}}{N_{jet}^{\uparrow\downarrow} + N_{jet}^{\uparrow\uparrow}}, \quad (1)$$

with the error:

$$\delta A_{LL} \simeq \frac{1}{\sqrt{N_{jet}^{\uparrow\downarrow} + N_{jet}^{\uparrow\uparrow}}}. \quad (2)$$

For detailed study of jets and dijets asymmetry at STAR we have used the Monte Carlo code SPHINX [12] which is 'polarized' version of PYTHIA [13].

Jet reconstruction was done by the JETSET-subroutine LUCCELL [13]. This routine defines jets in the two-dimensional (η, ϕ) -plane, η being pseudorapidity and ϕ the azimuthal angle. STAR detector covers full space in azimuth and pseudorapity region $-1 < \eta < 2$. In order to have segmentation expected at STAR ($\Delta\eta \times \Delta\phi = 0.1 \times 0.1$) we used 30 η -bins and 60 ϕ -bins in our calculation procedure. The values of LUCCELL-subroutine parameters E_{\perp}^{cell} and $R = \sqrt{\Delta\eta^2 + \Delta\phi^2}$ were $E_{\perp}^{cell} = 1.5 \text{ GeV}$ and $R = 0.7$.

The expected resolution of the STAR Electromagnetic Calorimeter, $\Delta E/E \simeq 0.16/\sqrt{E}$, was also taken into account. To obtain total rates ($Rate = \sigma \cdot \mathcal{L}$) of jets and dijets at STAR we taken into account designed luminosity at RHIC, $\mathcal{L} = 8 \times 10^{31} \text{ cm}^{-2} \text{ s}^{-1}$ at $\sqrt{s} = 200 \text{ GeV}$ ($\mathcal{L} = 2 \times 10^{32} \text{ cm}^{-2} \text{ s}^{-1}$

at $\sqrt{s} = 500 \text{ GeV}$) and effective run time of 100 days with 50% efficiency. The polarization of both beams was fixed at the value $P = 0.7$.

4 – Results of Monte Carlo simulations

Figure 3 shows the dependence of A_{LL} on the jet transverse energy E_T at $\sqrt{s} = 200 \text{ GeV}$. Points (open and black boxes) are simulation results with spin-dependent PDF [10] and $\Delta G^{>0}$ [7]. Errors on the figure are statistical only. One can see from Fig.3 that the absolute value of A_{LL} for both set of PDF is less than 5% at $E_T < 35 \text{ GeV}$. At higher transverse energy $E_T > 35 \text{ GeV}$ the asymmetry calculated with PDF $\Delta G^{>0}$ increases with E_T .

Dijet production in $p - p$ collisions allows to study so-called 'back-to-back' jets and to extract more correctly information on the dominant parton subprocess. In our simulations, the dijets were considered to be found if back-to-back deviations for the two jets don't exceed 30° . The error of the efficiency of the jet finder is estimated [14] to be at the level of 10 % for $E_T \simeq 30 \text{ GeV}$.

Figure 4 demonstrates the dependence of the asymmetry A_{LL} of dijet production in the $\vec{p} - \vec{p}$ collisions on the dijet transverse energy E_T at $\sqrt{s} = 200 \text{ GeV}$. The pseudorapidity range of jet production covers $-1 < \eta < 2$. Points (open and black boxes) are simulation results with spin-dependent PDF [10] and $\Delta G^{>0}$ [7]. Errors on the figure are statistical only. One can see from Fig.4 that the absolute value of A_{LL} for PDF[10] is practically constant ($\simeq (4 - 5)\%$) up to $E_T = 60 \text{ GeV}$. At higher transverse energy range $E_T > 60 \text{ GeV}$ the asymmetry decreases with E_T . The asymmetry calculated with PDF $\Delta G^{>0}$ [7] is small ($< 2\%$) at $E_T < 60 \text{ GeV}$ and increases up to (15-20)% at $E_T > 90 \text{ GeV}$.

We can consider 3 characteristic regions on both the Figures 3 and 4. In the low E_T region ($E_T < 20 \text{ GeV}$ for jets and $E_T < 50 \text{ GeV}$ for dijets) the value of the asymmetry A_{LL}^{Al-Si} obtained with parametrization [10] is larger than the asymmetry A_{LL}^{Tok} obtained with parametrization $\Delta G^{>0}$ [7]. The contribution of $g - g$ scattering for A_{LL}^{Al-Si} is 3 times higher than for A_{LL}^{Tok} . One can see from the Fig.1a that the ratio $\Delta G/G$ calculated with PDF [10] is larger than $\Delta G/G$ calculated with PDF $\Delta G^{>0}$ [7] at low x , so the behaviour of the asymmetry A_{LL} is reasonable. Moreover, it seems that this difference can be separated experimentally. On the basis of the obtained results we can conclude that, the information about ΔG could be extracted from (relatively) low E_T asymmetry values.

In the intermediate E_T region ($20 < E_T < 40 \text{ GeV}$ for jets and $50 < E_T < 70 \text{ GeV}$ for dijets) the asymmetry A_{LL}^{Al-Si} decreases and the asymmetry A_{LL}^{Tok} increases. The main contribution comes from $q - g$ scattering and $A_{LL} \sim \Delta G/G \cdot \Delta q/q \cdot a_{LL}$. So the difference of the Δq parametrizations $\Delta G^{>0}$ [7] and [10] becomes equally important as ΔG . This region gives us mixed information about ratio $\Delta G/G \cdot \Delta q/q$. The ratio $\Delta G/G$ for parametrization [10] decreases with x at $x > 0.2$ which results in the decreasing of asymmetry value A_{LL} . The asymmetry A_{LL}^{Tok} increases with E_T . The behaviour of A_{LL}^{Tok} is due to the growth of the ratio $\Delta G/G$ with x .

In the high E_T region ($E_T > 40 \text{ GeV}$ for jets and $E_T > 70 \text{ GeV}$ for dijets) the asymmetry $A_{LL}^{Al-Si} \simeq 0$ and A_{LL}^{Tok} increases with E_T and reaches (15-20)% for jet and dijets production at $E_T > 50$ and $E_T > 90 \text{ GeV}$, respectively. The main contribution comes in both cases $\Delta G^{>0}$ [7] and [10]) from $q - q$ scattering, so the resulting asymmetries reflect the difference between the Δq quark distributions. This region is very interesting because of possibility for checking the universality of factorization of spin-dependent PDF which are extracted from the results of DIS experiments.

Figure 5 shows the dependence of A_{LL} on the jet transverse energy E_T at $\sqrt{s} = 200 \text{ GeV}$ but for spin-dependent PDF with different sign of gluon distributions, $\Delta G^{>0}$ and $\Delta G^{<0}$ [7]. The asymmetry

calculated with PDF $\Delta G^{>0}$ increases with E_T , while the asymmetry calculated with PDF $\Delta G^{<0}$ is practically equal to zero in the whole region.

Figure 6 shows the dependence of the asymmetry A_{LL} of dijet production in the $\vec{p} - \vec{p}$ collisions on the dijet transverse energy E_T at $\sqrt{s} = 200 \text{ GeV}$ for the same combination of spin-dependent PDF's ($\Delta G^{>0}$ and $\Delta G^{<0}$ [7]).

On the basis of these results we can conclude that, the measurements of the jet and dijets asymmetry at $\sqrt{s} = 200 \text{ GeV}$ can give us information about the sign of ΔG .

5 – Conclusions

The asymmetry of jet and dijets production A_{LL} in $\vec{p} - \vec{p}$ collisions at RHIC energies was studied. The observable is expressed in the parton model via the $q-q$, $q-g$ and $g-g$ cross sections for different helicity and spin-dependent parton Δq and gluon ΔG distributions. The Monte Carlo simulation of A_{LL} taking into account parameters of the STAR EMC detector was made. Dependence of A_{LL} on jet transverse energy E_T for different parametrization of ΔG was studied. It was found that the value of A_{LL} is less than 5% at $E_T < 30 \text{ GeV}$ and $E_T < 50 \text{ GeV}$ for jet and dijets production, respectively. The asymmetry A_{LL} is sensitive for ΔG at lower E_T values and can give us information about the sign and shape of the $\Delta G(x, Q^2)$. At higher E_T range the asymmetry is sensitive for Δq and reaches (15-20)% for the jet and the dijets production at $E_T > 50$ and $E_T > 90 \text{ GeV}$, respectively. The obtained results can be verified in future experiments with polarized protons planed at RHIC.

References

- [1] M.Anselmino, A.Efremov, E.Leader, Phys.Rep. **261** (1995) 1.
- [2] RSC Collaboration, Proposal on Spin Physics using the RHIC Polarized Collider, August 1992.
- [3] Proceedings of the Workshop "Prospects of SPIN PHYSICS at HERA", DESY-Zeuthen, Germany, 28-31 August, 1995, DESY95-200, ed. by J.Blumlein, W.-D.Nowak
- [4] A. Penzo et al., Proc. VI Workshop on High Energy Spin Physics, p.238, Protvino, 1996.
- [5] R.D.Ball, S.Forte, G.Ridolfi, Preprint CERN-TH/95-266, 1995.
- [6] R.L.Jaffe, Phys. Lett. **B365** (1996) 359.
- [7] M.V.Tokarev, Preprint JINR, E2-96-304, Dubna, 1996.
- [8] W.-D.Nowak, A.V.Sidorov, M.V.Tokarev, Nuov. Cim. **A110** (1997) 757.
- [9] G.Bunce et al., Particle World, vol.3, (1992) p.1.
- [10] G.Altarelli, W. J.Stirling, Particle World, vol.1, (1989) p.40.
- [11] W.-D.Nowak, A.V.Sidorov, M.V.Tokarev, In: Proc. Int. Workshop SPIN'97, July 7-12, 1997, Dubna.
- [12] St.Gullenstern et al., Nucl. Phys. **A560** (1993) 494.
- [13] T.Sjostrand, Computer Physics Commun. **82** (1994) 74.
- [14] B.Christie, K.Shestermanov, STAR Note 196.

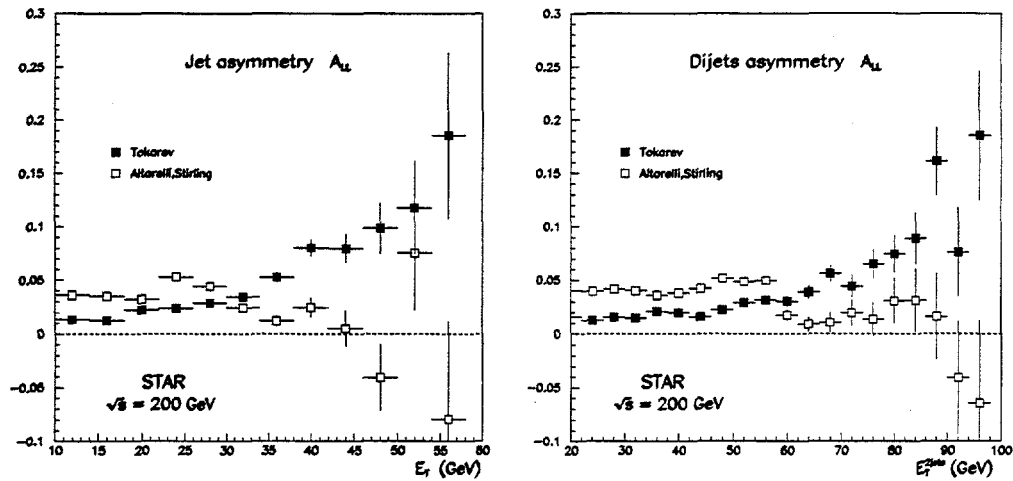


Figure 1.

Asymmetry of jet and dijet production A_{LL} in polarised pp collisions at $\sqrt{s} = 200$ GeV for two different sets of spin-dependent PDFs ($\Delta G^{>0}$ [7] and [10]) as a function of jet transverse energy E_T . The errors indicated are statistical only, based on the expected luminosity of RHIC and the properties of the STAR detector.

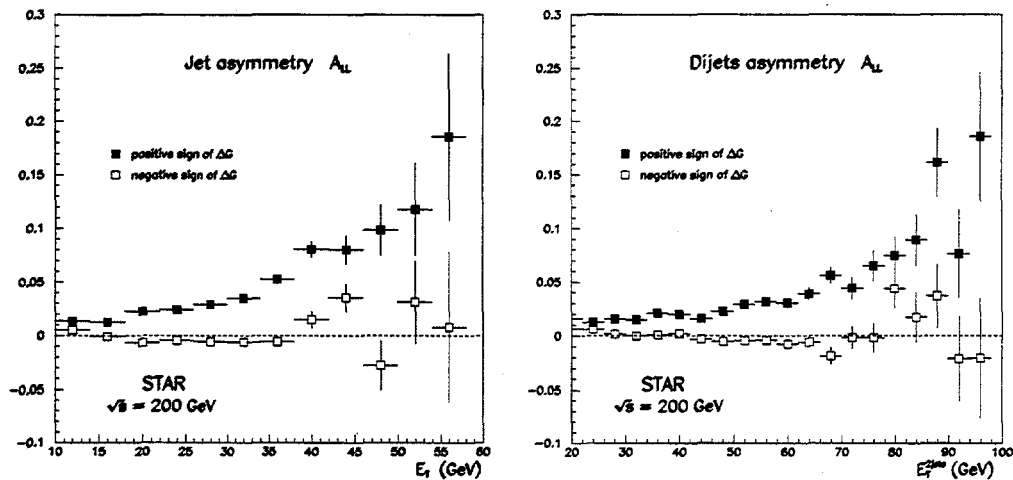


Figure 2.

Asymmetry of jet and dijet production A_{LL} in polarised pp collisions at $\sqrt{s} = 200$ GeV for two different sets of spin-dependent PDFs ($\Delta G^{>0}$ [7] and $\Delta G^{<0}$ [7]) as a function of jet transverse energy E_T . The errors indicated are statistical only, based on the expected luminosity of RHIC and the properties of the STAR detector.

Experimental Informations on the Gluon Polarization from Deep Inelastic Scattering

T.-A. Shibata ¹

Tokyo Institute of Technology / RIKEN

Deep inelastic scattering of charged leptons is an effective and well defined method to study the parton structure of the nucleon. Longitudinally polarized lepton beam and targets enable us to measure the spin dependent structure function $g_1(x)$. The EMC result in 1987 showed that only a small fraction of the nucleon spin is carried by the quarks, contrary to the expectation. The analyses showed that up quark is polarized in the same direction with the proton spin while down quark is oppositely polarized. Furthermore, strange quark is also polarized in the direction opposite to the proton spin. This result attracted much attentions and new several experiments were carried out to further study this problem with the proton and neutron targets.

In this talk two topics concerning the gluon polarization are presented. The first one is the polarized gluon distribution function derived by the $g_1(x)$ analysis with DGLAP Q^2 evolution equation. A few groups have studied the polarized parton distribution functions $\Delta u(x)$, $\Delta d(x)$, $\Delta G(x)$ etc. with this method. In view of recently increased data set and to investigate the problems in a systematic way in terms of choice of R-parameter etc., we have set up a program of the DGLAP Q^2 evolution and function parameterization. The result is that the integral of the polarized gluon distribution function $\Delta G(x)$ is positive. However, the size of the error is large.

The second topic is the measurement of $\Delta G(x)$ with charm productions in deep inelastic scattering. The charm production in the deep inelastic scattering goes through the photon-gluon fusion process where a gluon is dissociated to charm and anticharm, and one of them absorbs the virtual photon emitted by the lepton. The open charm, namely D^0 production and decay in the $K\pi$ channel is the cleanest signal. The excited states of D^0 can also be used. Other possibility is a bound charm system J/ψ . J/ψ production is dominated with the color singlet mechanism at small z where z is the energy carried by the hadron divided by the energy of the virtual photon. The asymmetry in J/ψ production at small z can be related to the gluon polarization. On the other hand, at high z , J/ψ production contains the color octet mechanism in which the relation with the gluon polarization is theoretically unclear. HERMES at DESY-HERA and COMPASS at CERN, among other planned experiments, are scheduled to take data of charm productions in the next years.

¹shibata@nucl.phys.titech.ac.jp

Polarized Parton Distribution Function

Working Group at RIKEN

Y. Goto, N. Hayashi, H. Horikawa, M. Hirai,
S. Miyama, T. Morii, S. Kumano,
N. Saito, T.-A. Shibata, E. Taniguchi

RIKEN, Kobe U, Saga U, TITech

Experimental Data Set



$\Delta U_V(x, Q^2)$, $\Delta d_V(x, Q^2)$, $\Delta S(x, Q^2)$
 $\Delta G(x, Q^2)$

(electron)
muon) - nucleon deep inelastic scattering

$$A^{\gamma N} = \frac{\sigma^{\uparrow} - \sigma^{\downarrow}}{\sigma^{\uparrow} + \sigma^{\downarrow}} \propto \frac{g_1(x)}{F_1(x)}$$

$$\begin{aligned} g_1(x) &= \frac{1}{2} \sum_i e_i^2 (q_i^{\uparrow}(x) - q_i^{\downarrow}(x)) \\ &= \frac{1}{2} \left[\frac{4}{9} (u^{\uparrow}(x) - u^{\downarrow}(x)) + \frac{1}{9} (d^{\uparrow}(x) - d^{\downarrow}(x)) \right. \\ &\quad \left. + \frac{1}{9} (s^{\uparrow}(x) - s^{\downarrow}(x)) \right] \quad ; \text{proton} \end{aligned}$$

$$\int_0^1 g_1(x) dx = \frac{1}{2} \left(\frac{4}{9} \Delta u + \frac{1}{9} \Delta d + \frac{1}{9} \Delta s \right)$$

$$\Delta u \equiv \int_0^1 dx (u^{\uparrow}(x) - u^{\downarrow}(x))$$

$$= \frac{1}{12} \left[(\Delta u - \Delta d) + \frac{1}{3} (\Delta u + \Delta d - 2\Delta s) \right]$$

neutron
β-decay

hyperon
decay

$$+ \frac{4}{3} (\Delta u + \Delta d + \Delta s) \Big]$$

$$\langle S_3 \rangle = \frac{1}{2} (\Delta u + \Delta d + \Delta s)$$

$$\Delta U_v(x, Q_0^2) = \eta_u A_u x^{\alpha_u} (1 + \gamma_u x^{\lambda_u}) U_v(x, Q_0^2)$$

$$\Delta d_v(x, Q_0^2) =$$

$$\Delta \bar{q}(x, Q_0^2) =$$

$$\Delta q(x, Q_0^2) =$$

16 parameters - 2

$$\eta_u = 0.918$$

$$\eta_d = -0.339$$

DGLAP Evolution Equation couples

Quarks and Gluon Distribution Functions

$$\eta_{\bar{q}} = -0.081 \pm 0.003$$

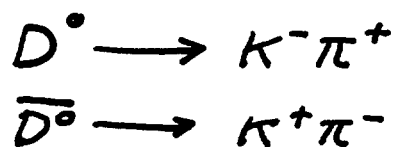
$$\eta_g = 2.00 \pm 1.01$$

from LO

Integral

NLO program is ready

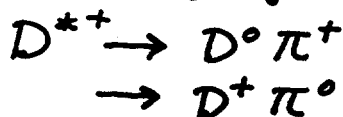
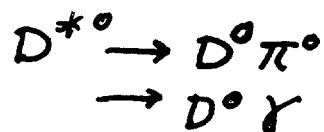
Open Charm



2 body decay, all charged
 π^\pm, K^\pm identification



semi leptonic decay
 $X = \nu + \dots$ μ identification



γ detection

Bound $c\bar{c}$

J/ψ

low z

color singlet model

$$0 < z = \frac{E_{J/\psi}}{\nu} < 1$$

$$\propto \frac{\sigma_Q(x)}{Q(x)}$$

high z

color octet model

theoretically uncertain

Conclusions

- Gluon Polarization Measurements with D.I.S. were presented.
- Efforts are being made in order to have a combined view of the spin-dependent Quark and Gluon distribution functions
- Analyses of g_2 data with DGLAP evolution equation provide a positive integral $\int_0^1 \Delta G(x) dx$ though the error is large
- Open Charm and J/ψ productions are access to Gluon polarization.
HERMES and COMPASS plan to measure.
Theoretical clarifications are needed.

Dennis SIVERS

Portland Physics Institute

BREMSSTRAHLUNG MODEL FOR GLUON POLARIZATION

There are several "models" for the spin-weighted gluon density, $\Delta G(x,t)$. However, it is worthwhile to present here another approach to modelling this distribution because the arguments involved are instructive on a couple of levels. This dynamic approach takes seriously the results of the nonrelativistic quark model for the hadronic spectrum and addresses the question of how these results constrain parton spin densities at low values of Q^2 . It also explicitly embodies the constituent-counting rule predictions at large x .

The model is defined by taking as input the Q^2 stability of the gluon polarization asymmetry,

$$\partial \Delta t (A^\circ(x,t)) = 0 \quad \text{where} \quad A(x,t) = \Delta G(x,t)/G(x,t)$$

and assuming that this stability holds in a region where the Altarelli-Parisi evolution equations are valid. The shape of the Q^2 independent asymmetry, $A^\circ(x)$, is determined by the "measured" distributions, $q(x,t)$, $\Delta q(x,t)$ and $G(x,t)$.

$$A^\circ(x) = \frac{\Delta P_{qg} \otimes \Delta q + \Delta P_{gg} \otimes (A^\circ(x) \cdot G)}{P_{qg} \otimes q + P_{gg} \otimes G}$$

We call this a Bremsstrahlung model because, at large x , it is equivalent to the assumption that intrinsic gluonic degrees of freedom are absent so that gluons are "radiated" from valence quarks. It extends the Close-Sivers perturbative Bremsstrahlung model to other values of x with a minimum of additional dynamical assumptions. The model can be solved recursively by Newton's method

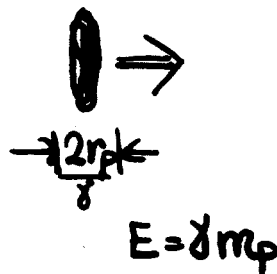
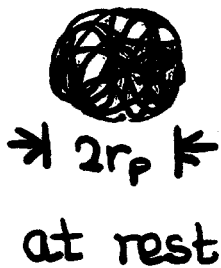
$$A_1^\circ(x) = \frac{\Delta P_{qg} \otimes \Delta q}{P_{qg} \otimes q} \quad A_n^\circ(x) = \frac{\Delta P_{qg} \otimes \Delta q + (A_{n-1}^\circ \cdot G) \otimes P_{gg}}{P_{qg} \otimes q + P_{gg} \otimes G}$$

At low x where gluon densities dominate the requirement of Q^2 independence for the asymmetry corresponds to self-similarity of the fractal structure of the branching in terms of spin content. It therefore provides a "natural" extrapolation to small x .

Partons Revisited

Proton structure

Picture of proton at rest clouded
by relativistic motion of constituents



transverse
motion of
constituents
"slowed" by
Lorentz contraction

Partons

If we want to take a ~~snapshot~~
of the proton it helps to look in
infinite momentum frame

This is the start of the parton
model

II. The non-relativistic quark model

By any objective measure, one of the most successful approaches to hadron spin structure (H. Lipkin + ... N. Isgur)

The spin & flavor degrees of freedom of low-lying hadrons are well-described by the restricted basis

$Q_i \bar{Q}_j$ mesons

$Q_i Q_j Q_k$ baryons

P. Geiger & N. Isgur (PR D55, 299, 1977)

"The first major degree-of-freedom problem is the absence of any sign of gluon degrees of freedom in the low-lying spectrum"

III. Brems. Model & Condition

$$\frac{\partial}{\partial \ln(Q^2)} [\Delta G/G] = 0$$

The approximate stability of the quark asymmetry

$$A_q = \Delta q/q$$

with Q^2 variation and the absence of any gluon structure in spectrum suggests that

$$\frac{\partial}{\partial \ln(Q^2)} [\Delta G/G] = \frac{G \Delta G' - \Delta G G'}{G^2} = 0$$

$$G \{ \Delta G' - \alpha_G G' \} = 0 \quad \text{Spin Stability}$$

$$\alpha_G = \frac{\Delta G'}{G'}$$

DGLAP evolution equations

$$\Delta_G^o(x) = \frac{\Delta P_{Gq} \otimes \Delta q + \Delta P_{GG} \otimes (\alpha_G \cdot G)}{P_{Gq} \otimes q + P_{GG} \otimes G}$$

this nonlinear equation can be solved for $Q_G^0(x)$ given parameterization of

$$q(x, Q^2) = u(x, Q^2) + d(x, Q^2) + s(x, Q^2)$$

$$\Delta q(x, Q^2) = \Delta u(x, Q^2) + \Delta d(x, Q^2) + \Delta s(x, Q^2)$$

$$G(x, Q^2)$$

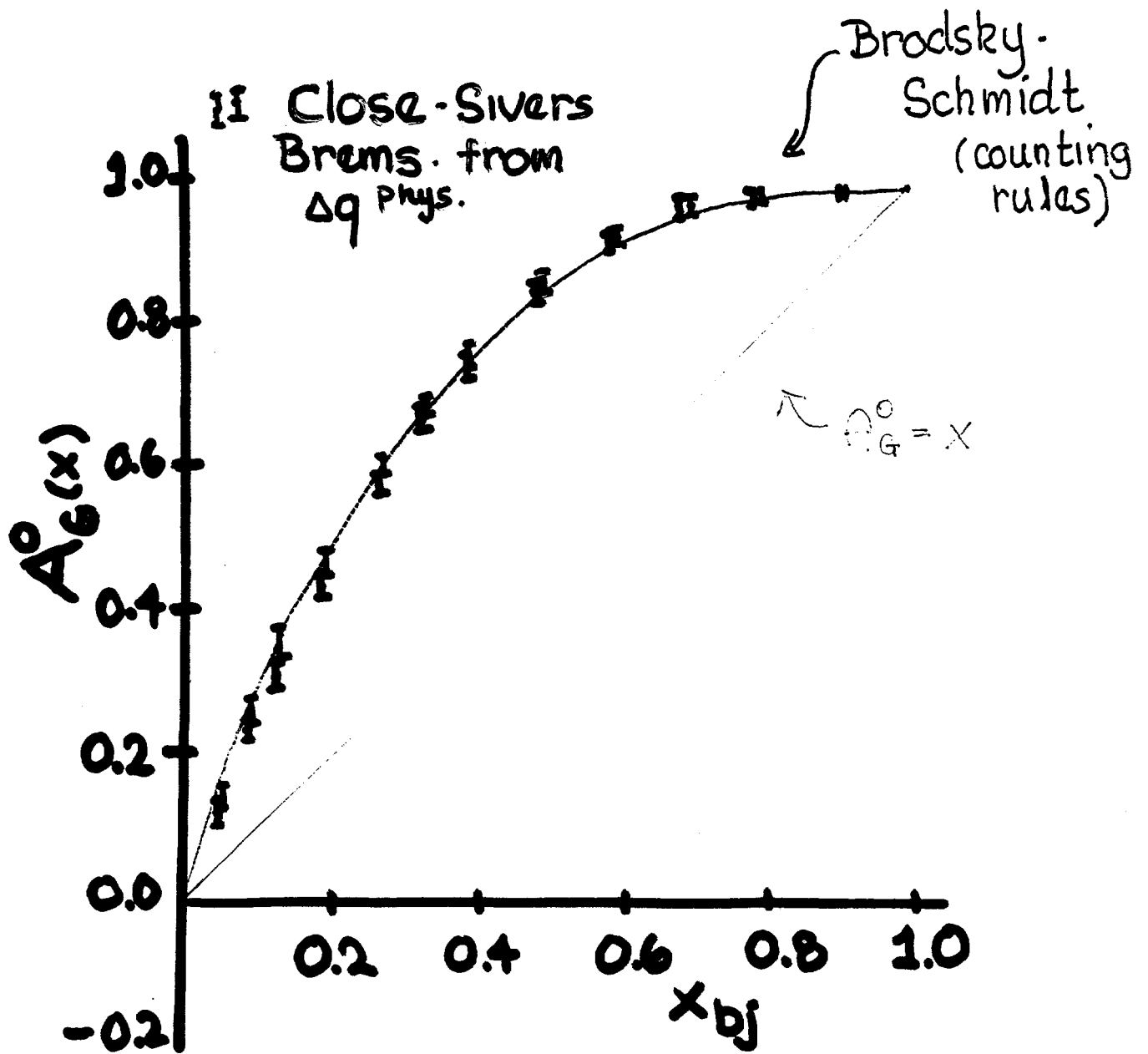
$$Q^{0(n)}(x) = \frac{\Delta P_{Gq} \otimes \Delta q}{P_{Gq} \otimes q}$$

$$Q^{0(n)}(x) = \frac{\Delta P_{Gq} \otimes \Delta q + \Delta P_{Gf} \otimes (Q^{0(n-1)} G)}{P_{Gq} \otimes q + P_{Gf} \otimes G}$$

newton's meth.

convolution

$$C(x) = A \otimes B = \int_x' dy A(y) B(x/y)$$



for the quark parameterizations
studied so far

$$A_G(x, Q^2=2) \stackrel{\text{Close-Sivers}}{\cong} \stackrel{\text{Brodsky-Schmidt}}{A_G(x)}$$

$x \geq 0.1$

bremg

intrinsic

The low- Q^2 asymmetry insensitive to
the relative amounts of intrinsic vs. radiated
gluons for $x \geq 0.1$

The difference between our model &
Brodsky Schmidt parameterization comparable
to experimental errors on planned experiments

$$\Delta G/G \approx .05 \quad \text{"future" plans}$$

This is still incomplete since integrals
have only been done with "leading-order"
 $\Delta P, P \dots$ & no attention paid to quark factorization
prescription & NLC parameterizations

$$\langle \Delta G \rangle / Q^2 \approx 0.8 \pm 0.2$$

How to Extract the Gluon Polarization using RHIC Probes: a Critical Analysis.

Jacques SOFFER¹

Centre de Physique Théorique
CNRS Luminy Case 907
13288 Marseille Cedex 09 France

The total amount of the proton spin carried by gluons is of crucial importance to achieve a precise understanding of the proton structure. This contribution is given by the first moment of the polarized gluon distribution $\Delta G(x, Q^2)$, which is presently, very poorly known. This is due to the fact that Deep-Inelastic Scattering (DIS) experiments do not allow a direct determination of the gluon properties, because of the absence of photon-gluon coupling. Moreover, unlike unpolarized DIS at HERA, polarized DIS experiments, so far, have given access to a rather limited Q^2 range. As a consequence, the numerous next-to-leading order (NLO) analysis of the data, on the spin-dependent structure function $g_1(x, Q^2)$, leave $\Delta G(x, Q^2)$ largely unconstrained.

It is the purpose of this talk to show that polarized proton-proton collisions at RHIC-BNL offer several new options, which will yield the gluon polarization in a rather broad kinematic domain, in particular with very large Q^2 values. The spin observable we will mainly consider is the double helicity asymmetry A_{LL} , corresponding to the case where the two initial protons are longitudinally polarized, for single or double inclusive reactions. Considerations will be given to the energy dependence of A_{LL} , as well as its p_T and rapidity behaviours. We will examine in turn, the different probes which have been proposed in the literature namely, direct photon production, single-jet and dijet productions, charmonium and heavy quark productions. We will discuss in some cases the effects of NLO corrections and more generally the theoretical uncertainties related to the choice of the set of polarized parton distributions. In the case of double inclusive production (i.e. direct photon + jet or dijet), since A_{LL} is directly proportional to $\Delta G(x, Q^2)$, it is easier to extract it from the data and one can also study rapidity correlations. For charmonium and heavy quark productions, the dynamical mechanism is still subject to discussions and the NLO corrections remain to be completed, so the predictions appear to be less reliable. Finally, one should also keep in mind that in single particle inclusive production (i.e. π or Λ), since the subprocess gluon-quark is important, these reactions might also be excellent and simple probes for the determination of the gluon polarization.

¹E-MAIL: SOFFER@CPT.UNIV-MRS.FR

event rates for
 $(\Delta\eta=3 \quad \Delta E_T^\gamma=5 \text{ GeV}) \quad \sqrt{s} = 500 \text{ GeV}$

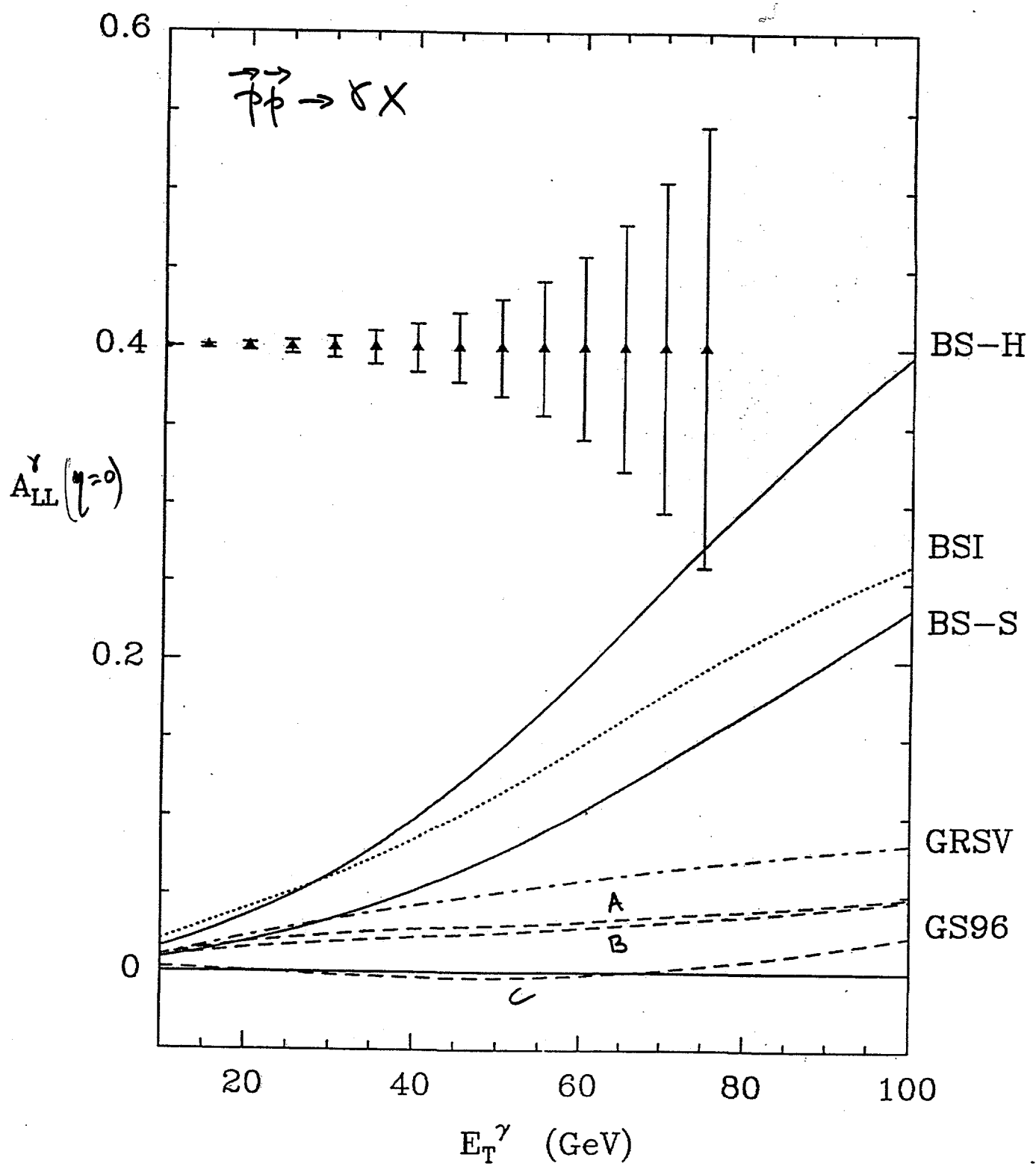


Fig 1

J.M. VIREY, J.S.
 NP B.509 297 (1998)

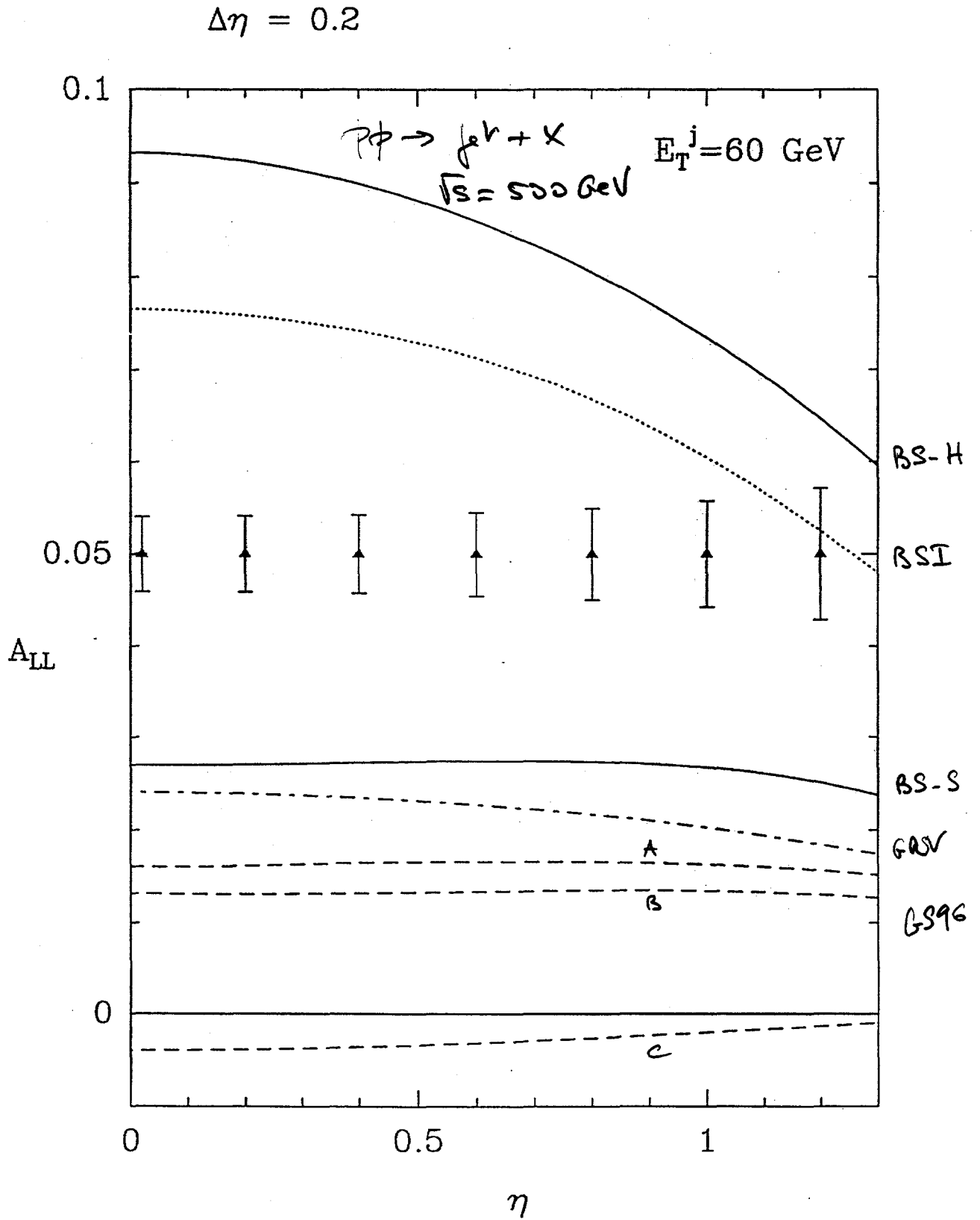
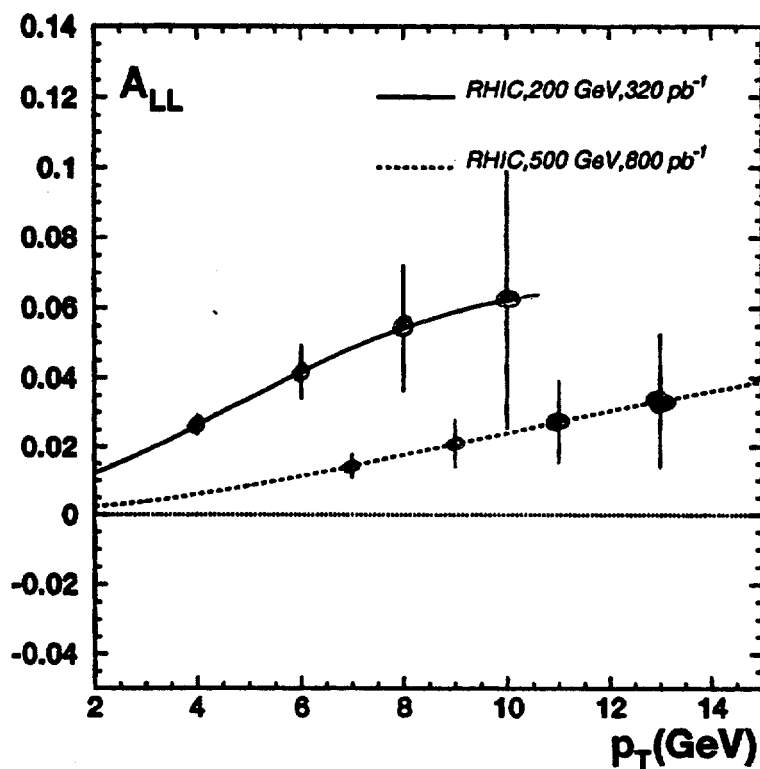


Fig 4 a

$$pp \rightarrow J/\psi + X$$

NLO GS DISTRIBUTIONS



O. TERYAEV, A. TKABLADEE

Phys. Rev. D56 (1997) 7331

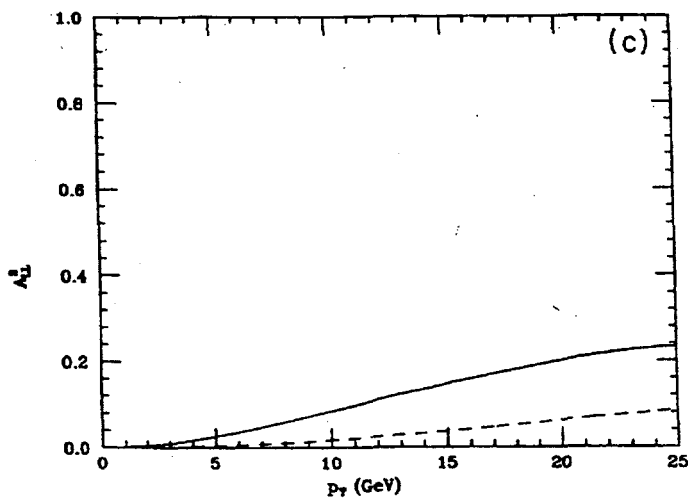
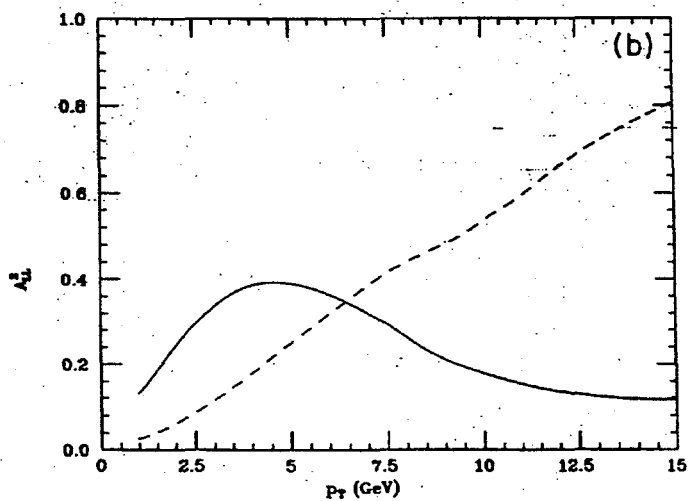
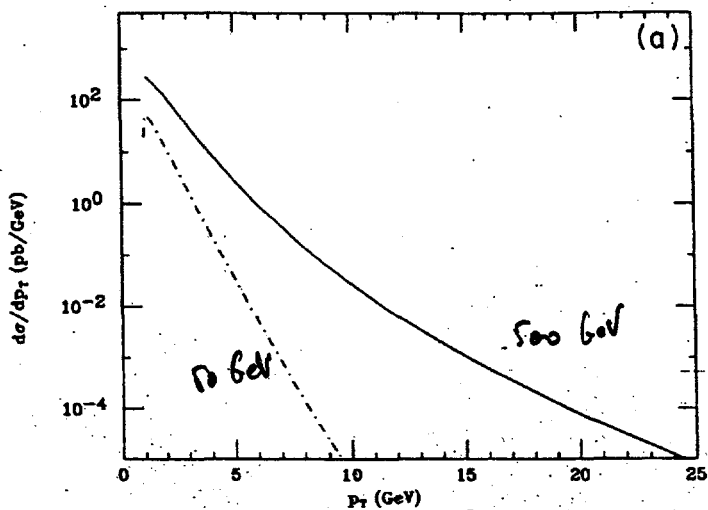


FIG. 3. p_T distribution, $\frac{d\sigma}{dp_T}$ vs p_T (a) for RHIC at $\sqrt{s} = 500$ GeV (solid line) and at $\sqrt{s} = 50$ GeV (dot-dashed line), and A_{LL}^2 vs p_T for RHIC at $\sqrt{s} = 50$ GeV (b) and at $\sqrt{s} = 500$ GeV (c) for large $\Delta g(x, Q^2)$ (solid line) and for moderately large $\Delta g(x, Q^2)$ (dashed line).

$$pp \rightarrow J/\psi + \gamma + X$$

M.A. JONCHERSKI AND C.S. KIM
PR 349 (1994) 4463

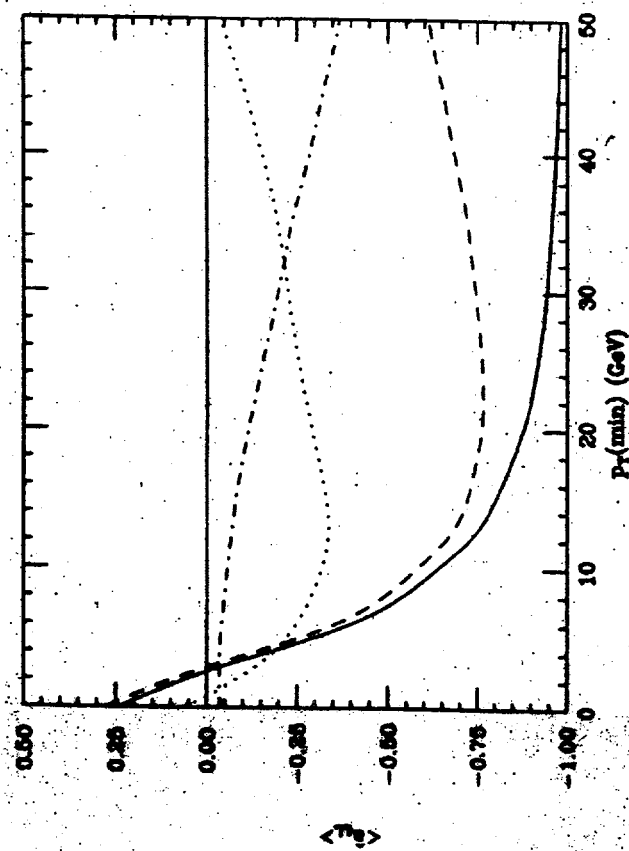


Fig. 3. The average asymmetry, $\langle \hat{a}_{LL} \rangle$, for b -quark production in pp collisions at $\sqrt{s} = 500$ GeV using only $2 \rightarrow 2$ processes. Solid line, total $2 \rightarrow 2$, dashes: gg , dot-dashes: $q\bar{q}$. The dotted line corresponds to the $2 \rightarrow 2$ contributions taken together with the 'regularized' $2 \rightarrow 3$ subprocesses described in the text.

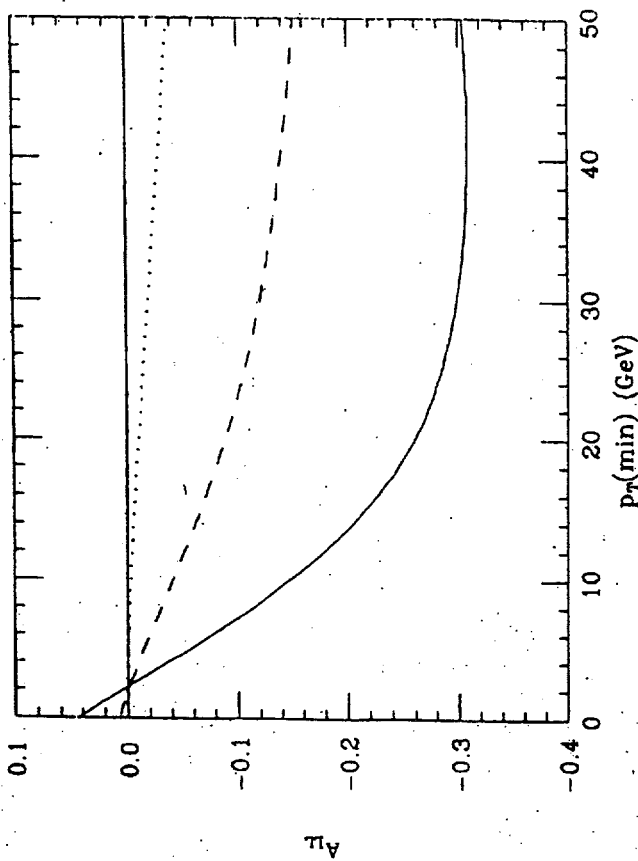


Fig. 4. The observable asymmetry A_{LL} in the integrated b -quark cross-section $\sigma(p_T > p_T(\text{min}))$, vs. $p_T(\text{min})$ (GeV), assuming $\Delta G(x, Q^2) = x^\alpha G(x, Q^2)$, where $\alpha = 1.0$ (0.5, 0.25): dots (dashes, solid). The sea quarks are assumed unpolarized for simplicity.

x-Dependent Polarized Parton Distributions for RHIC
Gordon P. Ramsey, Loyola University Chicago and Argonne National Lab
Talk given at the BNL/RIKEN Spin Workshop, April 27-29, 1998

Using QCD motivated constraints and polarized deep-inelastic scattering (PDIS) data, we have constructed x-dependent polarized parton distributions for each quark flavor. These satisfy positivity constraints and are evolved using the NLO DGLAP equations. Three models of the polarized gluon are used to allow representation in terms of different factorization prescriptions. [See hep-ph/9803351 for details].

The polarized valence distributions are constructed using a modified SU(6) model, with a spin dilution factor to modify the small-x behavior of the polarized valence quarks. The one free parameter is fixed by the Bjorken Sum Rule. The polarized sea is constructed using the following assumptions:

- (1) the SU(3) symmetry is broken by suppressing the strange sea polarization, using information from PDIS experiments [see Phys. Rev. D55, 1244 (1997)],
- (2) the polarized sea is generated from the unpolarized flavors assuming that $\langle \eta(x) \rangle = \langle [\Delta q(x)] / [xq(x)] \rangle = a + bx^{1/2}$, where a and b are free parameters, and $\langle \eta \rangle = \langle \Delta q \rangle / \langle xq \rangle$. This ensures that the overall spin carried by each constituent, obtained from data, is preserved.
- (3) the free parameters are determined from six sets of g_1 data, two each of proton, neutron and deuteron, then averaged for each sea flavor of light quarks.

The three polarized gluon models used to determine the anomaly term in the factorization prescription are shown in the following transparencies. The distributions are generated at Q_0^2 of 1 GeV² and then evolved using the NLO DGLAP evolution equations with 3 flavors, until reaching the charm threshold, where the fourth flavor is included. The overall parametrization is shown in the following transparencies along with a plot of g_1^p , showing the SMC data and the distributions using the three polarized gluon models.

x -Dependent Polarized Parton Distributions

Gordon P. Ramsey

**Loyola University Chicago
Argonne National Lab**

References

GR: Phys. Rev. D55, 1244 (1997)

GGR: hep-ph/9803351

Collaborators

L. Gordon, TJNL and HU (USA)

M. Goshtasbpour, CTPM and SBU (Iran)

SEA Parametrizations:

1.. Polarized to unpolarized sea ratio ($Q^2 = 1 \text{ GeV}^2$):

$$\eta_i(x) \equiv \frac{\Delta q_i(x)}{x q_i(x)} = a_i + b_i x^{1/2}$$

for each quark flavor, i . Here a_i and b_i are free parameters, fixed by theoretical arguments or data.

2. Broken SU(3) Sea flavors

$$\Delta \bar{u} = \Delta u_s = \Delta \bar{d} = \Delta d_s = (1 + \epsilon) \Delta \bar{s} = (1 + \epsilon) \Delta s$$

3. γ_5 anomaly: $\langle p | \bar{q} \gamma^\mu \gamma_5 q | p \rangle$

$$\text{For each quark flavor: } \Delta q_5 = \Delta q_c - \frac{\alpha_s}{4\pi} \hat{\gamma} \otimes \Delta G$$

Refs: Efremov and Teryaev; Altarelli and Ross
Carlitz, Collins and Mueller; Berger and Qiu

$\hat{\gamma}$ is convention dependent

physical observables are related to Δq_5

Δq_c do not evolve with Q_2 in LO

$$\sum_i (\langle \Delta q_5^i \rangle - \langle \Delta q_c^i \rangle) = \frac{N_f \alpha_s(Q^2)}{2\pi} \langle \Delta G(Q^2) \rangle \equiv \Gamma(Q^2)$$

Polarized Gluon Models:

1. Moderate:

$$\Delta G(x, Q^2) = xG(x, Q^2)$$

2. Zero (GI factorization):

$$\Delta G(x, Q^2) = 0$$

3. Instanton Induced (negative):

$$\Delta G(x, Q^2) = 7(1-x)^7[1 + 0.474 \ln(x)]$$

All at $Q_0^2 = 1 \text{ GeV}^2$.

CTEQ parametrization for the unpolarized gluon

**Gauge invariant factorization equivalent to
results obtained for model 2**

The resulting functions $\eta(x)$ for each gluon model are:

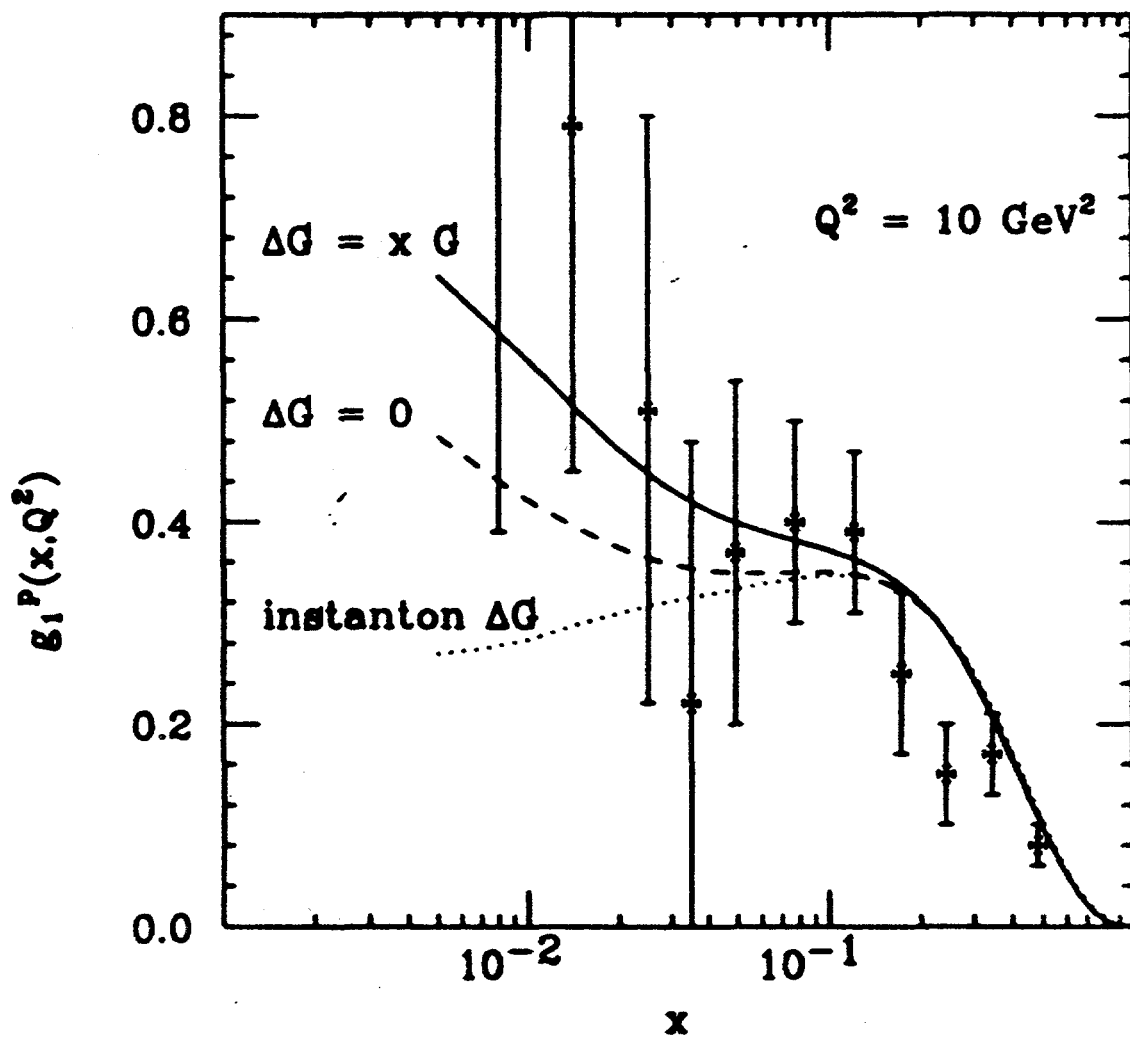
Quantity	$\eta_{u,d}(x)$	$\eta_s(x)$
$\Delta G = xG$	$-2.49 + 2.8\sqrt{x}$	$-1.67 + 2.1\sqrt{x}$
$\Delta G = 0$	$-3.03 + 3.0\sqrt{x}$	$-2.71 + 2.9\sqrt{x}$
$\Delta G < 0$	$-3.25 + 3.1\sqrt{x}$	$-3.31 + 3.3\sqrt{x}$

$$\Delta q_i(x) = -Ax^{-0.143}(1-x)^{8.041}(1-B\sqrt{x})[1 + 6.112x + P(x)]. \quad (4.1)$$

Flavor	ΔG	A	B	$P(x)$
$\langle \Delta u \rangle_{sea}$	xG	0.317	1.124	$-0.278x^{0.644} - 1.682x^{0.937}(1-x)^{-3.368}(1 + 4.269x^{1.508})$
$\langle \Delta d \rangle_{sea}$	xG	0.317	1.124	$+0.278x^{0.644} - 1.682x^{0.937}(1-x)^{-3.368}(1 + 4.269x^{1.508})$
$\langle \Delta s \rangle$	xG	0.107	1.257	$-3.351x^{0.937}(1-x)^{-3.368}(1 + 4.269x^{1.508})$
$\langle \Delta u \rangle_{sea}$	0	0.386	0.990	$-0.278x^{0.644}$
$\langle \Delta d \rangle_{sea}$	0	0.386	0.990	$+0.278x^{0.644}$
$\langle \Delta s \rangle$	0	0.173	1.070	0
$\langle \Delta u \rangle_{sea}$	Neg	0.414	0.954	$-0.278x^{0.644} - 10.49x^{1.143}(1-x)^{-1.041}(1 + 0.474 \ln x)$
$\langle \Delta d \rangle_{sea}$	Neg	0.414	0.954	$+0.278x^{0.644} - 10.49x^{1.143}(1-x)^{-1.041}(1 + 0.474 \ln x)$
$\langle \Delta s \rangle$	Neg	0.212	0.997	$-20.89x^{1.143}(1-x)^{-1.041}(1 + 0.474 \ln x)$

Key Elements:

- 1. Separate sea and valence**
- 2. BSR is Basis for valence**
- 3. Include NLO QCD corr. to BSR**
- 4. Separate strange sea (mass effect, ϵ)**
- 5. Separate parametrization for each flavor**
- 6. Different factorizations included**
- 7. 3 Different Gluon Models**
- 8. NLO DGLAP evolution**
- 9. All evolution in x -space**
- 10. Positivity holds**
- 11. Excellent agreement with data**
- 12. Results Compared with others**



Measuring the Gluon Helicity Distribution via $\bar{p}\bar{p} \rightarrow \gamma + \text{jet} + X$ with STAR

S.E. Vigdor

Dept. of Physics, Indiana University, Bloomington, IN 47405, U.S.A.

Measurement of the net gluon contribution to a proton's longitudinal spin projection with a precision better than ± 0.5 would substantially advance our understanding of the spin substructure, clarifying also the contributions from quarks and from orbital angular momentum. This precision is attainable, along with high-quality measurements of the dependence of the gluon polarization on Bjorken x , via γ -jet coincidence detection in STAR.

Among contemplated methods, the detection of γ -jet coincidences from hard $\bar{p}-\bar{p}$ collisions allows one to approach most closely the ideal of extracting $\Delta G(x_g)$ directly from the data, at experimentally determined x_g values (see Fig. 1). Still, the envisioned extraction involves simplifying assumptions, whose (model-dependent) effect is important to estimate from simulations.

STAR will be well-suited for γ -jet coincidences when the baseline detector is supplemented by the barrel electromagnetic calorimeter (EMC), already under construction, and by an endcap EMC to be proposed to the National Science Foundation in Fall 1998. As detailed in Fig. 2, the endcap provides access to kinematic regions where the greatest statistical precision in $\Delta G(x_g)$ and the cleanest experimental determination of x_g are possible. To distinguish single γ 's from π^0 or η -meson decays up to 60 GeV, the endcap will include a shower-maximum detector (SMD) comprising two orthogonal planes of scintillator strips of triangular cross section.

Simulation results (Fig. 3) indicate realistic statistical, plus some systematic, uncertainties achievable with STAR. The extracted values deviate systematically from $\Delta G(x, Q^2)$ *input* to the simulation (solid curve, based on model A of Gehrmann and Stirling, Ref. 1), because the simple data analysis neglects a number of effects included in the event generation: *e.g.*, contributions from $q\bar{q} \rightarrow g\gamma$, $qg \rightarrow q\gamma$ with $x_g > x_q$, and k_T smearing. The deviations are manageable ($\lesssim 30\%$) in magnitude, hence correctable, and become unimportant at $x_g < 0.1$, where the dominant contributions to the *integral* $\Delta G(Q^2) \equiv \int_0^1 \Delta G(x, Q^2) dx$ arise.

Simulations also demonstrate that the subtraction of π^0 and η -meson background does not seriously compromise the impact of the attainable results. As seen in Fig. 4, the imposition of isolation cuts and cuts on the shower profile measured in the SMD reduce the background/signal ratio from about 13 (generated by PYTHIA) to 0.6–0.8, roughly independent of the pseudorapidity of the detected particle or of the reconstructed x_g value. The background subtraction procedure outlined in Fig. 5 would increase error bars, over the statistical uncertainties included in Fig. 3, by a factor of 1.5–2.0, if we can determine the probability that mesons survive the SMD cut to $\pm 15\%$ from simulations. All other information needed to determine $A_{LL}(x_g)$ for direct γ production is *measured* in the experiment itself.

Measurements at two energies, $\sqrt{s}=200$ and 500 GeV, will yield $\Delta G(x_g)$ over the range $0.02 \leq x_g \leq 0.3$, with a net statistical plus background subtraction uncertainty $\lesssim \pm 0.2$ in the integral ΔG over this range. It appears feasible to control other systematic errors (including beam polarization calibration) sufficiently to maintain an overall error $< \pm 0.5$ in $\int_0^1 \Delta G(x, Q^2) dx$. Comparison of results from two energies at overlapping x_g -values will test the importance of k_T -smearing and other questionable issues in the theoretical description of direct photon production.

[1] T. Gehrmann and W.J. Stirling, Phys. Rev. **D53**, 6100 (1996).

ADVANTAGES OF $\vec{p} + \vec{p} \rightarrow \gamma + \text{jet} + X$

- one dominant partonic subprocess: $q + g \rightarrow q + \gamma$
- NLO effects relatively small
- extensive experience from unpolarized $G(x)$ fits

- event-by-event kinematic determination of $x_{1,2}, \theta^*$
(without reliance on poor resolution $p_T(\text{jet})$): **(neglecting k_T)**

$$x_1 = \frac{p_T(\gamma)}{\sqrt{s_{pp}}} [\exp(\eta_\gamma) + \exp(\eta_{\text{jet}})]$$

$$x_2 = \frac{p_T(\gamma)}{\sqrt{s_{pp}}} [\exp(-\eta_\gamma) + \exp(-\eta_{\text{jet}})]$$

$$|\cot \theta^*| = \left| \sinh \left(\frac{\eta_{\text{jet}} - \eta_\gamma}{2} \right) \right|$$

- $\hat{\sigma}(\theta^*)$, parton distribution functions both favor assignment:

$$x_g = \min \{ x_1, x_2 \}; \quad x_q = \max \{ x_1, x_2 \}$$

\Rightarrow removes ambiguity re sign of $\cot \theta^*$ (preference strongest when $|x_1 - x_2| > 0.1$, $|\cos \theta^*| \geq 0.5$), allows approx. LO direct extraction:

$$\frac{\Delta G(x_g)}{G(x_g)} \cong \frac{\varepsilon_{LL}^{\text{meas.}}}{P_{b_1} P_{b_2} A_1^{\text{DIS}}(x_q, Q^2) \hat{a}_{LL}^{\text{Compton}}(\theta^*)}$$

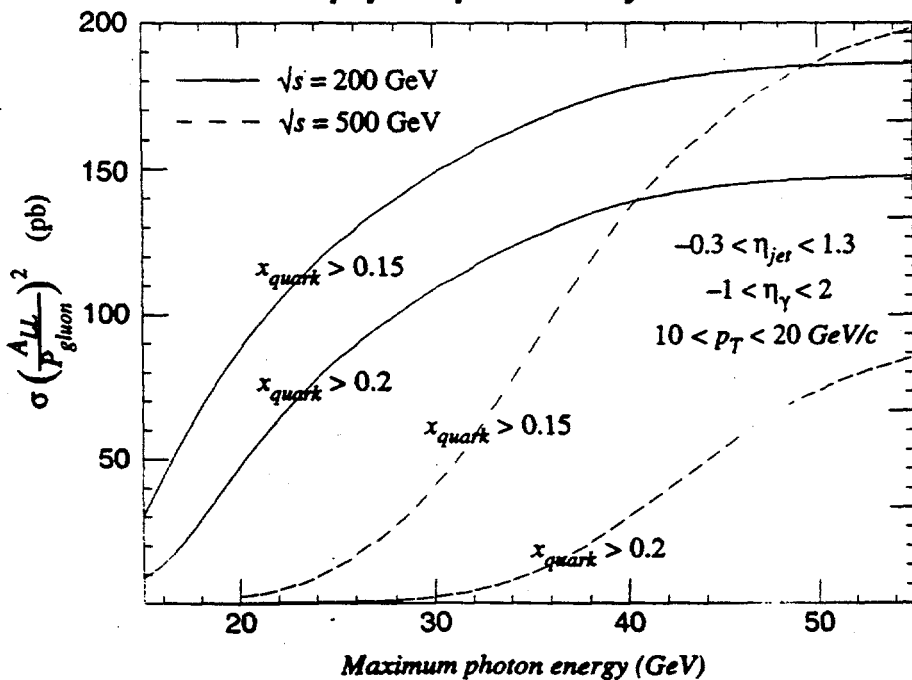
- perform simulations to test effects of neglecting:

$q \bar{q} \rightarrow g \gamma$; $x_g \leftrightarrow x_q$ misidentification;
 θ^* reconstruction errors; k_T - smearing + g radiation;
 eventually, NLO contributions

Endcap \Rightarrow Access To:

- 1) highly asymmetric partonic collisions:
 \Rightarrow highly pol'd quarks @ $x_q > 0.2$ to probe gluon pol'n @ $x_g < 0.1$
- 2) backward θ^* in $q + g \rightarrow q + \gamma$
 \Rightarrow peak $\hat{\sigma}$ and $\hat{a}_{LL} \Rightarrow$ greatest figure of merit for determining $\Delta G/G(x)$
- 3) least confusion in assigning x_g vs. x_q
 \Rightarrow both $\hat{\sigma}(\theta^*)$ and PDF's favor $x_g = x_{\min}$
- 4) greatly enhanced jet acceptance
 \Rightarrow enhanced coverage at large x_g

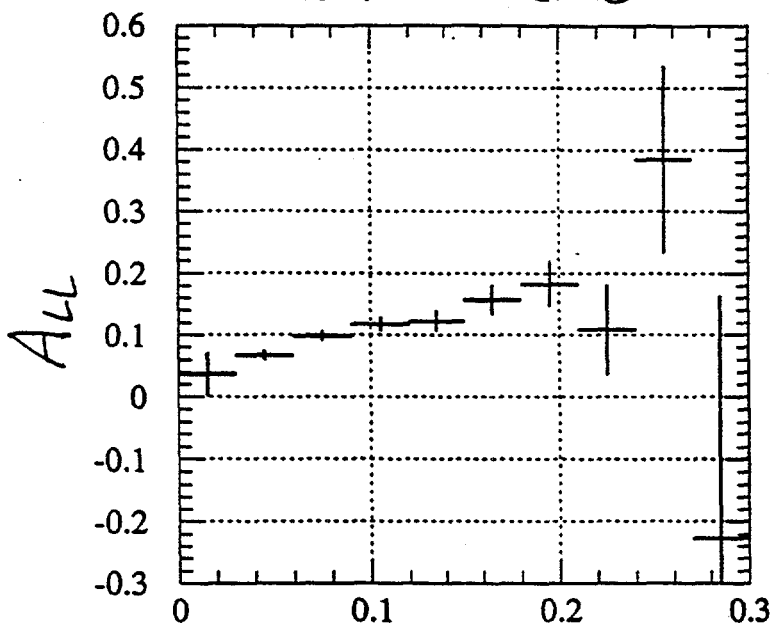
Fig. of Merit for $\frac{\Delta G(x)}{G(x)}$



Max. E_γ detected

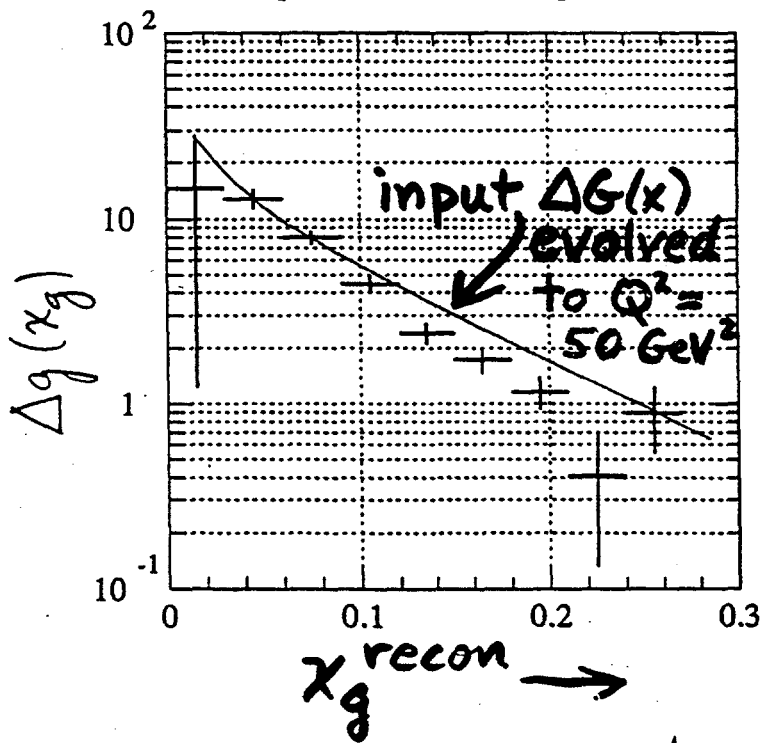
Simulated Data for $\vec{p} + \vec{p} \rightarrow \gamma + \text{jet} + X$
 for STAR + endcap EMC
 $\sqrt{s} = 200 \text{ GeV}; 320 \text{ pb}^{-1}$

BEMC + EEMC



error bars are
 statistical
 (± 0.005 syst.
 instrumental
 asym. included
 in $\epsilon_{LL}^{\text{meas.}} \Rightarrow \pm 0.010$
 in A_{LL})

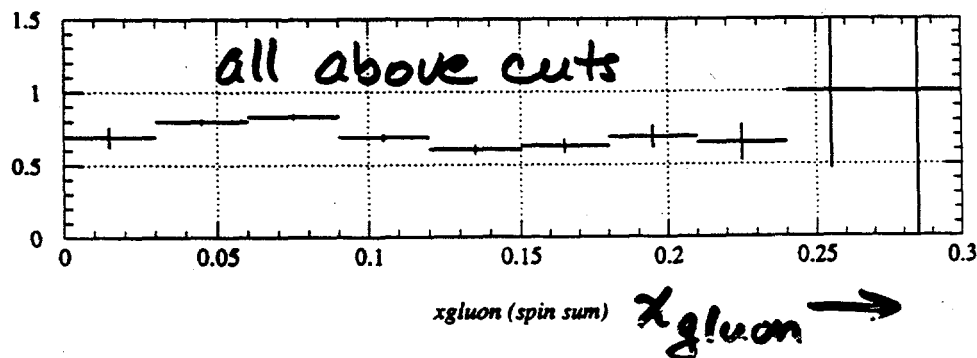
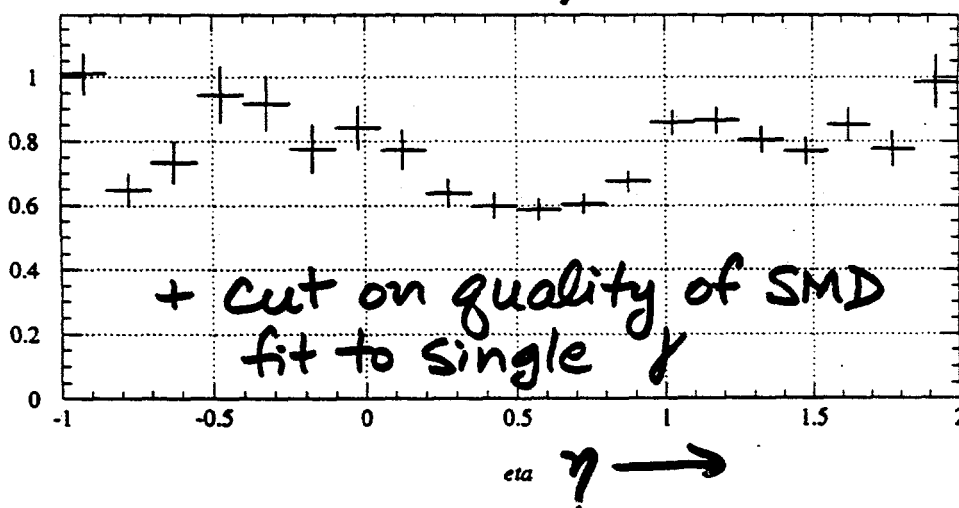
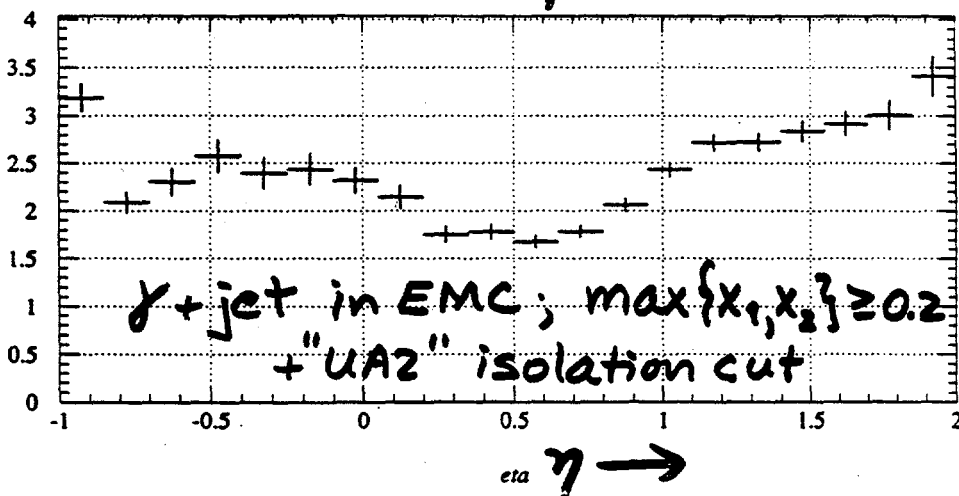
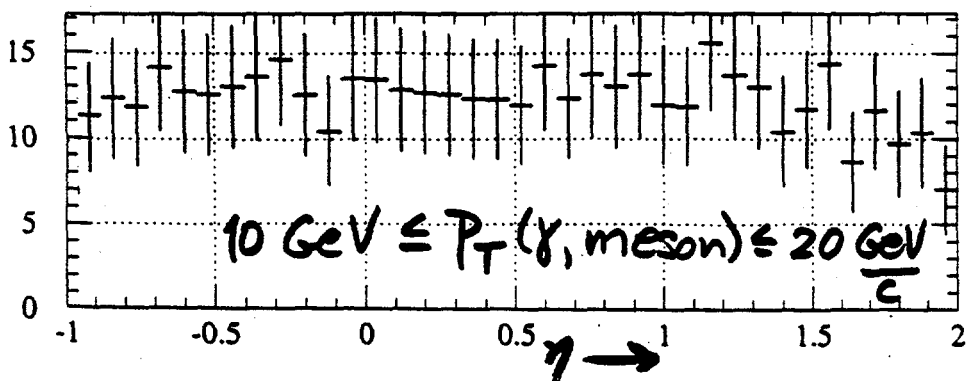
spin correlation vs x_{gluon}



Systematic deviation
 from input $\Delta G(x, Q^2)$
 from neglect of:
 $q\bar{q} \rightarrow \gamma g$
 $x_g \leftrightarrow x_q$
 $\cos \theta^*$ resol'n } all
 tend to
 reduce
 $\epsilon_{LL}^{\text{meas.}}$!
 k_T -smearing
 Effects ≈ 0 at
 $x_g < 0.1$, where get
 largest contrib'n's to $\int_0^1 \Delta G(x)$

$\sqrt{s} = 200 \text{ GeV}$

Ratio of $(\pi^0 + \eta^0) / \text{direct } \gamma$



π^0/η^0 Background Subtraction Analysis: 118.

For each x_g^{recon} bin, measure:

N, A_{LL} for SMD pass & SMD fail samples
+ use simulations, tuned to fit $\frac{N_{\text{pass}}}{N_{\text{fail}}}$ (SMD cut),
to predict*:

$P_{\pi} = \text{prob. that meson passes SMD cut}$
 ≈ 0.2

$$\Rightarrow A_{LL}^{\delta} = A_{LL}^{\text{pass}} + \frac{(A_{LL}^{\text{pass}} - A_{LL}^{\text{fail}})}{\left[\left(\frac{N_{\text{pass}}}{N_{\text{fail}}} \right) \left(\frac{1}{P_{\pi}} - 1 \right) - 1 \right]}$$

Simulation results then \Rightarrow

$$\sigma_{A_{LL}^{\delta}} \approx \left\{ 2.2 \sigma_{A_{LL}^{\text{simul. stat.}}}^2 + 25 A_{LL}^2 \sigma_{P_{\pi}}^2 \right\}^{1/2}$$

Assuming $\sigma_{P_{\pi}} \approx \pm 0.03$ (\Rightarrow 15% error in P_{π} !)

\Rightarrow increase simulated stat. errors
by factor $\approx \underline{1.5 - 2.0}$ to account for
bkgd. subt. uncertainty

* P_{π} can also be constrained independently
via preshower conversion probabilities

Prompt Photon at PHENIX

Yuji Goto, *RIKEN*

High p_T prompt photon in polarized proton collision is a good probe to investigate ΔG , gluon polarization in the proton. Prompt photon production is dominated by the gluon Compton process. With the asymmetry (A_{LL}) measurement, we can obtain $\Delta G/G$ by using knowledge of the quark polarization and the asymmetry of elementary process. Detection of the prompt photon is experimentally challenging because of many background mainly from $\pi^0 \rightarrow 2\gamma$.

The prompt photon is detected by an EM calorimeter (EMCal) system at PHENIX. Parameters of the EMCal system are summarized in Table ???. Using these parameters we are studying the prompt photon measurement with PYTHIA5.7/JETSET7.4. For the background reduction, isolation cut is studied by using the generated events. Around each photon, isolation cone is defined with half-angle $R = \sqrt{\Delta\eta^2 + \Delta\phi^2}$. All hadronic energy deposit in the cone is summed up and the sum is required to be less than a certain fraction of the photon energy. This cut discards background photon mainly from π^0 in the jet which is accompanied by other particles. On the other hand, the prompt photon is not accompanied by other particles and survives this cut.

We can impose other conditions, for instance, to use some constant value as the limit of energy in the cone, to use 1 central arm instead of isolation cone, etc. We need to consider that we cannot detect neutral hadron without detecting decay photons. There might be some theoretical issues in using any possible isolation cut to show the experimental result. We need to know how much uncertainty we have due to these cuts. This issue should be addressed to theorists.

For ΔG measurement, we need to know gluon's x value using p_T value of the prompt photon. Naive estimation of gluon's x is given by $x_T = 2p_T/\sqrt{s}$, but this shows the case that 2 colliding partons, i.e. gluon and quark, are balanced. From the simulation study, gluon's x value is estimated by specifying p_T region of the prompt photon. There is big difference between these two estimations. This uncertainty must be evaluated.

By considering yield and background, the accessible p_T ranges of prompt photon production are $10\text{GeV}/c < p_T < 30\text{GeV}/c$ for $\sqrt{s}=200\text{GeV}$ and $10\text{GeV}/c < p_T < 40\text{GeV}/c$ for $\sqrt{s}=500\text{GeV}$. This correspond to $0.1 < x < 0.3$ for $\sqrt{s}=200\text{GeV}$ and $0.04 < x < 0.16$ for $\sqrt{s}=500\text{GeV}$ by using the x_T to evaluate the x value. The statistical errors on the $\Delta G/G$ in this region are 5-30% for $\sqrt{s}=200\text{GeV}$ and 5-20% for $\sqrt{s}=500\text{GeV}$, although these will be affected by uncertainties in x value estimation.

All transparencies of this talk is accessible on the Web;

<http://www.phenix.bnl.gov/WWW/publish/goto/>

	η	ϕ	$\delta\eta$	$\delta\phi$	σ_E/E (%)	σ_x (mm)	σ_t (psec)
PbSc	± 0.35	$90^\circ + 45^\circ$	0.011	0.011	$7.8/\sqrt{E} \oplus 1.5$	$10/\sqrt{E}$	$70/\sqrt{E} \oplus 70$
PbGl	± 0.35	45°	0.008	0.008	$5.8/\sqrt{E} \oplus 1.0$	$5./\sqrt{E} \oplus 1.0$	$143/\sqrt{E} \oplus 75$

Table 1: Parameters of the PHENIX EMCal system. η and ϕ show pseudo-rapidity and azimuthal angle coverages. $\delta\eta$ and $\delta\phi$ show granularity per module. Energy resolution, position resolution and timing resolution are also listed.

PYTHIA Simulation

- PYTHIA5.7/JETSET7.4

- PDFLIB GRV94LO

- prompt photon production as a signal

- QCD jet as a background

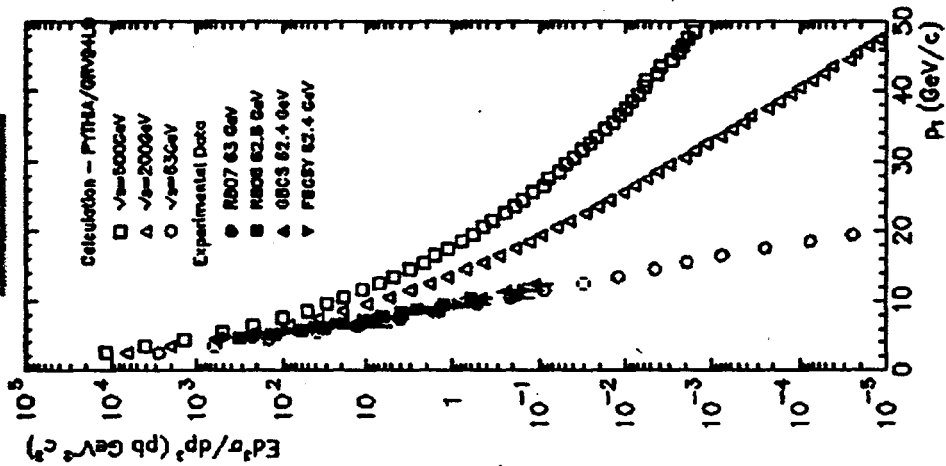
- Luminosity

$$\int Ldt = 320 \text{ pb}^{-1} \text{ for } \sqrt{s} = 200 \text{ GeV}$$

$$\int Ldt = 800 \text{ pb}^{-1} \text{ for } \sqrt{s} = 500 \text{ GeV}$$

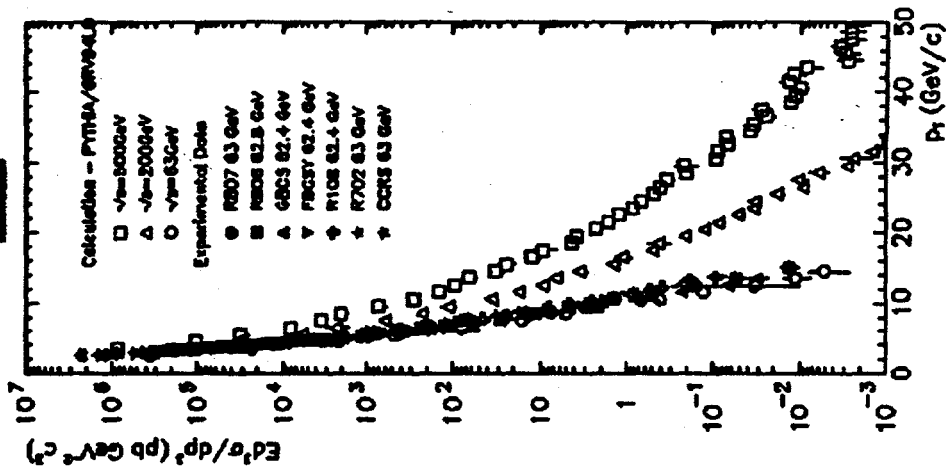
- 10 weeks run with 70% efficiency and 70% pol.

photon



(a) photon cross section

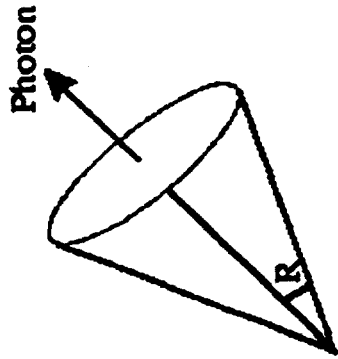
π⁰



(b) π⁰ cross section

Isolation Cut

- Around each photon, a cone of a certain radius R is defined.



$$R = \sqrt{\Delta\eta^2 + \Delta\phi^2}$$

– $\Delta\eta$: rapidity interval $\Delta\phi$: azimuthal angle

- Hadronic energy deposit in the cone (E_{sum}) is required to be less than a certain fraction of the photon energy (E_γ).

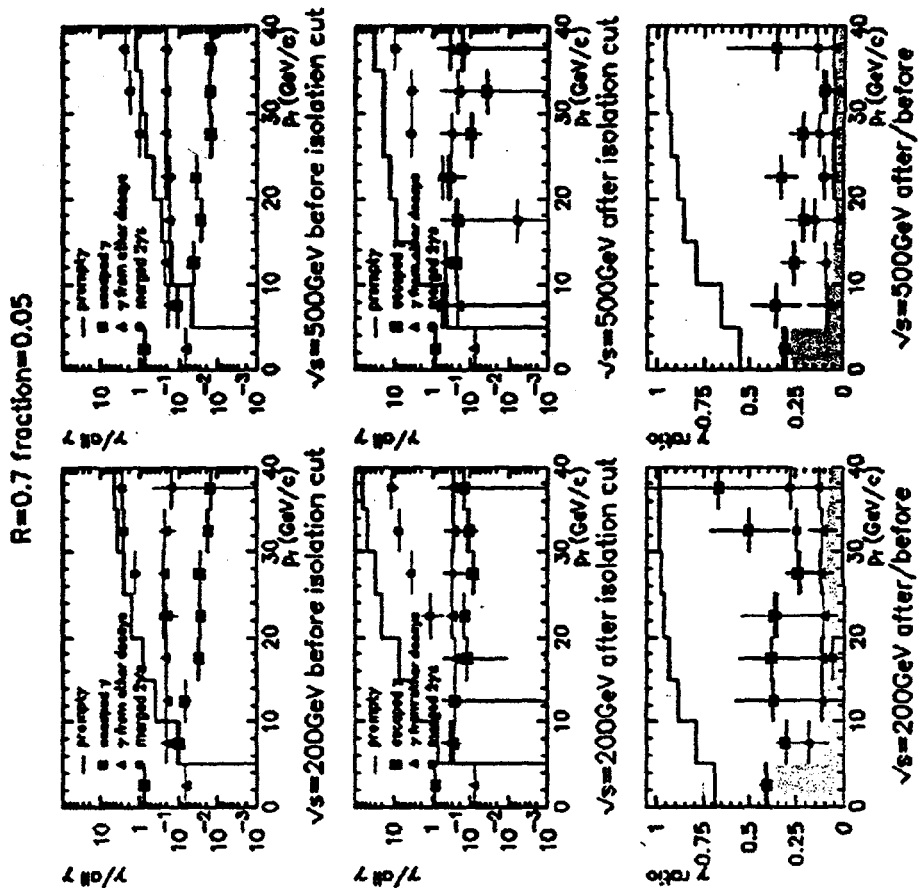
$$E_{sum} < \epsilon \cdot E_\gamma$$

- other isolation cut
 - fixed value instead of fraction
- $E_{sum} < \text{const.}$
- neutral hadron (other than π^0) undetectable
- 1 central arm instead of isolation cone ...

- theoretical issue ?
 - from experimental data to ΔG information directly ?
 - how much uncertainty ?

ISOLATION CUT

- background for prompt photon
 - before isolation cut
 - normalized by all background photon before isolation cut
 - after isolation cut
 - normalized by all background photon after isolation cut
- ratio before and after isolation cut
 - red line: prompt photon
 - yellow hatch: all background photon



* $\pi^0 \rightarrow 2\gamma$ is assumed to merge
 when 2γ merge is less than 0.05

ΔG Measurement

- statistics

- P_B : beam polarization ~70%
- N^{++} : parallel spin direction
- N^{+-} : anti-parallel spin direction
- A_{1P} : GS95

$$A_{LL} = \frac{1}{P_B^2} \cdot \frac{N^{++} - N^{+-}}{N^{++} + N^{+-}}$$

$$\delta A_{LL} = \frac{1}{P_B^2} \cdot \frac{1}{\sqrt{N^{++} + N^{+-}}}$$

$$\frac{\delta \Delta G}{G} = \frac{\delta A_{LL}}{A_{1P} \cdot a_{LL}}$$

Photon pr	$\sqrt{s} = 200 \text{ GeV}$		$\sqrt{s} = 500 \text{ GeV}$	
	Yield	Errors on $A_{LL} \Delta G/G$	Yield	Errors on $A_{LL} \Delta G/G$
10 - 15 GeV/c	1.0×10^5	0.0062 0.046	9.0×10^5	0.0022 0.045
15 - 20 GeV/c	1.3×10^4	0.0168 0.089	1.8×10^5	0.0059 0.059
20 - 25 GeV/c	2.7×10^3	0.0376 0.171	5.3×10^4	0.0081 0.081
25 - 30 GeV/c	5.9×10^2	0.0799 0.309	1.9×10^4	0.0115 0.115
30 - 35 GeV/c			7.7×10^3	0.0141 0.141
35 - 40 GeV/c			3.3×10^3	0.0198 0.198

Table 1: Prompt photon yield and error estimation.

Photon pr	$\sqrt{s} = 200 \text{ GeV}$		$\sqrt{s} = 500 \text{ GeV}$	
	Yield	Errors on $A_{LL} \Delta G/G$	Yield	Errors on $A_{LL} \Delta G/G$
10 - 15 GeV/c	5.6×10^5		1.2×10^7	
15 - 20 GeV/c	4.2×10^4		1.5×10^6	
20 - 25 GeV/c	4.9×10^3		2.5×10^5	
25 - 30 GeV/c	8.5×10^2		7.4×10^4	
30 - 35 GeV/c			1.9×10^4	
35 - 40 GeV/c			7.1×10^3	

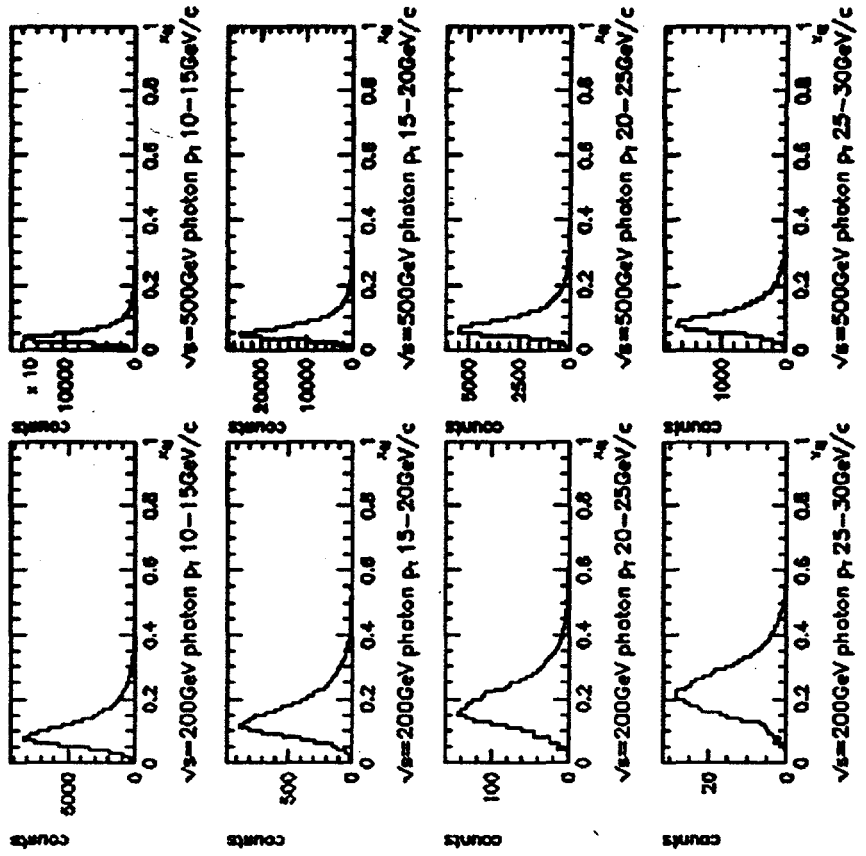
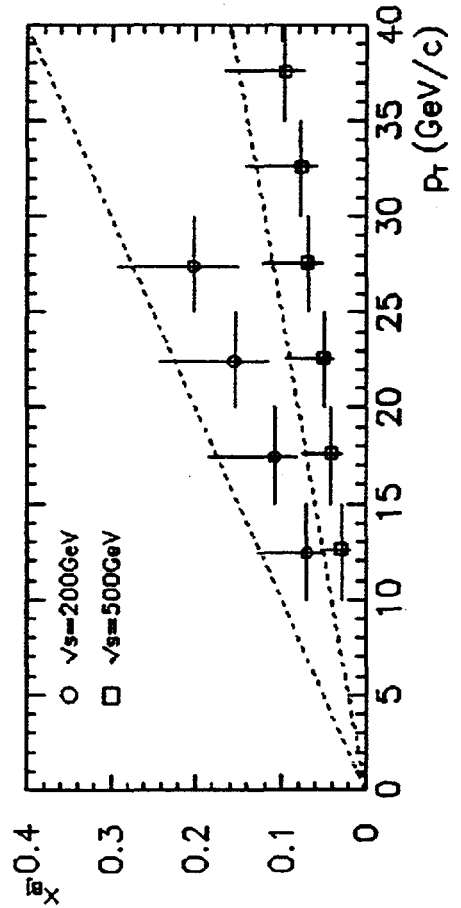
Table 2: Inclusive π^0 yield estimation.

ΔG Measurement

- P_T vs gluon's x
- naïve formula ?

$$x_T = \frac{2P_T}{\sqrt{s}}$$

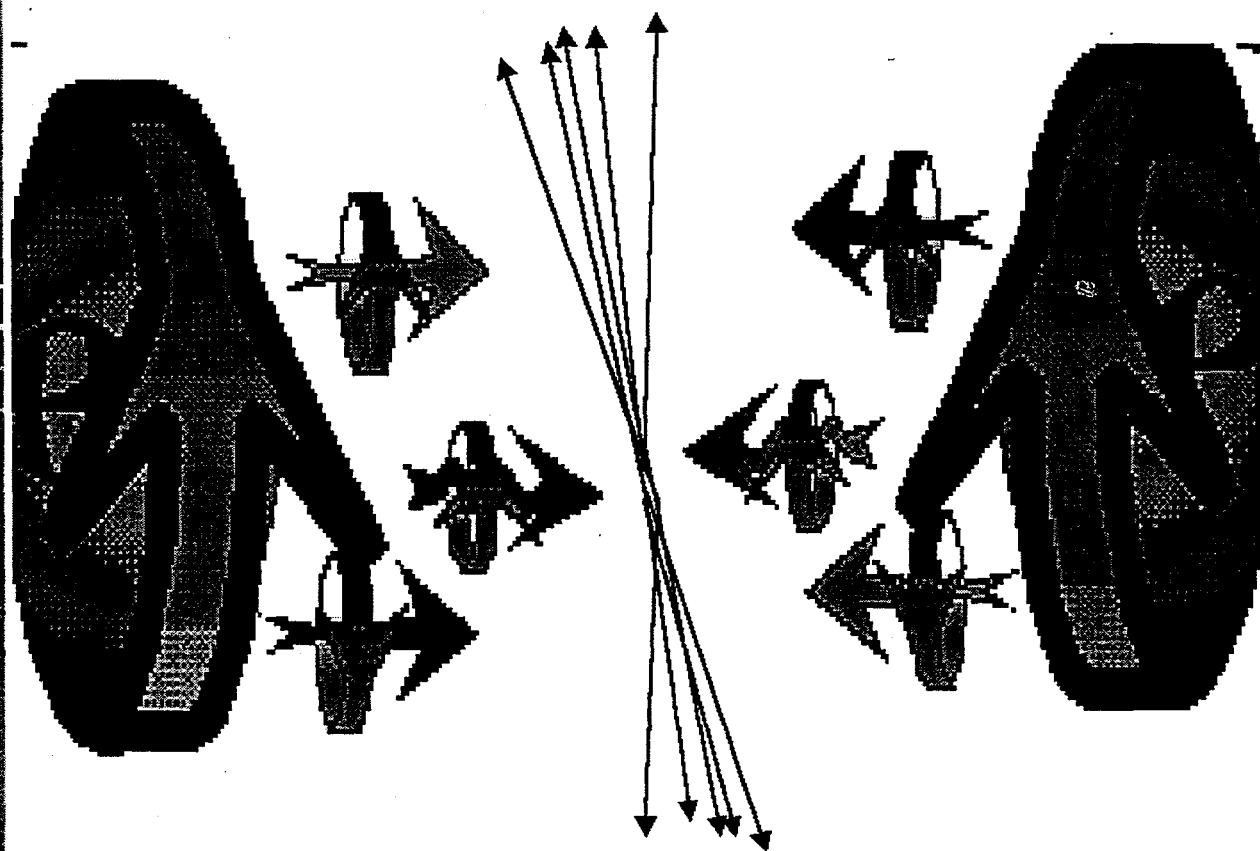
- or evaluation with simulation ?



Measuring ΔG with Jets

STAR

S. Heppelmann



Summary

The clean and easily interpreted method for measuring ΔG involves the measurement of longitudinal double spin asymmetry of direct photon + jet events. However detection of jet pairs may make up in statistics part of what is lacking in clarity of interpretation.

Focusing specifically here on dijets in the central rapidity region

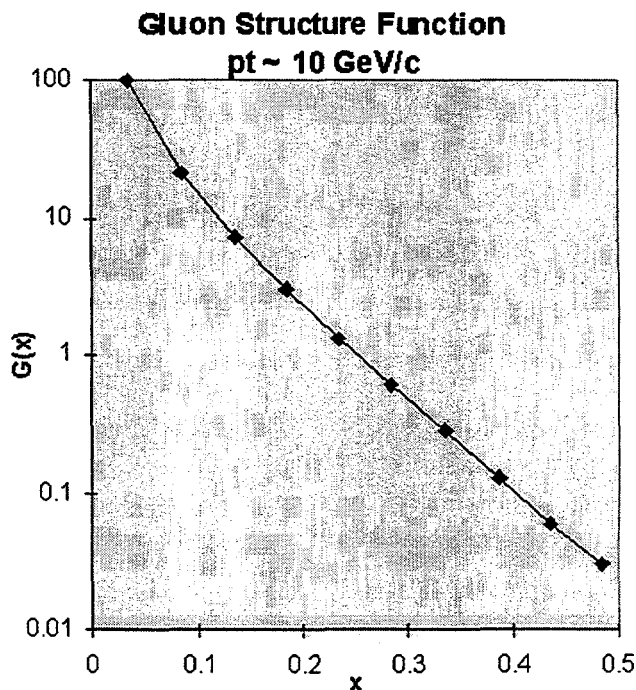
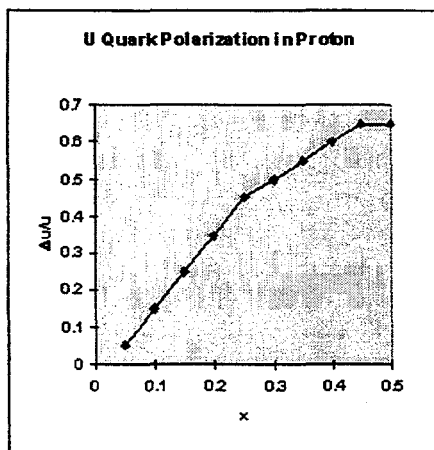
- > Luminosity = 800 pbarns^{-1}
- > $|Y_1| < .2$
- > $|Y_2| < .2$
- > $p_T > 5 \text{ GeV}/c$
- > $E_{cm} = 500 \text{ GeV}$

it is possible to make a determination of $\Delta G(x)$ around $x=.02$. This measurement may be the best handle on the low x part of the integral $\int_{x_{min}}^1 \Delta G(x) dx$. The error in this region is likely to dominate the error of the integral of the gluon spin. Measurements of $\Delta G(x=.02)$ at the 1% level would be very important to limit the low x contribution to the uncertainty of the integral. Such a 1% measurement would require the measurement of many ($\sim 10^7$) dijet events. If only 10^5 events were collected, the double spin longitudinal asymmetry would not be observable unless the gluon polarization in that region were to approach 10%.

1st Moment of the Gluon Polarization

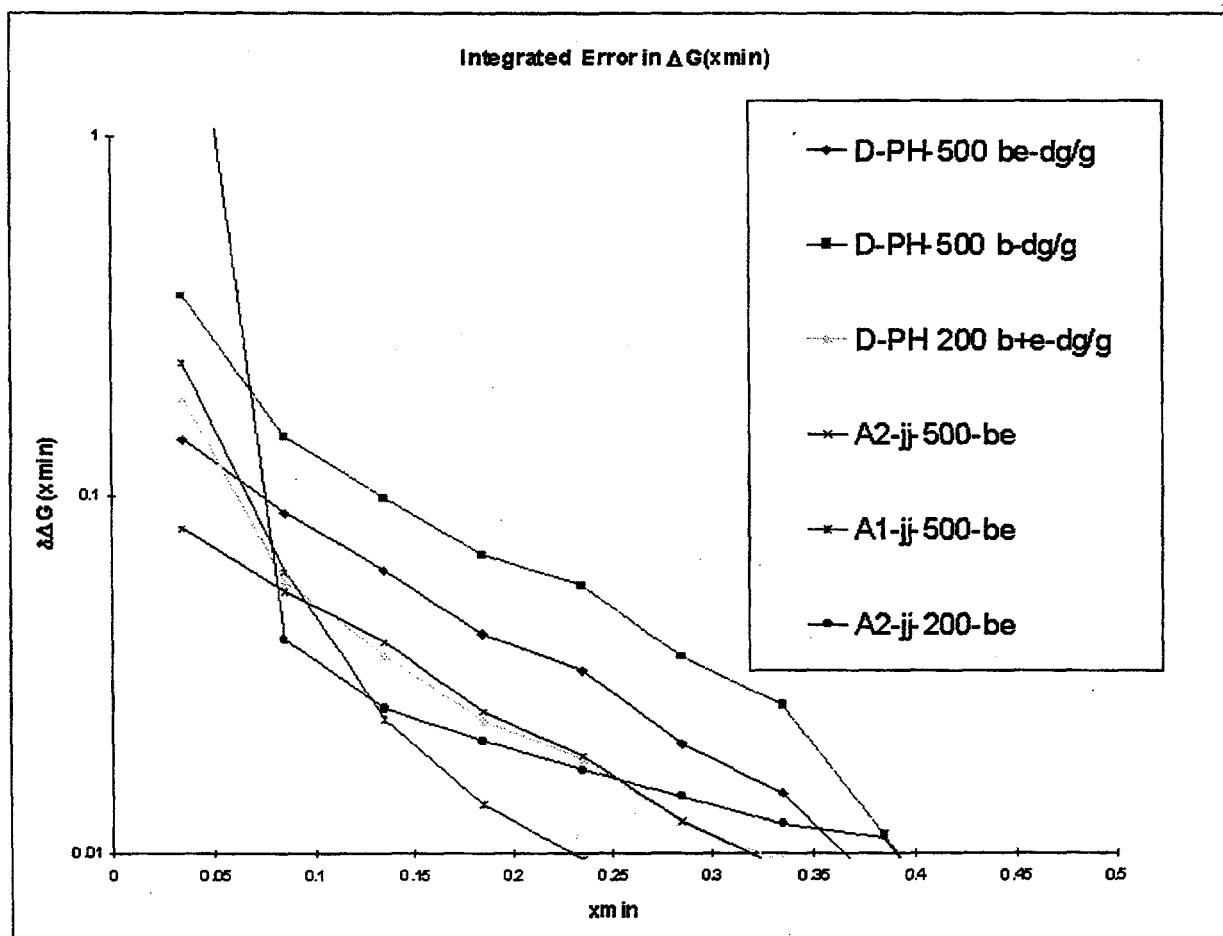
$$\Delta G(x \text{ min}) = \int_{x \text{ min}}^1 dx G(x) \left[\frac{\Delta G(x)}{G(x)} \right]$$

$$\delta[\Delta G(x \text{ min})] = \int_{x \text{ min}}^1 dx G(x) \delta \left[\frac{\Delta G(x)}{G(x)} \right]$$



Error in Integral $\Delta G(x_{min})$ For Various Measurements

Integrated Error in $\Delta G(x_{min})$



Using Jets

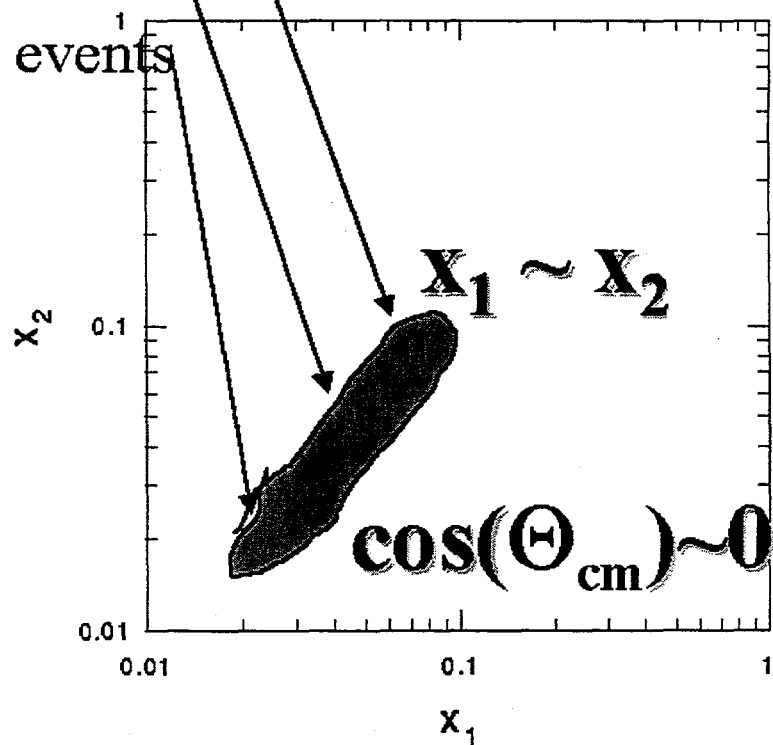
1. To many events.
2. Small $x \Leftrightarrow$ low pt
3. Messy

Selection: $|Y_1| < .2$ $|Y_2| < .2$

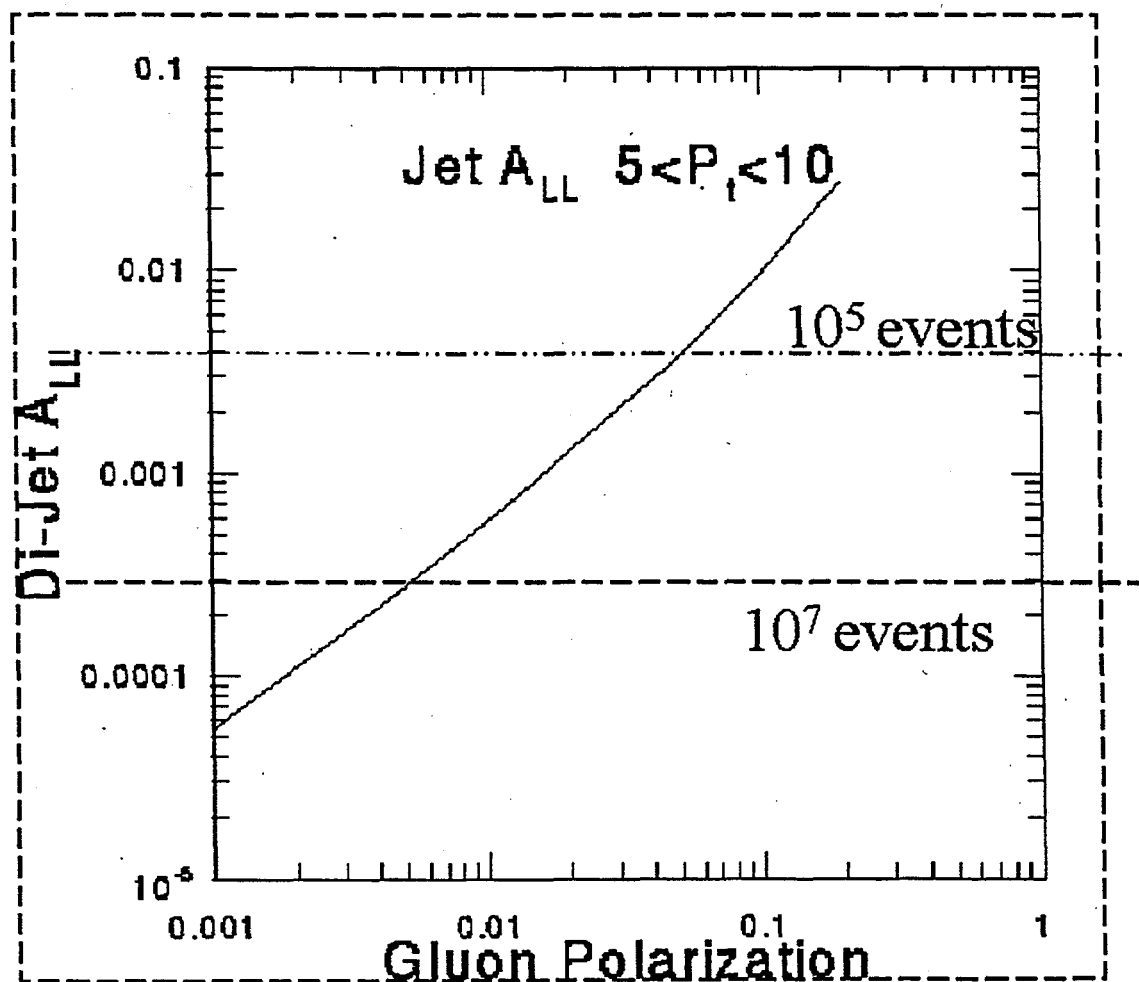
• $P_t > 20$ 10^5 events

• $P_t > 10$ 10^6 events

• $P_t > 5$ 10^7 events



Asymmetry vs Gluon Polarization around $x \sim .02$



Gluon Polarization and Dihadron Production at RHIC

Guanghua Xu

University of California, Riverside, CA 92521

J. C. Peng

Los Alamos National Laboratory, Los Alamos, NM 87545

1. Introduction

Recent Deep-Inelastic Scattering (DIS) experiments have indicated that gluons may play an important role in the spin structure of the proton. As an electromagnetic process, the DIS is not directly sensitive to the neutral gluons. In contrast, polarized p-p collisions at RHIC offers an opportunity to probe the gluon distributions via strong interaction processes. Indeed, one of the main goals of the RHIC-spin physics program is to determine the spin-dependent gluon structure functions. The processes sensitive to the gluon structure functions include direct-photon production, open-charm production, and jet production. Although the process of dijet production in hadron-hadron collisions have been studied in the literature [1], a closely related process, namely the high-mass dihadron production, has received little attention so far. The purpose of this note is to discuss the feasibility of using dihadron production at RHIC to extract information on the spin-dependent gluon structure functions.

For dijet and dihadron production, subprocesses involving quark-quark, quark-gluon and gluon-gluon scatterings can all contribute to the observed cross sections and double helicity asymmetries. To distinguish the effects of gluons from those of quarks, it is important to identify the kinematic region where gluon subprocesses play a dominant role. After identifying the region where gluon dominates, it is necessary to check how sensitively the measurements can separate different parametrizations of gluon structure functions.

In Section 2, we present the formula and calculations for the cross sections and double helicity asymmetries for both the dijet and the dihadron productions. The expected sensitivity of dihadron measurement at PHENIX for distinguishing various parametrizations of the spin-dependent gluon structure functions will be presented in Section 3. Summary and future prospect will be given in Section 4.

2. Dijet and Dihadron Productions in Hadron-Hadron Collisions

Consider two jets produced with rapidities y_1 and y_2 and with equal and opposite transverse momentum p_T . The differential cross section and the double helicity asymmetry A_{LL} can be written as[1]

$$\frac{d^3\sigma}{dM dy_1 dy_2} = \frac{M^3}{2s \cdot \cosh^2 y^*} \sum_{a,b} \frac{1}{1 + \delta_{ab}}$$

$$[f_A^a(x_A, Q^2) f_B^b(x_B, Q^2) \frac{d\hat{\sigma}_{ab}}{d\hat{t}}(\hat{s}, \hat{t}, \hat{u}) + (a \leftrightarrow b)], \quad (1)$$

$$A_{LL} = \left(\frac{d^3\sigma}{dM dy_1 dy_2} \right)^{-1} \frac{M^3}{2s \cdot \cosh^2 y^*} \sum_{i,j} \frac{1}{1 + \delta_{ab}} \cdot [\Delta f_A^a(x_A, Q^2) \Delta f_B^b(x_B, Q^2) \hat{a}_{LL}^{ab} \frac{d\hat{\sigma}_{ab}}{d\hat{t}}(\hat{s}, \hat{t}, \hat{u}) + (a \leftrightarrow b)], \quad (2)$$

where

$$M = 2p_T \cosh y^*, \quad Q^2 = p_T^2/4, \\ x_A = \sqrt{\tau} e^y, \quad x_B = \sqrt{\tau} e^{-y}, \quad (3)$$

with

$$\tau = \frac{M^2}{s}, \\ y^* = \frac{1}{2}(y_1 - y_2), \quad y = \frac{1}{2}(y_1 + y_2). \quad (4)$$

In Eqs. 1 and 2 the $d\hat{\sigma}_{ab}/d\hat{t}$ and \hat{a}_{LL}^{ab} are the cross section and the double helicity asymmetry of the hard scattering subprocesses[1], and $f_A^a(x_A, Q^2)$ and $\Delta f_A^a(x_A, Q^2)$ are spin-averaged and spin-dependent structure functions of parton a in hadron A . We will use the structure functions given by Gehrmann and Stirling (G-S) [2], which reproduce the DIS data well, as the inputs to our calculations. The $d^3\sigma/dM dy_1 dy_2$ and A_{LL} versus the jet-pair mass M at $y_1 = y_2 = 0$ and $\sqrt{s} = 500 \text{ GeV}$ are shown in Figs. 1(a) and 1(b), respectively.

Fig. 1 shows that the gluon-gluon scattering process dominates at most kinematic region. This is due to the facts that: (i) $(d\hat{\sigma}/d\hat{t})_{gg}$ is significantly larger than other processes, e.g. $(d\hat{\sigma}/d\hat{t})_{gg \rightarrow gg} : (d\hat{\sigma}/d\hat{t})_{qq \rightarrow qq} : (d\hat{\sigma}/d\hat{t})_{q\bar{q} \rightarrow q'\bar{q}'}$ = 30.4 : 3.26 : 0.22 at $\theta = 90^\circ$. (ii) $(\hat{a}_{LL})_{gg \rightarrow gg}$ has a large positive value ($(\hat{a}_{LL})_{gg \rightarrow gg} = 0.77$ at $\theta = 90^\circ$). (iii) gluons are more abundant than the quarks at the relatively small x region ($x \leq 0.3$) explored at RHIC. Therefore, as long as ΔG is not too small, we would expect important contributions to A_{LL} from gluon-gluon scatterings.

As the rapidity of the dijet increases, our calculations show that the quark-gluon scattering process becomes increasingly important. Hence, by choosing a small polar angle θ (which corresponds to a large dijet rapidity), one can detect dijets which are sensitive to the valence

quark distributions. More detailed discussion on the rapidity dependence of dijet production will be presented elsewhere [3].

To examine the sensitivity of dijet production to spin-dependent gluon structure functions, we show in Fig. 1(c) the double helicity asymmetries using three different G-S parametrizations[2] (sets A, B, and C). As shown in Fig. 1(c), different $\Delta G(x, Q^2)$ gives very different A_{LL} , suggesting that dijet production can be used to distinguish different parametrizations for the gluon polarization.

The cross section and double helicity asymmetry for dihadron production in hadron-hadron collisions ($A+B \rightarrow C+D+X$) are given by[3,4]

$$\frac{d^3\sigma}{dM dy_1 dy_2} = \frac{2x_{T_1} x_{T_2}}{\cosh y^*} \int_{p_{Tmin}}^{p_{Tmax}} dp_T \sqrt{\frac{p_T^C p_T^D}{(p_T^C)^2 + (p_T^D)^2}} \int_{z_{min}}^{z_{max}} \frac{dz_C}{z_C^3} \sum_{a,b} f_A^a\left(\frac{x_{T_1}}{z_C}, Q^2\right) f_B^b\left(\frac{x_{T_2}}{z_C}, Q^2\right) D_c^C(z_C) D_d^D(z_D) \frac{d\hat{\sigma}_{ab}(a+b \rightarrow c+d)}{d\hat{t}}, \quad (5)$$

$$A_{LL} = \left(\frac{d^3\sigma}{dM dy_1 dy_2}\right)^{-1} \frac{2x_{T_1} x_{T_2}}{\cosh y^*} \int_{p_{Tmin}}^{p_{Tmax}} dp_T \int_{z_{min}}^{z_{max}} \frac{dz_C}{z_C^3} \sqrt{\frac{p_T^C p_T^D}{(p_T^C)^2 + (p_T^D)^2}} \sum_{a,b} \Delta f_A^a\left(\frac{x_{T_1}}{z_C}, Q^2\right) \Delta f_B^b\left(\frac{x_{T_2}}{z_C}, Q^2\right) \hat{a}_{LL}^{ab} \frac{d\hat{\sigma}_{ab}(a+b \rightarrow c+d)}{d\hat{t}} D_c^C(z_C) D_d^D(z_D), \quad (6)$$

with

$$M = 2\sqrt{p_T^C p_T^D} \cosh y^*, \quad Q^2 = \frac{(p_T^C)^2}{4z_C^2} \\ x_{T_1} = \frac{p_T^C}{\sqrt{s}}(e^{y_1} + e^{y_2}), \quad x_{T_2} = \frac{p_T^D}{\sqrt{s}}(e^{-y_1} + e^{-y_2}) \\ p_T = |p_T^D| - |p_T^C|, \quad z_D = z_C |p_T^D/p_T^C|, \\ z_{min} = \max(x_{T_1}, x_{T_2}), \\ z_{max} = \begin{cases} 1 & \text{if } |p_T^D/p_T^C| < 1 \\ |p_T^C/p_T^D| & \text{if } |p_T^D/p_T^C| > 1 \end{cases} \quad (7)$$

where $d\hat{\sigma}_{ab}/d\hat{t}$, \hat{a}_{LL}^{ab} , $f_A^a(x, Q^2)$ and $\Delta f_A^a(x, Q^2)$ have the same definitions as in the dijet case, and (p_{Tmin}, p_{Tmax}) specifies the range of the net p_T of the dihadron. $D_c^C(z)$ and $D_d^D(z)$ are the fragmentation functions describing the probability for a parton to hadronize into a hadron carrying a fraction z of the parton momentum.

If we integrate over y_1 and y_2 , Eq. 5 can be written as

$$\frac{d\sigma}{dM} = \int_{-Y}^Y dy_1 \int_{y_{min}}^{y_{max}} dy_2 \frac{d^3\sigma}{dM dy_1 dy_2}, \quad (8)$$

and a similar expression for A_{LL} . The rapidity coverage for the detector is from $-Y$ to Y , and

$$y_{min} = \max(-Y, \ln \frac{M^2}{s} - y_1), \\ y_{max} = \min(Y, -y_1 - \ln \frac{M^2}{s}). \quad (9)$$

We have calculated the differential cross section and double helicity asymmetry A_{LL} for π^0 -pair production in p-p collision. We chose π^0 -pair production in our study for two reasons. First, the detection of π^0 is relatively straightforward since it only requires electromagnetic calorimeter. Second, there exist some π^0 -pair production data from ISR [5] and our calculations can be compared with these data.

Using the structure functions of [2] and the fragmentation functions given in [6], we calculated the differential cross section $d^3\sigma/dM dy_1 dy_2$ and A_{LL} for π^0 -pair production in p-p collision at $y_1 = y_2 = 0$ and $\sqrt{s} = 500 \text{ GeV}$ for $|p_T| < 1 \text{ GeV}/c$. The results are shown in Figs. 2(a) and 2(b). Comparing Fig. 2 with Fig. 1, one observes similar shapes for A_{LL} in dijet and dihadron productions. However, the predicted A_{LL} is shifted towards lower dihadron mass M for dihadron production versus dijet production. In other words, there appears to be a correspondence between the dijet production at a given M and the dihadron productions at a lower M .

This approximate correspondence between dijet and dihadron productions can be understood by considering the simple case of $y_1 = y_2 = 0$ and the net dihadron $p_T = 0$. We find $M_{dihadron} \sim \bar{z} M_{dijet}$, where \bar{z} is the mean value of z , and the dihadron production is sampling the x region very similar to that of the dijet production. This rough correspondence between dijet and dihadron productions has an important implication, namely, information which are obtained from high- M dijet measurement can already be obtained in dihadron measurement at significantly lower M .

To check the sensitivity of dihadron production to the gluon polarization, we show in Fig. 2(c) the predictions for A_{LL} for the three G-S $\Delta G(x, Q^2)$ parametrizations.[2] The results indicate good sensitivity to the spin-dependent gluon structure functions just like the case for dijet production. This is to be expected given the rough correspondence property discussed above.

An extensive study of π^0 -pair production in pp collisions has been performed at ISR by the CCOR collaboration.[5] In Fig. 3, we compare our calculations with the CCOR data. Note that a normalization factor of 2.5 has been applied to the calculations. This normalization factor is reminiscent of the K -factor in the Drell-Yan process and it reflects additional contributions from higher-order processes to the dihadron productions. The mass and the \sqrt{s} dependences of the CCOR data are well reproduced by our calculations.

3. Dihadron Productions at PHENIX

In this Section, we consider the expected rates and sensitivities for measuring π^0 -pair productions using the PHENIX detector at RHIC.

RHIC can accelerate polarized proton beams up to $\sqrt{s} = 500\text{GeV}$ at the luminosity of $2 \times 10^{32} \times (\sqrt{s}/500)\text{cm}^{-2}\text{sec}^{-1}$ with large polarization of 70%. In the following studies, we will assume the integrated luminosity of 800pb^{-1} for $\sqrt{s} = 500\text{GeV}$, which corresponds to 10 weeks of running time.

The azimuthal acceptance for PHENIX detectors is about 135° . For net $p_T < 1\text{GeV}/c$, and $\Delta y_1 = \Delta y_2 = 0.15$ around $y_1 = y_2 = 0$, we show in Fig. 2(c) the expected statistical errors for a 10-week run. The dihadron measurements can clearly separate the three ΔG 's given in [2].

If we integrate over the polar angles corresponding to the PHENIX acceptance in pseudo rapidity, $-0.35 < \eta < 0.35$, the expected yields for π^0 -pair production are listed in the following (where the unit of M is GeV/c^2):

Kinematic Range	Yield
$8 < M < 12$	$\sim 5.0 \times 10^6$
$12 < M < 16$	$\sim 6.1 \times 10^5$
$16 < M < 36$	$\sim 1.7 \times 10^5$
$36 < M < 52$	$\sim 1.2 \times 10^3$

The sensitivity of this measurement to the three ΔG 's is shown in Fig. 4. The integration over the polar angles will smear out the kinematic region x for a given M , but better statistics will be obtained for distinguishing the three ΔG 's.

As seen from Fig. 2(c) and Fig. 4, one can distinguish the three ΔG 's quite well at least up to $M \simeq 20\text{GeV}/c^2$, which corresponds to $x \simeq 0.13$. For distinguishing the three ΔG 's at higher M , more statistics is needed.

4. Summary and Future Prospect

We would summarize the above discussions as follows:

1. Dihadron and dijet productions at RHIC are sensitive to gluon structure functions.
2. A rough correspondence exists between dihadron and dijet productions. This feature makes it possible to use dihadron production as an alternative method to study spin-dependent gluon structure functions.
3. A two-month measurement for π^0 -pair production at PHENIX could clearly distinguish the various Gehrmann and Stirling polarized gluon structure functions.
4. Further studies are required to investigate the sensitivity of these results to fragmentation functions, and to extend the investigation to other dihadron channels such as $\pi^+\pi^-$.

Acknowledgements

We would like to thank Dr. Joel Moss of LANL and Dr. Mike Tannenbaum of BNL for valuable discussions.

-
- [1] C. Bourrely et al., Phys. Rep. **177** (1989) 319.
 - [2] T. Gehrmann and W.J. Stirling, Phys. Rev. D **53** (1996) 6100.
 - [3] G. Xu and J. C. Peng, to be published.
 - [4] R. Baier et al., Z. Physik C, Particles and Fields **2** (1979) 265.
 - [5] A.L.S. Angelis et al., Nucl. Phys. B **209** (1982) 284.
 - [6] P. Chiappetta et al., Nucl. Phys. B **412** (1994) 3.

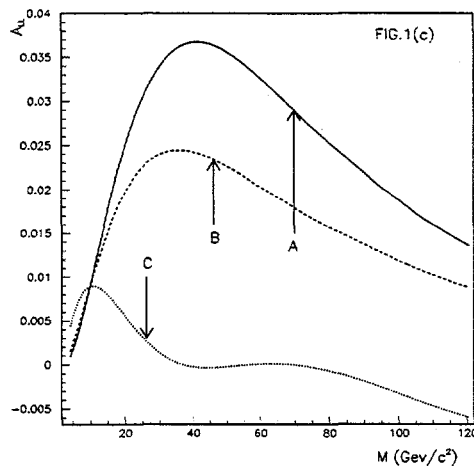
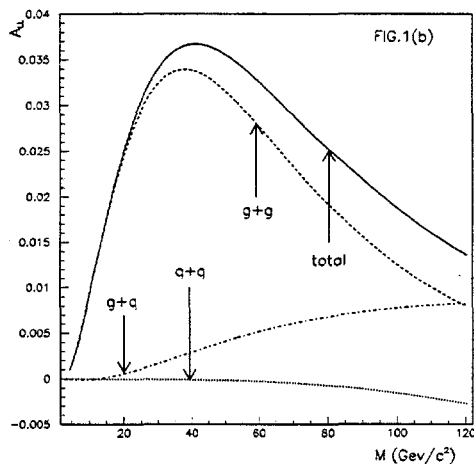
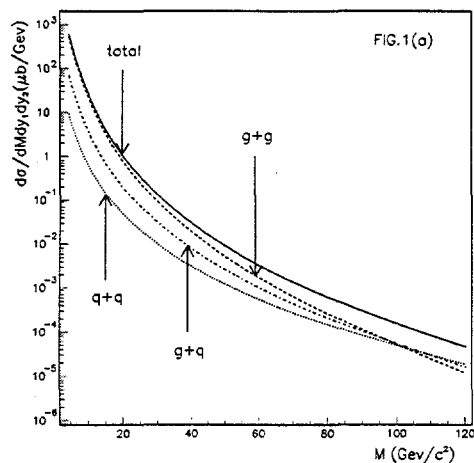


FIG. 1. Calculations of dijet productions in p-p collisions at $\sqrt{s} = 500\text{GeV}$ and $y_1 = y_2 = 0$. (a) and (b) show the contributions from various subprocesses to the cross section and double helicity asymmetry, and (c) shows the A_{LL} using three sets of parametrizations of gluon polarization given in [2].

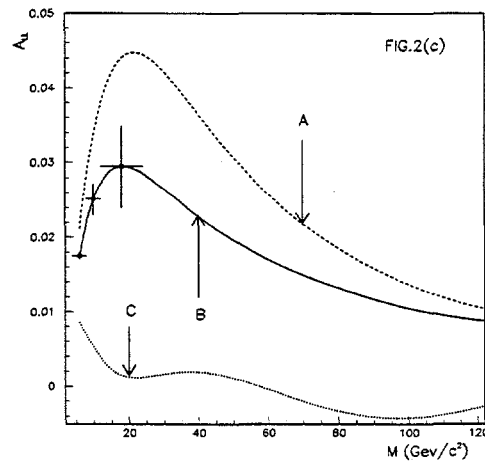
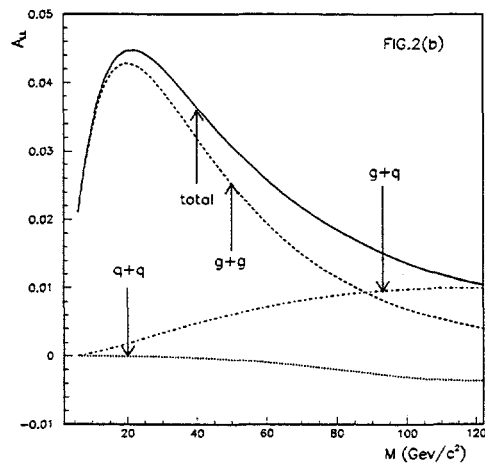
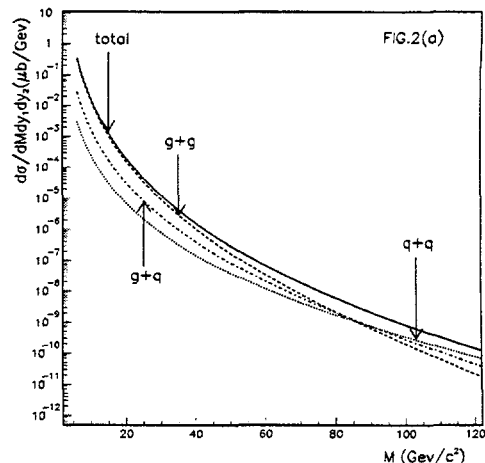


FIG. 2. Calculations of π^0 -pair productions in p-p collisions at $\sqrt{s} = 500\text{GeV}$ and $y_1 = y_2 = 0$. (a) and (b) show the contributions from various subprocesses to the cross section and double helicity asymmetry, and (c) shows the A_{LL} using three sets of parametrizations of gluon polarization given in [2] and the expected statistical errors for a 800pb^{-1} run in PHENIX.

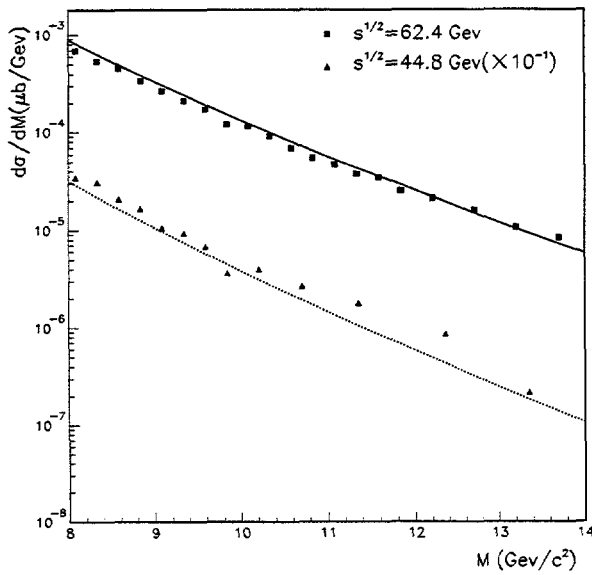


FIG. 3. Comparison between the calculations and the π^0 -pair production data in p-p collision from CCOR[5] at \sqrt{s} of 44.8 and 62.4 GeV. A normalization factor of 2.5 has been multiplied to the calculations at both energies.

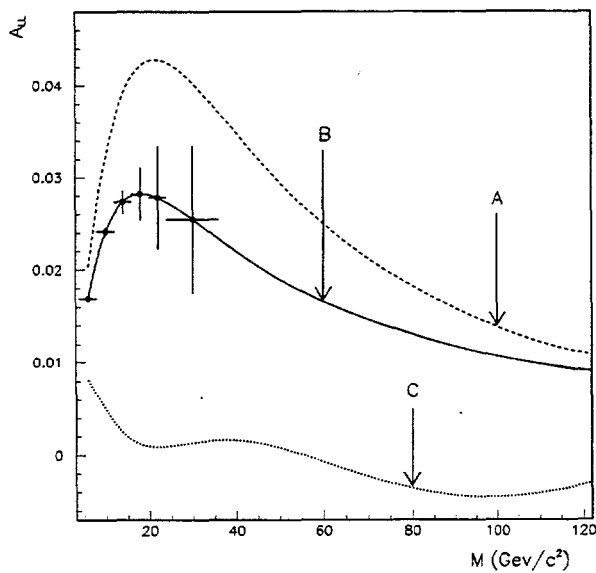


FIG. 4. Calculations of A_{LL} for π^0 -pair detection at $\sqrt{s} = 500\text{GeV}$ integrated over the full acceptance of the PHENIX detector. The expected statistical errors for a 800pb^{-1} run are also shown

Determination of ΔG from Open Heavy-Flavor Production*

Melynda Brooks, Joel Moss
Los Alamos National Laboratory

A study has been performed to look at the feasibility of getting a measure of $\Delta G/G$ by measuring the asymmetry in single muon production from heavy quarks, using the PHENIX muon detector. If the dominant production mechanism for heavy-quarks is assumed to be gluon-gluon fusion, then the asymmetry can be written as

$$A_{LL} = \Delta G/G(x_1) * \Delta G/G(x_2) * \hat{a} \quad (1)$$

$$\hat{a} = \frac{-(32y^2 - 16y^4 - 8x^2 - 8x^2y^2 + 8x^2y^4 + x^4 - x^4y^4)}{(32 - 32y^2 - 16y^4 + 8x^2 - 8x^2y^2 + 8x^2y^4 + x^2 - x^4y^4)} \quad (2)$$

where $x = \sqrt{\bullet}/m_Q$, $\bullet = s x_1 x_2$, and $y = \cos(\theta)$. If the analyzing power, \hat{a} , is large then a measurement of the asymmetry in heavy-quark production will provide a sensitive measurement of $\Delta G/G$ at the x_1, x_2 probed by the detector at the given \sqrt{s} running. For the PHENIX muon detector acceptance and $\sqrt{s} = 200$ GeV running, the analyzing power varies and is only found to be consistently large (and negative) at large p_t (>6 GeV) of the measured muon. Therefore, if you want to measure an asymmetry which is sensitive to the polarized gluon structure function, you should measure single muons at large p_t .

A simulation was performed to look at the overall sensitivity of an asymmetry measurement using the PHENIX detector's south muon arm. Muons from b and c quarks were produced using PYTHIA, tuned to match b and c experimental data. A detector acceptance cut was put on the muons, the x_1 and x_2 of the production obtained from PYTHIA, the analyzing power calculated from equation (2), and the resulting asymmetry determined using different polarized gluon structure functions from Gehrmann and Stirling [1] and equation (1). The asymmetry and its statistical error were then examined versus different p_t cuts on the accepted muon. The results showed that for an integrated luminosity of 320 pb^{-1} and $p_t > 6$ GeV, a significant measurement of A_{LL} , $\Delta G/G$ can be obtained which can easily distinguish between the B + C models of Gehrmann and Stirling (see figure from talk).

The background single muons, which come primarily from the decays of pions, kaons, and J/ψ s, were also examined and found to be produced well below the level of single muons from b and c for the PHENIX muon acceptance and $\sqrt{s} = 200$ GeV. In addition, any contribution to the asymmetry from muons from pion and kaon decay can be examined by looking at the single muons versus the event vertex since the decay muons will preferentially come from events that have a vertex far from the absorber material in front of the muon tracking volume rather than events with a vertex close to the absorber material.

*Talk can be found at:

<http://www.rhic.bnl.gov/phenix/WWW/publish/brooks/meetings/spin27apr98/index.htm>

*Paper can be found at:

http://www.rhic.bnl.gov/phenix/WWW/muon/working_group/muphysics/single_muon/singlemu.pdf

[1] T. Gehrmann and W. J. Stirling, Z. Phys. C65, 461 (1995).

Determination of ΔG from Open Heavy-Flavor Production

J. Moss*, M. Brooks

How to get a measure of $\Delta G/G$ with single muons

PHENIX Measurement:

PHENIX muon arms

Simulations performed to study sensitivity of measurement

Determination of ΔG from Open Heavy-Flavor Production

Heavy quarks (b,c) produced via two-gluon fusion
 Quarks produce single muons detected in 1 of the PHENIX muon arms
 Asymmetry in production is related to $\Delta G/G$ via the following equations:

$$A_{LL}(x_1, x_2) \cong \frac{\Delta G}{G}(x_1) \frac{\Delta G}{G}(x_2) \hat{a}$$

$$\hat{a} = \frac{-(32y^2 - 16y^4 - 8x^2 - 8x^2y^2 + 8x^2y^4 + x^4 + x^4y^4)}{32 - 32y^2 - 16y^4 + 8x^2 - 8x^2y^2 + 8x^2y^4 + x^2 - x^4y^4}$$

$$x = \sqrt{\hat{s}}/m_Q \quad \hat{s} = s x_1 x_2 \quad y = \cos(\theta)$$

If \hat{a} is large enough, A_{LL} measurement is sensitive to $\Delta G/G$.

Simulation of Single Muons

SIGNAL:

Generate charm and beauty events with PYTHIA ($\sigma=200\mu\text{barns}$, $2\mu\text{barns}$, $\sqrt{s}=200\text{ GeV}$)

BACKGROUNDS:

Generate pions and kaons using Boggild* parameterization

Generate J/ψ based on work by Vogt** ($\sigma_B=0.078\ \mu\text{barns}$)

Run events through "fast" simulator which includes acceptance of muon arm, simulates π and K decay before the tracking volume

Compare smaller set of events from full PISA/PISORP simulation to "fast" simulator to verify it works well

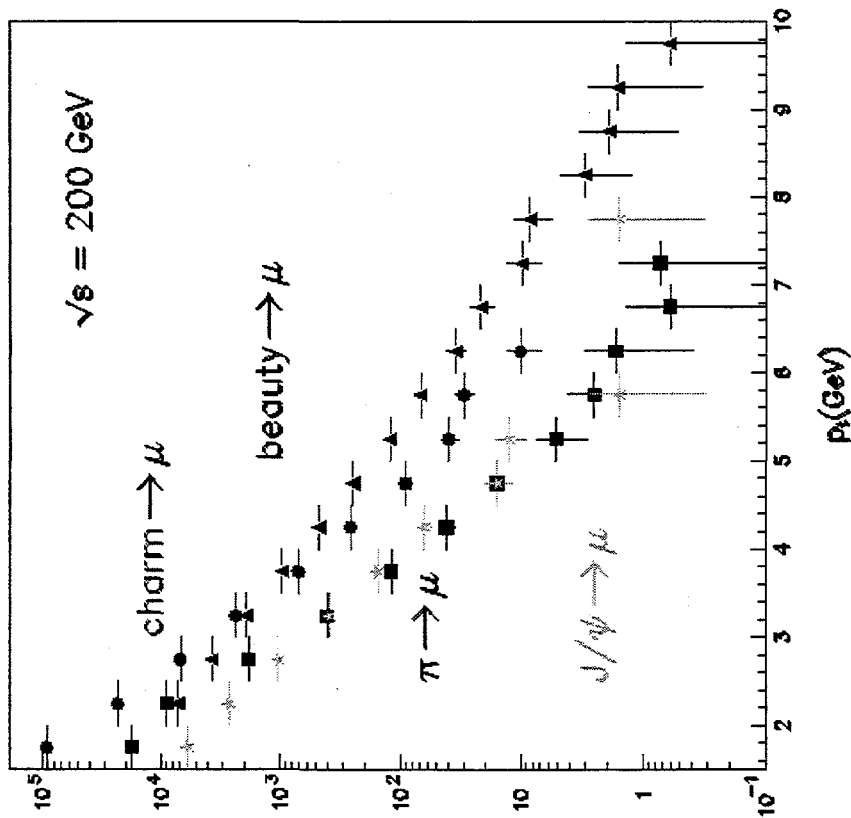
Calculate A_{LL} using x_1 , x_2 from event generator for each "accepted" event

Examine versus p_t of accepted muon

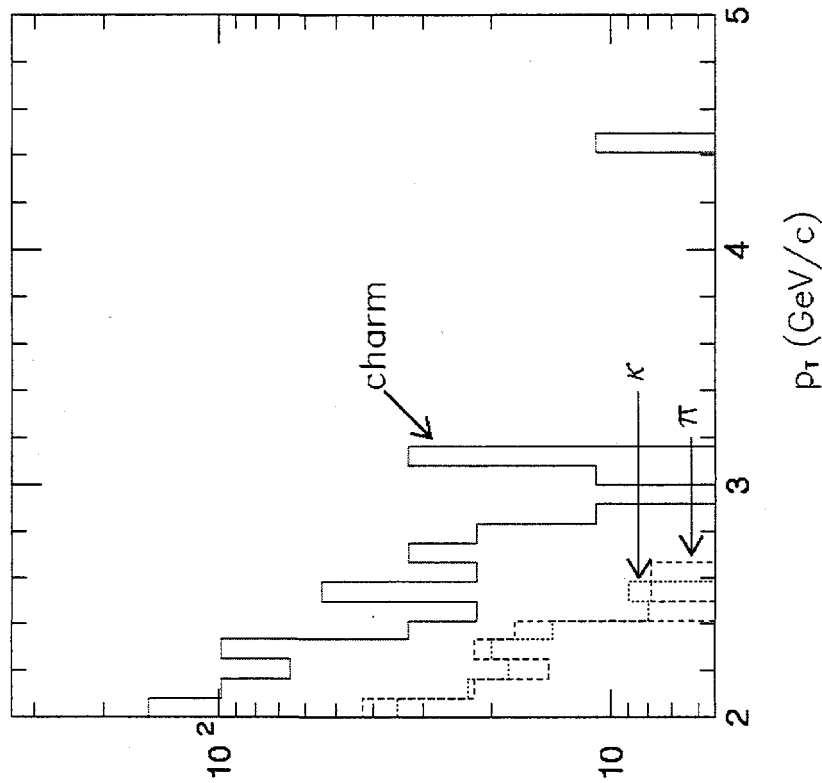
*from private communication with J. Moss

**Atom. Nucl. Data Tabl. 50, 343(1992)

Single muons from heavy quarks and "backgrounds" accepted into South Arm



"Fast" simulator



"Slow" simulator

PHENIX

Production from 10% Luminosity

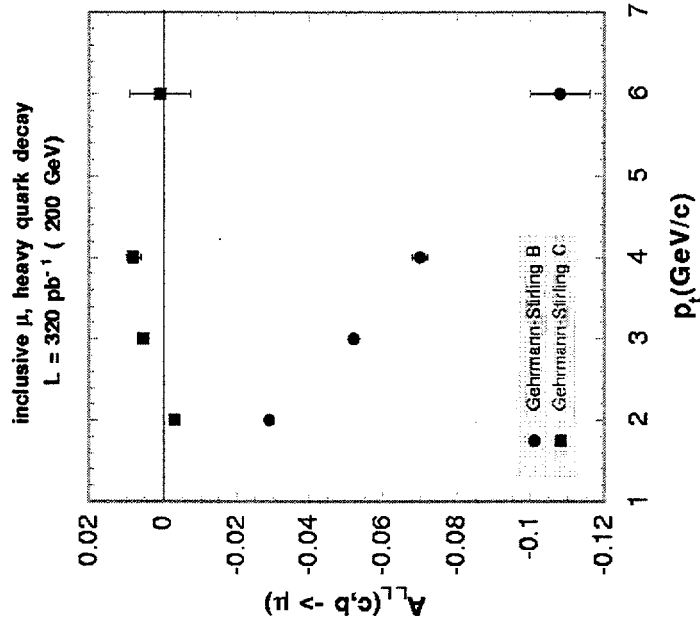
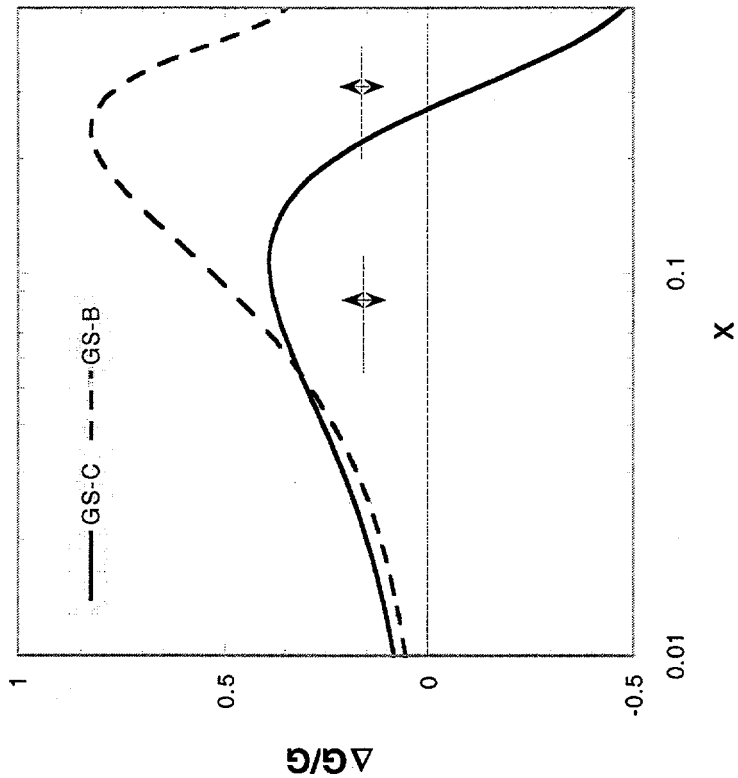
p_t (GeV/c)	charm	beauty
> 2	37300	32500
> 4	700	2370
> 6	21	222

Large production of c, b

p_t (GeV)	Quark	\hat{a}	A_{LL} (GS-B)	A_{LL} (GS-C)	δA_{LL}
> 2	c	-0.254	-0.044	-0.006	0.01
> 2	b	0.146	0.018	0.006	0.01
> 5	b	-0.135	-0.032	0.006	0.04
> 6	b	-0.501	-0.122	0.020	0.14

Need high p_t to get large \hat{a}

Asymmetry, ΔG Measurement at full luminosity running



$$A_{LL}(x_1, x_2) \cong \frac{\Delta G}{G}(x_1) \frac{\Delta G}{G}(x_2) \hat{a}$$

J/ψ Production in pp Collision at PHENIX

N.HAYASHI, Y. GOTO, K. KURITA and N. SAITO

The spin-dependent structure functions of the nucleon, particularly the quark spin contributions, have been studied extensively in polarized deep inelastic scattering experiments in the last decade. However, the gluon spin contribution to the nucleon spin remains as a weakly constrained quantity.

J/ψ production in proton-proton collision is dominated by gluon-gluon scattering process and relatively high rate is expected. Furthermore, the detection of J/ψ through its dilepton decay is experimentally rather unambiguous. Then, J/ψ production in pp is a good tool to study the gluon inside the proton.

However, theoretical understanding of the J/ψ production mechanism is not settled yet. There are three major models which describe J/ψ production and those were discussed in this talk. The best candidate is Color-Octet Model (COM) which has been developed in terms of NRQCD (Non-relativistic QCD) seems to agree the CDF J/ψ data, although still few problems remain.

The COM contribution is implemented into a physics event generator *PYTHIA* by following B.Cano-Coloma *et al.* prescription [1]. By using this program, we calculated that over 10^6 J/ψ ($p_T > 2$ GeV/ c) would be expected at PHENIX Muon-arm acceptance at $\sqrt{s} = 200$ GeV, which allows a precise asymmetry measurement. Sensitive x region of the gluon has a peak for larger $x \sim 0.1$, but much broader for the lower x . Subprocess asymmetries \hat{a}_{LL} have been calculated for each color-octet intermediate states. Next step is to calculate an inclusive J/ψ asymmetry basing on those facts for different ΔG predicted models.

References

- [1] B. Cano-Coloma, M.A. Sanchis-Lozano, Nucl. Phys. **B508** (1997) 753.

J/ψ Production Models

We have to start from production mechanism not only spin-dependent part.

- Color-Singlet Model (CSM):

R.Baier and R.Rückl, Z. Phys. ~~C21~~¹⁹ (198~~1~~)³ 251.

- J/ψ formation in color-singlet states $c\bar{c}$
- can't explain CDF direct J/ψ, ψ(2S) results

- Color-Octet Model (COM):

E.Braaten *et al.*, Annu.Rev.Nucl.Part.Sci. **46** (1996) 197.

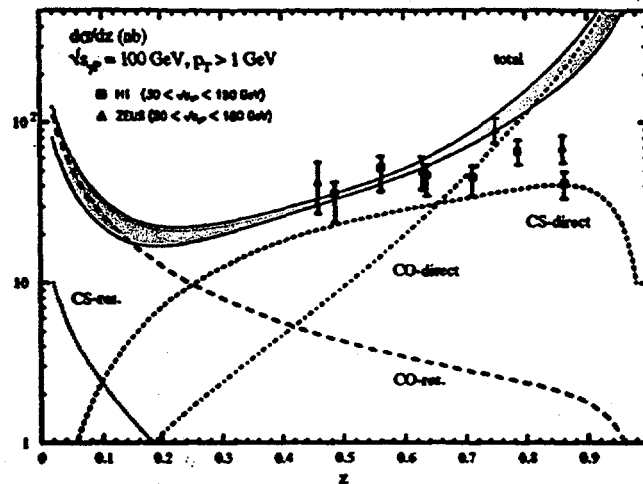
- color-octet states becomes J/ψ in non-perturbative region
- $g \rightarrow c$ fragmentation
- non-perturbative matrix elements ($\langle \mathcal{O}_8^{J/\psi}(^3S_1) \rangle$, etc.) determined by experimental data
- But HERA data not supportive

- Color Evaporation Model (CEM):

H.Fritzsch, Phys. Lett. **B67** (1977) 217.

- a certain fraction of $c\bar{c}$ pair forms J/ψ
- χ_c photoproduction rate can't be explained

J/ψ Photoproduction at HERA



M.Beneke, et al. Phys. Rev. D57(1998) 4258.

- How to interpret?
 - NLO correction
 - Modify non-perturbative matrix elements
 - $p_T(J/\psi) < 5$ is too sensitive ...
 - Small x behavior of the gluon ...

- Proof of COM
 - J/ψ polarization predicted by COM
 - Determination of non-perturbative matrix elements from other process ($b \rightarrow J/\psi$)
 - S.Fleming et al., Phys. Rev. D55 (1997) 4098
 - Lattice Calculation ...
 - G.T.Bodwin et al., Phys. Rev. Lett. 77 (1996) 2376.

Origin of J/ψ

$$J/\psi \left\{ \begin{array}{l} \text{prompt} \\ B \text{ decay} \end{array} \right. \left\{ \begin{array}{l} \text{direct} \\ \chi_c, \psi(2S) \text{ decay} \end{array} \right.$$

It was thought main contribution is B decay.
 CDF separated B decay origin by using SVX.
 They found that ...

Monte Carlo for J/ψ

PYTHIA : Monte Carlo generator
 CTEQ2L : parton parameterization

Color-Octet Model implemented into PYTHIA

hep-ph/9706270 B.Cano-Coloma, et al.

- tuned for CDF data
- For our study, only $g + g \rightarrow J/\psi + g$ is used.
 - Estimated 25% $g + q$ contribution is included by increasing a factor
- B decay contribution at CDF, 30%

J/ψ Yield

320 pb⁻¹ at $\sqrt{s} = 200$ GeV

800 pb⁻¹ at $\sqrt{s} = 500$ GeV

p_T (GeV/c)	$\sqrt{s} = 200$		$\sqrt{s} = 500$	
	Singlet	Octet	Singlet	Octet
2 - 4	720k	1.2M	540k	9.0M
4 - 6	2200	170k	19k	1.8M
6 - 8	140	3200	2200	520k
8 - 10			320	160k
10 - 12				62k
12 - 14				25k
14 - 16				11k
16 - 18				4700
18 - 20				2800

Summary

- J/ψ production in pp gluon-gluon process dominant
- J/ψ detection less problem and high statistics
- Color-Octet Model seems to be a choice...
 - But HERA data need to be explained
 - J/ψ polarization measurement is a test for the model
 - More theoretical progress should be done
- Color-Octet Model implemented into *PYTHIA*
- Consistency check with CDF J/ψ data
- J/ψ Yield Estimation for PHENIX

Yousef Makdisi
BNL, RHIC Project
RHIC Spin Collaboration Workshop
April 27 - 29, 1998

MEASURING THE BEAM POLARIZATION AT RHIC

(Introduction to the session)

We are within one year of witnessing the first heavy ion physics collisions at RHIC scheduled for June 1999. The hardware needed to commission one ring with polarized protons, two Siberian snakes and one polarimeter, should be installed prior to October 1999.

The road to develop a polarimeter for RHIC has been a long one. A committee was formed to choose from various polarimeter options with the target goal to measure the absolute beam polarization to 5%. This solution requires a polarized hydrogen jet target (A. Penzo) which will be used to calibrate the online polarimeters. This is envisaged beyond day-one.

The near term goal and financial constraints call for the installation of an inclusive pion polarimeter in one ring. This serves the commissioning phase and will measure the beam polarization to better than 10% between injection and 100 GeV/c. Towards this end, experiment E925 was installed on the AGS floor, ran with a polarized proton beam, and measured the asymmetries in inclusive pion production at RHIC injection energy from a carbon target with quite promising results (H. Spinka).

A parallel effort to develop a second polarimeter looking simultaneously at the same carbon target but utilizing the asymmetry in the Coulomb Nuclear Interference in P-C scattering has also netted interesting results in measurements at Kyoto (K. Imai) and at IUCF (D. Fields). If the concept proves viable at high energies, this is a promising method to measure the polarization of both beams in a single setup.

This session presents the status of these efforts and of course there is no shortage on new ideas, some of which will also be discussed. Our task is to finalize the designs, develop the hardware, and start installation in the RHIC tunnel starting this summer and continue during the periods when the tunnel is open in order to be ready by October 1999.

Constraints on the RHIC Polarimeter Design

The polarimeter(s) has to satisfy the following:

- Beam polarization monitor for Physics (5 %)
Several samples over the duration of a fill
- Beam polarization diagnostic tool
Sample on demand
Online
- Machine tuning tool
Fast/within few minutes
Online
- A large dynamic range Energy independent?
23 GeV/c at injection
250 GeV/c at top energy
- Measure A_N and if possible another component A_S
- Ideal Large analyzing Power &
Large Cross section &
Low background
- Reasonable Cost

Candidate Processes

- p-p Elastic scattering
The AGS internal polarimeter, the analyzing power is proportional to $1/p$. Experimental data good to 10%.
- Primakoff Production in the Coherent Coulomb region (E704)
 $p + Z \rightarrow \Delta / N^* + Z \rightarrow \pi^0 + p + Z$
 $(\gamma + p \rightarrow p + \pi^0)$ at $t < 0.001$

 Gave a large analyzing power of $-0.57 \pm 0.12 \pm .20$
 Large background.
 D. Carey et al Phys. Rev. Lett. **64**, 357 (1990)
- p-e elastic scattering
Calculable process with large analyzing power A_{NN} , A_{LL} in the forward direction of the electron and drops dramatically with large angles at few mr. A_{SL} possible at RHIC.

 I. V. Glavanakov et al. INP Tomsk preprint 2/95,1/96 and published in the proceedings of the Spin96.
- e-p Deep inelastic scattering, G. Igo (from SMC and SLAC)
- p-p elastic scattering in the CNI region using the PP2PP
- Inclusive Pion production from carbon,
E704 and ZGS from H₂
- P Carbon CNI (tests at Kyoto, IUCF, AGS)

The polarimeter Vs Energy

We envisage Two reference points:

23 GeV/c RHIC injection..... measured to 10%

200 GeV/c measured to 8-9%

A measurement at an energy inbetween involves:

- 1) Measure the asymmetry at a convenient anchor'
- 2) Move to the desired energy and measure the asymmetry there.
- 3) Return to the reference energy and measure again.

The assumption is that the dynamics of beam acceleration and deceleration will affect the polarization equally.

SATURNE II (500 - 3000 MeV).

A. Nakach et al. Determination of the Proton Beam Polarization at High Energies by Measurement After Deceleration. Proceedings of the 6th Symposium on High Energy Spin Physics, Marseille 1984, pp C2-647.

IUCF (200 - 400 MeV)

B. von Przewoski et al. Calibration of the Polarization of a Beam of Arbitrary Energy in a Storage Ring. Proceedings of SPIN96, pp 513.

C. Pollock at al. Sumbitted to Phys. Rev.

COST and Schedule

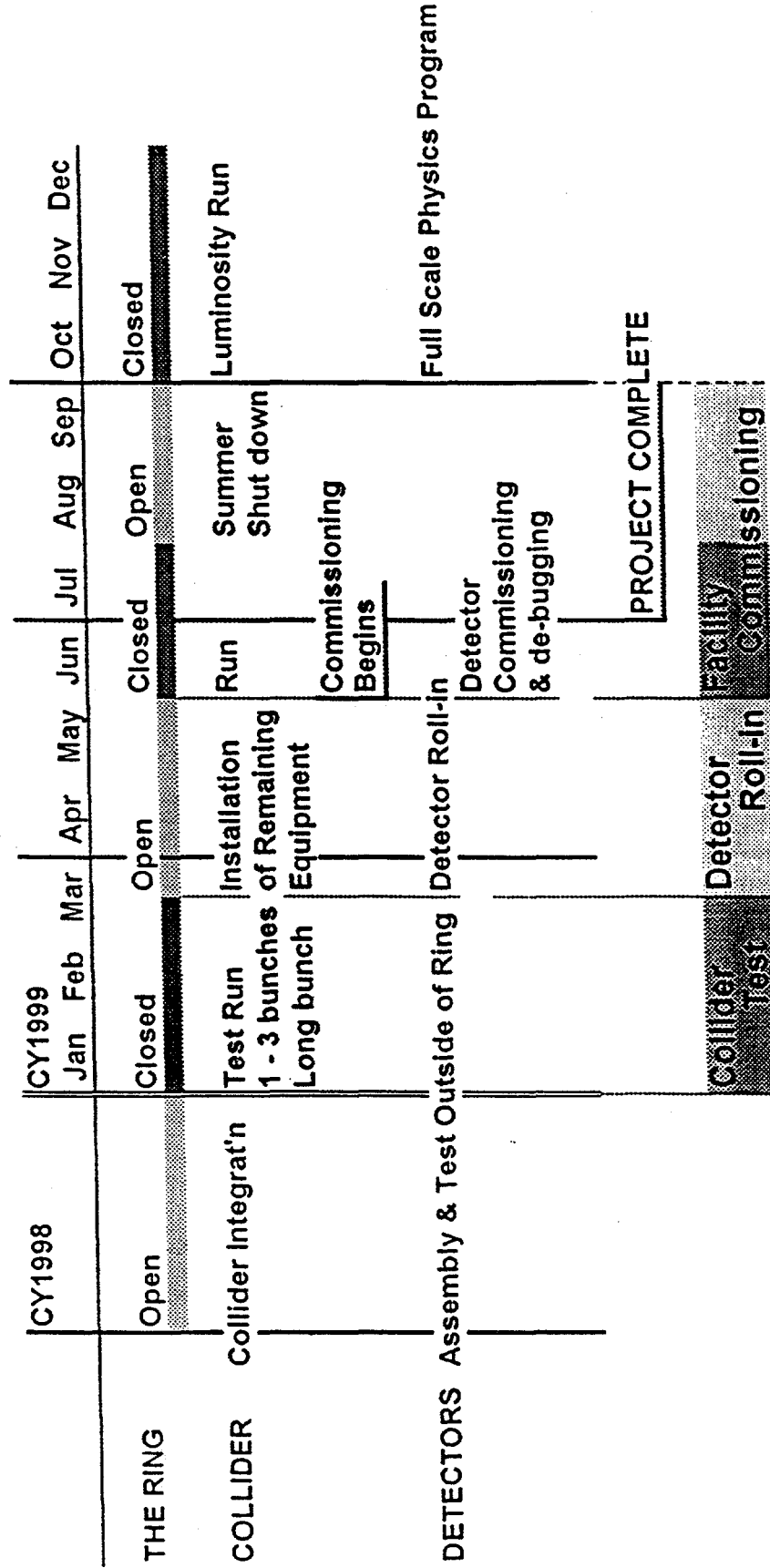
- At latest count the polarimeter cost has dropped from \$1.5 M to less than \$ 0.5 M.
- The profile sets the polarimeter(s) funding after the snake/rotator fabrication,
- This calls for a) creative financing, & b) recycling
- At least one polarimeter is required to allow commissioning in FY 2000,
- The work started now with construction and installation completed by Oct 1st, 1999.
- E880 and E925 are scheduled for another run in Feb 1999.

The 5% Solution and Long Range Plan

- Install a polarized hydrogen Jet Target,
- Measure the Jet target polarization to less than 5%,
- Measure the beam polarization,
- Calibrate analyzing power of the polarimeter to better than 5%,
- Use the calibrated polarimeter to measure the absolute beam polarization. This process could be done at any desired energy.

TOWARD THE COMMISSIONING, OPERATION & PHYSICS

Objective: Full scale physics program as early as possible



Full scale relativistic heavy ion physics program in the fall of 1999

Progress Report on the Design of the RHIC Pion Inclusive Polarimeter

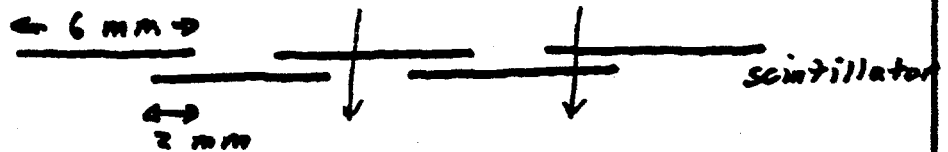
H. Spinka
27 April 1998

- Existing data (D.L. Adams et al., PL *B264*, 462 (1991) and W.H. Dragoset et al., PR *D18*, 3939 (1978) and preliminary data from BNL E925) suggest sizeable π^\pm inclusive asymmetries at large x_F . Both $\vec{p}p$ and $\vec{p}C$ reactions show these asymmetries.
- A revised pion inclusive polarimeter design is required by financial limitations. A carbon ribbon target, five dipole magnets, and scintillator hodoscopes will be used. The first three magnets will move for different beam momenta.
- The polarimeter design will cover beam momenta in the range 23 - 100 GeV/c, $x_F \geq 0.5$, and $P_T \geq 0.7$ GeV/c.
- It is suggested to record all scaler data for each bunch in both beams for use by RHIC experiments.
- The schedule is tight to complete the installation of the polarimeter hardware. The first polarized beam runs are expected to occur after Oct. 1999, but hardware from BNL E925 will not be available until after Feb. 1999.

Components of the Pion Inclusive

Polarimeter

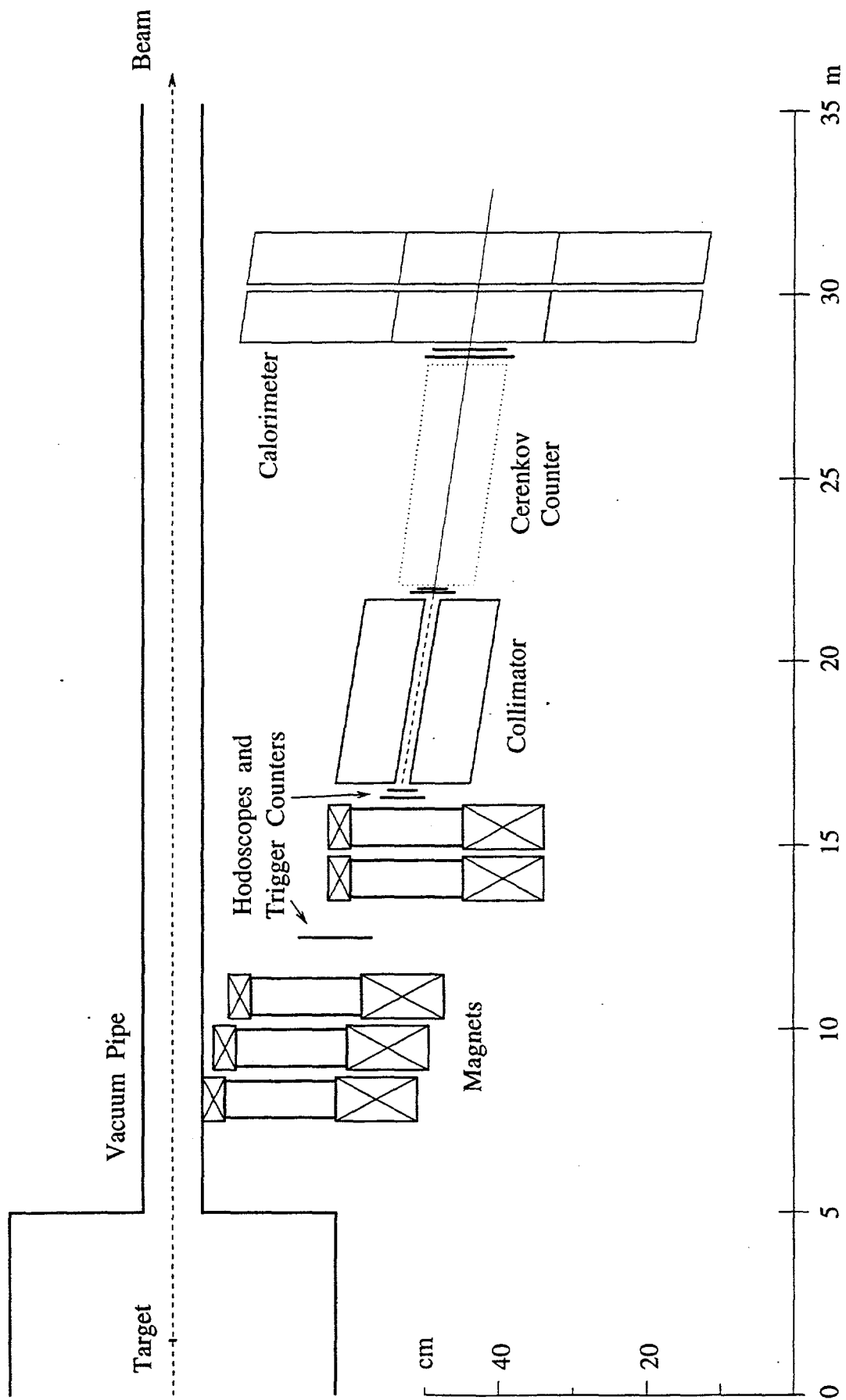
- Carbon Ribbon Target.
5 - 10 $\mu\text{gm}/\text{cm}^2$ 0.02 mm wide
plus a thin window in the vacuum box for pions to exit
- Five Dipole Magnets.
first three are movable, others are fixed
- Four Scintillator Hodoscopes.
modified from BNL E925 and FNAL E704
6 mm wide scintillators and 2 mm wide segments



#1	X plane	8-10 cm x 4 cm
#2	X, Y planes	3-4 cm x 5 cm
#3	X, Y planes	3-4 cm x 7 cm
#4	X, Y planes	10 cm x 10 cm

perhaps U and/or V planes in one or more hodoscopes

- ~5 m Long Collimator.
- Three Trigger Scintillators Near Hodoscopes #2-4.
- Optional Cerenkov Counter.
to identify pions from kaons and protons
- Hadron Calorimeter.
(borrow existing modules?)
- Luminosity Monitor Telescopes.
(three small scintillation counters per telescope, mounted above and below the beam looking at the carbon ribbon target)
- Cables, HVPS, Electronics.
- Data Acquisition Hardware.
including computer and associated software



Suggested Information Available

to RHIC Experiments

It is suggested to record in a file the following scalers for each bunch and beam whenever a polarimeter measurement is made:

- Luminosity monitor coincidences and accidentals.
- Coincidences and accidentals for each polarimeter arm.
- Duration of the measurement.

From this information, the expected average product of beam polarizations at each RHIC detector, weighted by the luminosities measured at the polarimeters, can be calculated and made available. However, each experiment may wish to calculate this product using luminosities measured in their intersection region or eliminating data from certain bunches. The data recorded in the file should allow such a calculation.

Schedule

The short-term schedule is:

- Feb. 1999 E925 run with liquid hydrogen
- Mar., April 1999 install some polarimeter hardware
- Mar.–Aug. 1999 modify E925 hodoscopes
- Aug., Sept. 1999 install additional polarimeter hardware
- after Oct. 1999 first polarized runs in one beam

After the first polarized runs, the polarimeter performance will need to be evaluated and perhaps changes or improvements made. A polarimeter in the other beam will need to be constructed before the first data taking with both beams polarized.

perhaps put down survey lines, install cables late 1998

Pion polarimetry issues.

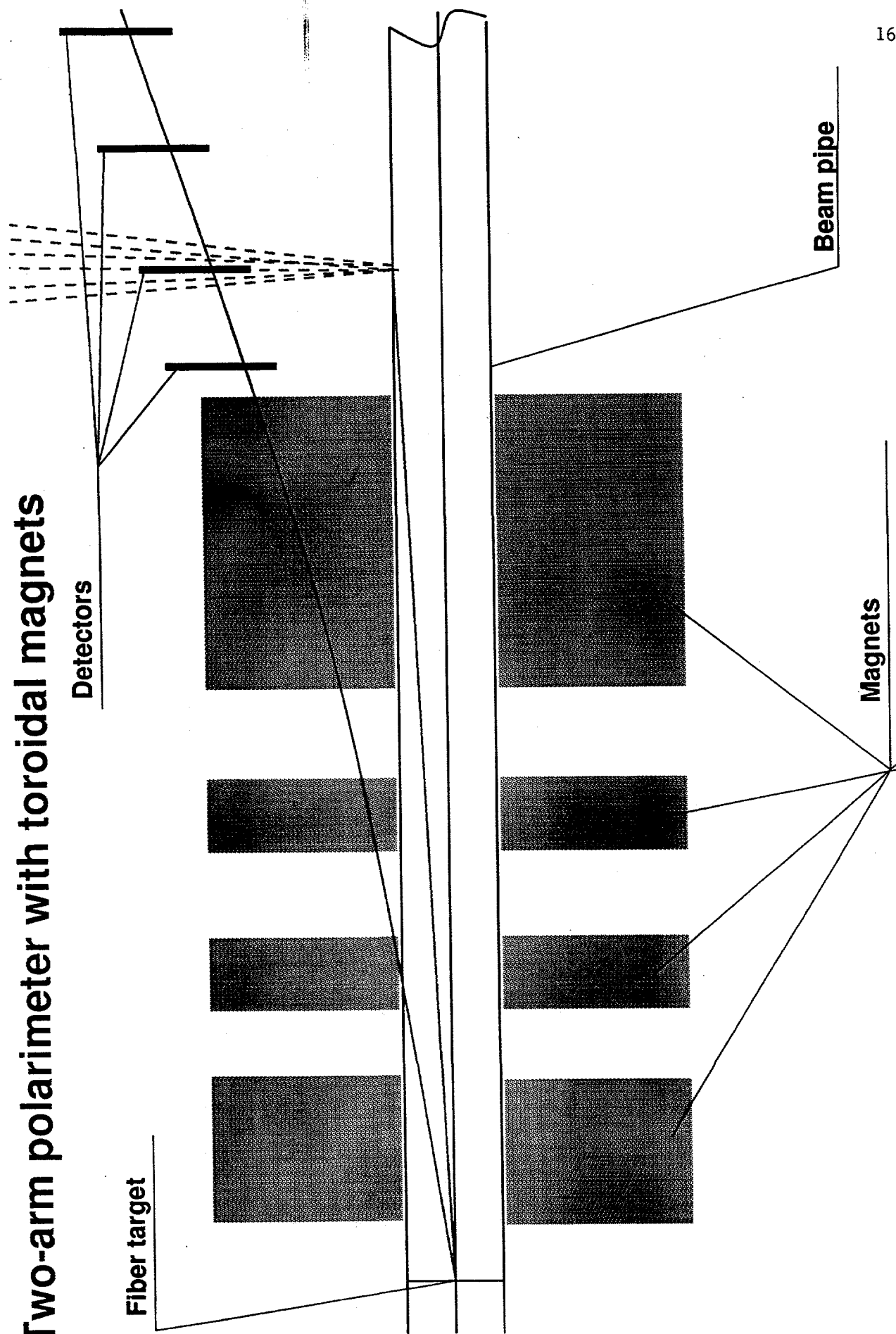
*I.G. Alekseev, V.P. Kanavets, B.V. Morozov,
V.M. Nesterov, D.N. Svirida.
(ITEP, Moscow)*

- **Some conclusions coming from background simulations.**

A simulation of detector acceptance and backgrounds was performed for two-armed polarimeter based on toroidal magnets. Our results could be interesting for understanding of current polarimeter design also.

- ◇ Inclusive pion polarimeter can work up to the highest intensities of RHIC: $P=250$ GeV/c, bunch filling $2 \cdot 10^{11}$ protons and 120 bunches per ring.
- ◇ Main source of parasitic particles comes from fast particles produced on the target, which go the most way in the beam pipe and then produce a shower on its wall. Due to the fact that detectors are too near to the tube this can not be cured by shielding.
- ◇ Acceptance is enough to ensure small measurement times, but the problem could come from emittance blowup at low energies, especially at small bunch filling. So we should not drop the acceptance without serious reasons.

Two-arm polarimeter with toroidal magnets



1 m.

- Absolute calibration of inclusive pion polarimeter with polarized jet target.

We can go on now with relative inclusive pion polarimeter and, if then a strong demand for precise absolute value arise, obtain it for old measurements also.

To have the same geometry for polarized target as for polarized beam we need:

$$p_{\text{beam}}^A/A = p_{\text{beam}}^P;$$

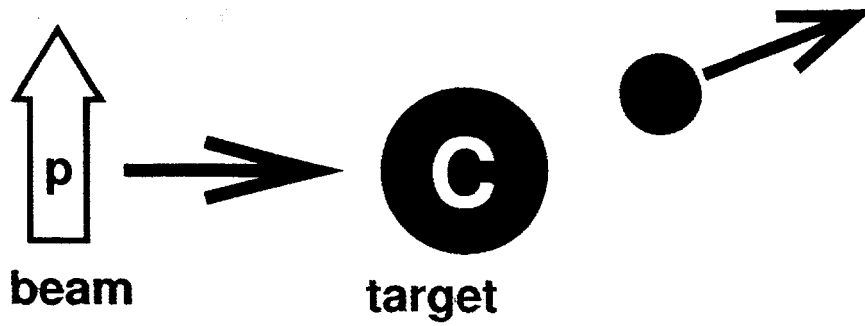
$$p'_t = p_t;$$

$$p'_{\parallel} \approx \frac{x_f}{2m_p} \left(m_p^2 - \frac{p_t^2 + m_{\pi}^2}{x_f^2} \right)$$

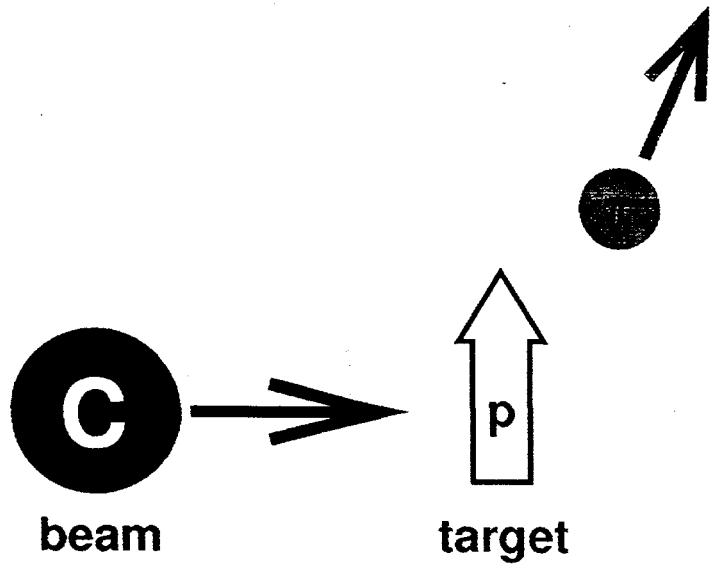
- Direction and momentum of pions does not depend on the beam momentum, so the two-arm setup covering angles $\theta_{\text{lab}}=45-78^\circ$ and $\varphi=0\pm 10^\circ, 180\pm 10^\circ$ and momentum range near 1 GeV will suit for all beam energies.
- The estimated time of gathering of 10^4 pions corresponding to "polarized beam" $x_f=0.5\pm 0.1$ and $p_t=0.8\pm 0.1$ GeV/c is 30 min. at 25 GeV and several seconds at 250 GeV on a polarized jet target with thickness 10^{13} atoms/cm².
- This method also votes for using hydrogen jet target in polarimeter because carbon can not be accelerated at RHIC to 250 GeV/nucleon, which we need to make calibration at 250 GeV.

Conclusion: Inclusive pion polarimeter is quite reasonable choice for polarimetry at RHIC.

Beam polarization measurement



Analysing power measurement



Notes on Elastic pp Polarimetry at High t for RHIC

I.G. Alekseev, V.P. Kanavets, B.V. Morozov, V.M. Nesterov, D.N. Svirida
ITEP, Moscow

RHIC Spin Workshop, BNL, April 27, 1998

Recently Boris Kopeliovich suggested to use the elastic proton-proton scattering near $|t| \approx 1$ (GeV/c)² for absolute polarimetry. These notes contain our estimates on the subject, concerning the possibilities of its realization. The available data at the energies above 40 GeV in $|t| \approx 1.2 \pm 0.2$ (GeV/c)² interval reveals the asymmetry about $A \approx -(0.05 \div 0.10)$. Unfortunately these results have large errors and new precise asymmetry measurements are necessary in advance in order to use it for polarimetry. This could be achieved either with a polarized jet target or by measurement of the recoiled proton polarization, which is equal to the asymmetry in elastic processes. The recoiled proton polarization can be determined by their second scattering on carbon in a standard and calibrated polarimeter. The inspection of available experimental data on crosssection and asymmetry leads to the conclusion that the "elastic" polarimetry at large momentum transferred is bounded to the energies above 40 GeV and relatively narrow t interval $\Delta t \sim 0.2$ (GeV/c)². Then we considered the principal features of the possible layouts separately for the measurement of the recoiled proton polarization and for the polarimetry itself. The instrumental restrictions are imposed by the elastic scattering kinematics and the properties of the carbon polarimeters. We also need a $\pm 90^\circ$ spin-rotator (solenoid) to cancel false asymmetries in the polarimeter. So the magnetic channel for the recoiled proton transportation to the polarimeter should include: a couple of wide aperture quadrupole lenses near the target, a dipole magnet for the proton momentum measurement, another couple of lenses and a spin rotator. In order to select the events of elastic scattering the precision measurements of both recoiled and forward proton angles is necessary, since the angular correlations are the most powerful selection criteria in the case. For the available experimental data we estimated the counting rates. We calculated the event number and time required to achieve 5% precision in beam polarization. For the same conditions taking into account "figure of merit" of standard carbon polarimeters we obtained that the time required to measure the recoiled proton polarization is approximately 75 times more than the time required to measure the beam polarization itself. Using of polarized jet target with thickness $\rho > 10^{13}$ proton/cm² has several obvious advantages. We concluded that the absolute polarimetry based on elastic pp scattering near $|t| = 1$ (GeV/c)² is possible in the energy range (40 \div 250) GeV, but requires large measurement times, particularly in the case of recoiled proton polarization analysis.

Instrumental restrictions from properties of carbon polarimeters:

$$P_{rec} = (1-1.5) \text{ GeV}/c, \quad A_C \approx 0.25$$

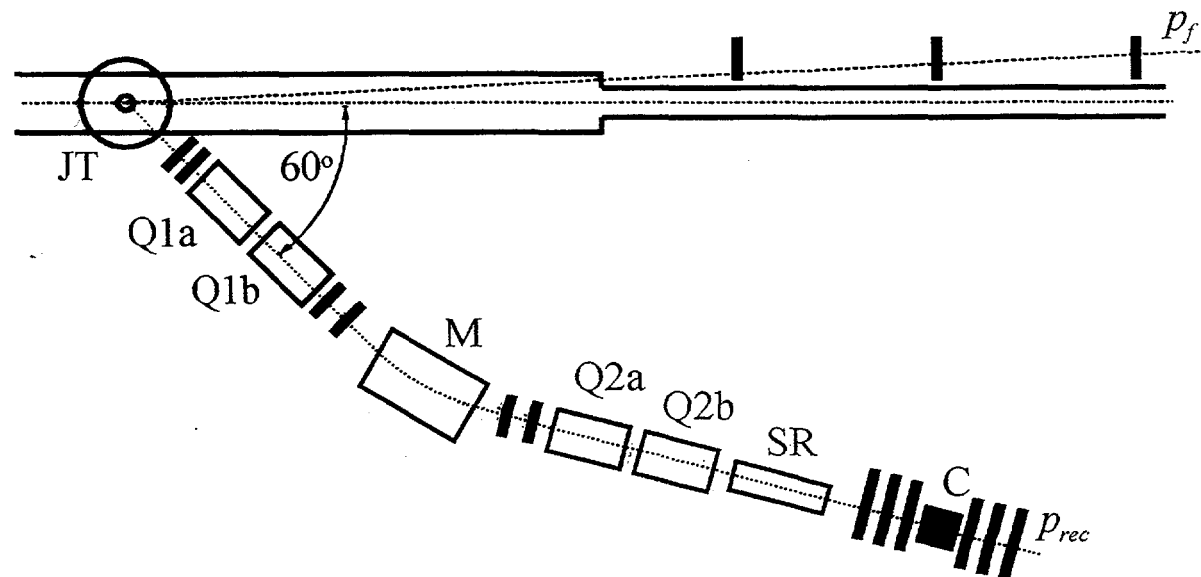
False asymmetries $\approx 0.002-0.005$ or $\approx (10-25)\%$ for $\rho = 0.08$

⇓ ⇓ ⇓

SPIN ROTATOR $\pm 90^\circ$ (solenoid) for systematic error compensation

Magnetic channel:

- Couple of wide-aperture quadrupole lenses
- Dipole magnet
- Couple of lenses for focusing
- Spin rotator
- Polarimeter



Selection of elastic scattering:

The most powerful criteria — angular correlations

⇓ ⇓ ⇓

Precise measurements of scattered and recoiled proton angles

Limitations $\begin{cases} \rightarrow \text{multiple scattering} \\ \rightarrow \text{internal beam angular divergence} \end{cases}$

Measurement of recoiled proton momentum $\Delta P/P < 1\%$

Counting rates:

with $|A| = 1.2 \pm 0.1 \text{ (GeV/c)}^2$, $\Delta\phi = 30^\circ$, $I_b = 10^{11}$, $N_b = 60$,
 $\rho = 10^{15} \text{ p/cm}^2$ - target thickness

$n=8 \text{ evt/c @ } 50 \text{ GeV/c}$, $n = 4 \text{ evt/c @ } 200 \text{ GeV/c}$

Event number and time required:

"FIGURE OF MERIT" : analyzing power and polarimeter efficiency:

$$\Delta P = \frac{\sqrt{2}}{F\sqrt{N}}$$

For standard carbon polarimeter, for example:

POMME: $F^2 = 0.015$ @ $P_{rec} = 1.25 \text{ GeV/c}$ NIM A288, 1990, 379

ITEP: $F^2 = 0.015/1.1$ @ $P_{rec} = 1.35 \text{ GeV/c}$

EVENT NUMBER: $8.3 \cdot 10^6$ (for $\rho = 0.08$, stat. error 5%)

TIME REQUIRED: 300 hours @ 50 GeV, 600 hours @ 200 GeV.

It is strongly DESIRABLE to increase the target density (1-2) order of magnitude

BUT: possible problems with background due to excessive number of secondaries per bunch

Convenient formula for time estimations:

$$T_A = \frac{2}{\alpha^2 A^2 F^2 c (d\sigma / dt)}$$

$c = \Delta t \cdot (\Delta\phi/360^\circ) \cdot \rho \cdot I_b \cdot N_b \cdot f$,

A - expected asymmetry,

$\alpha = \Delta A/A$ - required statistical accuracy,

f - collider frequency.

II. Beam polarization measurement

$$T_{P_b} = \frac{1}{\alpha^2 A^2 P_b^2 c (d\sigma / dt) \langle \cos \phi \rangle^2} \quad (1)$$

$\langle \cos \phi \rangle$ - averaged cosine to the scattering plane normal

At above conditions:

$$\frac{T_{P_b}}{T_A} = \frac{F^2}{2P_b^2 \langle \cos \varphi \rangle^2} \approx \frac{1}{75}$$

$$T_{P_b} = 4 \text{ hours @ } 50 \text{ GeV}, T_{P_b} = 8 \text{ hours @ } 200 \text{ GeV}$$

III. Polarized hydrogen target

Time measurement formula similar to (1)

For polarized jet target with thickness 75 times LESS:

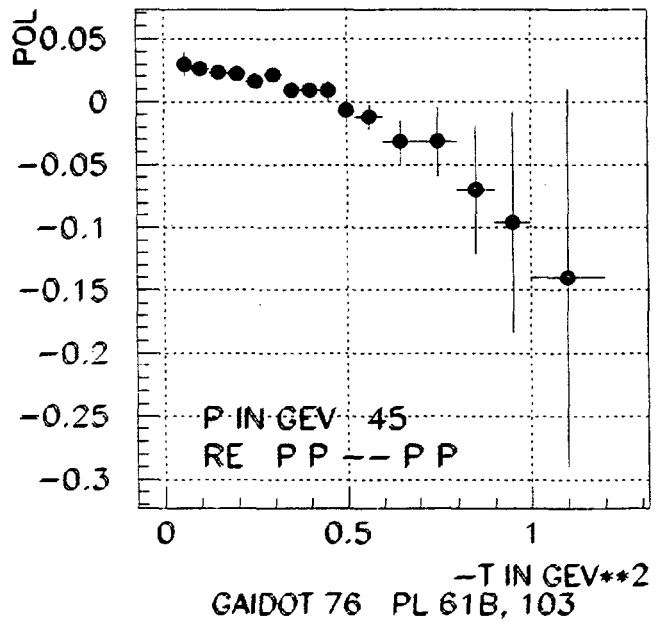
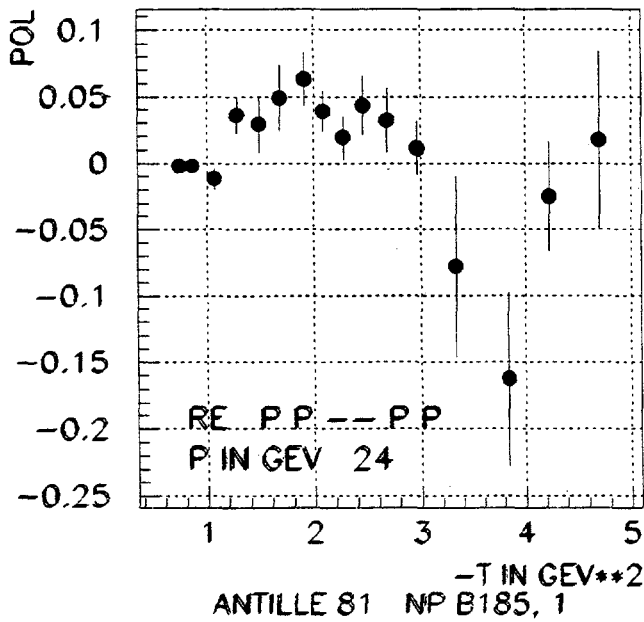
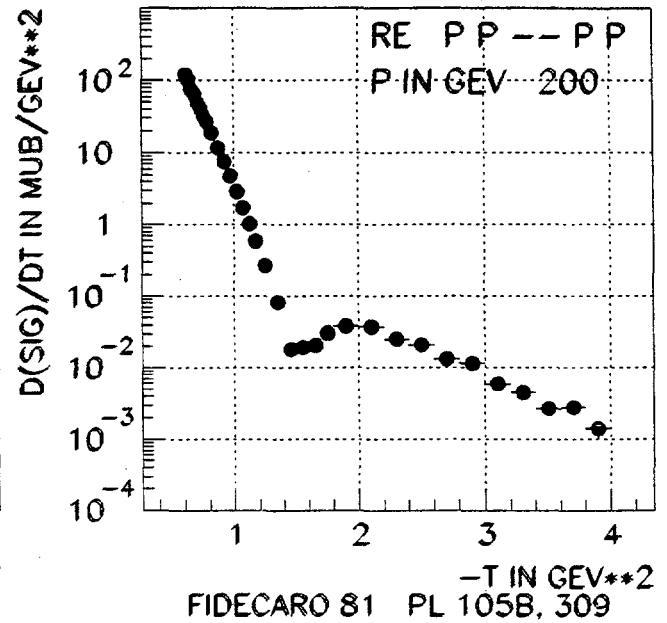
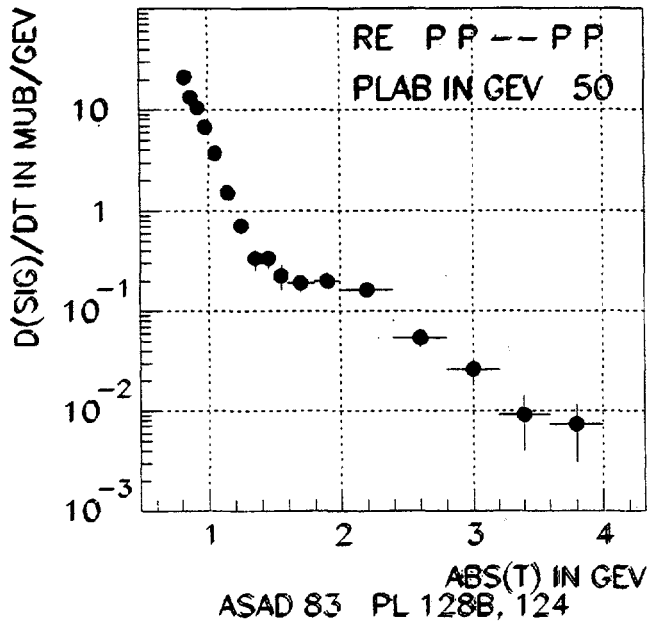
$$300 \text{ hours @ } 50 \text{ GeV}, 600 \text{ hours @ } 200 \text{ GeV}$$

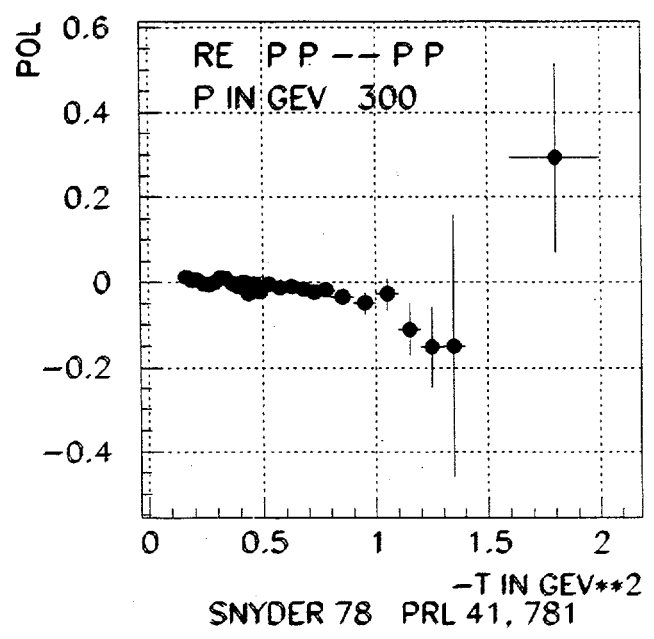
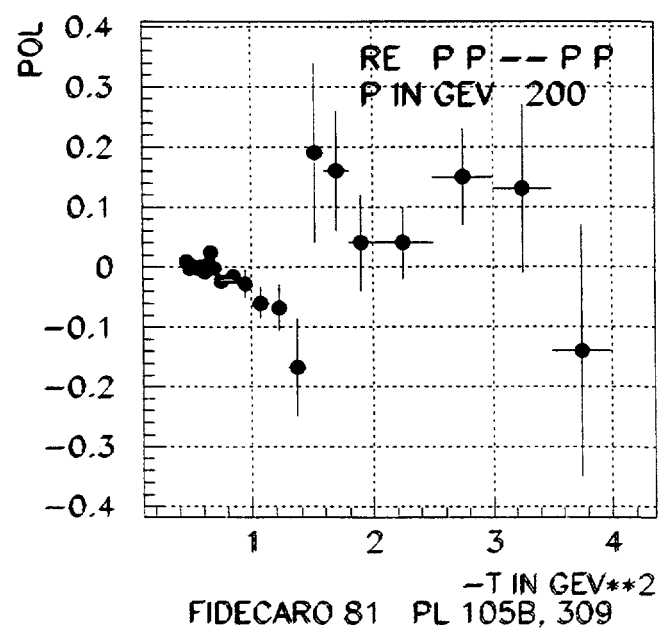
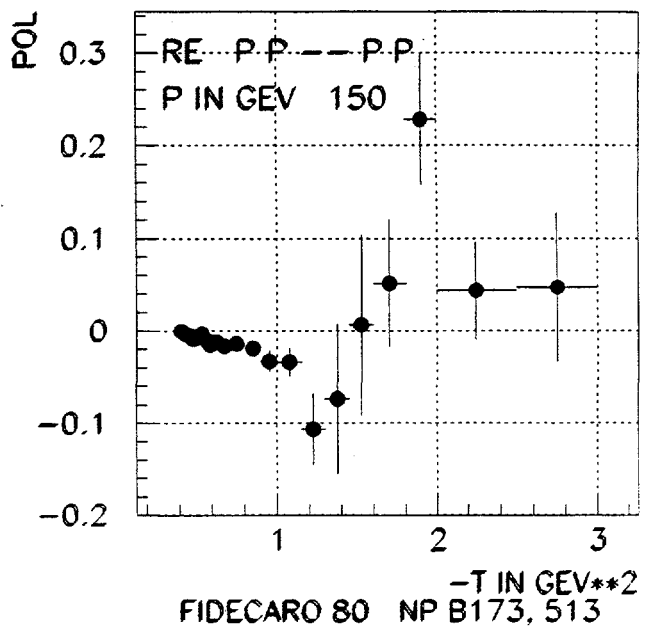
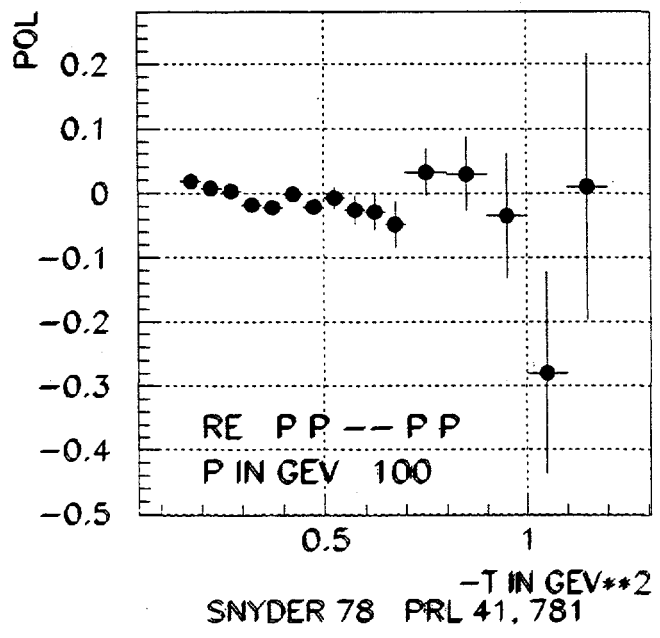
Obvious advantages:

- The setup simplifies much, no second scattering required
- The same detector layout can be used for the measurements of both the asymmetry and beam polarization
- High target polarization values (up to 75%) result in essential raw asymmetries, thus decreasing the relative false asymmetries

IV. Conclusions.

The absolute polarimetry based on elastic pp scattering with large momentum transferred is possible in the energy range (40-250) GeV , but requires large measurement times due to low crossection and small asymmetry values, particularly in the case of the recoiled proton polarization analysis.





Proton-Carbon CNI Polarimeter and MCP Detector

Ken'ichi Imai

Kyoto University and RIKEN

The polarization analyzing power of the elastic proton-carbon scattering at Coulomb-nuclear interference (CNI) region was recently proposed as a possible polarimeter for RHIC. It is quite attractive because measurement is compatible with the pion polarimeter and the detectors could be simple and inexpensive.

The analyzing power of p-C CNI scattering can be described by spinflip and nonflip amplitudes of nuclear and Coulomb interaction. Long time ago we measured them at $T_p = 65\text{MeV}$ which are shown in the Figure. At this low energy, the analyzing power at the CNI region mainly comes from the nuclear spin-flip amplitude. However, at high energy limit, nuclear spinflip amplitude is expected to be zero and nonflip amplitude as pure imaginary (diffractive scattering). Then the analyzing power can be reliably calculated and is 4% at maximum (Figure). The analyzing power of p-p CNI was measured at 200 GeV and consistent with the theoretical values within the errors. For the p-C CNI scattering, recoil carbon must be detected. The kinetic energy of the carbon ranges from 90 to 500 keV for the CNI region. We have tested the micro-channel plate (MCP) as a possible detector for the recoil carbon.

We have measured p-C elastic scattering using 10 MeV proton beam from the Tandem van de Graaf of Kyoto Univ. The scattered proton is detected with a scintillator and the carbon with the MCP in coincidence (Figure). The carbon was successfully detected with the MCP to about 100 keV. The energy spectra of the carbon were obtained at several angles by using the TOF between the proton and carbon (Figure). The TOF resolution was checked by p-p scattering and it was 240psec.

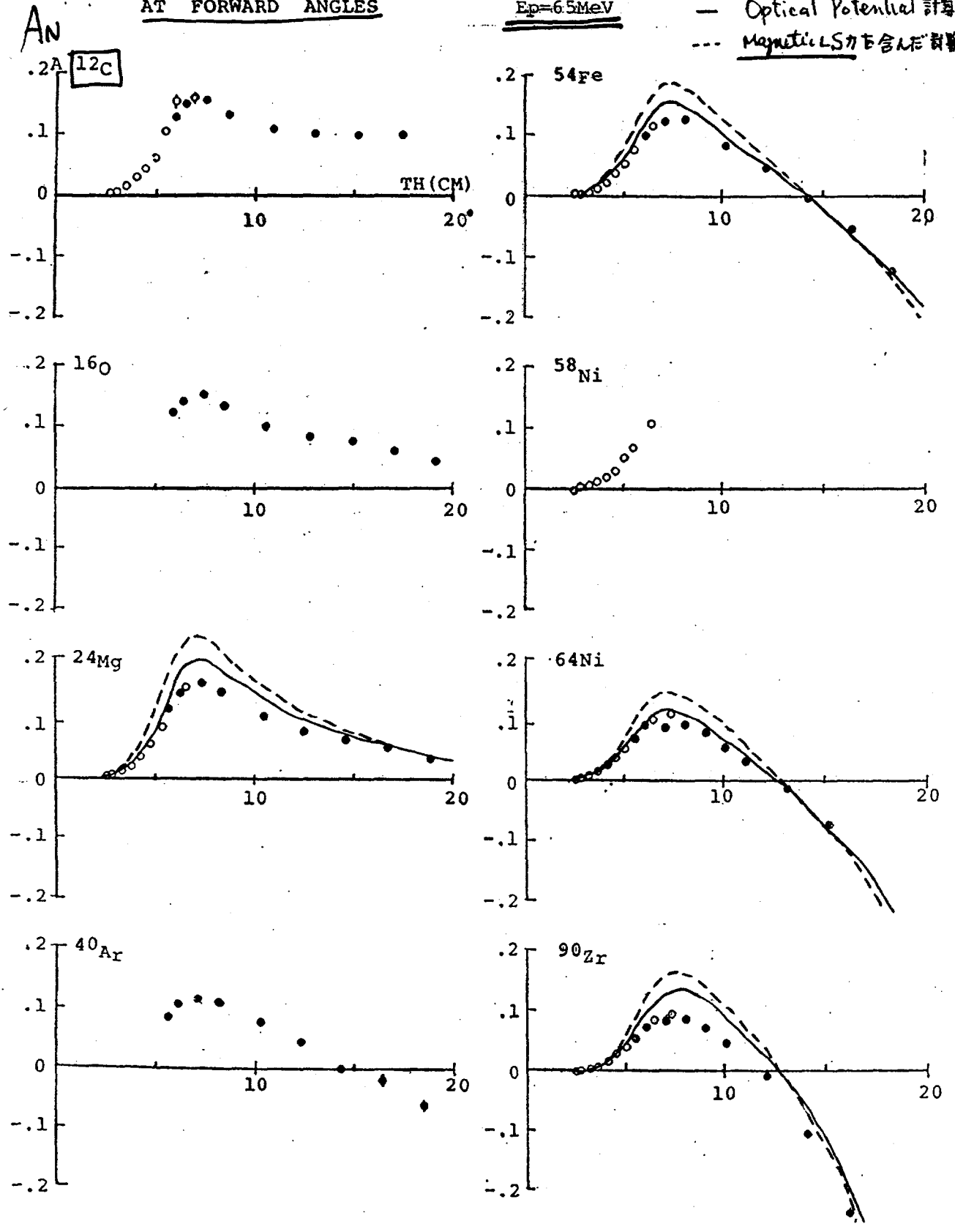
The present MCP is double-layered and has an effective area of 14mm dia. The MCP is easy to handle like a photomultiplier due to its high gain especially against electronical noises. However it is sensitive to the low energy electrons and X-rays. By using this MCP, we plan to study the multiple scattering and energy loss of the carbon in the carbon foil, and the charge states of the recoil carbons, which are important for the design of the RHIC polarimeter. The combination of the MCP and silicon detectors will be also studied. For the RHIC polarimeter, the rectangular shaped MCP with multi anodes will be used to obtain both timing and position information.

In summary, by the present test measurement we found the MCP as useful device to detect the recoil carbon for the RHIC p-C CNI polarimeter.

ANALYZING POWER IN ELASTIC P-NUCLEUS SCATTERING
AT FORWARD ANGLES

$E_p = 65 \text{ MeV}$

— Optical Potential 計算値
--- Magnetic LS 力を含む計算値

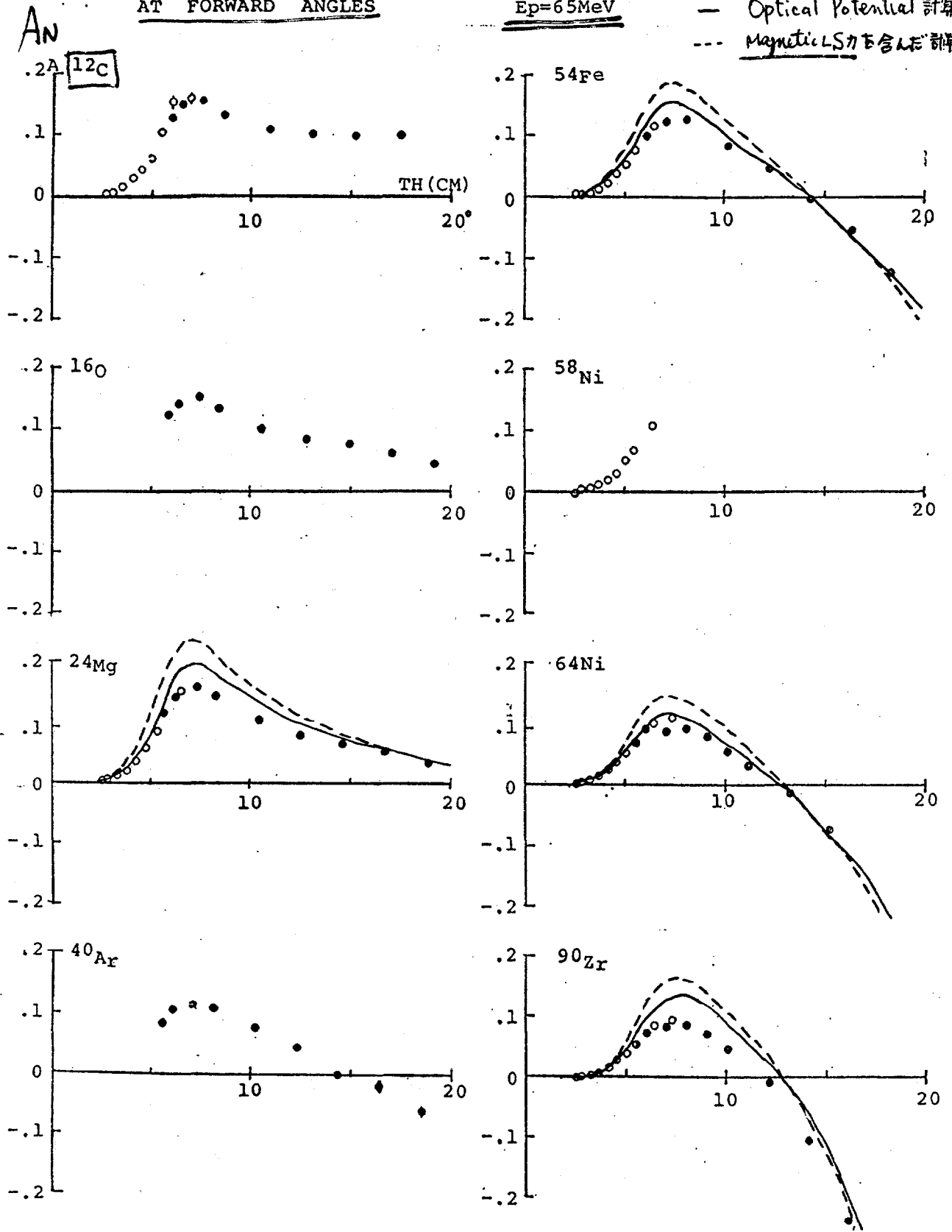


ANALYZING POWER IN ELASTIC P-NUCLEUS SCATTERING

AT FORWARD ANGLES

$E_p = 65 \text{ MeV}$

— Optical Potential 計算値
 --- Magnetic LS力を含む計算値



Hamamatsu MCP (F4655).

- Double layer
- sensitive area $14.5 \text{ mm } \phi$.
- diameter of channel $12 \mu\text{m}$
- HV max. (MCP) 2.4 KV .
- vacuum $< 1 \times 10^{-5} \text{ Torr}$.
- Gain. (2KV) 1×10^7
- dark count 3 c/sec/cm^2
- Rise time 250 psec .
- Pulse height Resolution $50\% \text{ (FWHM)}$

$T_{12} \approx 90 \sim 450 \text{ keV}$

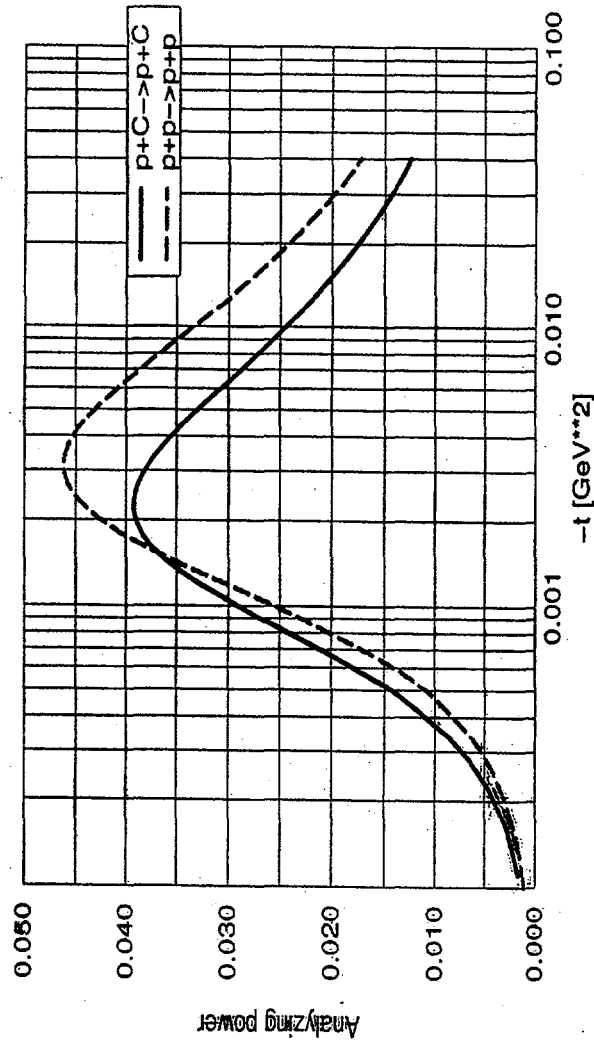


Figure 1. Coulomb-Nuclear interference analyzing power for pp and pC scattering at 250 GeV.

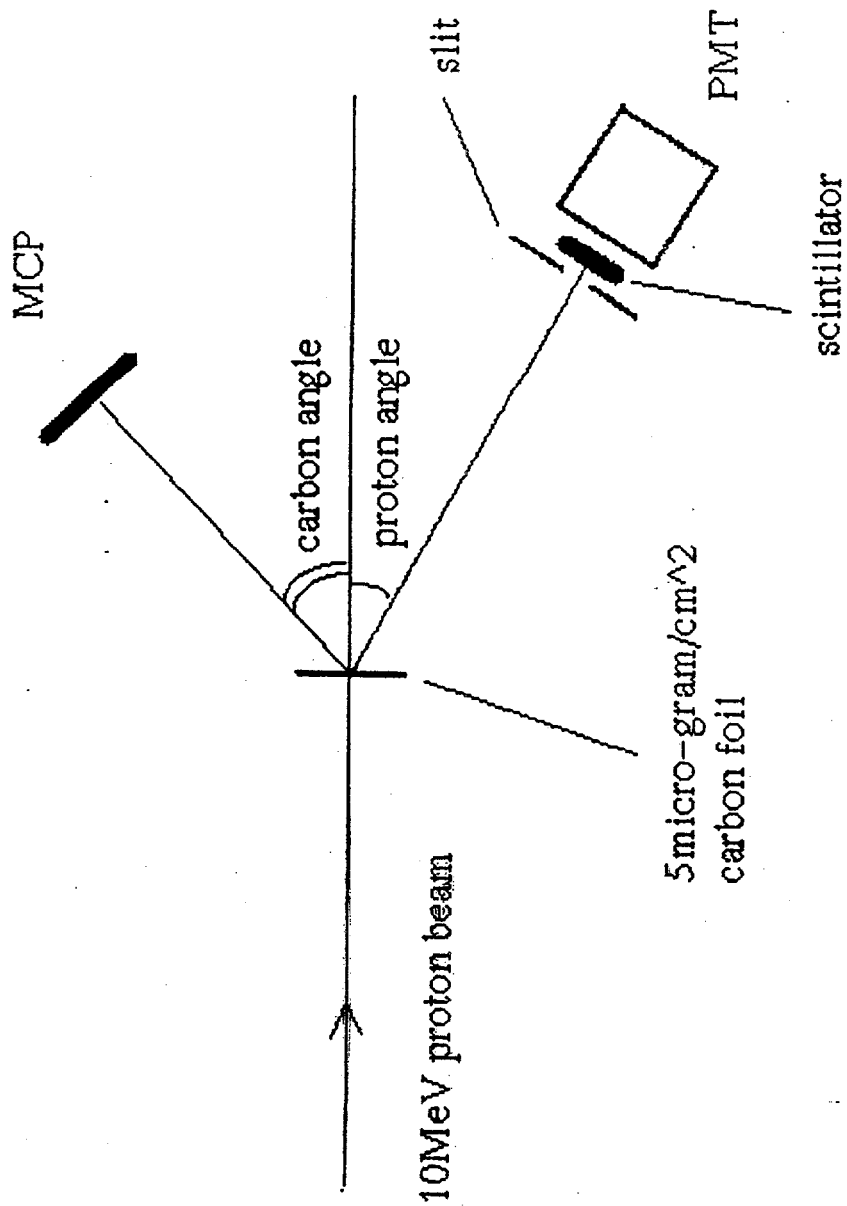


Fig.1 Experimental setup

θ_p	θ_{carbon}	F_{carbon}
27.7°	75°	190 <i>keV</i>
36.1°	70.5°	318 "
46.4	65.0	510 "
61.2	57.5°	824 "

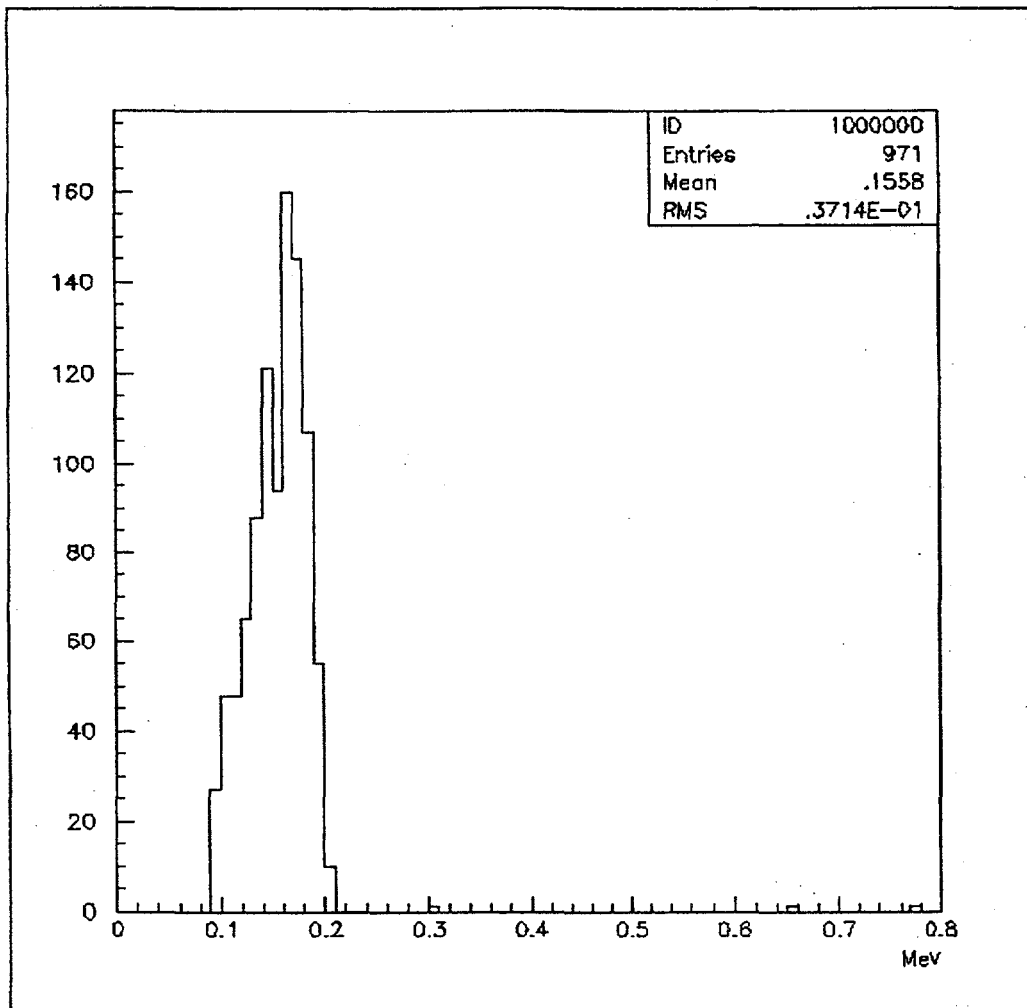
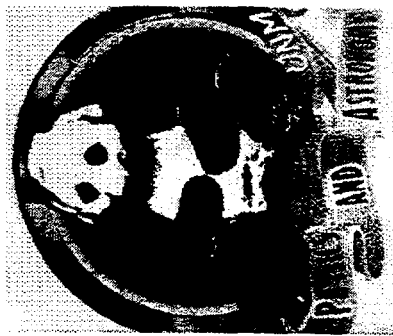


Fig.3 The energy spectrum of the carbon ions.
proton angle = 27.74 , carbon angle = 75.0

$$E_c = 190 \text{ keV}$$

A Proposal For A (p+C) CNI Polarimeter for RHIC



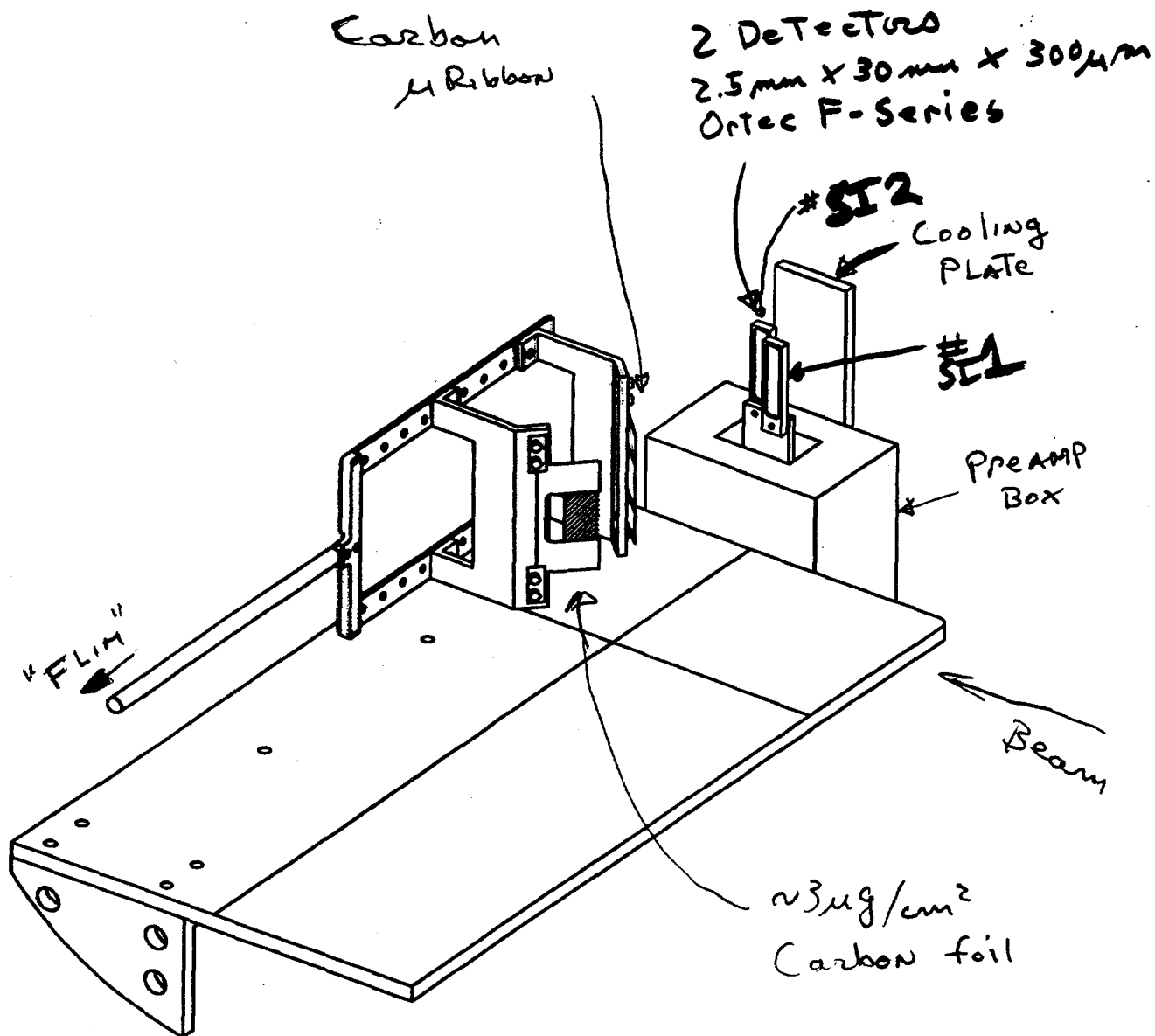
D.E. Fields*, T. Thomas, B. Smith,
J. Behrendt, D. Wolfe

- G. Bunce, H. Huang, Y. Makdisi, T. Roser, M. Syphers
Brockhaven National Laboratory
- J. Doskow, K. Kwiatkowski, B. Lozowski, H.O. Meyer, B. Przewoski, T. Rinckel*



4/24/98

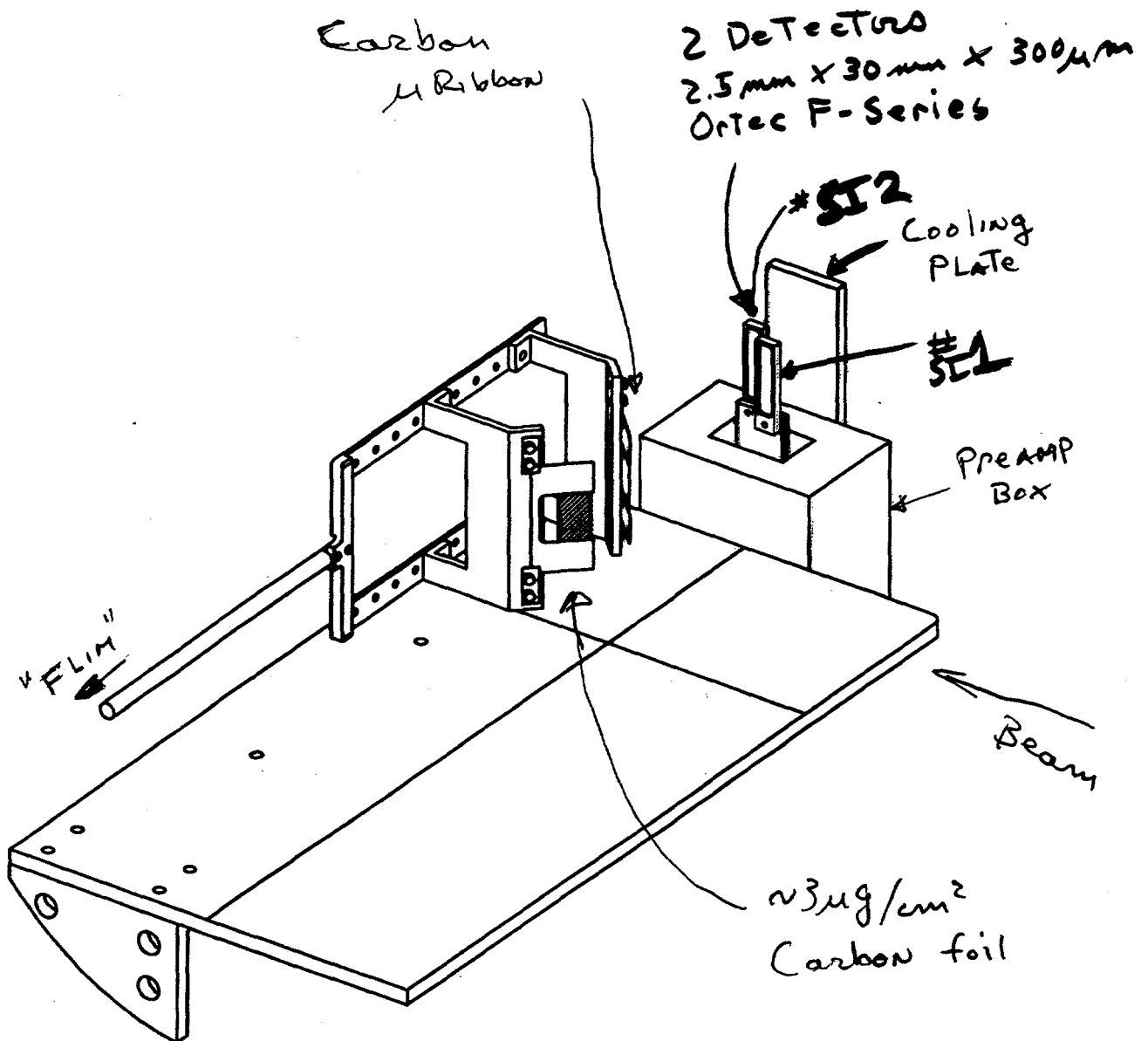
Douglas Fields

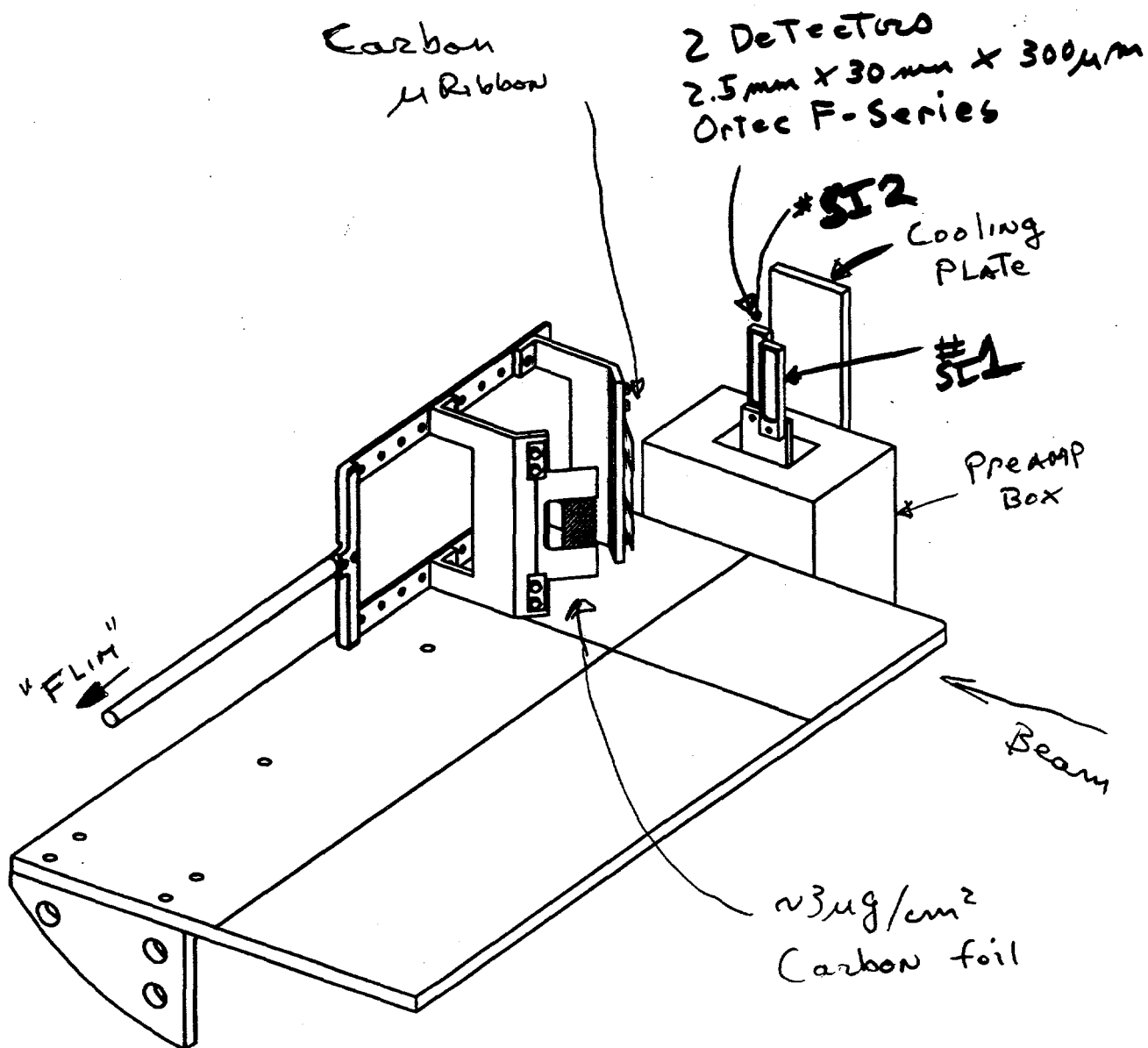


C75A

30-MAR-98

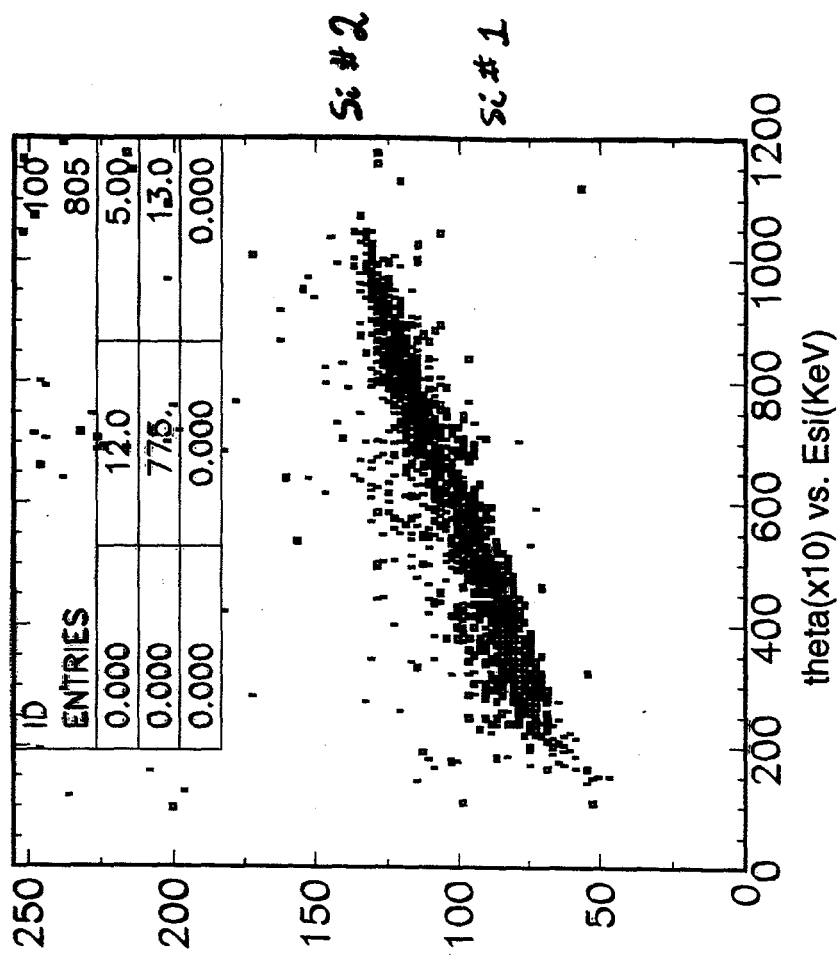
185





Calibrated Results

Silicon only as trigger. E_{thresh} is $\sim 250\text{KeV}$ and is from noise in the small angle detector.



Future Plans

- Build full detector system
 - Two boards with five Si channels each
 - Improve S/N
 - Improve crosstalk
- Run in Fall at IUCF to test full detector system and to measure analyzing power
- Run in Feb. 99 at AGS
- Add MCP trigger?

LUMINOSITY MONITOR

D. Underwood

High Energy Physics

Argonne National Laboratory

Presented at

Spin Meeting

BNL

April 27, 1998

Luminosity monitors are needed in each experiment doing spin physics at RHIC. We concentrate on the luminosity aspects here because, for example, with a 10^{-3} raw asymmetry in an experiment, an error of 10^{-4} in the luminosity is as significant as a 10% polarization error.

Because luminosity is a property of how two beams overlap, the luminosity at an interaction region must be measured at that interaction region in order to be relevant to the experiment at that interaction region.

We will have to do the physics and the luminosity measurements by using labels on the event sums according to the polarization labels on the colliding bunches. Most likely we will not have independent polarization measurement on each bunch, but only on all the filled bunches in a ring, or perhaps all the bunches that are actually used in an experiment.

Most analyses can then be handled by using the 9 combinations gotten from 3 kinds of bunches in each ring, +, - and empty bunches. The empty bunches are needed to measure beam-gas background, (and some, like 6 in a row, are needed for the beam abort.)

Much of the difficulty comes from the fact that we must use a physics process to represent the luminosity. This process must have kinematic and geometric cuts both to reduce systematics such as beam-gas backgrounds and to make it representative of the part of the interaction diamond from which the physics events come.

See Also
AGS/RHIC/SN No 035
AGS/RHIC/SN No 071

DEFINITIONS OF BEAM LUMINOSITY FOR RHIC SPIN

There could be two ways of defining the spin luminosity quantities:

1) Label the Bunches:

Luminosity Labels are based on Bunch Labels

A particle luminosity with Labels (+, -)

Independent of the Magnitude of Polarizations (+, -), etc

(eg + - for + bunch in A and - bunch in B)

$$\text{Polarization of bunch labeled + in beam A} = \frac{n(\text{up}) - n(\text{dn})}{n(\text{up}) + n(\text{dn})}$$

This is related to the useful Luminosity definition for experiments

Even though we can't usually measure this polarization for a single bunch.

We could still in principle do $\langle L_{\text{up dn}} \rangle$ for all up, dn protons in the beams

By doing proper sums

(but in practice we compromise)

2) Label an Ensemble of Particles with definite Spin Independent of Bunches:

Lum. = A product of fluxes of particles with Definite Spin direction

L+ - from all up protons in beam A with all down protons in beam B

This has a form similar to parton fluxes used in some calculations.

This is not possible to measure because

The best we can do is either polarization of a bunch or polarization of a beam.

(And we can't get L accurately from the flux of one beam x the flux of the other even if we could label particles.)

Note: Luminosity is really a property of 2 beams

You can't get it from individual beam properties without extra information.

WHAT WE WANT :

$$\begin{array}{c} \text{EVENTS}^{++} \\ \hline N_{\text{BUNCH}} \\ \sum_A \sum_B \\ 0 \quad 0 \end{array} \quad \begin{array}{c} P_A^+ \quad P_B^+ \\ P_{A_i} \quad P_{B_j} \\ L_{ij}^{++} \end{array}$$

$$\begin{array}{c} \text{EVENTS}^{+-} \\ \hline N_A \quad N_B \\ \sum_A \quad \sum_B \\ 0 \quad 0 \end{array} \quad \begin{array}{c} P_A^+ \quad P_B^- \\ P_{A_i} \quad P_{B_j} \\ L_{ij}^{+-} \end{array}$$

WHAT WE ARE MORE LIKELY TO GET :

$$\begin{array}{c} \text{EVENTS}^{++} \\ \hline \end{array} \quad \langle \alpha_{\text{STAR}} L_{\text{STAR}}^{++} \rangle \quad \langle P_A \rangle \quad \langle P_B \rangle$$

α COMES FROM
 PHYSICS PROCESSES
 KINEMATIC CUTS
 GEOMETRIC CUTS
 COUNTING METHODS
 STATISTICS

P IS LIKELY AN AVERAGE OVER $+, -$
 BECAUSE OF SYSTEMATIC ERRORS
 IN POLARIMETERS

WE CAN ACTUALLY DO SLIGHTLY BETTER
 THAN TAKING P FOR ALL OF ONE BEAM.

REQUIREMENT:

AVOID SATURATION EFFECTS IN COUNTING.

IMPLEMENTATION:

- << 1 COUNT / CROSSING AT FULL L
- CHOOSE PROCESS
- CHOOSE DETECTOR KINEMATIC THRESHOLD

REQUIREMENT:

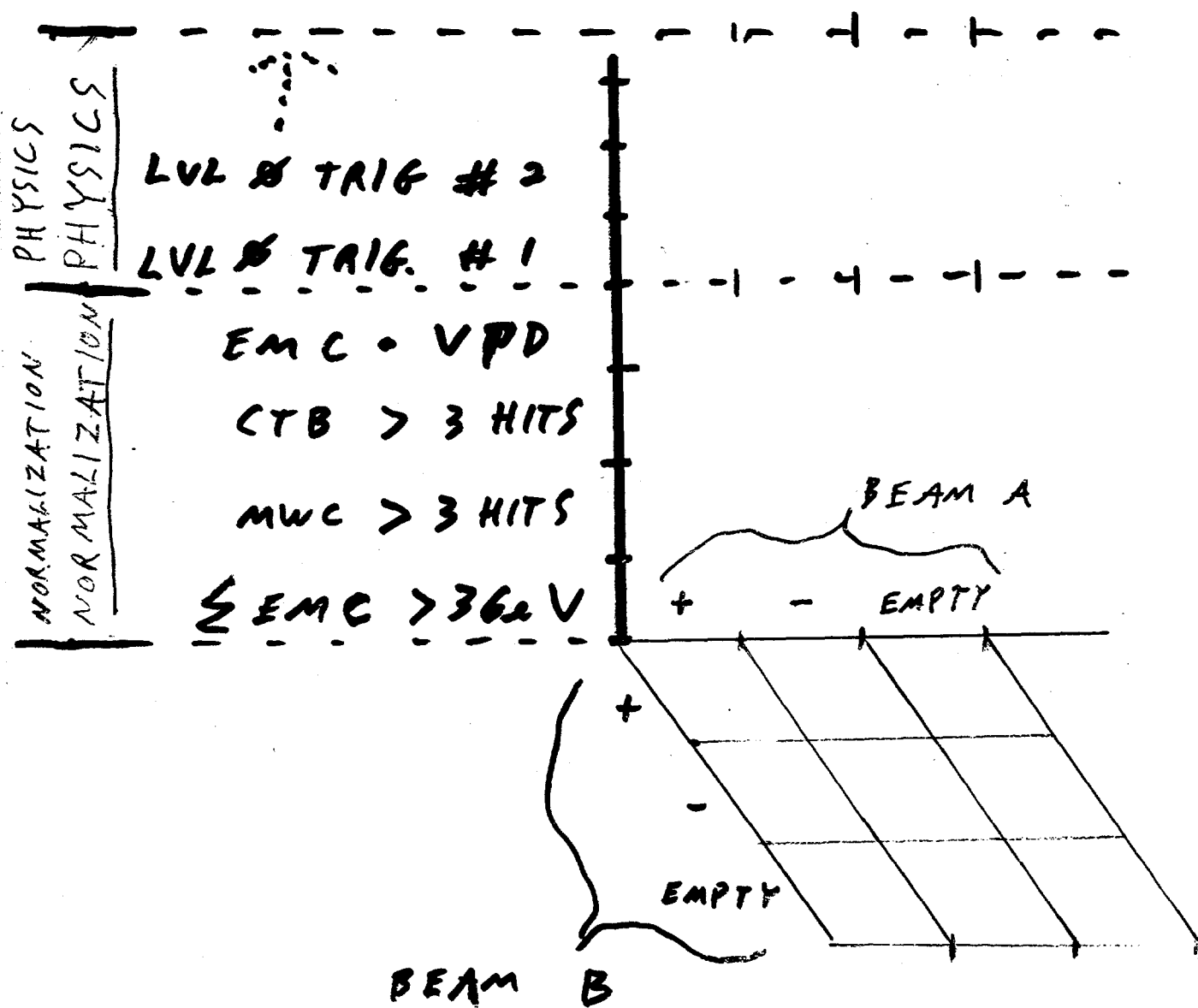
HAVE A WAY TO MEASURE ASYMMETRY IN LUMINOSITY MONITOR ITSELF.

IMPLEMENTATION:

- 1) USE MULTIPLE KINEMATIC THRESHOLDS AND COMPARE. (NORMALIZE ONE TO ANOTHER)
- 2) FOR ALL THERE ARE CERTAIN BUNCH COMBINATIONS THAT WORK. SEE PAPER AGS/RHIC/SN

SPIN LUMINOSITY MONITOR STAR CONCEPTUAL EXAMPLE

THIS SIMPLE EXAMPLE HAS $3 \times 3 \times 6 = 54$ SCALERS



ADIABATIC FLIPPER SWAPS +, - IN EACH BEAM

A Jet-Target for Polarimetry at RHIC

(Proposal and Project Status)

1. - Jet-Targets (J-T) fit Colliders :

- Low density \rightarrow negligible beam perturbation
- Luminosity as high as colliding- beams (C-B)

2. - Practical aspects :

- Design criteria \searrow
- Construction \rightarrow ENGINEERING
- Install./operation \nearrow
- Costs

3. - Additional advantages for polarimetry :

- * Fixed-target (F-T): \sqrt{s} overlaps present data ($pp \rightarrow pp, pp \rightarrow \pi X$)
- ** Recoil-particle accessible [$P_R \equiv A_N^{(B)}$] \searrow
($pp \rightarrow pp$) \rightarrow SELF-CALIBRATION
- *** Pol.Gas-Targets (PG-T) [$A_N^{(T)} \equiv A_N^{(B)}$] \nearrow

4. - Status of project :

- ✓ 3- year R&D prototype studies done (MC /PJ-T)
- ✓ Setup design (integrated with PP2PP: forward+ recoil detectors)
- ✓ Molecular cluster(MC) assembly available (ADONE/NIKHEF)
- Polarized J-T components existing; assembly in progress
- Funding request to complete vacuum parts in progress
- Need to finalize installation plans and schedule (target year 2000)

1. - Successful & dependable experience with MC J-T:

<u>Laboratory</u>	<u>Experiment (Accelerator)</u>				
CERN	UA6 (SPS)	R704 (ISR)	PS202 (LEAR)		M C J T
FNAL	E760 (AAR)				
TSL	(CELSIUS)	[Light-heavy (A=1-131) gases]			
LNF	BTPB (ADONE)	" "	(A=1-40)	"	
NIKHEF	↓	" "	" "	" "	
⋮					
DESY	HERMES (HERA)	H↑/D↑ storage cell			P G T
BINP	(VEPP-2/3)	" "	" "	" "	
IUCF	(Cooler Ring)	" "	" "	" "	
⋮					

1.1 - Typical parameters for J-T systems

Target Type	Target Material [A]	Target Thickness [g/cm ² ; at/cm ²]	Pressure Bump [mbar]	Beam Aperture [Ø, cm]	Detection Clearance [$\Delta\Omega/4\pi$]	Recoil Detection [MeV/c]
MC J-T	1-131	0.2-4 10 ⁻⁹ ; $\geq 10^{14}$	$\leq 10^{-7}$	≥ 10	≈ 0.7	≥ 30 (p)
AB PJ-T	1-2	0.02 10 ⁻⁹ ; $\approx 10^{12}$	$\leq 10^{-8}$	≥ 10	≈ 0.7	≥ 30 (p)
SC PG-T	1-3	0.2 10 ⁻⁹ ; $\approx 10^{14}$	$\leq 10^{-7}$	≤ 2	≈ 0.7	≥ 200 (p)
Fiber (*)	12,95,184	$\approx 5 \cdot 10^{-4}$; $\approx 10^{17}$	10 ⁻⁹	≈ 5	≈ 1	≥ 240 (C)
Ribbon(*)	12, 197	$\approx 5 \cdot 10^{-6}$; $\approx 10^{15}$	10 ⁻⁹	≈ 5	≈ 1	≥ 50 (C)

(*) Shown for comparison; average thickness sweeping through beam.

1.2 - Luminosity: $L = N_B \times n_B \times n_T \times l_T \times q \times f_0$

RHIC Parameters for p-p (polarized)	
Energy (Injection - Top)	28 - 250 GeV
Number of bunches (n_B)	120
Number of protons/bunch (N_B)	$2 \cdot 10^{11}$
Revolution frequency (f_0)	$78 \cdot 10^3$ Hz
Beta at crossing point (β^*)	10 m
(low beta)	2 m
Normalized emittance (ϵ)	20π mm mrad
Circumference	3834 m
Beam pipe diameter (\varnothing)	80 mm
Vacuum (warm regions)	$7 \cdot 10^{-10}$ mbar
Beam store time (T_S)	5-10 hours
Beam polarization (P_B)	$\approx 70\%$

Typical MCJ-T parameters (UA6)	
Total gas input (@ 1 bar)	20 mbar . l/s
Nozzle diameter	0.1 mm
Nozzle temperature	28 K
Distance nozzle - beam	25 cm
Jet density (n_T)	$2 \cdot 10^{14}$ atoms/cm ³ ($3.4 \cdot 10^{-10}$ g/cm ³)
Jet sectional area ($w \cdot l_T$)	6×8 mm ²
B-T overlap factor (q)	typically ≈ 1
Target thickness (t_T)	$1.6 \cdot 10^{14}$ atoms/cm ²
Background gas (n_b)	$< 2 \cdot 10^9$ atoms/cm ³
Residual pressure bump	$6 \cdot 10^{-8}$ mbar (≈ 5 m)

$$L = 2 \cdot 10^{11} \times 120 \times 1.6 \cdot 10^{14} \times 79 \cdot 10^3 = 3 \cdot 10^{32} \text{ cm}^{-2} \text{ s}^{-1}$$

1.3 - Effects on the beams: losses and emittance growth

Order of magnitude estimate:

- Compare effects of J-T and associated pressure bump with the effects of residual gas in the rings;
- Ignore specific (nuclear) effects [$\approx A^\alpha$]: they might be significant in the overall rings, but not relevant for the J-T region (H gas).

Influence on beam lifetime and emittance						
	Pressure P [mbar]	Length L [cm]	n [at./cm ³]	n . L [at./cm ²]	L _S /L _I	L _S /L _R
RHIC average	1.8 10 ⁻¹⁰	3.8 10 ⁵	$\approx 2 \cdot 10^7$	0.8 10 ¹³	8 10 ⁻⁴	6.2 10 ⁻⁴
Target region	$\leq 2 \cdot 10^{-7}$	≈ 500	$\leq 5 \cdot 10^9$	$\leq 2.5 \cdot 10^{12}$	$\leq 3 \cdot 10^{-4}$	$\leq 2.2 \cdot 10^{-4}$
Jet	4 10 ⁻³	0.8	2 10 ¹⁴	1.6 10 ¹⁴	1.8 10 ⁻²	1.5 10 ⁻²

Assuming 4 10⁴ sec store time (T_S):

$$L_S = f_0 \times L \times T_S \quad \text{effective integrated path length of beam particles}$$

$$L_I = 1/n \sigma \quad \text{effective interaction length}$$

$$L_R = \chi_0/\rho \quad \text{effective radiation length}$$

The two parameters L_T/L_I and L_T/L_R, control the lifetime of the beams and the rate of emittance growth during a store:

$$\tau^{-1} = f_0 \times n \times L \times \sigma \quad \text{represents the beam lifetime } [N_B(t) = N_B e^{-t/\tau}]$$

Emittance growth is given by

$$d\varepsilon/dt = \beta^* \Theta_{ms}^2/2,$$

with $\Theta_{ms}^2 = (15/p)^2 (L/L_R)$ and p in MeV/c. Lifetime is given by $\tau = T_S / (L_T/L_I)$ and $\Delta\varepsilon = \beta^* (15/p)^2 (L_S/L_R) T_S$, measures the total emittance growth during one store. The region surrounding the target, although with sizable pressure, does not introduce appreciable deterioration of the beams; the jet target (at $\approx 2 \cdot 10^{14}$ at./cm³ density) affects significantly, but not catastrophically the losses and emittance of the beams; at $\approx 10^{13}$ at./cm³ the effects are quite tolerable.

2. - Engineering and cost

The jet-target system should provide

- jet density $\geq 10^{12}$ atoms/cm³
- free standing pure H jet unobstructed over 8 cm \varnothing
- maintain machine vacuum of 10^{-10} torr away from immediate vicinity of jet by differential pumping
- design and construction criteria appropriate for easy installation, reliable operation and simple maintenance

Objectives: Providing a target assembly with MC and PAB sources easily interchangeable. In combination with PF2PP a suitable J-T should provide absolute polarization measurements in times shorter than one colliding-beam fill with 5% precision.

2.1 - Cost estimate

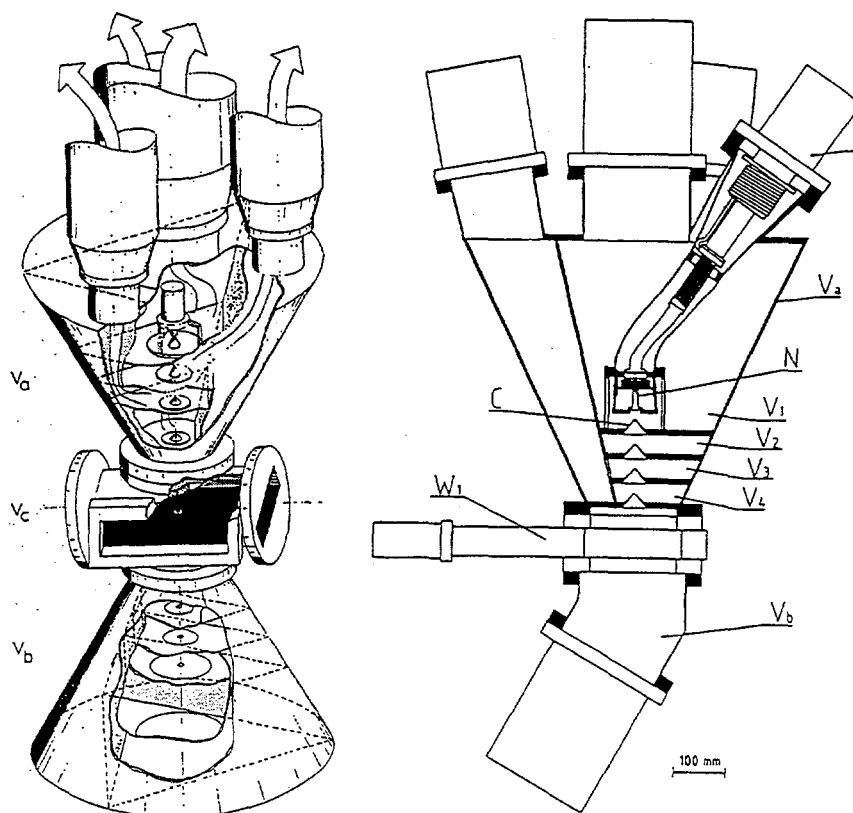
Jet production stage:		381 k\$
chamber	20. k\$	
nozzle/skimmer	8. k\$	
cold head+compressor	36. k\$	
turbo pumps	246. k\$	
primary pumps	39. k\$	
vacuum gauges	32. k\$	
Target Stage:		41 k\$
Chamber	11. k\$	
Valves	30. k\$	
Dump Stage:		24 k\$
Chamber	6. k\$	
Cold head+compressor	18. k\$	
Infrastructure		51 k\$
Cables, pipes	23. k\$	
Support structure	8. k\$	
Controls	20. k\$	
Polarized jet (additional cost)		200 k\$
Dissociator	15 k\$	
Extra pumps	120 k\$	
RF transitions	20 k\$	
Polarimeter	45 k\$	
Total (with overhead and contingency)		697 k\$

2.2 Cheap Scheme

Recover existing equipment (Genova) of MC J-T used at ADONE

Net cost of supplementary parts to refurbish and commission the system, divided by item:

Pumps and vacuum equipment	$44 + 38 + 25 = 107$ k\$
Polarized source	$15 + 29 = 44$ k\$
Mechanical parts	$6 + 8 = 14$ k\$
Controls	20 k\$
Total	175 k\$



The Genova molecular -cluster Jet-Target at ADONE

For the polarized atomic beam source the basic components (dissociator and sextupole magnets) exist already; a design to integrate the source into the Genova assembly is in progress.

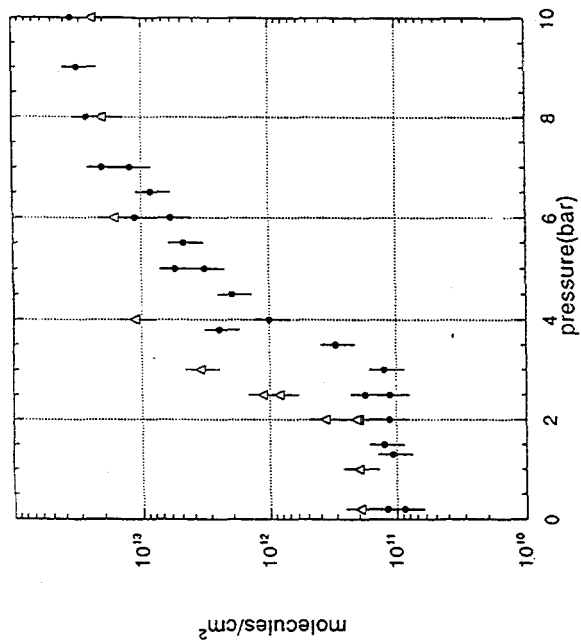


Fig. 3. Target thickness in molecules/cm² vs. inlet pressure deduced from the residual vacuum measured in the dump volume V_b . Full dots: N₂ at 130 K nozzle temperature, open triangles: O₂ at 160 K.

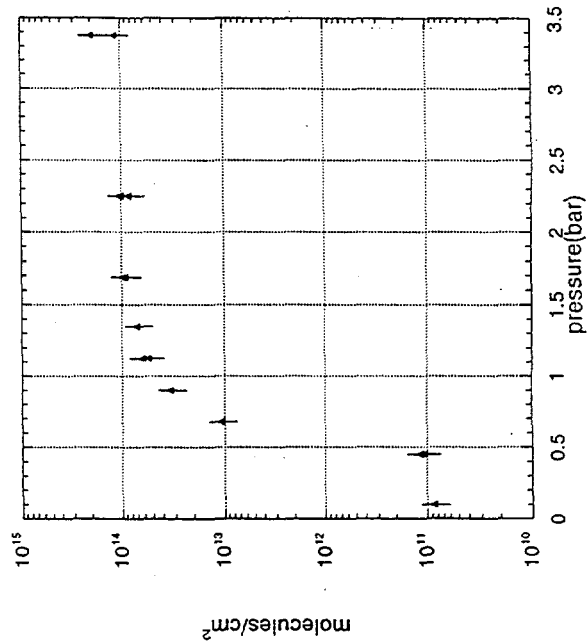


Fig. 4. Same measurement as Fig. 4 with H₂ gas at nozzle temperature of 40 K.

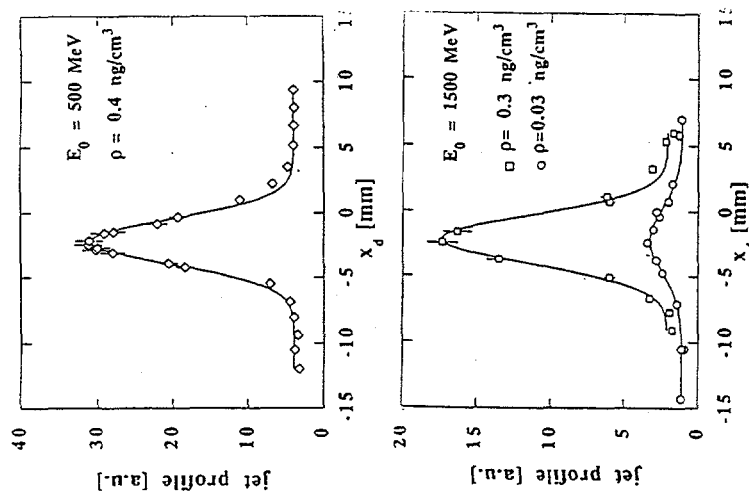
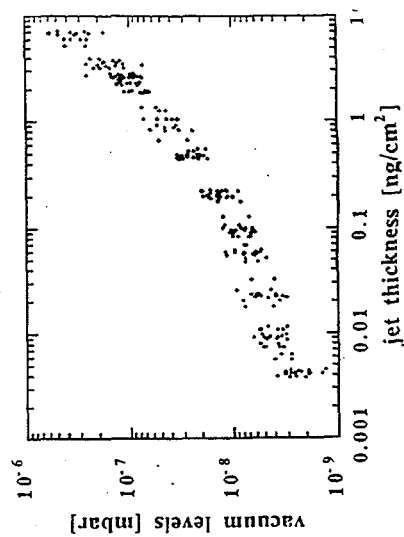


Fig. 6. Jet profiles measured at the given electron energies and jet thicknesses. The solid line curve are the convolutions obtained from eq. (15) with $d_{ip} = 5.4$ mm.



Conclusions

- significant progress in securing a suitable gas jet-target for polarimetry at RHIC

- possibility of performing absolute polarization measurements at the required 5% level in the conceptually cleanest way:
 - pure hydrogen target
 - unbiased detection of $pp \rightarrow pp$
 - self-calibrating by recoil analysis

- polarized jet option included

- integration with PP2PP
 - cost effective
 - forward-recoil detection
 - infrastructure

- unpolarized jet can be rapidly implemented
 - feedback needed to focus plans

Gauge Invariant Quark and Gluon Spin and Orbital Angular Momentum Distributions*

Sergei Bashinsky†

Typically in (semi)-inclusive deep inelastic scattering the Bjorken variable x_{Bj} is fixed, and only forward hadron matrix elements are accessible. In order to accommodate these experimental conditions, we propose to describe a hadron in terms of those observables Γ that are diagonal in the basis formed by quark and gluon partons. We then construct gauge invariant x_{Bj} -distributions associated with such an observable. The gauge covariant definition of parton states in fully interacting QCD are chosen so that the parton distributions are given by the physical structure functions $q(x_{Bj})$ and $g(x_{Bj})$. To satisfy these requirements, quark and gluon partons must be eigenstates of the generators of the covariant translations,

$$\begin{aligned} T_-^q &: \psi(x) \rightarrow U(x, x+a^-) \psi(x+a^-), \\ T_-^g &: D_\lambda(x) \rightarrow U(x, x+a^-) D_\lambda(x+a^-) U(x+a^-, x), \end{aligned} \quad (1)$$

and the operator of the observable Γ must commute with T_-^q and T_-^g .

A hadron angular momentum is completely described by four scale dependent x_{Bj} -distributions. Two of them coincide with the polarized quark and gluon structure functions Δq and Δg . The other two,

$$f_{L_q}(x_{Bj}) = \frac{\int d\xi^- e^{ix_{Bj}P^+\xi^-} \langle P | \int d^2x^\perp \psi^\dagger(x^\perp) (x^1 i\mathcal{D}_2 - x^2 i\mathcal{D}_1) \psi_+(x^\perp + \xi^-) | P \rangle}{2\pi\sqrt{2} (\int d^2x^\perp)}$$

and

$$f_{L_g}(x_{Bj}) = \frac{\int d\xi^- e^{ix_{Bj}P^+\xi^-} \langle P | \int d^2x^\perp F^{+\lambda}(x^\perp) (x^1 i\mathcal{D}_2 - x^2 i\mathcal{D}_1) F_\lambda^+(x^\perp + \xi^-) | P \rangle}{4\pi x_{Bj} P^+ (\int d^2x^\perp)}$$

are naturally regarded as the x_{Bj} distributions of quark and gluon orbital angular momentum. They are well defined physical objects and are gauge invariant by means of the residual gauge covariant derivative $\mathcal{D}_i = \partial_i - ig\mathcal{A}_i$, where \mathcal{A} is given by

$$\mathcal{A}_\lambda(x^+, x^1, x^2) = \frac{1}{\int dx^-} \int dx^- A_\lambda(x) \quad (2)$$

in $A^+ = 0$ gauge. They are observable in principle and can be calculated in models or within lattice QCD. However, it remains an open question whether the x_{Bj} -distributions of quark and gluon orbital angular momentum which we have defined can be measured in a practical experimental process.

†CTP, MIT; Email address: sergei@mit.edu; phone: (617)-577-5828; fax: (617)-253-8674.

*S. V. Bashinsky, R. L. Jaffe, hep-ph/9804397.

GAUGE INVARIANT QUARK AND GLUON ANGULAR MOMENTUM DISTRIBUTIONS

(S. Bashinsky)

HEP-PH/9804397: S.B.,
R.L. JAFFE

- RECENT "BURST" OF
THEORETICAL INTEREST:
P. Hägler, A. Schäffe (9802362)
A. Harindranath, R. Kundu (9802406)
O.V. Teryaev (9803403)
P. Hoodbhoy, X. Ji, W. Lu (9804337)

- Remember the naive parton model: $p^+ = x_{Bj} P^+$

p^+ characterizes transformation properties under $x^- \rightarrow x^- + a^-$:

$$\begin{aligned}\psi_{p^+} &\rightarrow e^{-ip^+ a^-} \psi_{p^+}, \\ A_{p^+}^\lambda &\rightarrow e^{-ip^+ a^-} A_{p^+}^\lambda\end{aligned}$$

- Generalize to \rightarrow States of interacting fields \rightarrow gauge-covariant, independent t-n.

$$T_1^{\mathcal{Q}}: \psi(x) \rightarrow U(x, x+a^-) \psi(x+a^-)$$

$$T_1^{\mathcal{Q}}: D_\lambda(x) \rightarrow U(x, x+a^-) D_\lambda(x+a^-) U(x+a^-, x)$$

$$(U(x, x+a^-) \equiv P e^{ig \int_{x+a^-}^x ds^- A^+(s)},$$

$$D_\lambda(x) = \partial_\lambda - ig A_\lambda(x))$$

- gauge covariance: \checkmark

- non-interacting limit: \checkmark^*

- reproduce $q(x_{Bj}), g(x_{Bj})$: \checkmark^*

*) $T_{\underline{9}}$ and $T_{\underline{9}}$ become ordinary translations in $A^+ = 0$

- Unphysical gauge degrees of freedom: Take $A^+ = 0$ gauge. Still have the residual gauge invariance:

$$\psi(x) \rightarrow e^{i\alpha(\tilde{x})} \psi(x)$$

$$A_{\lambda}(x) \rightarrow e^{i\alpha(\tilde{x})} \left(A_{\lambda}(x) + \frac{i}{g} \partial_{\lambda} \right) e^{-i\alpha(\tilde{x})}$$

$$\tilde{x} = (x^+, x^-, x^2)$$

As for the usual gauge invariance introduce $\mathcal{A}_{\lambda}(\tilde{x})$, s.t.

$$\mathcal{A}_{\lambda}(\tilde{x}) \rightarrow e^{i\alpha(\tilde{x})} \left(\mathcal{A}_{\lambda}(\tilde{x}) + \frac{i}{g} \partial_{\lambda} \right) e^{-i\alpha(\tilde{x})}$$

($\mathcal{D}_{\lambda} \equiv \partial_{\lambda} - ig \mathcal{A}_{\lambda}$ ← the res. g. cov. der.)

$$A(x) = \mathcal{A}(\tilde{x}) + G(x), \quad G_{\lambda}(x) \rightarrow e^{i\alpha(\tilde{x})} G_{\lambda}(x) e^{-i\alpha(\tilde{x})}$$

DESCRIPTION OF NUCLEON PROPERTIES

207

- Restricted to sectors of $\tilde{\Psi}$ and \tilde{G} with $p^+ = x_{Bj} P^+$
 - \Rightarrow propose to work with observables, Γ , that are diagonal in $\{\tilde{\Psi}(p^+), \tilde{G}(p^+)\}$
 - \Rightarrow Γ 's are entirely specified by their $x_{Bj} \equiv P^+/p^+$ densities $f_{r,q}(x_{Bj}), f_{r,g}(x_{Bj})$

Necessary
& sufficient: $[\Gamma, T_-^9] = [\Gamma, T_-^8] = 0$
($[\delta_r, \delta_-^9] = [\delta_r, \delta_-^8] = 0$)

- Construct Γ x_{Bj} -distributions as $\Gamma \xrightarrow{1} \delta_\Gamma \xrightarrow{2} \delta_{\Gamma, q, g}^{(x_{Bj})} \rightarrow f_{\Gamma, q, g}(x_{Bj})$

EXAMPLE:

$$\begin{aligned} & \text{chirality} \xrightarrow{1} \delta\psi(x) = i\epsilon\gamma^5\psi(x) \xrightarrow{2} \\ & \rightarrow \delta\tilde{\psi}(p^+) = i\epsilon\gamma^5\tilde{\psi}(x_{Bj}, p^+) \delta(p^+/p^+ - x_{Bj}) \xrightarrow{3} \\ & \rightarrow \frac{1}{2\pi\sqrt{2}} \int d\zeta^- e^{ix_{Bj}p^+\zeta^-} \langle P | \psi_+^\dagger(0) \gamma^5 \psi_+(\zeta^-) | P \rangle \\ & \quad (\psi_+ \equiv \frac{1}{2} \gamma^- \gamma^+ \psi) \end{aligned}$$

- The result for $f_{\Gamma, q}(x_{Bj})$, $f_{\Gamma, g}(x_{Bj})$ is
 - gauge invariant (Wilson lines in an arbitr. gauge)
 - Lorentz boost invariant
 - Properly normalized
($q+g$ 1st moments = $\langle \Gamma \rangle$,
in free theory $f_{\Gamma, q, g} = \Gamma^{q, g} \delta(1-x_{Bj})$)
 - Reproduce $q(x_{Bj})$, $g(x_{Bj})$
(also $\Delta q(x_{Bj})$, $\Delta g(x_{Bj})$)

ORBITAL ANGULAR MOMENTUM

209

Remember:

$$[\underline{L}, T_9] = [\underline{L}, T_8] = 0$$

\Rightarrow work with γ^3 :

$$\delta\psi = i\epsilon \left[\frac{1}{2} \gamma^0 \gamma^3 \gamma^5 + (x^1 i \mathcal{D}_2 - x^2 i \mathcal{D}_1) \right] \psi$$

$$\delta G_\lambda = i\epsilon \left[\underbrace{-i(\delta_\lambda^1 \delta_2^\lambda - \delta_\lambda^2 \delta_1^\lambda)}_{-i\epsilon^{+-\lambda}} + (x^1 i \mathcal{D}_2 - x^2 i \mathcal{D}_1) \right] G_\lambda$$

$(\mathcal{D} = \partial - ig\mathcal{A})$

Substituting the generators,
obtain $f_\Sigma, f_{L_9}, f_{\Delta G}, f_{L_9}$,

e.g.

$$f_\Sigma(x_{Bj}) = \frac{i}{4\pi x_{Bj} P^+} \int d^3\xi e^{i x_{Bj} P^+ \xi^-} \times \langle P | F^{+\lambda} | 0 \rangle \langle F_\lambda^{*+} | \xi^- \rangle | P \rangle$$

$$f_{L_9}(x_{Bj}) = \frac{1}{2\pi\sqrt{2} (S d^2 x^\perp)} \int d^3\xi e^{i x_{Bj} P^+ \xi^-} \times \langle P | \int d^2 x^\perp \psi_+^\dagger(x^\perp) \underline{(x^1 i \mathcal{D}_2 - x^2 i \mathcal{D}_1)} \psi_+(x^\perp + \xi^-) | P \rangle$$

- Construct Γ x_{Bj} -distributions
as $\Gamma \xrightarrow{1} \delta_\Gamma \xrightarrow{2} \delta_{\Gamma, q, g}^{(x_{Bj})} \rightarrow f_{\Gamma, q, g}(x_{Bj})$

EXAMPLE:

$$\begin{aligned} & \text{chirality} \xrightarrow{1} \delta\psi(x) = i\epsilon\gamma^5\psi(x) \xrightarrow{2} \\ & \rightarrow \delta\tilde{\psi}(p^+) = i\epsilon\gamma^5\tilde{\psi}(x_{Bj}, p^+) \delta(p^+/p^+ - x_{Bj}) \xrightarrow{3} \\ & \rightarrow \frac{1}{2\pi\sqrt{2}} \int d\zeta^- e^{ix_{Bj}p^+\zeta^-} \langle P | \psi_+^\dagger(0) \gamma^5 \psi_+(\zeta^-) | P \rangle \\ & \quad (\psi_+ \equiv \frac{1}{2} \gamma^- \gamma^+ \psi) \end{aligned}$$

- The result for $f_{\Gamma, q}(x_{Bj})$, $f_{\Gamma, g}(x_{Bj})$ is
 - gauge invariant (Wilson lines in an arbitr. gauge)
 - Lorentz boost invariant
 - Properly normalized
($q+g$ 1st moments = $\langle \Gamma \rangle$,
in free theory $f_{\Gamma, q, g} = \Gamma^{q, g} \delta(1-x_{Bj})$)
 - Reproduce $q(x_{Bj})$, $g(x_{Bj})$
(also $\Delta q(x_{Bj})$, $\Delta g(x_{Bj})$)

DETECTOR LIMITATIONS, STAR

D. Underwood

High Energy Physics

Argonne National Laboratory

Presented at

Spin Meeting

BNL

April 28, 1998

Every detector has limitations in terms of solid angle, particular technologies chosen, cracks due to mechanical structure, etc. If all of the presently planned parts of STAR were in place, these factors would not seriously limit our ability to exploit the spin physics possible in RHIC.

What is of greater concern at the moment is the construction schedule for components such as the Electromagnetic Calorimeters, and the limited funding for various levels of triggers.

What is good in STAR

(before I launch into a limitations talk)

Large solid angle

Good tracking with Momentum	$-1 < \eta < 1$	-all ϕ
Some tracking with some Momentum info	$1 < \eta < 2$	-all ϕ
Tracking	$2.5 < \eta < 4$	-all ϕ
EMC	$-1 < \eta < 2$	-all ϕ
SVT	$-1 < \eta < 1$	-all ϕ

This is good for Gamma + Jet, Jet-Jet, e^+e^- , etc

Kinematic coverage over a range in x for gluon (see S. Vigdor Talk)

Z0 statistics

W statistics

options for $h1 \times h1$ other than $h1 \times h1$ bar

TALKS YESTERDAY:

→ DIRECT PHOTON AT STAR - STEVE VIGDOR
 JETS - STAR - STEVE HEPPELMAN

Limitations

**No Hadron Calorimeter > Jet trigger is not sharp
Must set EM threshold low to be efficient,
and then take lots of low energy stuff**

**EM Calorimeter coming on Late in Program > Partial Detector for
Early Spin Physics**

Year	Fraction of Barrel coverage	End Cap
End-1999 /2000	10%	?
End 2001 /2002	50%	?
End 2003 /2004	100%	?

**Much of Trigger is Unfunded > Low level trigger rate is limited to
DAQ and Tape rate**

**so energy thresholds are driven up
in order to to get rate down**

**(miss low x physics until funded)
(low statistics until funded)**

**Vertex Pos. Det. Unfunded > More processing to find correct vertex
out of 800 in TPC**

Trigger

The basic idea is that with all the STAR trigger present we could have 1000 HZ at level 0 (summed over all triggers) , and certain thresholds.

However, since most of STAR trigger is deferred, the Level 0 rate can't be more than 60 Hz with < 50% deadtime (and maybe the rate is lower)

This drives some of the thresholds up about a factor of 4 to get the rate down.

Particularly:

jets | (large EMC patch trigger)

less so:

electrons |

gammas | (single EMC tower trigger)

di-electrons |

Trigger that will be there : *EARLY*

Level 0

towers 0.2 x 0.2 for jet trigger

highest .05 x .05 tower for gamma / e trigger

Global Et for jet-jet

maybe simple 2-hits

charge multiplicity (CTB , MWC)

Unfunded Trigger:

Level 0

VPD to select 20 out of 800 vertices stored in TPC
SMD to get a factor of 3-5 on single tower trig rate

Level 2 Spatial Information using:

Calorimeter
Shower Max. Detector
Charged Multiplicity Counters
Silicon Vertex

A factor - 5 in trigger rate

Shower width for e to pi
Size of Jet in EM
Charged multiplicity(CTB + MWC) + neutral energy (EMC)
to define jet
refined jet-jet, gamma-jet, e+ e-
possible isolation cut for gamma using energy ratios
finding correct interaction point for tracking using SVT

Level 3

- **Using momentum in trigger (as opposed to just writing to tape)**
- **Using Momentum + EMC to sharpen jet trigger threshold**
- **Tracking using EMC hits as seeds**
(fast way to find 30 tracks out of 2400)
- **Optimizing tracking so that at least some raw data can go to tape**
from a few tracks to improve momentum resolution offline

Signal	\sqrt{s} (GeV)	Events	x Range	Sensitivity
W^+	500	72,000	0.05-0.3	$\Delta u(x)/u(x) \sim 0.01 - 0.02$
				$\Delta \bar{d}(x)/\bar{d}(x) \sim 0.01 - 0.02$
W^-	500	21,000	0.05-0.3	$\Delta d(x)/d(x) \sim 0.02 - 0.04$
				$\Delta \bar{u}(x)/\bar{u}(x) \sim 0.02 - 0.04$
Z^0	500	3,200	0.05-0.3	$\Delta h_1/q \sim 0.2$
$\gamma + \text{jet}$	500	3×10^6	0.02-.3	$\Delta G(x)/G(x) \sim 0.03$
	200	3×10^5	0.05-.3	$\Delta G(x)/G(x) \sim 0.04$
Dijets	500	5×10^7	0.03-.4	$\Delta G(x)/G(x) \sim 0.03$
	200	2×10^7	0.08-.4	$\Delta G(x)/G(x) \sim 0.05$

Uncertainties in ΔG Measurement at PHENIX

Yuji Goto, *RIKEN*

I will list what should be considered as uncertainties in ΔG measurement at PHENIX. Mainly I will show the case of prompt photon measurement.

x -independent uncertainties We have uncertainties in beam polarization measurement and luminosity measurement. We expect 10% error at the first stage of the experiment, and 5% at the final stage for the absolute value measurement of the polarization. For the relative value measurement of the polarization, our goal is less than 1%. For luminosity measurement, we expect 10% error at first, and 5% finally about the absolute value measurement. As for relative value measurement, 10^{-4} level precision is required to measure 10^{-3} level asymmetries, because this is used as normalization factor of asymmetry calculation.

x -dependent uncertainties I have reported statistics and subtraction of background mainly from $\pi^0 \rightarrow 2\gamma$ at the previous talk. We also need to subtract 10-20% contribution from the annihilation process. It is important to estimate how much asymmetry remains after subtracting backgrounds considering their asymmetries. As for event selection, what should be considered are efficiency corrections for trigger and offline cuts, detector acceptance, etc.

For the prompt photon process, quark polarization is necessary information to evaluate contribution from both the gluon Compton process and the annihilation process. The x region of PHENIX prompt photon measurement is covered by the high precision data of SLAC-E143. Anti-quark polarization is also necessary to evaluate the annihilation process. This information has not been provided yet. We can measure it by ourselves using weak boson measurement.

Theory also includes uncertainties, for instance, in estimation of the annihilation process, higher order corrections, fragmentation function, what Q^2 value should be used, etc.

uncertainties in x estimation There are uncertainties in momentum scale and in photon's p_T vs gluon's x relation. Uncertainty in momentum scale includes momentum resolution and systematic uncertainty by non-linearity of the EM calorimeter. The non-linearity originates from PMT, electronics, shower leakage, etc. Our goal of the non-linearity is 1%, because, for instance, this is enhanced to 6% cross section error at $\sqrt{s}=500\text{GeV}$ and $p_T=20\text{GeV}/c$. In addition, there is uncertainty due to intrinsic k_T . In PYTHIA simulation, we can switch off initial radiation for k_T . There is difference in low x region between ' k_T on' setting and ' k_T off' setting. This effect for gluon's x estimation is small, but it is interesting topic to investigate.

All transparencies of this talk is accessible on the Web;
<http://www.phenix.bnl.gov/WWW/publish/goto/>

The Asymmetry and Gluon Spin

$$A_{LL}(p_T, x_1, x_2)$$

$$= \frac{1}{r_{PP}} \left(\frac{N_1/L_1 - N_2/L_2}{N_1/L_1 + N_2/L_2} \right) - A_{LL}^{background} - A_{TL/TT}$$

For Jets:

$$= F_{qg}(\hat{a}_{qg}^{LO} + HO(Q^2, \alpha_s)) \left(\frac{\Sigma \Delta q(x, Q^2)}{\Sigma q(x, Q^2)} \right) \left(\frac{\Delta G(x, Q^2)}{G(x, Q^2)} \right)$$

$$+ (qq \text{ term}) + (GG \text{ term})$$

For Direct Photon:

$$= F_{qg}(\hat{a}_{qg}^{LO} + HO(Q^2, \alpha_s)) \frac{g_1}{F_1}(x, Q^2) \left(\frac{\Delta G(x, Q^2)}{G(x, Q^2)} \right)$$

$$+ (q\bar{q} \text{ term})$$

List of Systematic Errors

Error Source	Estimated Size
Error on A_{LL}	
Beam Polarization magnitude	$\Delta A/A = 0.1 \rightarrow 0.05$
Relative Luminosity Measurement	$\Delta A \leq 0.001$
Polarization and Luminosity Correlation	small
Backgrounds	
Polarized Backgrounds	
Kinematic Resolution	
Transverse Components of Polarization	small
Spin dependent rate (dead time, pile up, etc)	very small
Detector Stability	very small
Detector Asymmetry	very small
Error on ΔG	
Uncertainty on g_1/F_1	$\Delta A/A = 0.05 - 0.1$
Unpolarized quark/gluon PDF	
Polarized quark PDF	
Unfolding PDFs with $x_1, x_2 \rightarrow x_q, x_g$	
QCD Higher Order	
QCD scale factor	
Uncertainty on α_s	
Isolation cut and photon fragmentation function	
QCD k_T smearing	

Uncertainties in X Estimation

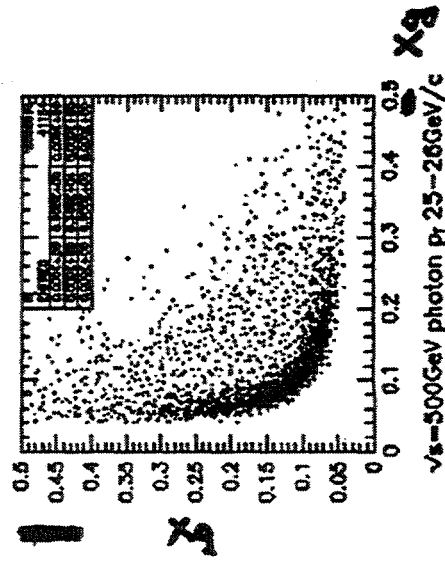
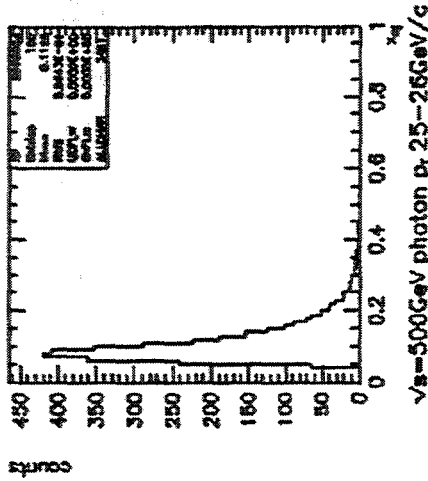
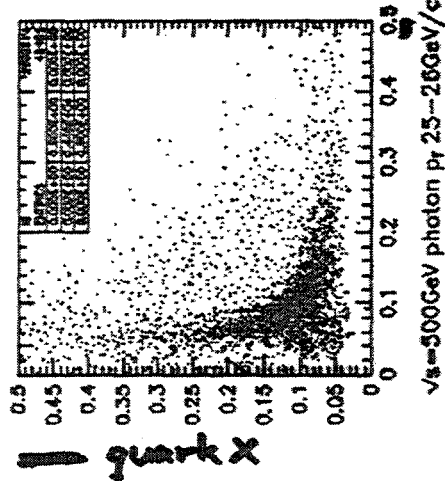
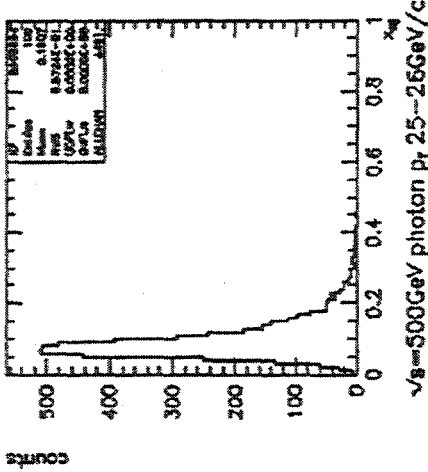
- P_T vs gluon's X - uncertainty by k_T

- in PYTHIA initial radiation

$$k_T^2 = (1-z)Q^2$$

z: splitting fraction of initial radiation

$$k_T^2 = 0$$



Summary

x-independent uncertainties					
beam polarization	absolute		10% -> 5%		
	relative		Goal: <1%		
luminosity	absolute		10% -> 5%		
	relative		10**-4 ?		
x-dependent uncertainties					
statistics	(for prompt photon)		5% - 30%		(for sqrt(s)=200GeV, pT 10 - 30GeV/c, 5GeV/c bin)
background subtraction	(for prompt photon)		<20% background		(for sqrt(s)=200GeV, pT 10 - 30GeV/c, 5GeV/c bin)
hadron & bremsstrahlung			?		
event selection			<1%		
theoretical	annihilation process		<20% background		
	higher order correction, etc.		(* uncertainty of quark pol.)		
	quark polarization		?		
uncertainties in x estimation			20% - 8%		(for x=0.04 - 0.25 in 15 bins)
momentum scale			Goal: 1%		
pT vs x			>50% * slope of asymmetry		
kT			?		
global analysis			?		

Next-to-Leading Order Issues in Spin Pdf Determinations

B. Kamal

*Physics Department, Brookhaven National Laboratory, Upton, New York 11973,
U.S.A.*

SUMMARY

It was demonstrated that the leading order (LO) pdf's are process dependent to $\mathcal{O}(\alpha_s)$, while the next-to-leading order (NLO) ones are process dependent only to $\mathcal{O}(\alpha_s^2)$. Using NLO, or higher, pdf's it is thus possible to test the validity parton model by verifying explicitly the reduction in process dependence as one goes to higher orders in perturbation theory. The same applies to the ratio of the polarized to unpolarized pdf's. This should manifest itself through a convergence of the perturbation series to the experimental result for new processes which were not included in the fits. The issue of factorization scheme dependence was discussed and the mechanism for the evolution of $\Delta\Sigma$ was illustrated without making explicit use of the ABJ anomaly. The result for that evolution is in exact agreement with that obtained via the above mentioned anomaly, at two-loops, as is required.

Consistent NLO predictions for all longitudinal Drell-Yan type processes at RHIC (W^\pm , Z and γ^*) were made using polarized parton distributions which fit the recent DIS data. Particular attention was paid to regularization and factorization scheme dependences. The HOC increased the cross sections substantially and had a major impact on the asymmetries, while preserving the features of the LO asymmetries. The exact sign and magnitude of the HOC depended on the details of the parton distributions used, especially the polarized gluon distribution. Faced with either low rates or small asymmetries, γ^* production didn't prove very interesting for longitudinal polarization (unless the agreement between the various parton distributions at small- x is an artificial one). The Z -asymmetries were all quite sensitive to the sea quarks; the parity violating ones being the largest, with unexpected sensitivity due to a coincidental cancellation between u and d valence contributions. With large rates and asymmetries, W^\pm production can directly measure the sea and valence distributions as well as the unpolarized \bar{u}/\bar{d} ratio. Lower energy running could measure directly \bar{u} and \bar{d} at rather large x (both polarized and unpolarized).

NLO Issues in Spin pdf Determinations

- Process Independence of pdf's
Provides best test of Parton Model (PM) for pol. & unpol. processes.

Why?

Can almost always fit some specific piece of data just by playing with pdf's.

But

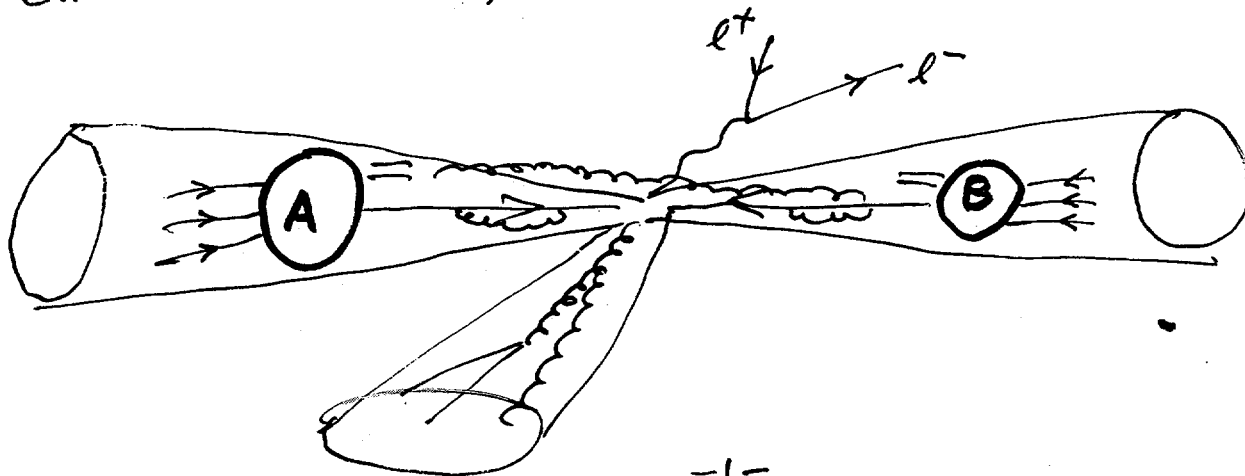
PM expression in reality involves all-orders pdf's & x-sctns (or high order in pert. theor: N-loop, $N \gg 1$, where series best approximates reality).

Specifically:

$$[\Delta] \sigma_{AB}^{\text{exp}}(M^2) \simeq \sum_{ij} \int dx_1 dx_2 [\Delta] f_{i/A}^N(x_1, M^2) [\Delta] f_{j/B}^N(x_2, M^2) [\Delta] \sigma_{ij}^N(M^2, \dots)$$

↑ Physical scale
 ← arbitrary scale
 ← All orders \simeq N-loop

Validity of PM relies on process independence of $[\Delta] f_{i/A}^N$ since experimental cuts can never eliminate collinear, soft & virtual partonic radiation



Hence, even with most stringent cuts, need to know $\hat{\sigma}_{\text{virt+soft+collin.}}^N \rightarrow$ contains all scheme, scale dep's

\rightarrow cancel w/ opposite scheme, scale dep's in f_i^N to $\mathcal{O}(\alpha_s^{N+1})$

$$\Rightarrow \sigma^{\text{exp}} = \sigma_{\text{theor.}}^N + \mathcal{O}(\alpha_s^{N+1}) \quad \text{if PM works}$$

$\Leftrightarrow [\Delta]f_i^N$ process indep., since $[\Delta]\hat{\sigma}_{ij}^N$ based only on PQCD \rightarrow not a source of problems if expansion well-behaved.

Now:

Process indep. of $[\Delta]f_{i/A}^N(x, \mu^2)$ [to $\mathcal{O}(\alpha_s^{N+1})$]
 \Rightarrow process dep. of $[\Delta]f_{i/A}^{\text{LO}}(x, \mu^2)$ of $\mathcal{O}(\alpha_s)$

because σ^{exp} is unique, but $\hat{\sigma}_{ij}^N$ & $\hat{\sigma}_{ij}^{\text{LO}}$ differ by a (K-) factor which is different in magnitude and x dependence from process to process.

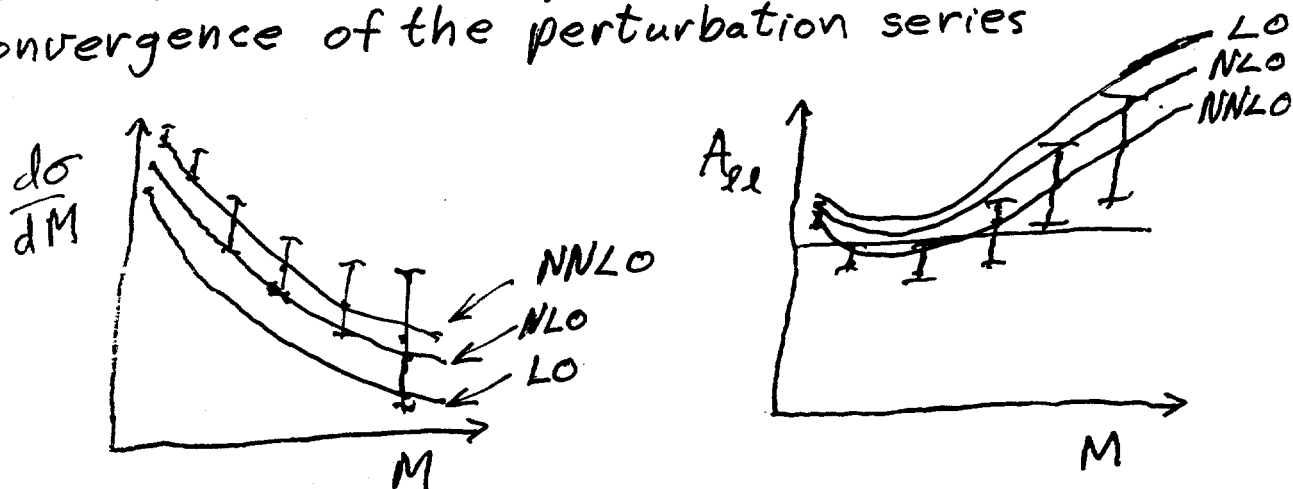
Also, new $\hat{\sigma}_{ij}$ enter @ NLO, NNLO, ...

\Rightarrow Roughly speaking, processes w/ larger (smaller) K-factors will tend to give $[\Delta]f_i^{\text{LO}}$ which are larger than (closer to) $[\Delta]f^N$, etc...

Ex: DIS has small K-factor, DY has large K-factor $\rightarrow [\Delta]f^{\text{LO}}$ determined from DIS closer to $[\Delta]f^N$ than $[\Delta]f^{\text{LO}}$ determined from DY, which will be larger.

Similar issue for $\Delta f_i^{LO}/f_i^{LO}$ since asymmetries receive a K-factor as well, which is also process dependent.

Then, ideally, if we measured $[\Delta]f^N$ in some set of processes (DIS, etc...), we could go to another set of processes (DY, etc...) and test the convergence of the perturbation series



In this way, we test the process independence of the pdf's.

⇒ Just need to pick a factorization scheme.
At NLO, can work in any scheme & differences $\mathcal{O}(\alpha_s^2)$. → Use whatever available.

At LO, differences $\mathcal{O}(\alpha_s)$ → traded a process dependence for a scheme dependence. But, ...
now A_{22} , etc... represent first term in a (hopefully) meaningful expansion.

• How does factorization scheme dependence enter?

In order to cancel mass singularities @ 1-loop, must express bare parton dists in terms of renormalized ones, similar to UV renormalization:

"Master Eq'n"

$$f_{i/A}^0(x) = f_{i/A}^r(x) + \frac{C(\epsilon)}{\epsilon} \frac{\alpha_s}{2\pi} \sum_j \int \frac{dy}{y} f_{j/A}^r(y) [P_{ij}(x/y) + \epsilon T_{ij}(x/y)]$$

$\frac{1}{\epsilon} - \gamma_E + \ln 4\pi$ ← AP splitting fn defines fact. scheme

Can determine rel'n between $f_{i/A}^r$ of different schemes using above eq'n since $f_{i/A}^0$ factoriz'n scheme indep. (depends only on regularization scheme)

The possibilities are endless:

$$(\Delta_r P_{ij} \equiv \Delta P_{ij}, \Delta_u P_{ij} \equiv P_{ij}) \quad k=u,d$$

	\overline{MS}	\overline{MS}_{HC} (2-loop pol split fn's)	\overline{MS}_E (BK)	\overline{MS}_p (Gordon + Vogelsang)
$\Delta_k T_{qq}$	0	$\Delta_r P_{qq}^E - \Delta_u P_{qq}^E$	$\Delta_k P_{qq}^E$	$\Delta_r P_{qq}^E - \Delta_u P_{qq}^E$
$\Delta_k T_{qg}$	0	0	$\Delta_k P_{qg}^E$	$\Delta_r P_{qg}^E$
$\Delta_k T_{gq}$	0	0	$\Delta_k P_{gq}^E$	$\Delta_r P_{gq}^E$
$\Delta_k T_{gg}$	0	0	$\Delta_k P_{gg}^E$	$\Delta_r P_{gg}^{E, <}$

most commonly used GRSV, GS

• How do we know pdf's so obtained contain any meaningful physics? Pdf's should satisfy positivity

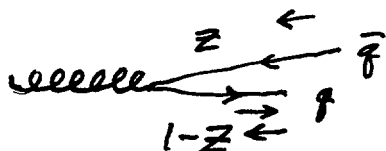
$$\Delta f_i < f_i$$

What else?

Note the following peculiarity of DREG/HVBM regularization

$$P_{gg,++}^n(z) \neq P_{gg,-+}^n(1-z) \quad [\mathcal{O}(\epsilon) \text{ effect}]$$

Hence, in n -dimensions, when a gluon splits into a collinear $q\bar{q}$ pair, they don't necessarily have opposite chirality



\Rightarrow indirectly violates chirality conservation & leads to the evolution of $\Delta\Sigma$ via ΔP_{gg}^{PS} , in \overline{MS}_{HC} .

Question: Do we need to enforce chirality conservation strictly to obtain meaningful pdf's? Answer: Not clear.

Note: Schemes like \overline{MS}_p , \overline{MS}_E , ... restore chirality conservation and prohibit the evolution of $\Delta\Sigma$
 \rightarrow Makes life simpler if nothing else.

• Drell-Yan

Working in \overline{MS}_{HC} scheme & using corresponding NLO pdf's throughout, all mass differential Drell-Yan observables were calculated for longitudinal polarization (W^\pm, Z^0, γ^*)

see

B.K. hep-ph/9710374 & PRD online, June 1.

DETERMINATIONS OF THE POLARIZED GLUON DISTRIBUTION⁽⁺⁾

A.P. Contogouris^{a,b}, Z. Merebashvili^{b(*)}, G.Grispos^a, V. Spanos^a and G. Veropoulos^a

a. Nuclear and Particle Physics, University of Athens, Athens 15771, Greece

b. Department of Physics, McGill University, Montreal H3A 2T8, Canada

SUMMARY

Photoproduction of heavy quarks in polarized photon-proton collisions, including higher order corrections (HOC), is studied. It is found that the HOC significantly enhance the Born contribution (K-factors well exceeding unit). The resulting asymmetries permit a distinction between various scenarios for the size and shape of the polarized gluon distribution. The results are compared to earlier work on large- p_T direct photon production in polarized proton-proton collisions at RHIC and fixed-target energies.

(+) Also supported by the General Secretariat of Research and Technology of Greece and by the Natural Sciences and Engineering Research Council of Canada.

(*) Now at the High Energy Physics Institute, Tbilisi State University, Tbilisi, Republic of Georgia.

Phys. quantities:

$Q=c$. Let $y = \text{c.m. rapid. of } c$:

$$\Delta \frac{d\sigma}{dp_T dy}(s, p_T, y), \quad \Delta \frac{d\sigma}{dp_T}, \quad \Delta \frac{d\sigma}{dy}$$

K-factors corresp. to $\Delta d\sigma/dp_T = \Delta\sigma$

$$K = \frac{\Delta\sigma_B + \Delta\sigma_{HOC}}{\Delta\sigma_B} \quad \text{vs } x_T$$

Asyms:

$$A = \Delta\sigma/\sigma$$

Results at $\sqrt{s}_{\gamma\gamma} = 10 \text{ GeV}$; also at 40 & 150, typical
HERA (pre-proposal).

NOTE: Results for photopr. by real γ ; for leptopr.
at $q^2 \approx 0$: Weisz.-Will. involu. $\int_{\text{over}} [\Delta]P = \frac{17(1-z)^2}{2}$
 \Rightarrow asymmetries smaller.

CONCLUSIONS

Det. HOC of $\bar{\gamma}\bar{p} \rightarrow Q(\bar{Q}) + X$ due to domin. subpr.

$\bar{\gamma}\bar{q} \rightarrow Q\bar{Q}$; also resolved γ contribtn (small):

(a) K-factors (large $z > 0$)

(b) Asymmetries: COMPASS can disting. set A from B, C;

to disting. B from C need good stat. at larger x_T .

Best way disting all A, B, C: $\sqrt{s}_{\gamma\gamma} \sim 40-150 \text{ GeV}$ (preproposal)

COMPARE: COMPASS $\bar{\mu}\bar{p} \rightarrow \mu + c + X$ vs RHIC $\bar{p}\bar{p} \rightarrow \gamma + X$:

Better is RHIC

Phys. Rev. D55, 2718 (97)

DETERMINATIONS OF THE POLARIZED GLUON DISTRIBUTION

A.P. Contogouris, Z. Merebashvili, G. Grigoris, V. Spanos &
G. Veropoulos

Central problem of Spin Physics:

Size & shape of polzed gluon distr. Δg

Best way: Study polzed reactions domtd by
subprs with initl gluons. One case:

$\vec{p}\vec{p} \rightarrow \gamma(\text{large-}p_T) + X$ Kamal-Hereb-Tkachou-C
domtd by $\vec{q}\vec{q} \rightarrow \gamma q$. Another: Gordon-Vogelsang

domtd by $\vec{\gamma}\vec{p} \rightarrow Q(\bar{Q}) + X$
 $\vec{\gamma}\vec{q} \rightarrow Q\bar{Q}$

Expt: COMPASS (CERN) $\sqrt{s_{pp}} \sim 10$ GeV

Pre-proposal: HERA; (SLAC-E156)

Present HOC for contribtn of subpr. γq to $\vec{\gamma}\vec{p}$;
present asymms A & discuss possib. to disting.
between various scenarios for Δg ;

compare with corresp. A of $\vec{p}\vec{p} \rightarrow \gamma + X$ (RHIC)

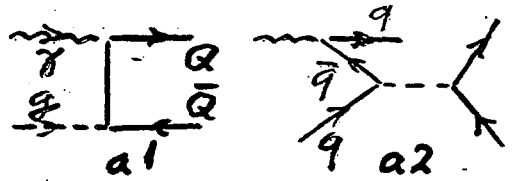
NOTE: Interested in whole Δg : all moments
(not just in 1st mom.)

Leading order (α_s)

(a1) Born

(a2) Resolved γ via

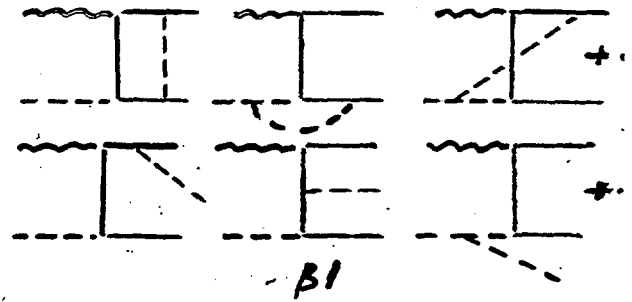
$\bar{q}q \rightarrow Q\bar{Q}$
 γ str. fn $\Delta F_{q/\gamma}$



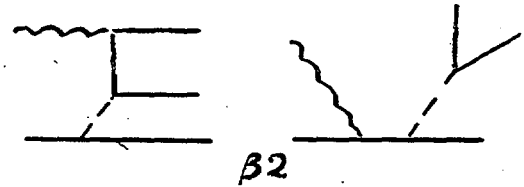
$\bar{q}q \rightarrow Q\bar{Q}$
 $\Delta F_{q/\gamma}$ known only theo.

NLO (α_s^2)

(B1) Loops & Brems
HARDEST part due
 to $m_Q \neq 0$.
 Results for this.



(B2) Subpr.
 $\bar{q}q \rightarrow Q\bar{Q}q$
 no loops
 Prelim. results: small



Req. (a2): Using theoret. $\Delta F_{q/\gamma}$ $\Delta F_{q/\gamma}$
 contribtns small in \bar{MS} & phys. scales.

Hassan & Pilon

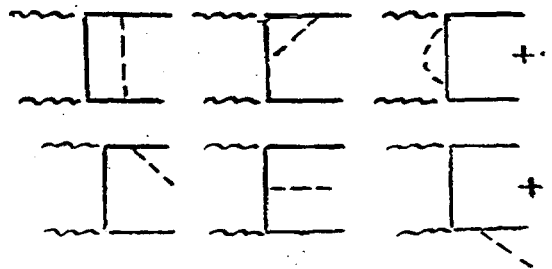
NOTE

Abelian part of (B1) provides HOC to

Kamal-Mereb. - C
 Phys. Rev. D51, 4802
 199.

$\bar{\gamma}\bar{\gamma} \rightarrow Q\bar{Q}$

This of interest in itself
 in Higgs search when
 $m_H < 2m_V$



Determinn of HOC:

Loops via Passarino-Veltman, Brems integrals via
Gottfr.-Jackson frame of final $q + \bar{Q}$.

Eliminm of singuls ($1/\epsilon^2$ & $1/\epsilon$): Dimnl reduction;
to satisfy Ward's id add finite vertex cterterm

$$\gamma^\mu \rightarrow \frac{-g^2}{(4\pi)^2} C_F \left(g^{\mu\nu} - \frac{q^\mu q^\nu}{q^2} \right) \gamma_\nu$$

Renormaliztn: Of heavy Q mass & w-fn: on-shell.

Of charge: In scheme with internal loops of heavy Q
subtracted out (heavy Q decoupled).

Polzd parton distrs: 2-loop split fns: several groups.

use distrs of one group, 3 sets Gehrm.-Stirl.

set A: $\Delta g(x) > 0$, reltvely large

B: > 0 , " small

C: $\Delta g(x)$ changes sign; for $x > 1$ $\Delta g < 0$;

even for A, signif. $<$ old Δg

These parton distrs in modif. t'Hooft-Veltman ($\sim \overline{MS}$)

since our HOC in dimnl redctn: conversion terms.

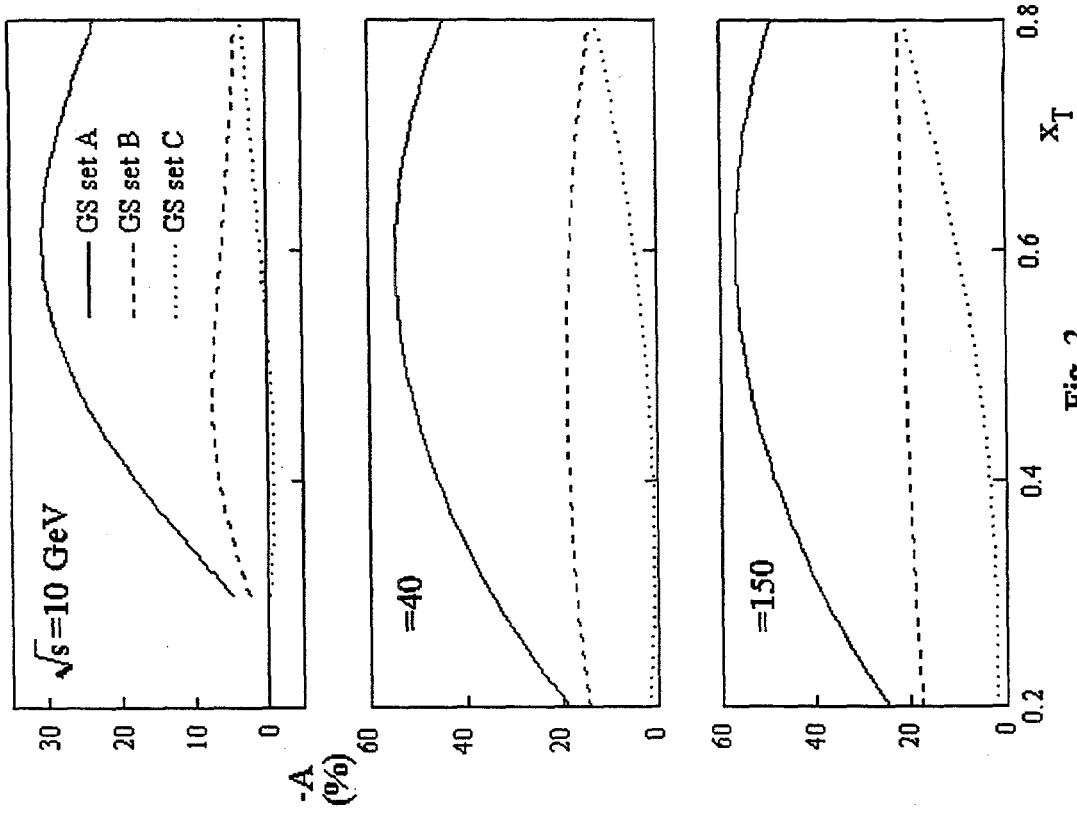


Fig. 2

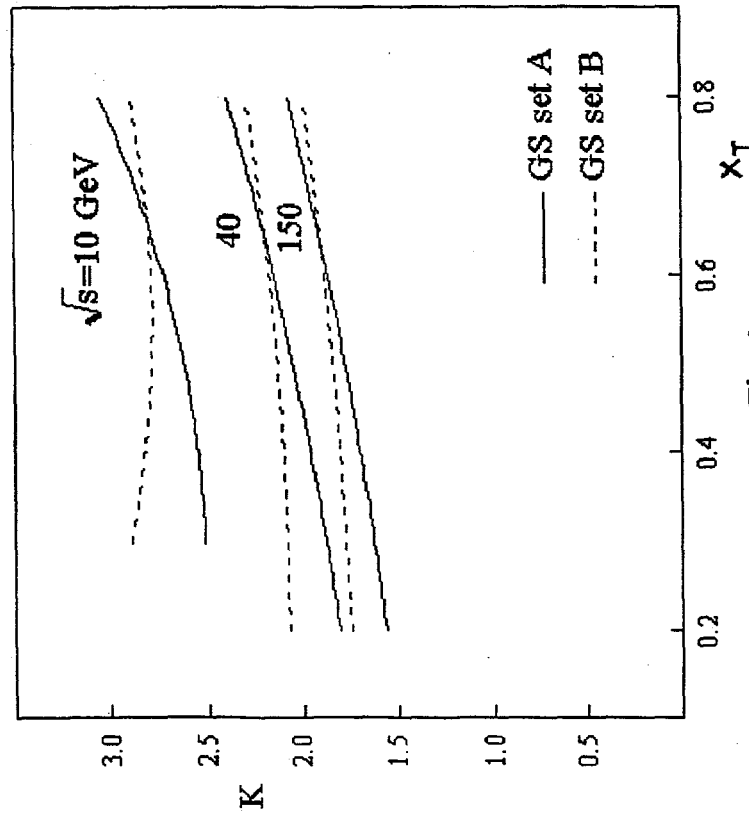
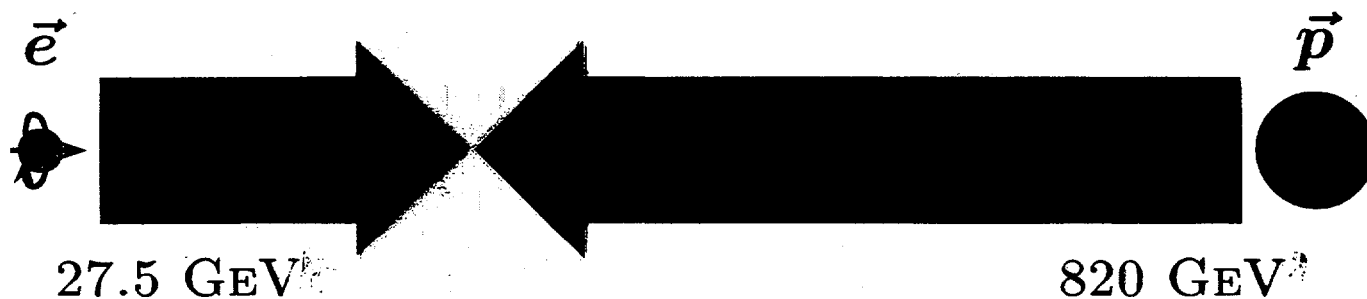


Fig. 1

PHYSICS WITH POLARISED PROTONS AT HERA

ALBERT DE ROECK
CERN/DESY

BNL, RHIC-SPIN, APRIL 27-29, 1998



$$\sqrt{s} = 300 \text{ GeV}$$

- ★ BEHAVIOUR OF $g_1(x, Q^2)$ AT SMALL x AND LARGE $Q^2 \rightarrow$ TIGHT CONSTRAINTS ON QCD FITS
- ★ $\Delta G(x, Q^2)$ FROM SEVERAL METHODS:
 - TRACKS AND JETS: SHAPE OF $\Delta G(x, Q^2)$ IN THE RANGE $0.002 < x_g < 0.2$
 - NLO FITS TO g_1 : $\delta \int \Delta G dx \rightarrow 20\%$
 - NLO FITS $g_1 + \text{JETS}$: $\delta \int \Delta G dx \rightarrow 10\%$
 - PHOTOPROD. OF JETS AND HIGH P_T TRACKS
- ★ POLARISED PARTON DISTRIBUTIONS IN THE PHOTON Δq_γ FROM PHOTOPRODUCTION STUDIES
- ★ DIRECT DETERMINATION OF $\Delta q_V = \Delta q - \Delta \bar{q}$ FROM CHARGED CURRENT EVENTS
- ★ $\vec{N}N$ AND $\vec{N}\vec{N}$ SCATTERING AT $\sqrt{s} = 40$ GEV: SHAPE OF $\Delta G(x, Q^2)$ FOR $0.1 < x_g < 0.4$

...AND MUCH MORE

MANY OF THESE ARE UNIQUE TO HERA

STATUS

- MACHINE + PHYSICS REVIEW WORKSHOP
PLANNED FOR \approx MAY '99
- $\vec{e}\vec{p} \geq 2004$?

POLARIZED
HERA

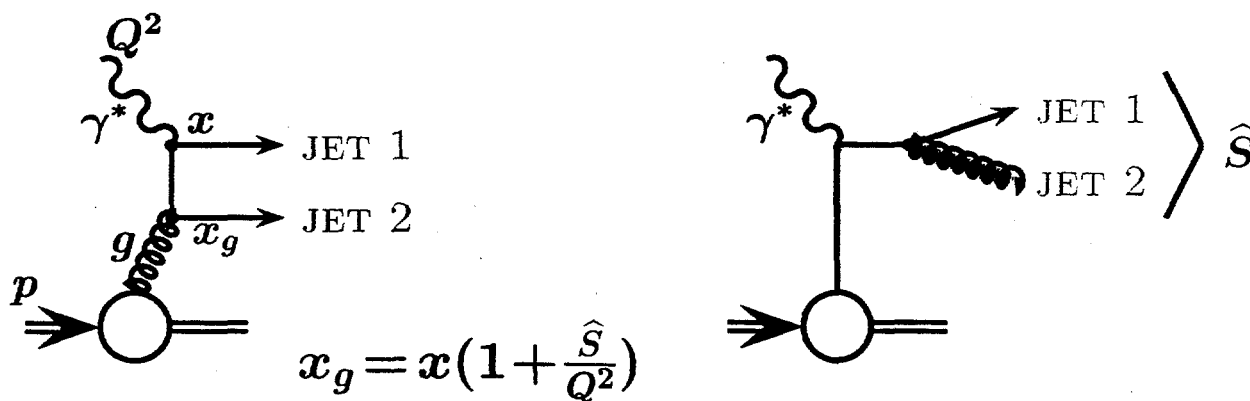
HUNTING ΔG ...

237
A. DE ROECK
(DESY / CERN)

[HTTP://WWW.DESY.DE/~GEHRT/HERASPIN](http://www.desy.de/~gehrt/HERASPIN)

★ ΔG FROM NLO FITS TO g_1 "INDIRECT"

★ ΔG FROM 2-JET EVENTS (LO) "DIRECT"



"BOSON GLUON FUSION (BGF)"

SIGNAL

"QCD-COMPTON"

BACKGROUND

★ ΔG FROM 2-HIGH- p_T TRACKS WITH OPPOSITE
AZIMUTH, SAME DIAGRAMS AS ABOVE
EXCHANGE "JET" \leftrightarrow "TRACK"

★ ΔG FROM A COMBINED FIT ($g_1 + \text{JETS}$)

★ ΔG FROM JETS/TRACKS IN
PHOTOPRODUCTION DATA

★ ΔG FROM VECTOR MESON
AND CHARM PRODUCTION

⊖ AT HERA

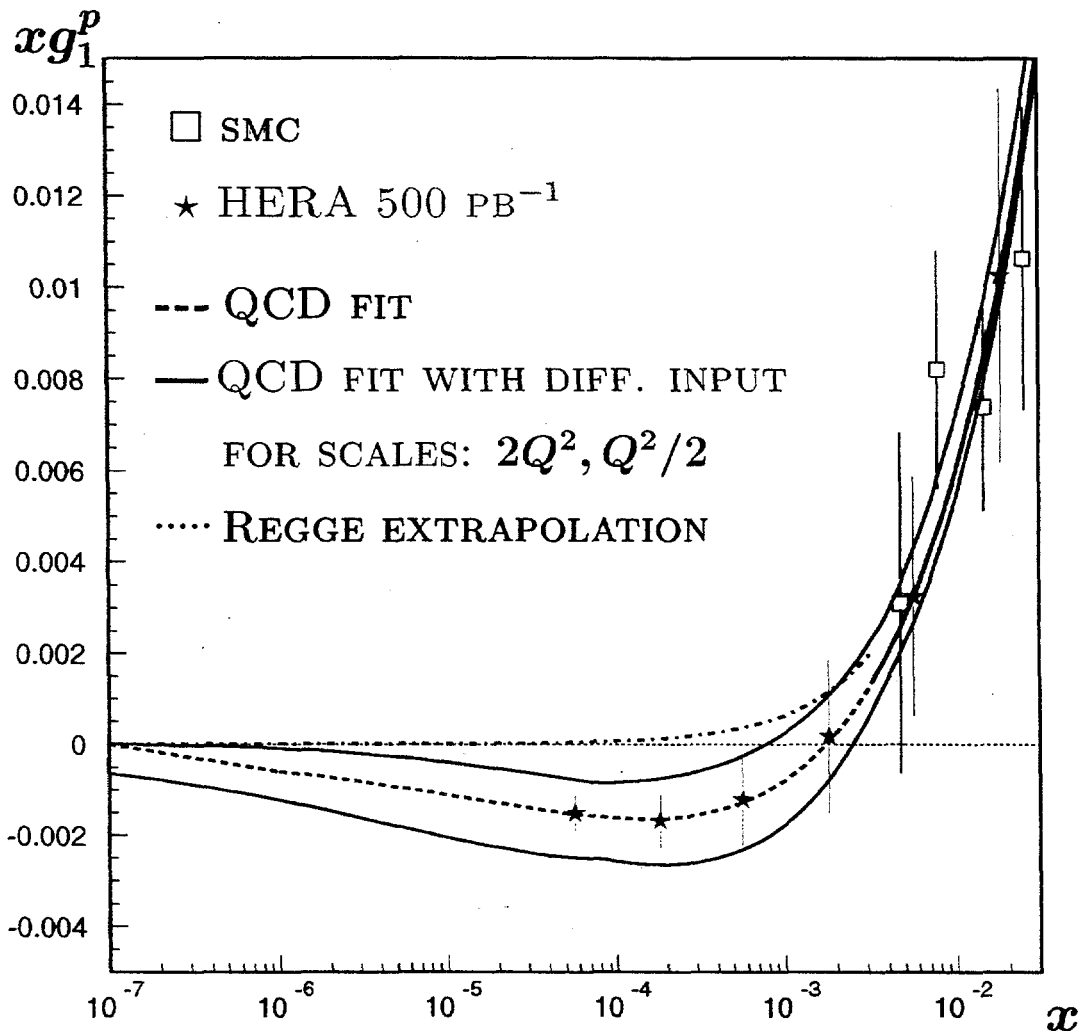
ΔG TODAY FROM SCALING VIOLATIONS, E.G.:

$$\delta(\Delta G) = \pm 0.3 \text{ (EXP)} \pm 1.0 \text{ (THEORY)}$$

(SMC, PLB 412 (1997), 414)

+ HERA 'DATA': $\delta(\Delta G) = \pm 0.2 \text{ (EXP)}$

LARGEST CONTRIBUTIONS TO THEORETICAL ERROR:
RENORMALIZATION & FACTORIZATION SCALES (Q^2)



HERA DATA DIFFERENTIATES BETWEEN SCALES
 $\rightarrow \delta(\Delta G)_{\text{SCALES}}$ DECREASES BY \approx FACTOR 3

ΔG FROM 2-JET PRODUCTION

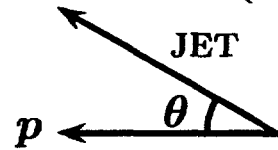
A. DE ROECK, M. MAUL, G. RÄDEL

SELECTION:

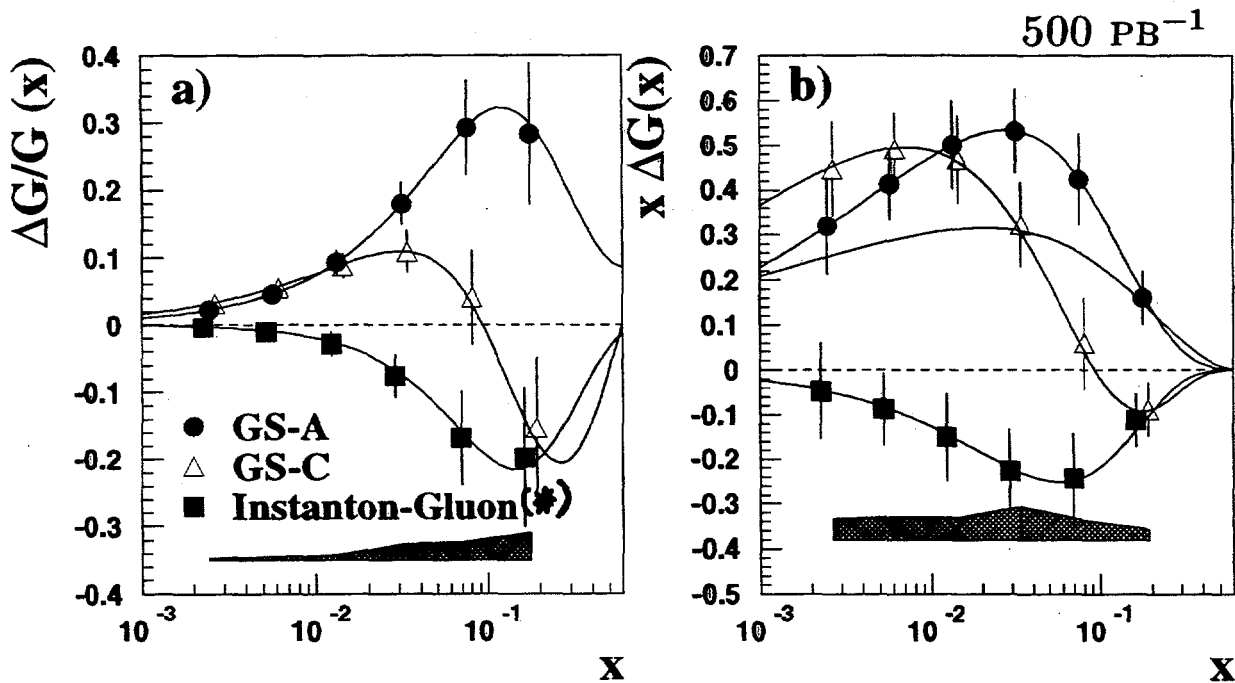
- $5 < Q^2 < 100 \text{ GEV}^2$
- $0.3 < y < 0.85$
- $p_T^{\text{JET}} > 5 \text{ GEV}$
- $|\eta_{\text{LAB}}^{\text{JET}}| < 2.8$

DETECTOR EFFECTS INCLUDED

$$\eta = -\ln \tan(\theta/2)$$



EXTRACTED GLUON (LO) AT $Q^2 = 20 \text{ GEV}^2$



→ MEASURE THE POLARISED GLUON DISTRIBUTION

FOR $0.002 < x_g < 0.2$

NLO CORRECTIONS STUDIED: $\sim 10\%$ SMALL !

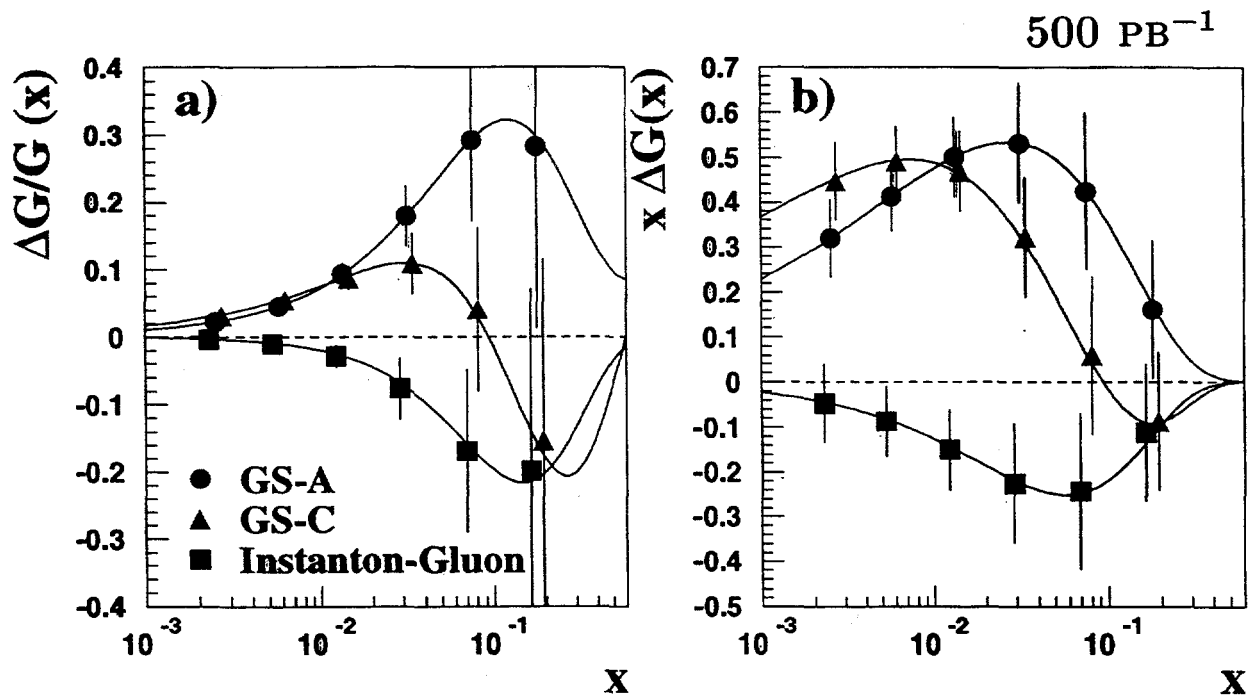
E. MIRKES, S. WILLFAHRT

* N. KOICHELEV HEP-PH/9707418

A. DE ROECK, G. RÄDEL

SELECTION:

- $5 < Q^2 < 100 \text{ GEV}^2$
- $0.3 < y < 0.85$
- $p_T^{\text{HAD}} > 1.5 \text{ GEV}$
- $-1.5 < \eta_{\text{LAB}}^{\text{HAD}} < 2.5$
- $|\Phi_{\text{HAD } 1} - \Phi_{\text{HAD } 2}| < 60^\circ$

EXTRACTED GLUON (LO) AT $Q^2 = 20 \text{ GEV}^2$ 

→ SIMILAR RESULT AS FOR 2-JET ANALYSIS, BUT:

- WORSE AT HIGHEST x (CAN BE IMPROVED)
- POTENTIAL TO REACH LOWER x

OVERLAP 2-JET/2-HADRON SAMPLE $\sim 40\%$

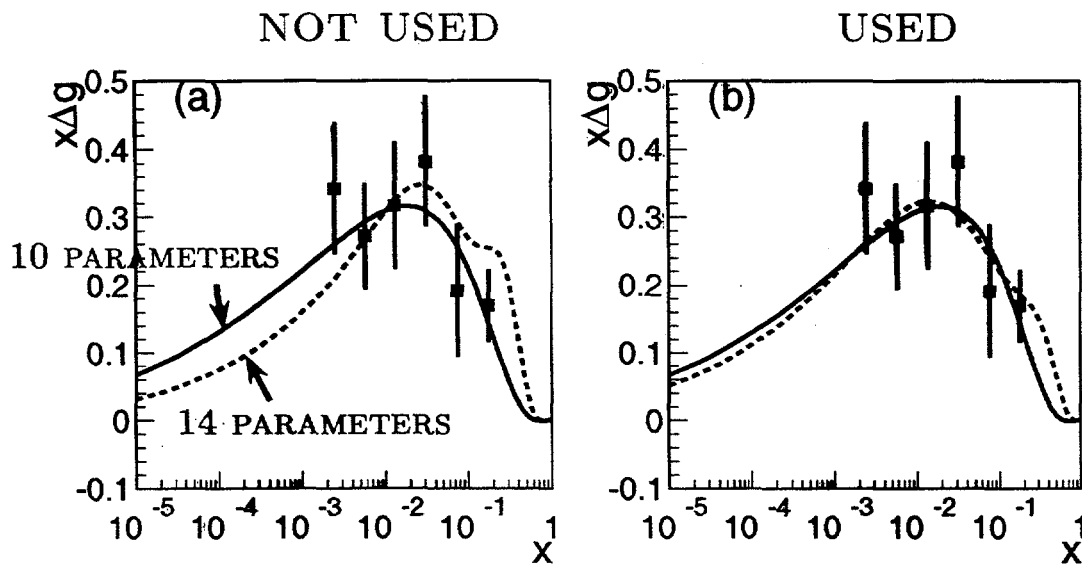
A.DE ROECK, A.DESHPANDE, V.HUGHES, J.LICHTENSTADT, G.RÄDEL

USE DATA ON $g_1(x, Q^2)$ AND ΔG FROM
2-JET EVENTS IN A COMBINED FIT

CHECK IMPACT ON: ★ $\delta(\int \Delta G dx)$

★ SHAPE OF $\Delta G(x)$

FIT RESULT: JET INFORMATION



DATA USED

$\delta(\int \Delta G)_{\text{EXP}}$

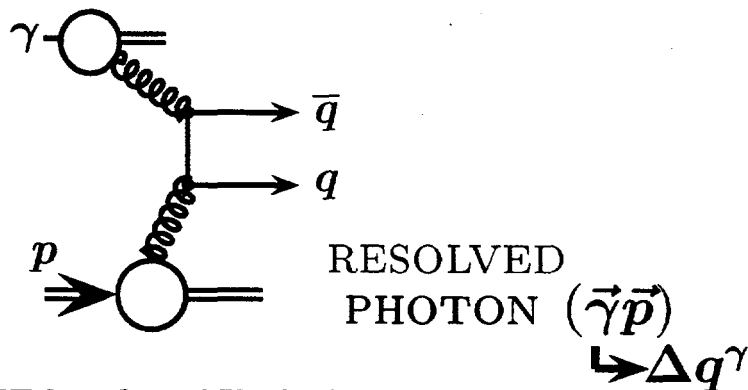
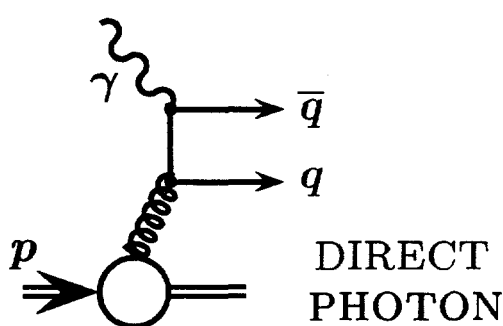
PRESENT FIXED TARGET g_1	→	30%
+ HERA $g_1(x, Q^2)$	→	20%
+ HERA 2-JETS	→	10%

→ SIGNIFICANT IMPROVEMENT ON $\delta(\int \Delta G)_{\text{EXP}}$
SHAPE BETTER CONSTRAINED

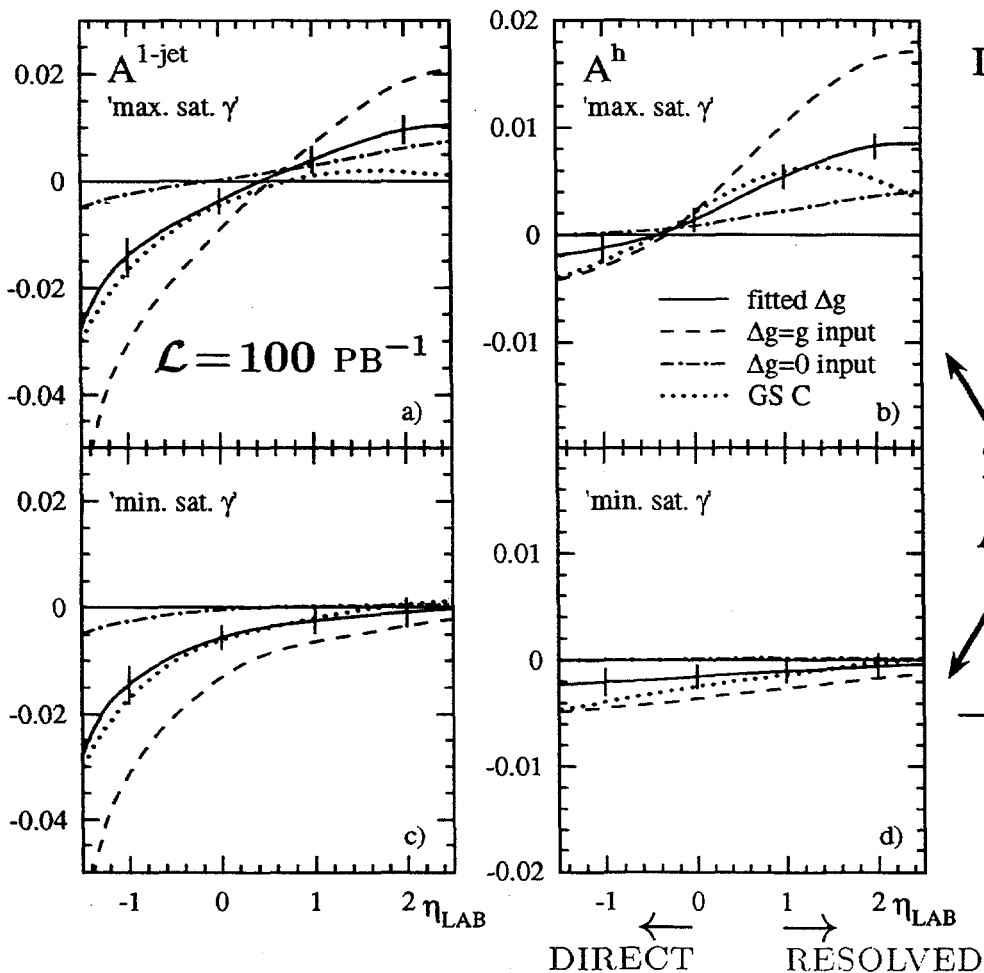
PHOTOPRODUCTION ($Q^2 \approx 0$)

J. BUTTERWORTH, N. GOODMAN, M. STRATMANN, W. VOGELSANG

HIGH- p_T JET/HADRON PRODUCTION:



INCLUSIVE ASYMMETRIES FOR SINGLE
 JETS: $p_T > 8$ GeV HADRONS: $p_T > 2$ GeV

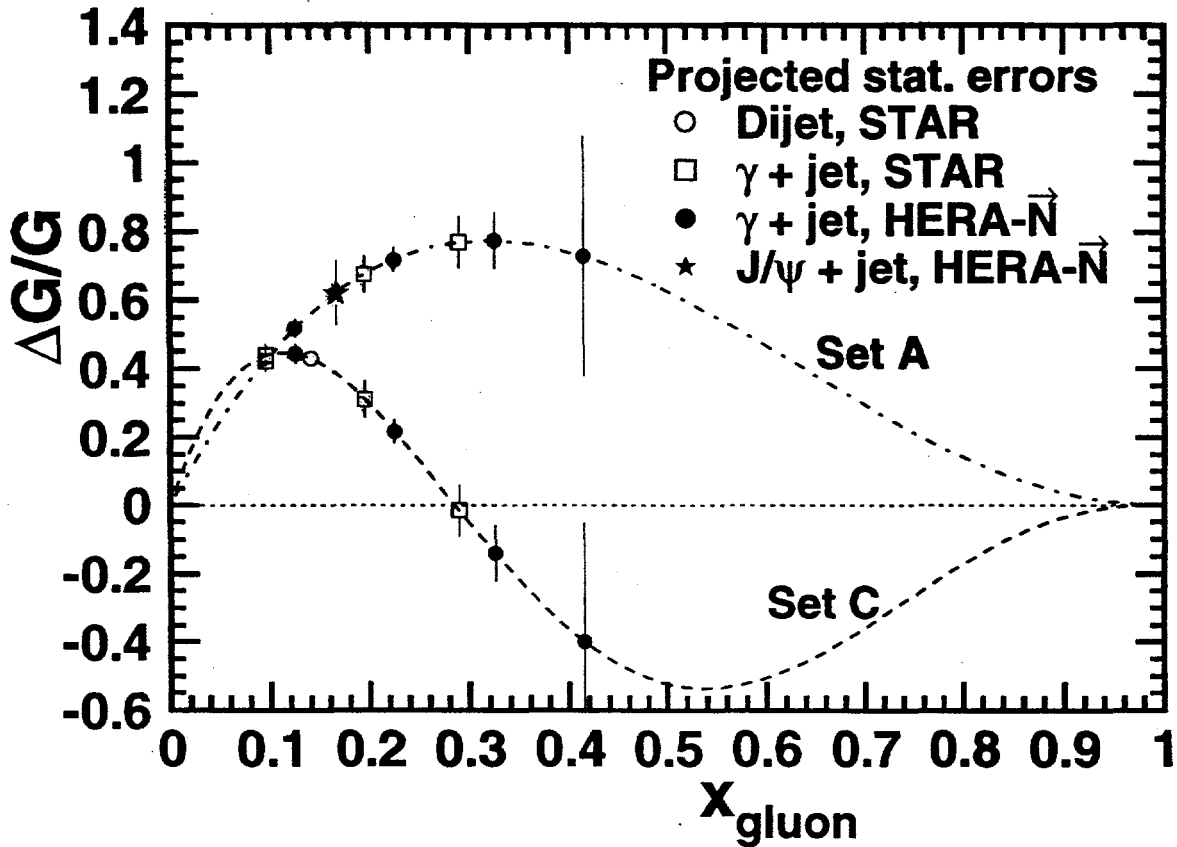


INFORMATION
 ON Δq^γ
 UNIQUE
 TO HERA

2 DIFFERENT
 ASSUMPTIONS
 FOR Δq^γ

→ SENSITIVITY
 TO Δq^γ
 AND ΔG

$\vec{p}\vec{p} \rightarrow \gamma + \text{JET} + X, \vec{p}\vec{p} \rightarrow J/\Psi + \text{JET} + X$



	<u>STUDY $\Delta G/G$ IN</u>				
HERA- \vec{N}	2	4	6	8	$p\text{QCD ONSET REGION}$
RHIC	10	20	30		$\text{DEEP PERTURB. REGION}$
	—————→ p_T				

COMPLEMENTARY EXPERIMENTS!

(V. KOROTKOV)

Polarized Protons Project Status and Plans

Mike Syphers, BNL
RSC Workshop, 27 April 1998

RHIC Requirements for Polarized Proton Operation

- 25 GeV ----> 250 GeV
- Longitudinal polarization at major experiments
- Full Siberian Snake(s)
 - ⇒ $(1.8)(250 - 25) = 405$ imperfection resonances, plus many intrinsic resonances
- Need fine vertical orbit control / correction
 - ⇒ investigating harmonic and other correction schemes

Project Funding -- Primarily from RIKEN

- Funding for Accelerator Components: 1B Yen (\$10 M)

(Less, due to exchange rate!)

constant issue... (4/27/98: 132 Y/\$)

Superconducting Magnet System Requirements

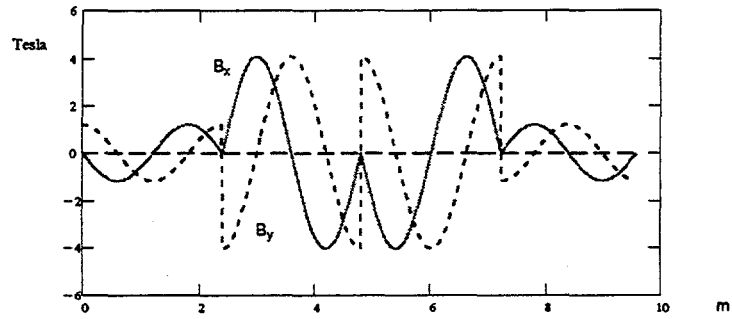
For the Siberian Snakes and Spin Rotators in RHIC:

- Works for 250 GeV Protons with reasonable field strengths
- Large aperture, for necessary orbit distortions, ...
- ... yet high field to keep orbit distortions small and local
- Low current (low heat-leak through power leads) and tunable
- Fits in available space in RHIC ring
- Minimize number of different components to be built

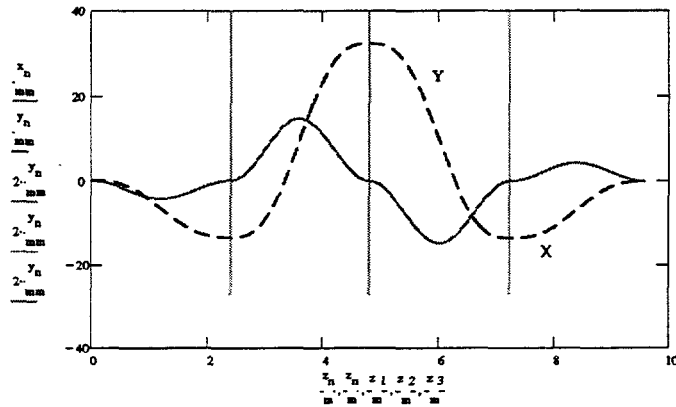
Nice solution for Snakes and Rotators proposed by Ptitsin and Shatunov (BINP), and refined at BNL over past few years, using helical dipole magnets...

- high field superconducting helical dipole magnets keep orbit distortions small and allow for the spin manipulations to be performed in a compact region
- four helical dipoles fit within standard RHIC straight section, keeping the assembly between already cold superconducting quadrupoles Q7 and Q8
- Rotators located in "warm" regions (which must be modified slightly), but modular design allows Snake and Rotator hardware to be as similar as possible
- low current, many-turn magnet designs being considered

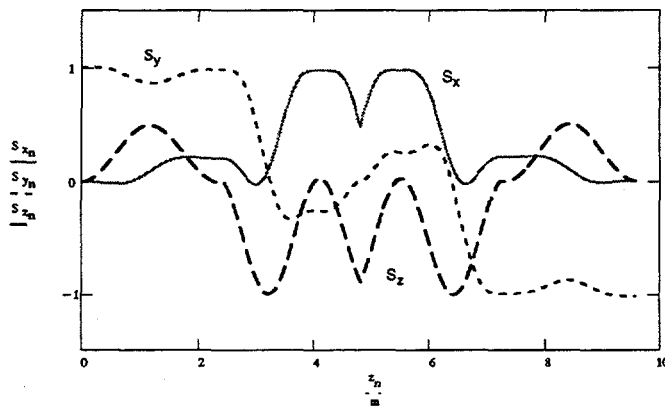
Magnetic Field through Snake Magnets

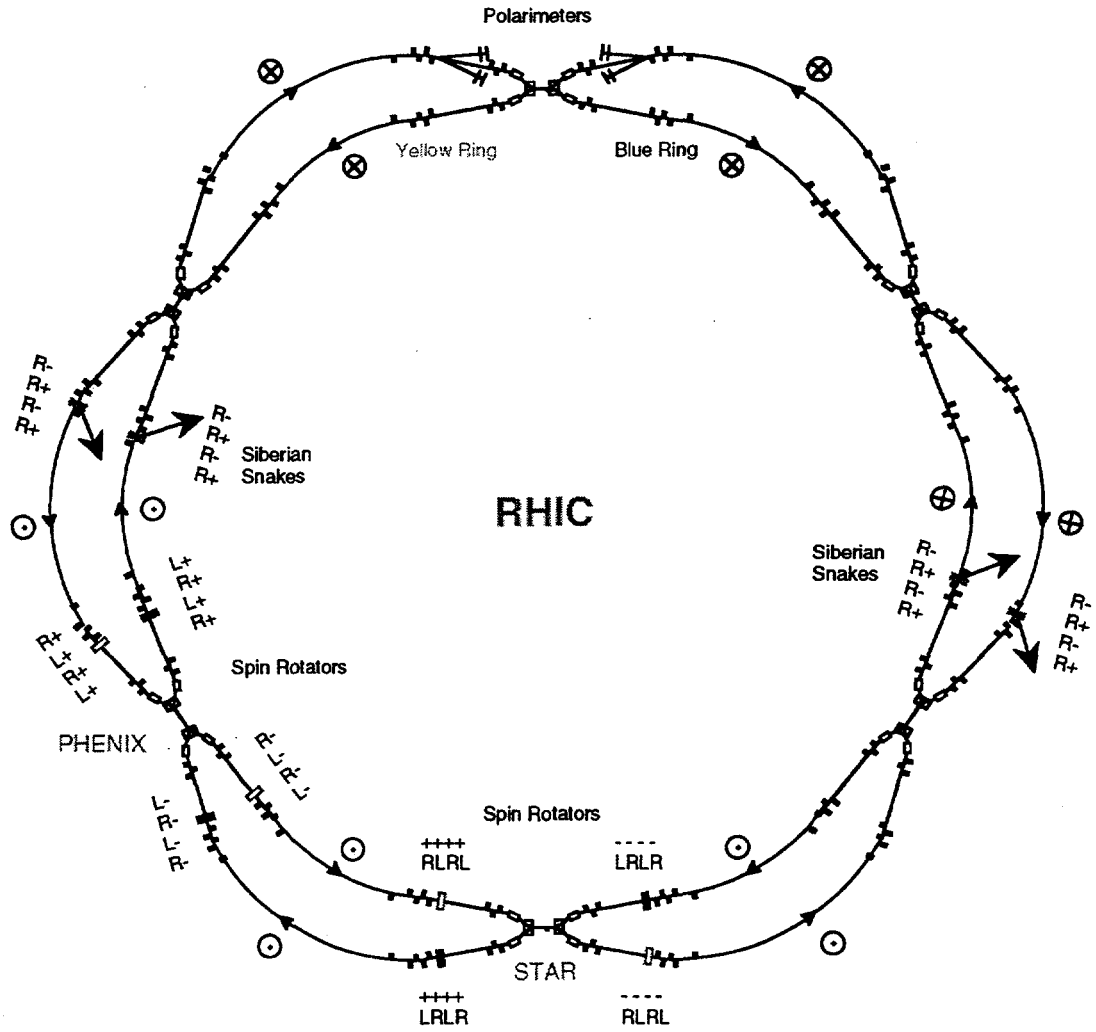


Proton Trajectory through Snake Magnets



Proton Spin through Snake Magnets





Rotators = Hor field (at ends), + = radially "out," - = radially "in"
 Snakes = Ver field (at ends), + = "up," - = "down"

Present Project Status:

Accelerator Physics:

- Spin tracking studies concentrating on closed orbit correction schemes, crossing of strongest intrinsic resonances.

Magnets:

- Magnet R&D: success with both methods in making 4 Tesla helical dipole magnets! Slotted magnet more robust, chosen as design. >80% of Mechanical/Electrical drawings complete; most of remaining work is in cryostat assembly.
- Tooling (winding machine) is complete; most operational issues have been worked out. (Will still be learning things as we build first magnet.) Lamination stacking fixture nearly complete.
- Procurement of long-lead-time items (aluminum tubes, iron yoke laminations, superconductor) in good shape.
- First full-length production magnet was to begin in January; delays, primarily in tube machining. First full-length tube now mounted on winding machine and winding has begun.

Polarimeter:

- Toroid double-arm polarimeters are too expensive for our "actual" budget. Considering scaled-down, "day one" system.
- Looking at CNI system as second "day one" polarimeter, and future systems such as jets.

Roadmap Toward First Polarized Proton Run (Proposal)

T. Roser, M. Syphers

Goal: First polarized proton physics run in YEAR TWO (Oct. 2000 --->)

- 100 GeV on 100 GeV
- Longitudinal polarization at STAR and PHENIX

Need: Polarized proton commissioning during YEAR ONE (Oct. 1999 --->)

- one ring, two Snakes, one polarimeter; energies up to 100 GeV

A 4-week commissioning plan proposal for YEAR ONE (Oct. 1999 --->):

- Transfer of polarized beam from the AGS and injection into RHIC. Commission filling of RHIC with bunches of alternate polarization sign. (6 days)
- Commissioning of the polarimeter at 25 GeV. Check for systematic errors. (7 days)
- Measurement of beam polarization in RHIC at 25 GeV with and without Snakes.(4 days)
- Accelerate polarized beam to 40, 60, 80, and 100 GeV. Commission polarimeter and measure polarization at each energy. (11 Days)

Schedule calls for:

1. Two Siberian Snakes available for one RHIC ring by Summer 1999.
2. One polarimeter available for one (same!) RHIC ring by Summer 1999
-- operating range 25 GeV to 100 GeV.
3. Remaining components (2 Snakes, 8 rotators, 2nd polarimeter system) installed by Summer 2000.

AGS RF dipole Experiment

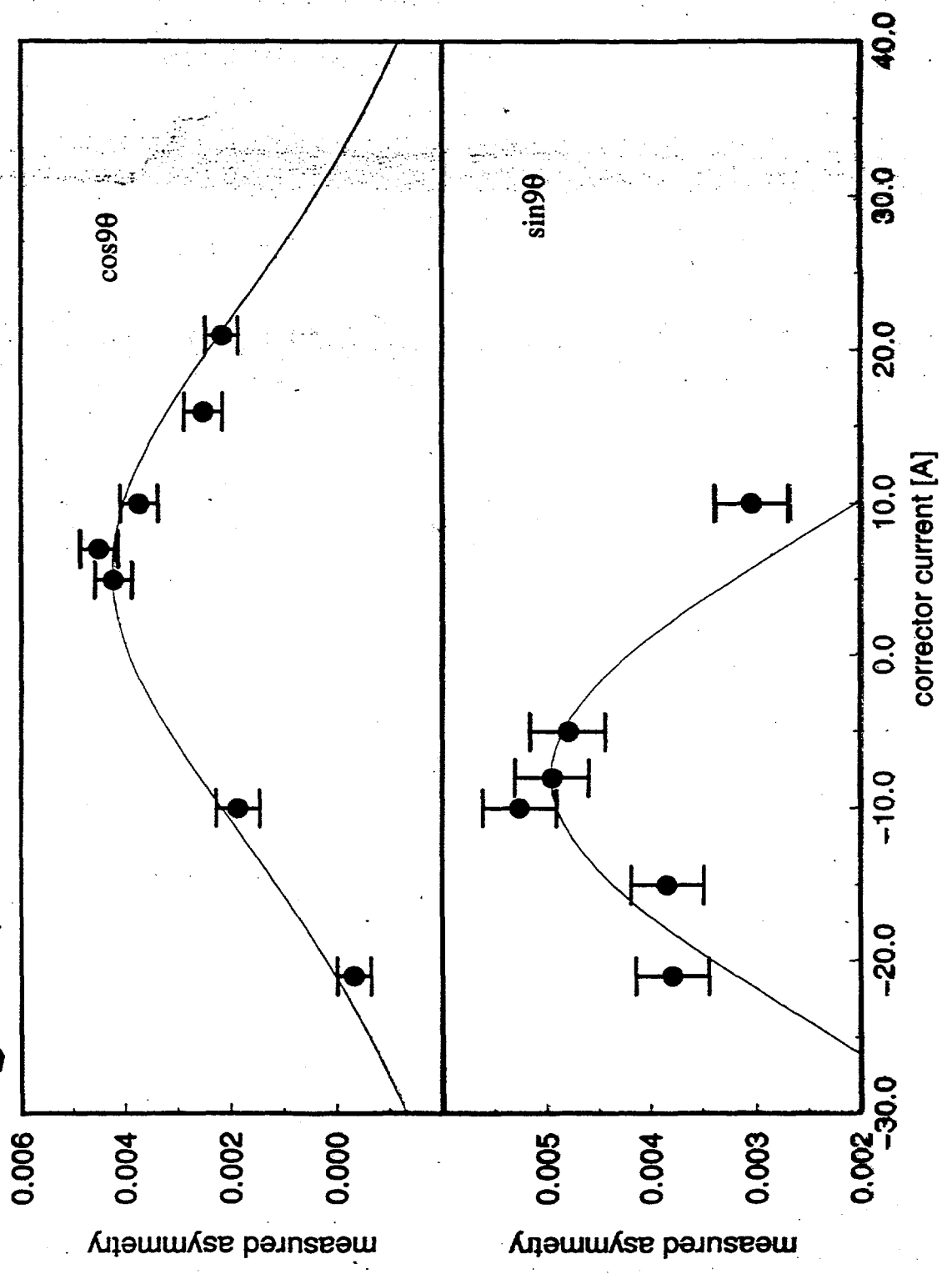
M. Bai

Indiana University

Normally, particles in a beam with different oscillation amplitudes have different spin resonance strengths. The smaller the oscillation amplitude, the weaker the spin resonance strength. Therefore after crossing a spin resonance, the spin vectors for different particles spread out and the beam polarization, which is the ensemble average of all the particles spin vectors, is decreased. To avoid this happen, one can excite a coherent betatron oscillation to force all the particles have large oscillation amplitudes to enhance the beam spin resonance strength and obtain a full spin flip. An adiabatic coherent betatron oscillation can be excited and maintained without causing beam emittance growth by using an RF dipole. This technique was successfully tested in the recent polarized proton experiments at the Brookhaven AGS to overcome three strong intrinsic spin resonances at $0 + \nu_z$, $12 + \nu_z$ and $36 - \nu_z$. The experimental data show that measured beam polarization became saturated at large oscillation amplitude which indicates a full spin flip was achieved.

A new type of spin resonance at $G\gamma = 60 - \nu_z - 9$ was found in the most recent polarized proton run at the AGS. This resonance was found to be associated with horizontal closed orbit distortion and can be understood as a 2nd order effect of the spin precession tune modulation due to the horizontal focusing fields when large horizontal closed orbit distortion occurs. In the experiment, the horizontal harmonic correctors were employed to eliminate the horizontal closed orbit distortion and correct this semi-intrinsic resonance.

Fitting Model : $S_f = S_0 \frac{1 - b [(x-c)^2 + (y-s)^2]}{1 + b [(x-c)^2 + (y-s)^2]}$
 Best fit θ : $S_0 = (4.99 \pm 0.26) \times 10^{-3}$
 $b = (1.287 \pm 0.18) \times 10^{-3}$
 $c = 5.59 \pm 1.5$
 $s = -7.95 \pm 1.2$



$$G\gamma = 60 - \nu_z - 9$$

cause: modulation of spin precession tune due to the horizontal focusing field. This resonance can be treated as the 2nd order effect parasitic to the intrinsic spin resonance $G\gamma = 60 - \nu_z$.

Generally,

$$G\gamma = K - m \cdot n \text{ is parasitic to the spin resonance } G\gamma = K$$

integer

harmonic of horizontal closed orbit

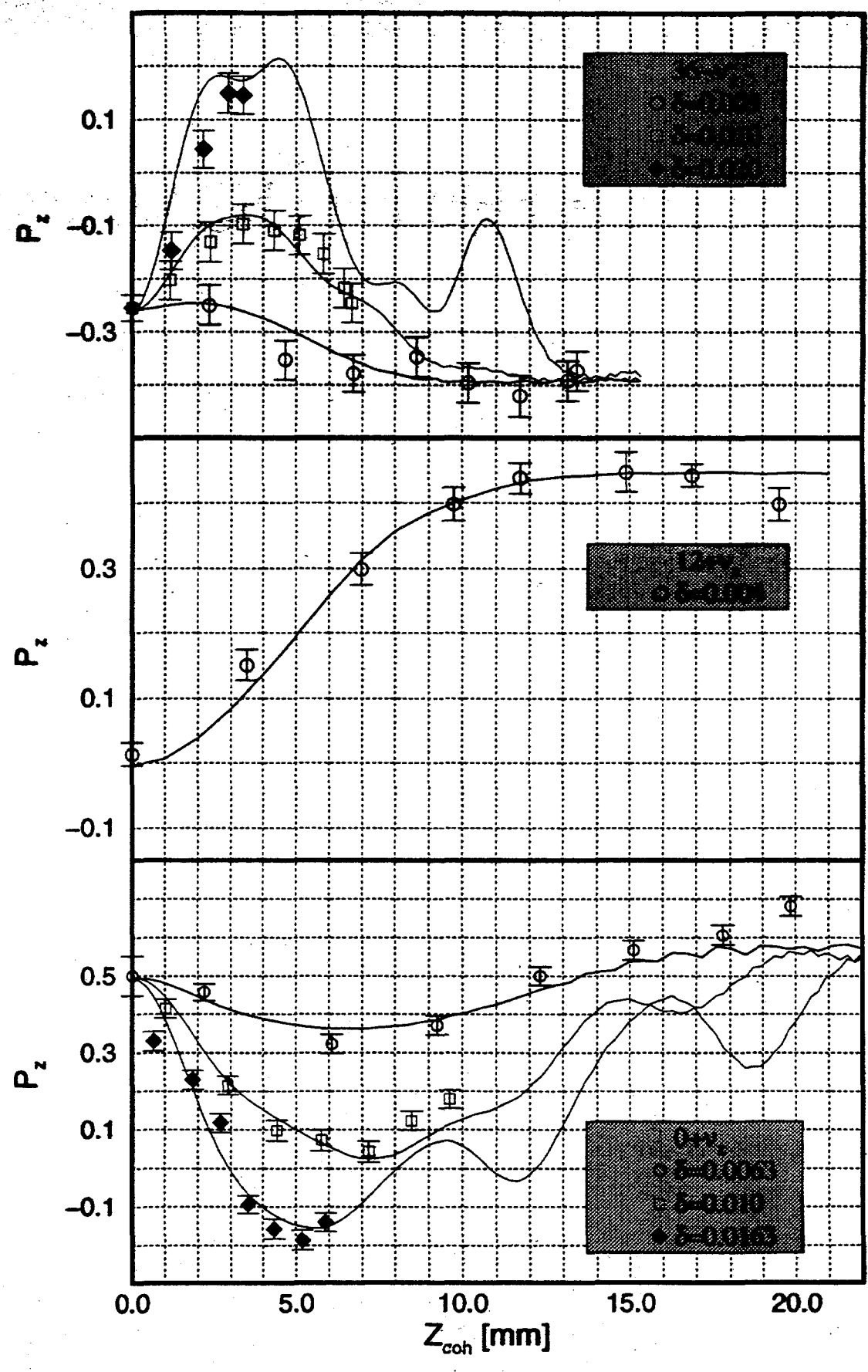
$$\mathcal{E}_{K - m \cdot n} = \mathcal{E}_K J_m(g)$$

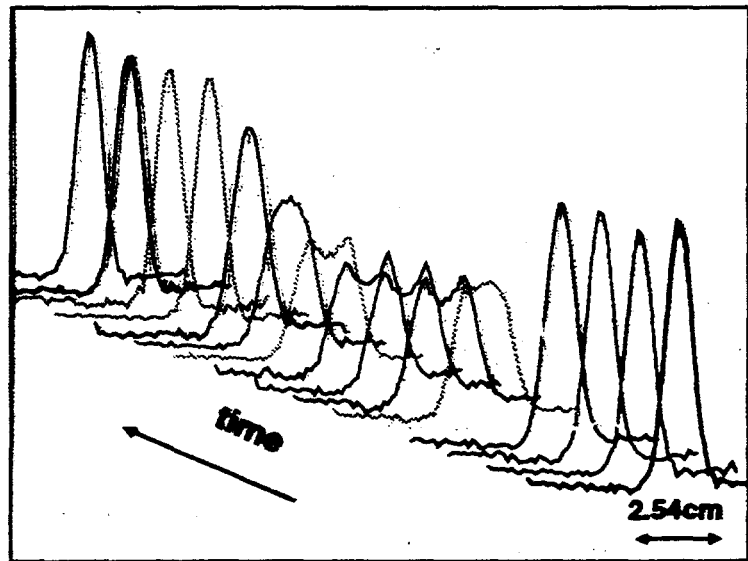
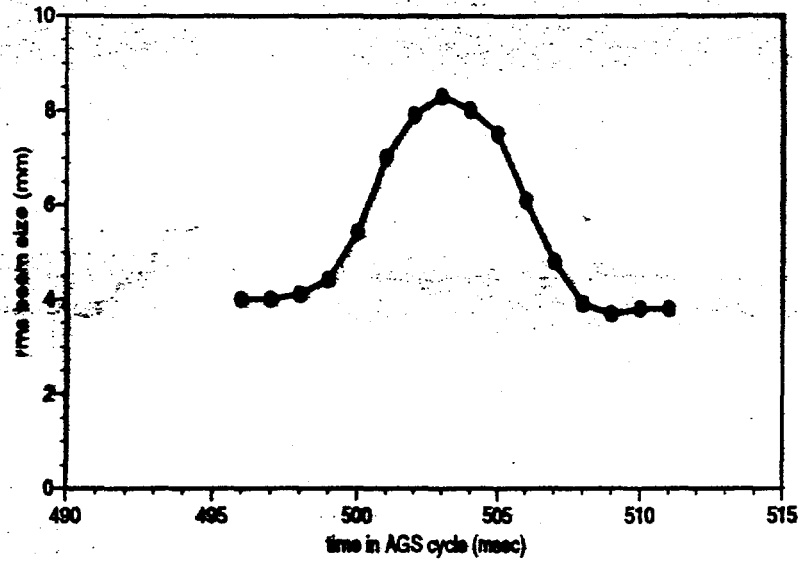
Resonance strength of $G\gamma = K - m \cdot n$

Resonance strength of $G\gamma = K$

$$g = 9 \cdot X_{co} \cdot (1 + G\gamma) / R$$

Bessel Function

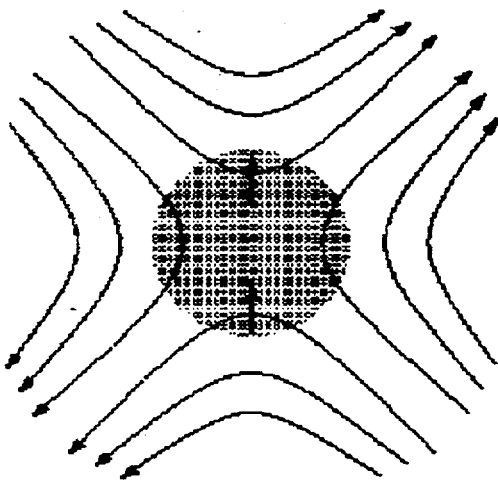




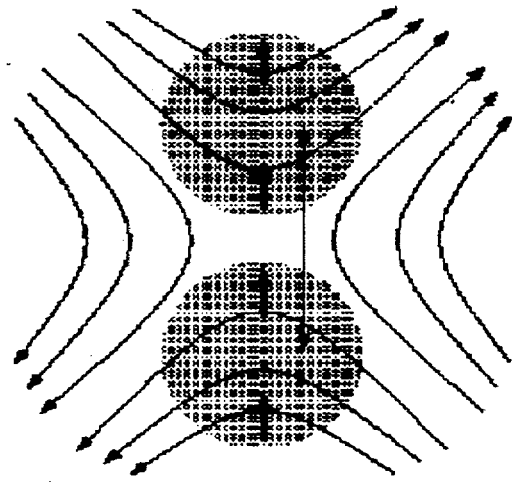
Exciting coherent betatron oscillation when crossing the intrinsic spin resonance

The idea of exciting a vertical coherent betatron oscillation is to let all the particles have strong resonance strength so that a full spin flip can be obtained under the nominal acceleration rate

Intrinsic Resonance Crossing



Vertical focusing fields
causes depolarization



Driven beam oscillation
 ➤ whole beam sees the
the same field
 ➤ spin flip

Introduction:

An RF dipole magnetic field is given by: $B = B_m \cos(2\pi\nu_m n)$

where B_m : RF dipole magnetic field amplitude

n : number of revolutions around the accelerator

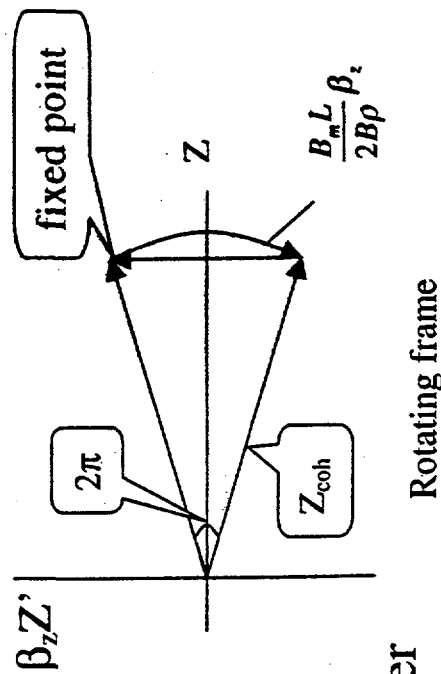
ν_m : RF dipole modulation tune defined as the ratio of its oscillation frequency to the accelerator revolution frequency

Advantage over using a pulsed kicker:

- ① beam emittance can be preserved.
- ② operation is easier to control

The coherent oscillation amplitude Z_{coh} is:

$$Z_{coh} = \frac{B_m L}{4\pi B \rho \delta} \beta_z$$



$\delta = |\nu_m - \nu_z|$ is the resonance proximity parameter

How Do We Reach 70% Polarization in the AGS?

Haixin Huang

Brookhaven National Lab

Abstract

This presentation gives some thoughts on how to reach 70% polarization in the AGS. A 5% partial Siberian solenoidal snake and a 18 G-m rf dipole have been tested successfully in the AGS^[1]. A spin tracking code^[2] is used to understand the behavior of the beam polarization during acceleration in the AGS. The simulation results show that much of the remaining depolarization occurring in the AGS is associated with transverse coupling resonances. And in fact, a major source of the coupling is the solenoidal field of the partial Siberian snake. If a helical dipole partial snake^[3] is used in the AGS, in addition to a stronger rf dipole(28 G-m) and energy jump scheme^[4], 70% polarization in the AGS is feasible. Among these upgrade options, a helical dipole partial snake is crucial.

REFERENCES

1. M.Bai, these proceedings.
2. H. Huang, T. Roser, A. Luccio, Spin Tracking Study in the AGS, AGS/RHIC/SN-043, November, 1996.
3. T. Roser, et al., Helical Partial Snake for the AGS, AGS/RHIC/SN-072, March, 1998.
4. H. Huang, et al., Polarized Proton Experiment in the AGS with a Partial Snake, AGS/RHIC/SN-044, November, 1996.

The "visible" spin resonances in the AGS can be divided into four categories:

Imperfection Resonances

$$G\gamma = 5, 6, \dots, 45$$

arising from vertical closed orbit distortion

$$G\gamma = n \text{ (integer)}$$

Intrinsic Resonances

$$G\gamma = 0 + \nu_y, 12 + \nu_y, 36 \pm \nu_y \text{ (strong)}$$

$$24 \pm \nu_y, 48 - \nu_y \text{ (weak)}$$

caused by vertical betatron motion

$$G\gamma = kP \pm \nu_y$$

Coupling Resonances

$$G\gamma = 0 + \nu_x, 12 + \nu_x, 36 \pm \nu_x$$

horizontal betatron motion coupled to vertical betatron motion by some coupling elements: solenoid

$$G\gamma = kP \pm \nu_x$$

Semi-Intrinsic Resonance

$$G\gamma = 60 - \nu_y - 9$$

caused by strong 1st order intrinsic resonance combined with large horizontal closed orbit distortion

$$G\gamma = kP \pm \nu_y \pm [\nu_\beta]$$

Current schemes to overcome these resonances.

261

Imperfection Resonances 5% partial snake (solenoid)

Intrinsic Resonances

Strong ones

18 Gm RF dipole

Weak ones

Coupling Resonances

Reduce the resonance strength
by separating the two betatron tunes
with 0.15 unit.

Semi-Intrinsic Resonance

7th harmonic
orbit correction

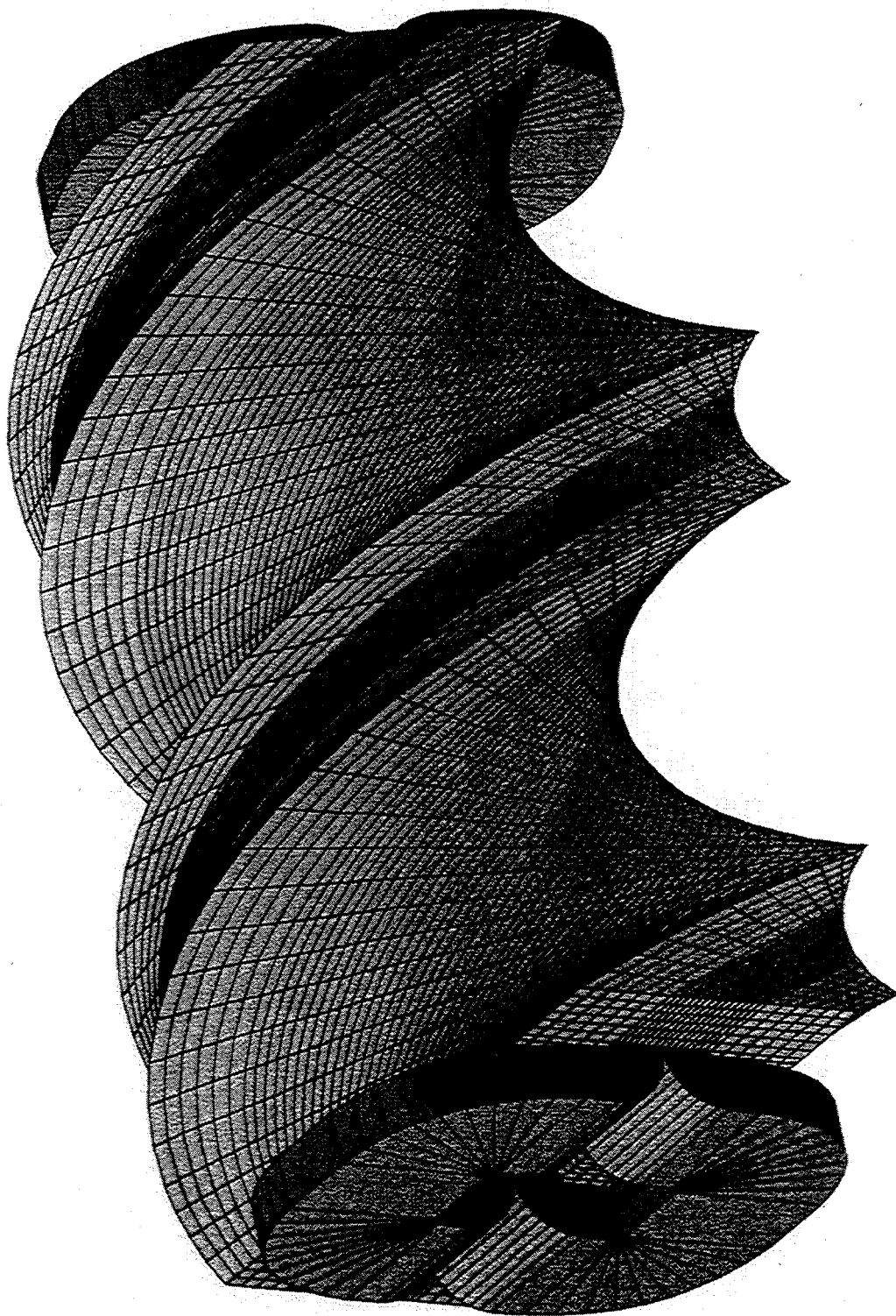
$$\frac{P_f}{P_i} = 0.547 \quad (\text{simulation})$$

With 75% polarization from the source,

the polarization at $G\gamma = 47.5$ is

41%

5% helical partial snake



New Schemes

Improving factor

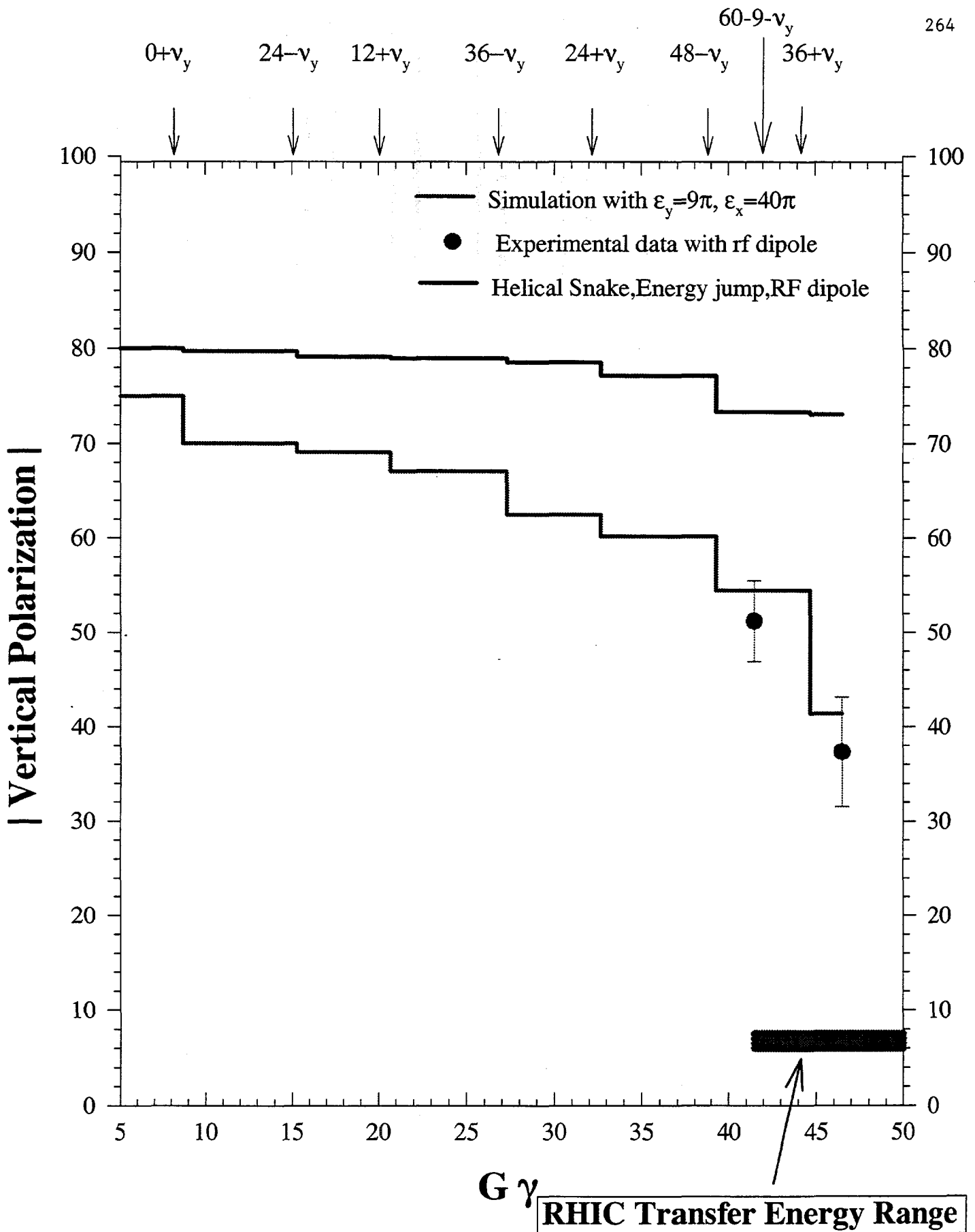
Imperfection Resonances	5% helical partial snake	1
Intrinsic Resonances	Strong ones	28 Gm RF dipole
	Weak ones	Energy jump
Coupling Resonances	Eliminating the source of coupling with the 5% helical partial snake	1.47
Semi-Intrinsic Resonance	9th harmonic orbit correction	1

$$\frac{P_f}{P_i} = 0.915 \quad (\text{simulation})$$

The new polarized source will give 80% initial polarization

The polarization at $G\gamma = 47.5$ will be

73%



RHIC Transfer Energy Range

Helical Magnets

Workshop on RHIC Spin Physics

April 28, 1998

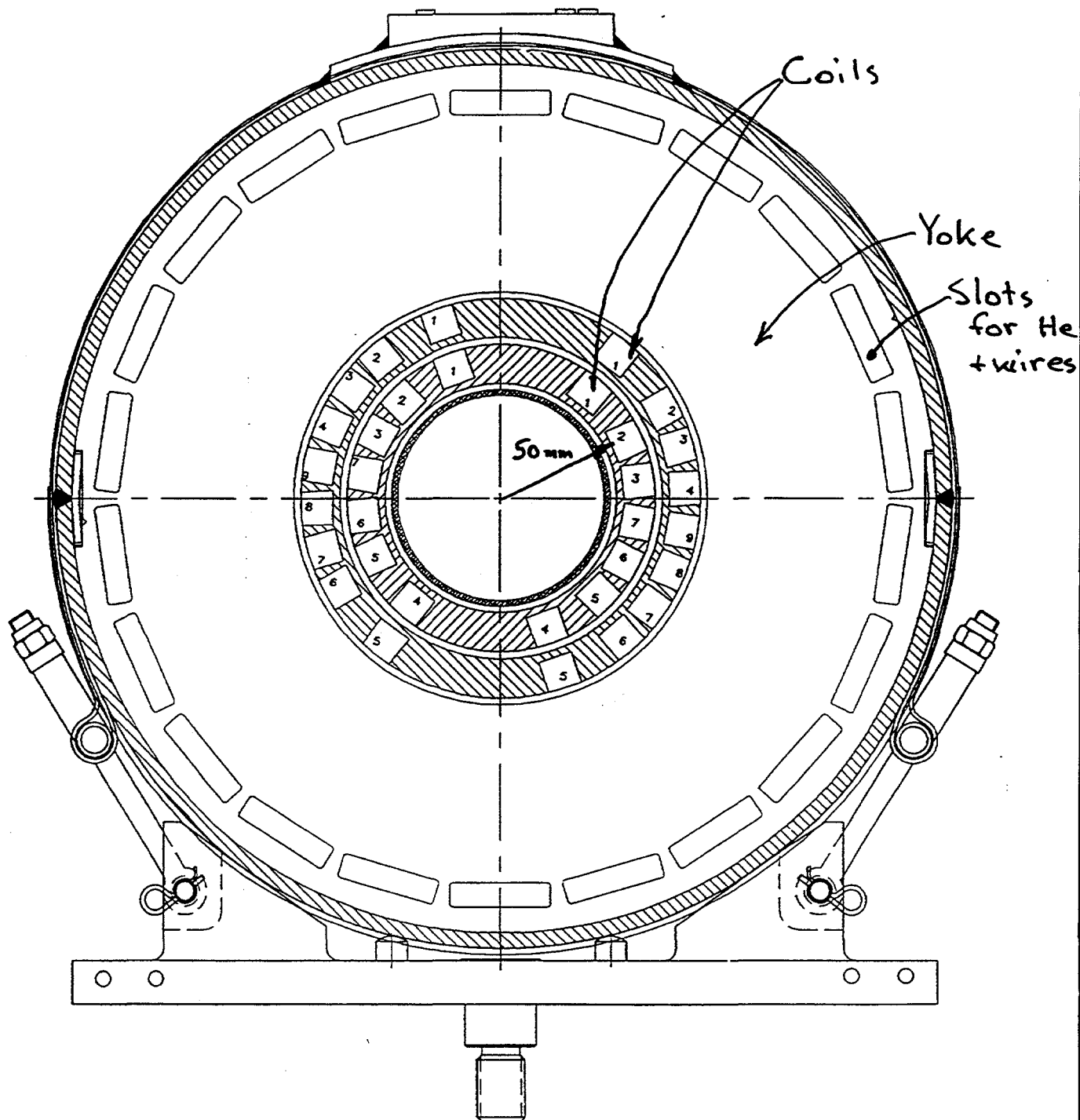
Erich Willen

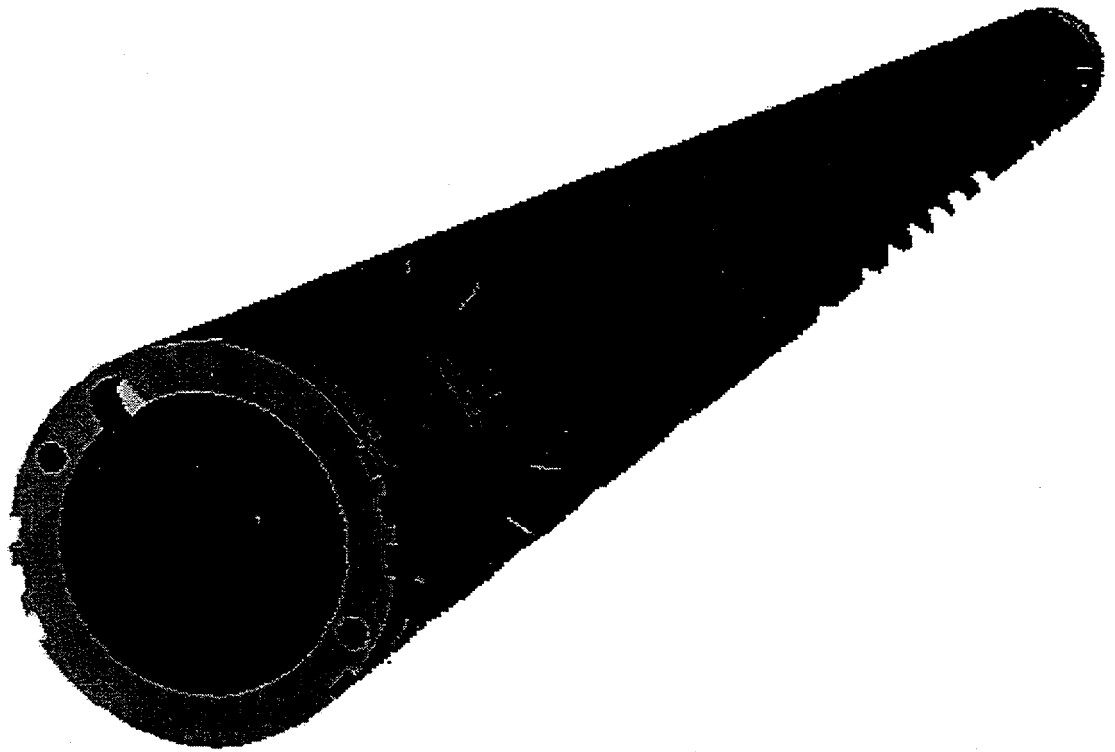
Helical dipole magnets are being built at Brookhaven to control proton spin in RHIC. These magnets are designed to fit into the RHIC lattice at appropriate points and with minimal disruption to the existing hardware. A half-length model has been built and tested to validate the design. It produced a good quality, helical 4 T field with sufficient margin to be acceptable for machine use. Plans are under way for the production of the full complement of magnets, based on this design, over the next few years. A needed piece of equipment, an automated coil winding machine, is undergoing final checkout and debug. Production is expected to begin by Summer.

The attached drawings and tables show some of the technical features of the magnets.

Helical Magnets

Σω
4/20/98

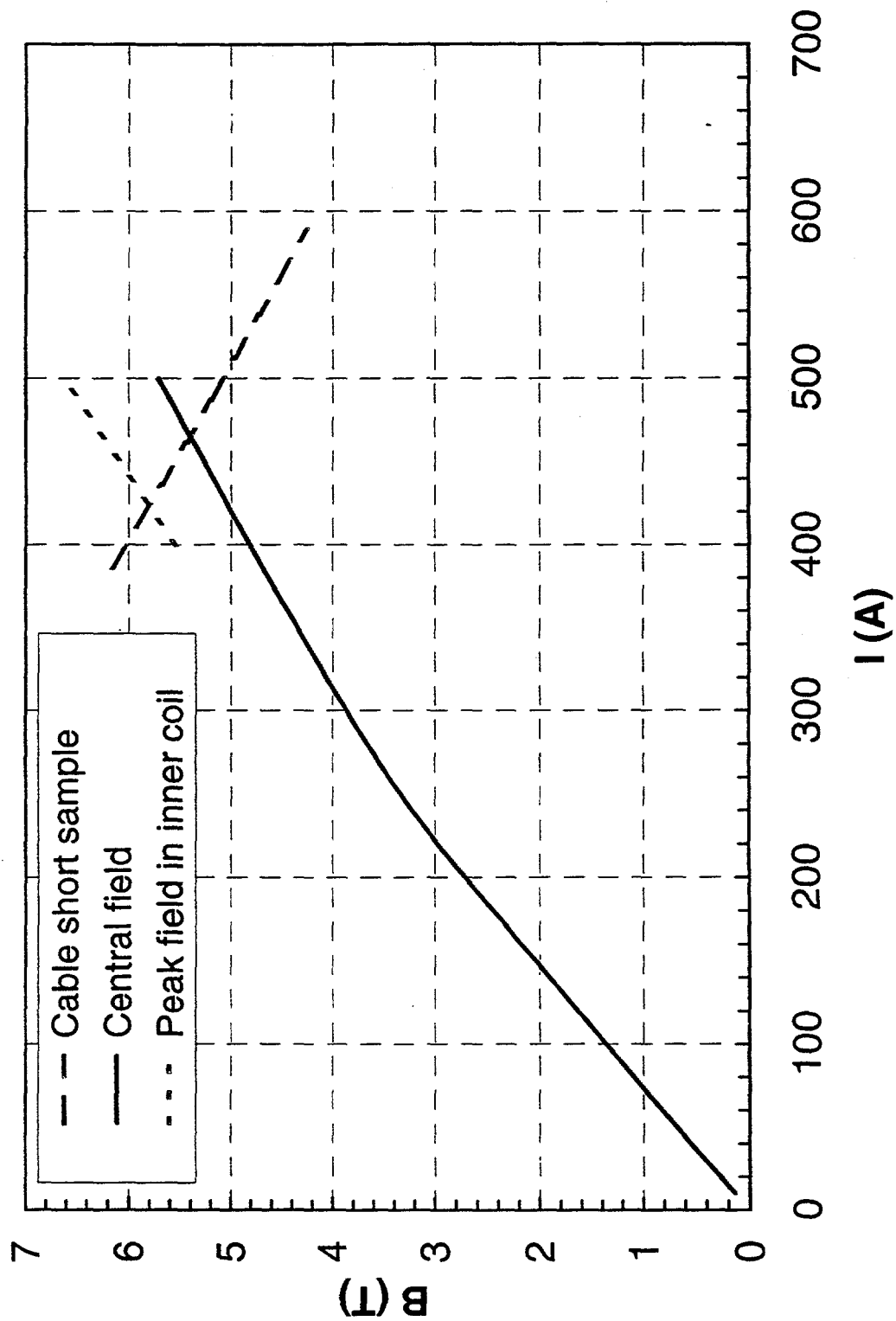




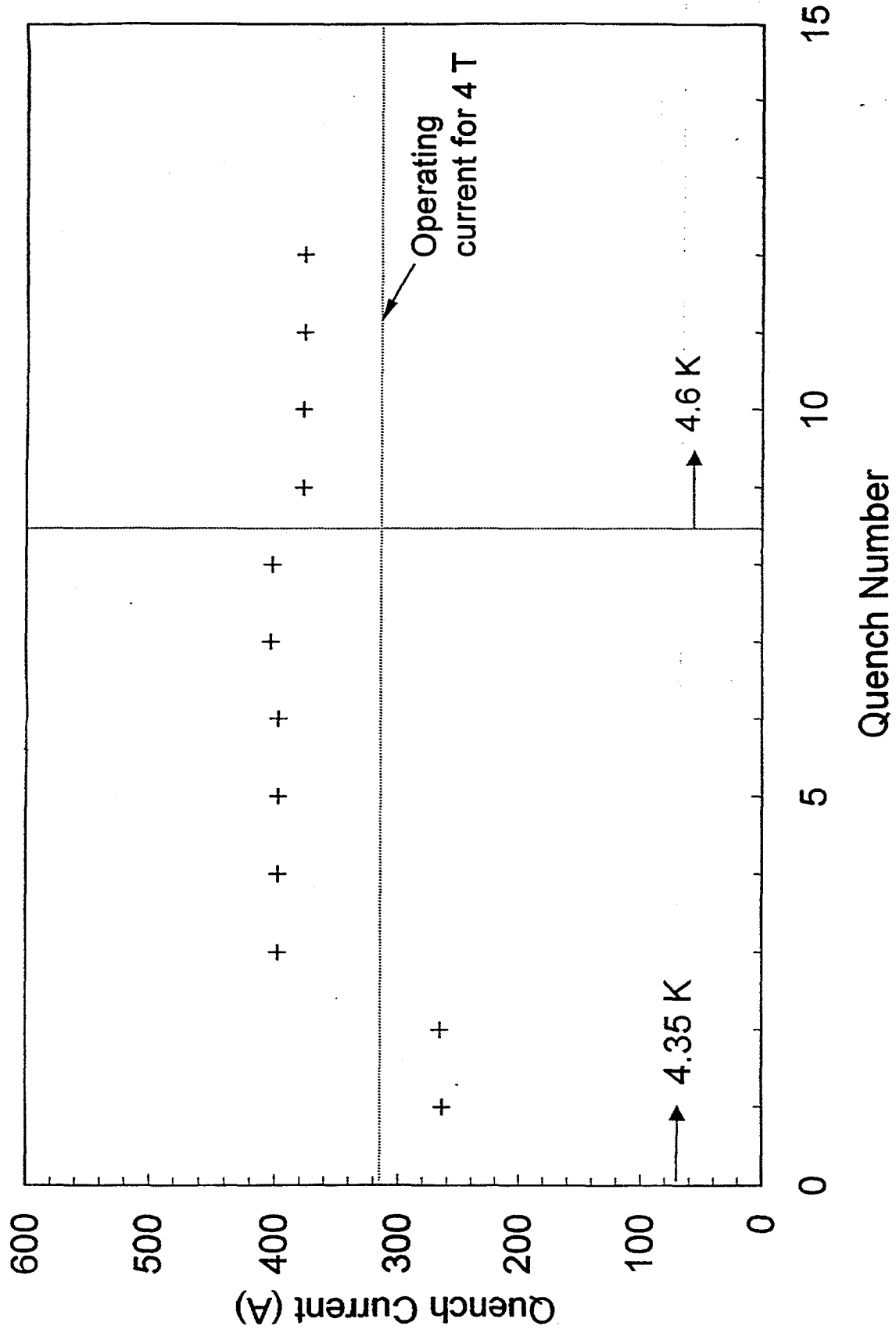
Selected mechanical parameters of the helical magnet.

268

Parameter	Value
	Inner, Outer
Number of cylinders	2
Num of current blocks per cylinder	7, 9
Num of cable turns per layer	12, 12
Num of layers per current block	9, 9
Num of cable turns per block	108, 108
Num of cable turns per cylinder	756, 972
Total turns	1728
Coil inner radius (mm)	49.7, 68.6
Coil outer radius (mm)	60.0, 78.9
Helix, magnetic length (mm)	2400
Helix, rotation (deg)	360
Yoke IR in straight section (mm)	84.5
Yoke IR in ends (mm)	114.4
Yoke outer radius (mm)	177.8



Measured quench performance of the helical magnet.



Polarized protons acceleration in HERA

Vladimir A. Anferov

*Physics Department, University of Michigan,
Ann Arbor, Michigan 48109-1120*

1 Introduction

The interest in spin phenomena has significantly increased in recent years. It is now clear that spin effects in high energy interactions provide essential information about properties of the elementary particles and their fundamental interactions. The polarized proton beam capability at HERA would provide a powerful tool for high energy physics; it would allow unique spin studies in a polarized $e-p$ collider.

While high energy electron and positron beams have selfpolarization mechanism due to the synchrotron radiation, an intense high energy polarized proton beam could only be obtained by acceleration from the source to the ring's maximum energy. Wide range of spin instabilities that become stronger at higher energies make the polarized protons acceleration a challenging problem. However, recently developed methods and techniques of overcoming the spin depolarizing resonances allow one to consider polarized proton beam acceleration in the high energy proton machines such as RHIC (250 GeV), HERA (820 GeV) and Tevatron (900 GeV).

The SPIN Collaboration and DESY Polarization Team have been studying the possible acceleration of a polarized proton beam to 820 GeV/c in the HERA ring at DESY [1]. While most of the polarized beam problems appear to have straightforward solutions using existing techniques, two main problems will need further study:

- increasing the accumulated polarized beam intensity,
- providing adequate spin stability for polarized beam acceleration and storage in HERA.

The required changes for each stage of polarized beam acceleration are shown in Fig. 1.

2 Polarized Ion Source

A state-of-the-art polarized H^- ion source should be acquired and installed at DESY. This might be either an atomic beam source (ABS), or an optically pumped polarized ion source (OPPIS). Both types of sources have made tremendous progress in the recent years; the best ABS at INR (Moscow) has now achieved a current of 1 mA in pulsed operation [2], while the best OPPIS at TRIUMF (shown in Fig. 2) has recently obtained H^- current of 1.6 mA in DC mode with the beam emittance of 2π mm·mrad [3]. The source performance together with accumulation efficiency will be crucial issues for attaining a high intensity polarized proton beam at 820 GeV/c. Recent experimental tests at TRIUMF indicate that a 10 mA polarized H^- current could be obtained in the pulsed mode using the OPPIS technology. Such a source would bring the polarized beam intensity in HERA close to the intensity of unpolarized beam.

3 Polarized beam acceleration

Various methods would be used in HERA in order to preserve the beam polarization during the acceleration, but the biggest problems arise in the 820 GeV/c HERA ring.

Accelerating polarized protons in HERA is difficult not only because of the very strong depolarizing resonances that occur during the acceleration, but also because of the requirement

of a several hours polarization life time at the top energy in order to be useful for the experiments. Four Siberian snakes could be installed in each of the existing long straight sections. However, earlier studies by the DESY Polarization team have shown that the vertical orbit bumps around the interaction regions in HERA would interfere with any standard Siberian snake configuration. A solution to this problem was found, which would require four additional snakes to make the HERA ring "flat" for the spin motion. We called these snakes "flattening snakes" to emphasize their purpose of making the vertically bending beam lines near the interaction regions spin transparent.

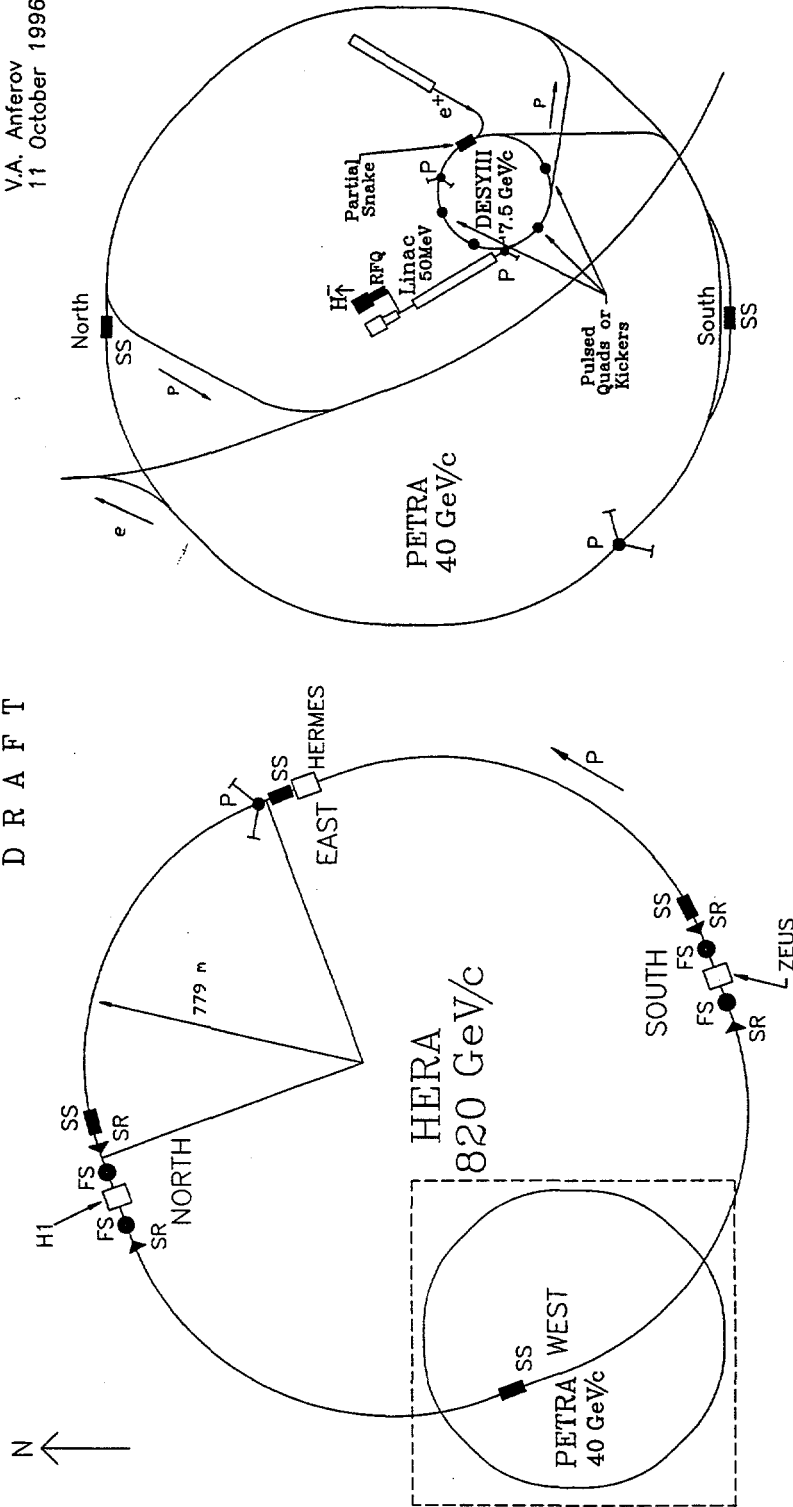
Even after "flattening" the HERA lattice the spin perturbation remains very strong and four snakes in HERA would not provide adequate spin stability during the polarized beam acceleration. To reduce the strength of the spin perturbations we consider various correction techniques that could reduce the rms orbit error to perhaps 0.2 mm and the emittance of the polarized beam to perhaps 5π mm mrad. One could also consider installing additional four regular or type-3 snakes into each bending arc. Both options are now under careful analysis using various spin tracking techniques developed by the SPIN Collaboration and DESY Polarization team.

References

- [1] SPIN Collaboration, "Acceleration of Polarized Protons to 820 GeV/c at HERA", University of Michigan Report UM-HE 96-20, November 1996.
- [2] A.S. Belov *et al.*, Proc. 6th Int. Conf. on Ion Sources (Whistler); Rev. Sci. Instrum. **67**, 1293 (1996).
- [3] A.N. Zelenski *et al.*, Proc. of PAC97 (Vancouver); Rev. Sci. Instrum. **67**, 1359 (1996).

V.A. Anferov
11 October 1996

D R A F T

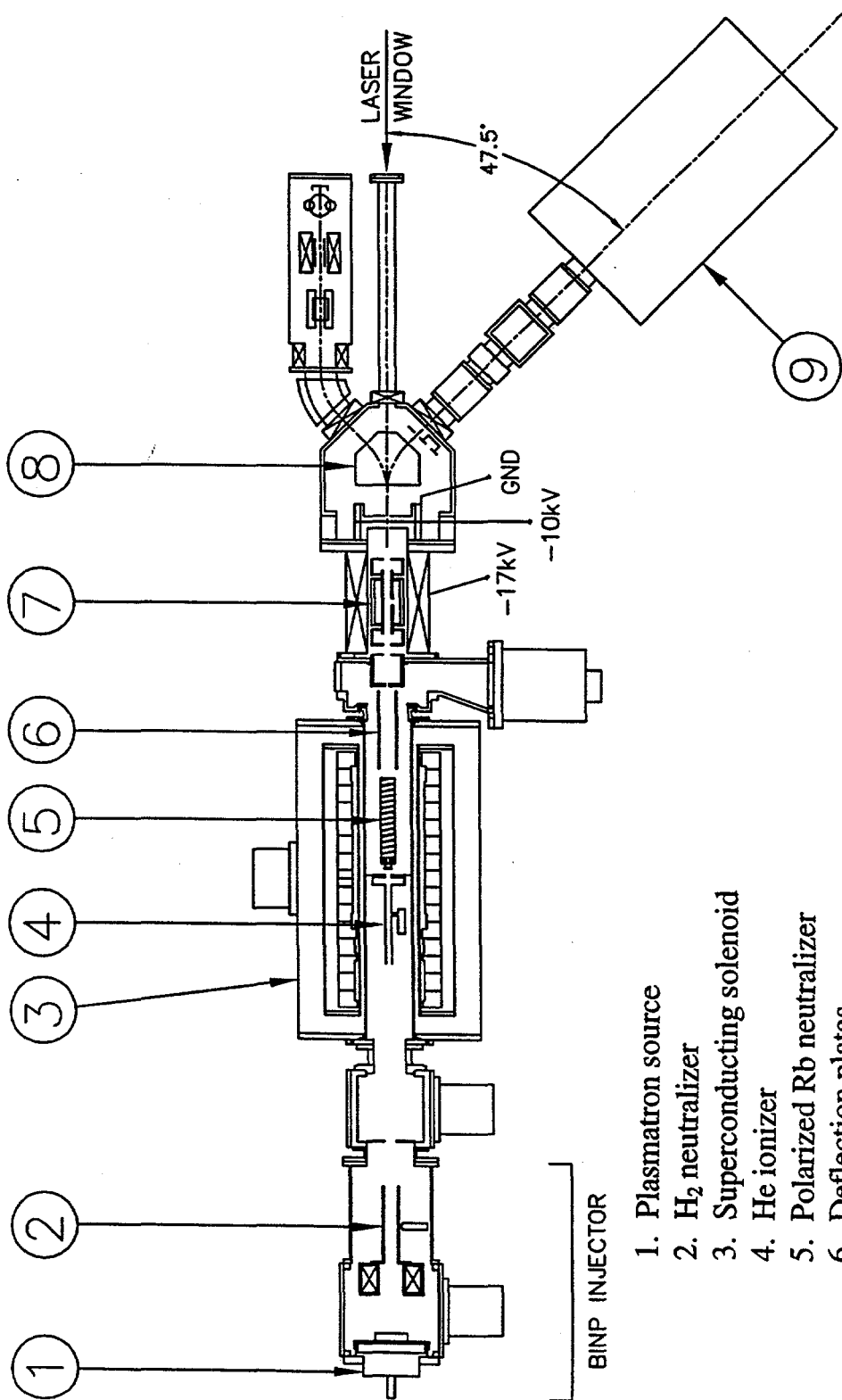


- SS - Siberian snake
- ▴ SR - Spin Rotator
- FS - Flattening snake
- P - Polarimeters

Optically-Pumped Polarized Ion Source

TRIUMF-INR-KEK

1.6 mA output DC H^- current with 2π mm-mrad emittance
 20 mA in 100 μ sec pulses at 0.25 Hz rate might be possible
 (would equal unpolarized intensity)



- 1. Plasmatron source
- 2. H_2 neutralizer
- 3. Superconducting solenoid
- 4. He ionizer
- 5. Polarized Rb neutralizer
- 6. Deflection plates
- 7. Na^- ionizer
- 8. Bending magnet
- 9. RFQ

Polarized Neutrons in RHIC

Ernest D. Courant

April 29, 1998

There does not appear to be any obvious way to accelerate neutrons, polarized or otherwise, to high energies by themselves. To investigate the behavior of polarized neutrons we therefore have to obtain them by accelerating them as components of heavier nuclei, and then sorting out the contribution of the neutrons in the analysis of the reactions produced by the heavy ion beams.

The best "neutron carriers" for this purpose are probably ^3He nuclei and deuterons. A polarized deuteron is primarily a combination of a proton and a neutron with their spins pointing in the same direction; in the ^3He nucleus the spins of the two protons are opposite and the net spin (and magnetic moment) is almost the same as that of a free neutron. In tritium (^3H), on the other hand, the net spin is essentially that of the proton, and the spins of the two neutrons cancel.

Let us see what the problems are in accelerating polarized ^3He or deuterons.

For ^3He :

Anomalous magnetic moment factor

$$G = \mu \frac{A}{2ZS} -$$

$$= -4.191$$

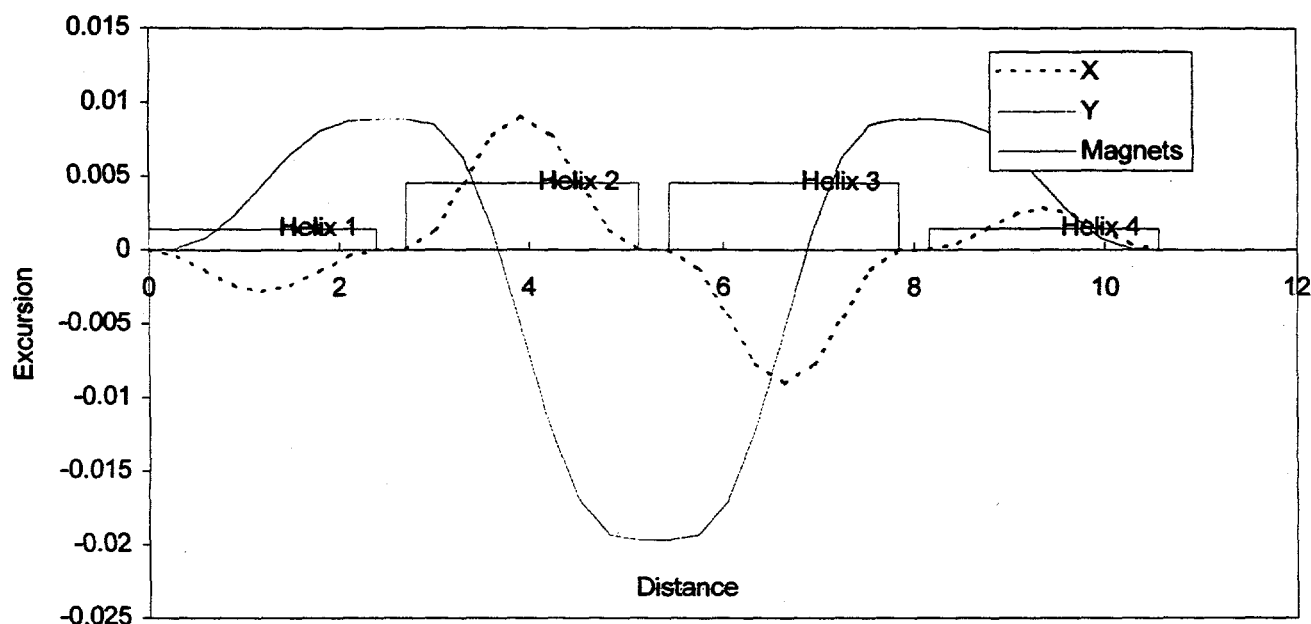
more than twice the magnitude for protons.

Siberian snakes need field strength scaled by factor A/ZG

$$= (3/2)(1.793/4.191) = 0.642$$

for ^3He as compared to protons:

Helical snakes need field of 2.6 T instead of 4.0.



The resonances in the AGS are likewise stronger and more closely spaced than with protons. But there should be no great difficulty in overcoming them with the partial snake for imperfections and the rf dipole for intrinsic resonances (as described by T. Roser and M. Bai). - The rotators that bring the spin into the longitudinal direction also have to be reduced by the same 64% factor as the snakes, and should function as in the proton case.

Other light nuclei that could, if desired, be handled the same way include tritium and/or ^{19}F .

Deuterons:

Here the magnetic anomaly is very small: $G = -.143$.

Result: Only ~ 18 imperfection resonances, 12 intrinsic.

But still strong enough to cause trouble.

Siberian snakes impossible (field required would be 25 times that for protons).

Intrinsic resonances can, however, be handled by the rf dipole method just as is done in the AGS; inducing coherent oscillations of amplitude 1 mm or so should be sufficient to make each intrinsic resonance strong enough for spin flip (the one at $\gamma = 120.15$ is anyway strong enough without help).

As for the imperfection resonances:

Use solenoids. Just as in the AGS, a solenoid of given strength BL rotates the spin by an angle

$$\mathcal{G} = (1 + G)BL / (B\rho)$$

producing integral resonances of strength $\varepsilon = \mathcal{G} / 2\pi$ at all integral values of $G\gamma$. If the value of ε is large enough such that Froissart-Stora factor

$$F = 2 \exp[-(\pi\varepsilon)^2 / \Delta] - 1$$

is practically equal to -1 we get complete spin flip ($\Delta =$ increment of $G\gamma$ per turn).

For deuterons $G = -.143$. With T (ramp time from $\gamma = 15$ to 135) = 1 minute, we have $\Delta = |G|(\gamma_f - \gamma_i)C/cT$ with $C = 3834$ m the circumference of RHIC, giving $\Delta = 3.66 \times 10^{-6}$. Thus to get $F < -0.99$ (99% spin flip) we need $\varepsilon > (\Delta \ln 200)^{1/2}/\pi = 1.4 \times 10^{-3}$; using (5) and (6) we find that at top energy ($B\rho = 840$ T-m) we need a solenoid of strength of 8.7 Tesla-meters, i.e. just twice the "partial snake" solenoid in use at the AGS. Such a solenoid, which could be warm or cold, would easily fit in one of the long Q3-Q4 gaps in an insertion. This solenoid will give complete spin flip at each of the 19 integer resonances in the acceleration range, provided only that the imperfection resonances we would have without the partial snake are weaker than 1.4×10^{-3} . Calculations using the SYNCH and DEPOL computer programs show that, with one particular random-number generator seed, and with rms alignment errors of $1/4$ mm in the quads in the arc, the resulting closed orbit has an rms excursion of 2.5 mm, and the strongest depolarization resonance (at $\gamma = 119$) has strength 0.003, but the resonances below $\gamma = 100$ are weaker than 0.001. Thus our 8 T-m solenoid should be able to cope with all integer resonances below about 200 GeV. If the MICADO orbit correction scheme is used, the calculations show that the rms orbit excursion is reduced to 0.6 mm and the strongest integer resonance is well below the strength of .001; thus the partial-snake solenoid should work just fine.

With the partial-snake solenoid scheme. the spin is very nearly vertical in the whole machine when the energy is reasonably far (more than several times ε) from the resonance. But just exactly at the resonance energy the closed-orbit spin vector will precess in the horizontal plane, and just 180° from the snake it will be longitudinal. Therefore experiments with longitudinal spin will be possible at this discrete set of energies, $-G\gamma = 1, 2, 3, \dots, 19$ (energy at multiples of about 13.6 GeV). For helicity experiments at STAR (6 o'clock) the solenoid should be in the

12 o'clock insertion; for experiments at PHENIX (8 o'clock) it should be at 2 o'clock.

Parity-violating Asymmetries in W^\pm Production with STAR

L.C. Bland

Dept. of Physics, Indiana University, Bloomington, IN 47405 USA

In addition to its crucial role in accurately determining the polarized gluon structure function for the proton via measurements of the longitudinal spin correlation coefficient (A_{LL}) in $pp \rightarrow \gamma + \text{jet}$ reactions at $\sqrt{s} = 200$ GeV, the proposed end-cap electromagnetic calorimeter (EEMC) upgrade to STAR also allows important determinations of flavor-specific quark and antiquark polarizations through measurements of the $e^\pm(\nu)$ decay of W^\pm bosons produced in collisions of longitudinally polarized protons at $\sqrt{s} = 500$ GeV. The ability to relate the measured parity-violating single-spin asymmetry (A_L) directly to the quark or antiquark polarization is greatest when the e^\pm from W^\pm decays are detected at large pseudorapidity, $1 < \eta < 2$, corresponding to the acceptance of the proposed EEMC.

Fig. 1 shows the expected η distribution of e^\pm from W^\pm decays for pp collisions at $\sqrt{s} = 500$ GeV as generated by PYTHIA [1]. Simple expressions for the W^\pm production cross section from ref. [2] provide substantial insight. In particular, when the W^\pm are produced at large rapidity, y_W , then in leading-order, we expect the most asymmetric collisions in the initial state corresponding to the partonic momentum fractions, $x_1 \gg x_2$. For such asymmetric collisions, we expect (Fig. 2) a direct relationship between the measured A_L and the $u(d)$ and $\bar{d}(\bar{u})$ polarizations.

To test this idea, a simulation model for the $\bar{p}p \rightarrow W^\pm X \rightarrow e^\pm(\nu)X$ reaction at $\sqrt{s} = 500$ GeV was developed. Events were generated for W^\pm production, excluding the proton polarization, using PYTHIA. The partonic kinematics for the event were then used to evaluate the expected A_L for each of the two beam longitudinally polarized beams (assuming $P_{beam} = 0.7$) using the expressions from ref. [2] and polarized structure functions from ref. [3]. The detection of e^\pm from W^\pm decays was modeled by including only the acceptance of the STAR TPC and barrel and end-cap EMC. The events were subjected to particle identification cuts to distinguish e^\pm from the most important background arising from the prolific production of hadrons ($h^\pm \equiv$ protons(anti-protons), K^\pm and π^\pm) with large transverse momentum, $p_T > 10$ GeV/c. Other backgrounds such as Z^0 decay, with only a single e^\pm detected and single electrons from the Dalitz decay of high- $p_T \pi^0$ have been considered and found to be negligible. Clean distinction between e^\pm and h^\pm relies on (1) *isolation cuts* applied to the candidate e^\pm , (2) the much smaller response of the EMC to incident h^\pm relative to e^\pm , and (3) rejecting events that have an accompanying jet with $p_T > 5$ GeV/c in the azimuthal angle range, $|\pi - (\phi_{jet} - \phi_h)| < 1$ radian. The first two of these cuts have been discussed before [4]; the third cut further reduces the hadronic background by an additional order of magnitude. The end result is that STAR can cleanly detect e^\pm from W^\pm decays.

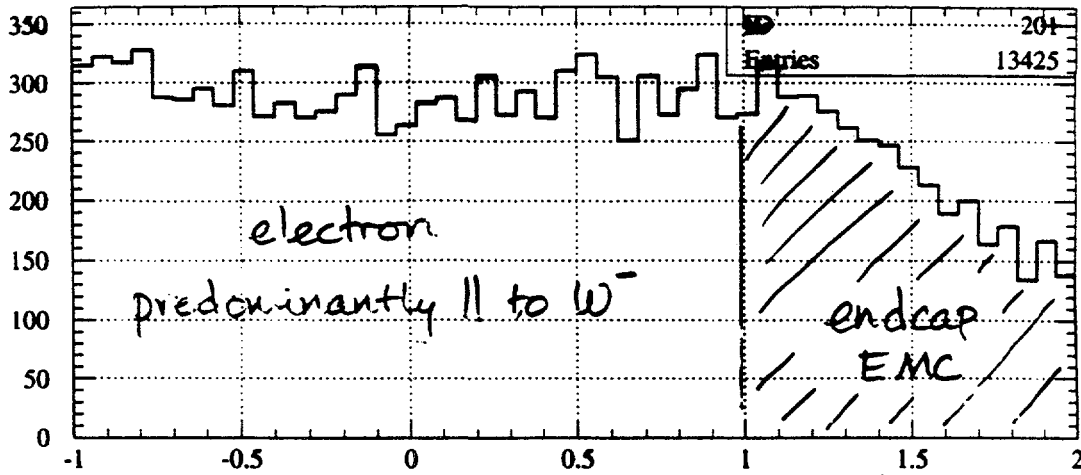
Fig. 3 shows the expected A_L for the four independent quantities that can be measured (asymmetries from either beam longitudinally polarized, and detection of either e^+ or e^-). To examine if the measured asymmetries are directly related to quark and antiquark polarizations, the identities of the partons involved in the W^\pm production were examined. Figs. 4 and 5 show the x distribution of the initial-state partons, available from PYTHIA for two different ranges of e^\pm pseudorapidity. It's clear that only when the e^\pm are detected at large η that A_L can be directly related to $u(d)$ and $\bar{d}(\bar{u})$ polarizations.

The next step to take with the simulation model is to attempt the reconstruction of the initial-state $u(d)$ and $\bar{d}(\bar{u})$ momentum fractions (x) assuming collinear collisions. As well, a more accurate simulation of the response of the STAR detector is essential to quantitatively establish the accuracy of the determination of the $u(d)$ and $\bar{d}(\bar{u})$ polarizations.

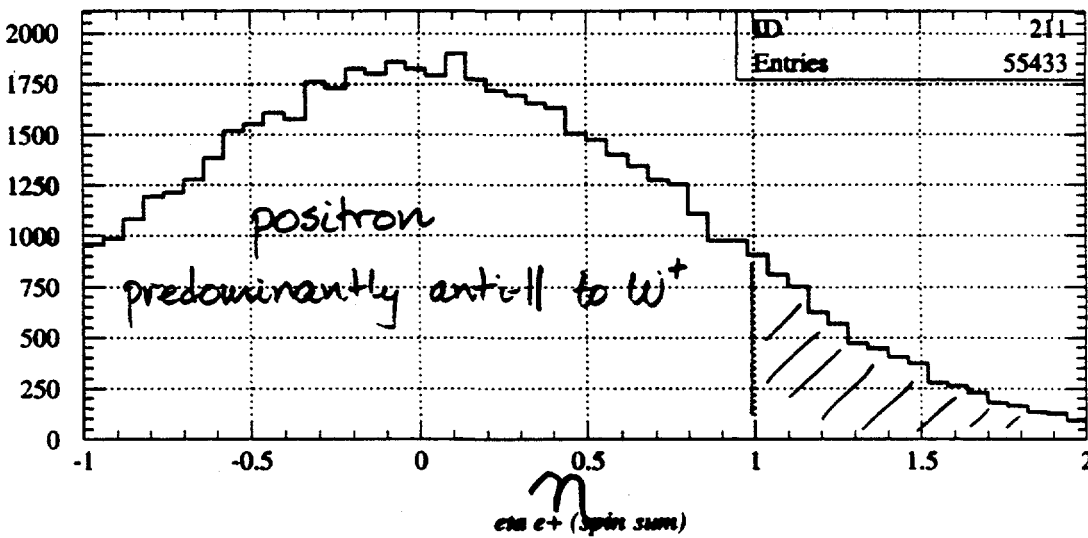
- [1] PYTHIA 5.7 / JETSET 7.4 T. Sjöstrand, Comp. Phys. Comm. **82** (1994) 74.
- [2] C. Bourrely, J. Soffer, F.M. Renard and P. Taxil, Phys. Rept. **177** (1989) 319.
- [3] T. Gehrmann and W.J. Stirling, Phys. Rev. **D53** (1996) 6100.
- [4] A.A. Derevschikov, V.L. Rykov, K.E. Shestermanov and A. Yokosawa in *Proc. 11th Intl. Symp. on High Energy Spin Physics*, Bloomington, 1994, eds. Kenneth J. Heller and Sandra L. Smith, AIP Conf. Proc. No. 343 (1995) p. 472.

AVERY

Np/Np



$pp \rightarrow W^\pm X \rightarrow e^\pm(\nu) X$
 800 pb^{-1}
 $\sqrt{s} = 5006 \text{ GeV}$
 (PYTHIA)



$$\frac{d\sigma}{dy} (W^\pm) = G_F \frac{\sqrt{2}}{3} \pi \tau \left[u(x_a, M_W^2) \bar{d}(x_b, M_W^2) + (a \leftrightarrow b) \right]$$

$$\tau = \frac{M_W^2}{s_{pp}} \quad x_1 = \sqrt{\tau} e^{-y_W} \quad x_2 = \sqrt{\tau} e^{+y_W}$$

If $y_W \sim y_e$ then endcap $\Rightarrow x_2 \gg x_1$
 \Rightarrow Interpret A_L in terms of $\frac{\Delta q}{q} \pm \frac{\Delta \bar{q}}{q} ?$

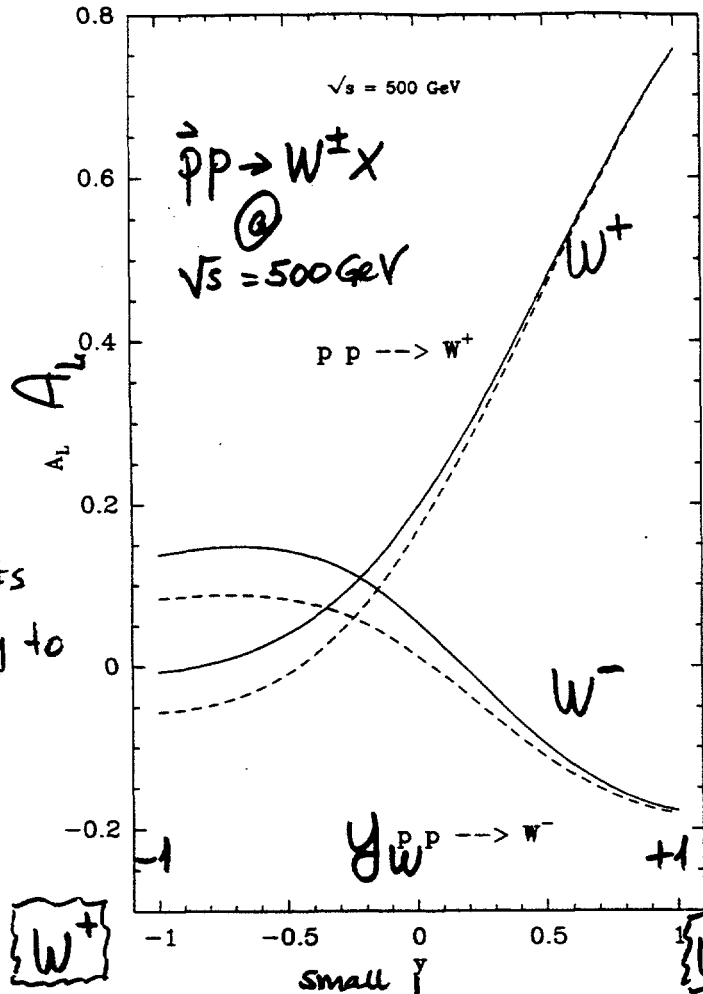
Fig. 1

Bourrely
&
Soffer

A_L measurements
give sensitivity to

$$\Delta q = q_{\uparrow} - q_{\downarrow}$$

$$\Delta \bar{q} = \bar{q}_{\uparrow} - \bar{q}_{\downarrow}$$



$u \bar{d} \rightarrow W^+$

$d \bar{u} \rightarrow W^-$

"a"
polarized

$$\frac{\Delta u(x_a) \bar{d}(x_b) - \Delta \bar{d}(x_a) u(x_b)}{u(x_a) \bar{d}(x_b) + \bar{d}(x_a) u(x_b)}$$

$$\xrightarrow{x_a \gg x_b} \frac{\Delta u(x_a)}{u(x_a)}$$

$$\frac{\Delta d(x_a) \bar{u}(x_b) - \Delta \bar{u}(x_a) d(x_b)}{d(x_a) \bar{u}(x_b) + \bar{u}(x_a) d(x_b)}$$

$$\xrightarrow{x_a \gg x_b} \frac{\Delta d(x_a)}{d(x_a)}$$

"b"
polarized

$$\frac{u(x_a) \Delta \bar{d}(x_b) - \bar{d}(x_a) \Delta u(x_b)}{u(x_a) \bar{d}(x_b) + \bar{d}(x_a) u(x_b)} \text{ Small}$$

$$\xrightarrow{x_a \gg x_b} \frac{\Delta \bar{d}(x_b)}{\bar{d}(x_b)} - \frac{\bar{d}(x_a) \Delta u(x_b)}{u(x_a) \bar{d}(x_b)}$$

$$\frac{d(x_a) \Delta \bar{u}(x_b) - \bar{u}(x_a) \Delta d(x_b)}{d(x_a) \bar{u}(x_b) + \bar{u}(x_a) d(x_b)} \text{ small}$$

$$\xrightarrow{x_a \gg x_b} \frac{\Delta \bar{u}(x_b)}{\bar{u}(x_b)} - \frac{\bar{u}(x_a) \Delta d(x_b)}{d(x_a) \bar{u}(x_b)}$$

(Fig. 2)

$\bar{p}p \rightarrow W^\pm X \rightarrow e^\pm(\nu) X$ $\sqrt{s} = 500 \text{ GeV}$
 800 pb^{-1} $P_{\text{beam}} = 0.7$

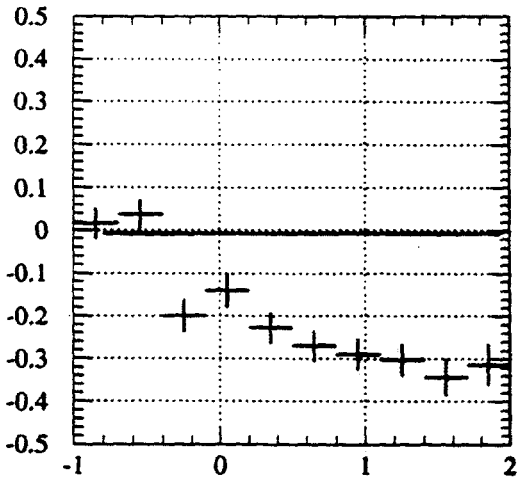
beam a polarized

beam b polarized

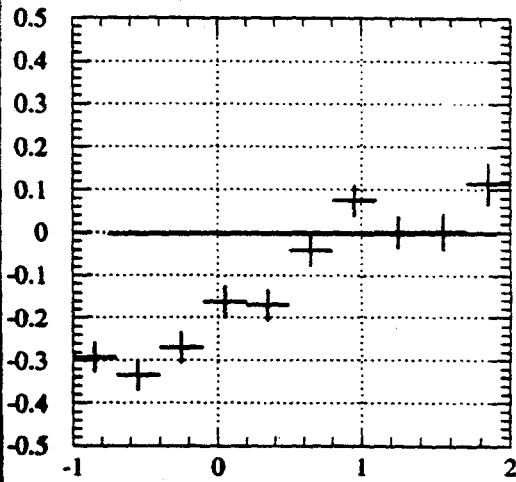
98/04/29 06.57

AVERY

AL

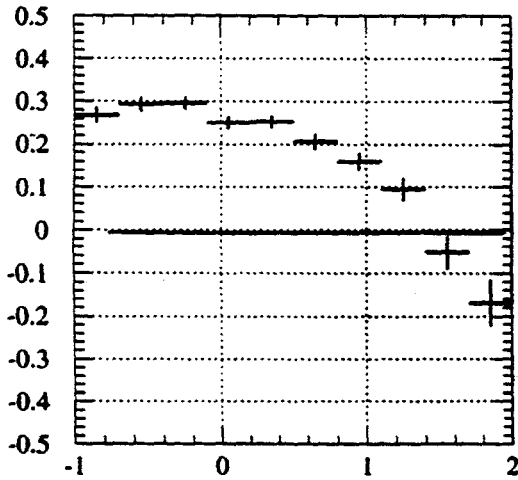


Pos pz beam spin asym vs eta e-

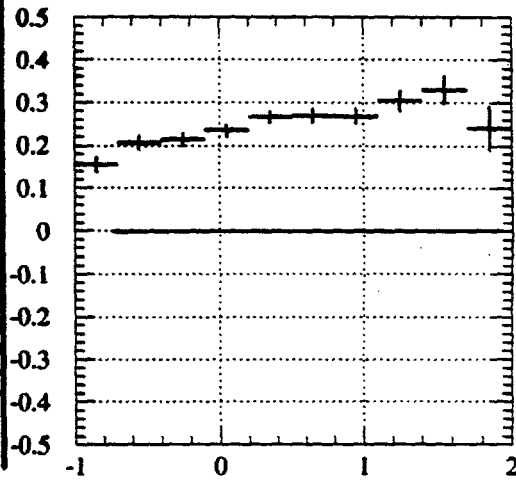


Neg pz beam spin asym vs eta e-

$W^- \rightarrow e^-(\bar{\nu})$



Pos pz beam spin asym vs eta e+



Neg pz beam spin asym vs eta e+

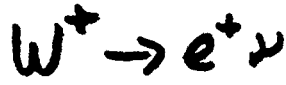
$W^+ \rightarrow e^+(\nu)$

η_{e^\pm}

Do A_1 values determine $\frac{\Delta q}{q}$, $\frac{\Delta \bar{q}}{\bar{q}}$?

→ Look in different η ranges

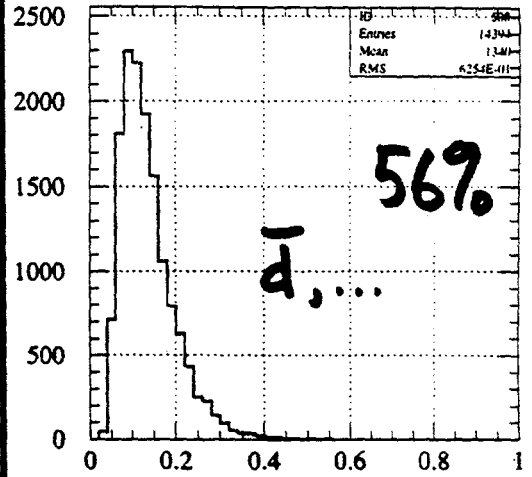
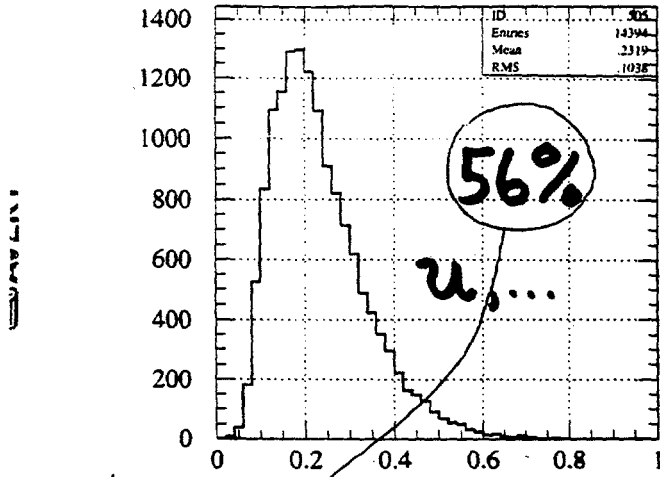
Fig. 3



beam a

beam b

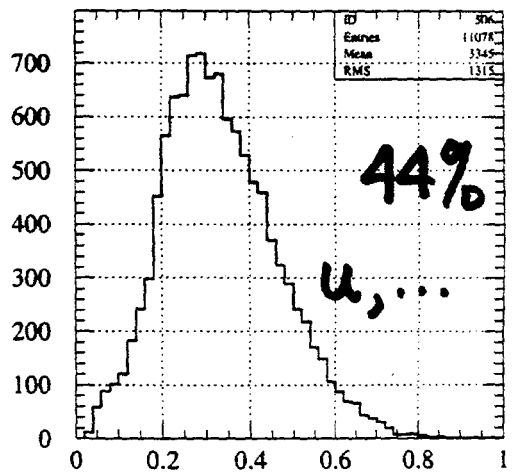
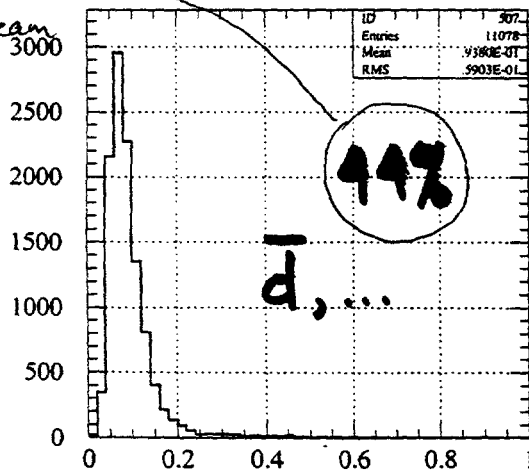
98/04/25 21.58



parton composition of beam

$x q$ for e^+ and q pz pos

$x qbar$ for e^+ and $qbar$ pz neg



$x qbar$ for e^+ and $qbar$ pz pos

$x q$ for e^+ and q pz neg

$\langle A_L \rangle \sim +0.3$

$\langle A_L \rangle \sim +0.2$

$-1 < \eta_{e^+} < 0$

$\Rightarrow A_L$ not directly related to $\frac{\Delta u}{u}$ or $\frac{\Delta \bar{d}}{\bar{d}}$

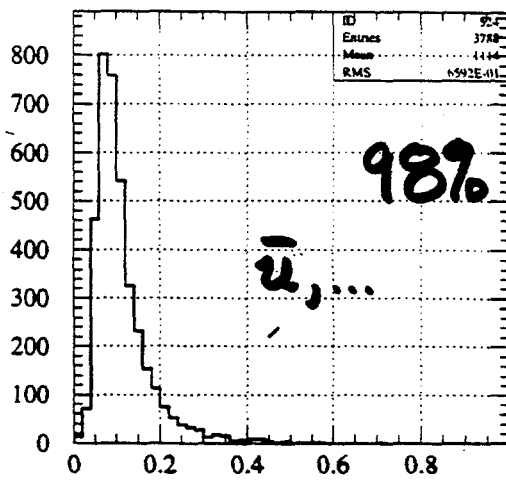
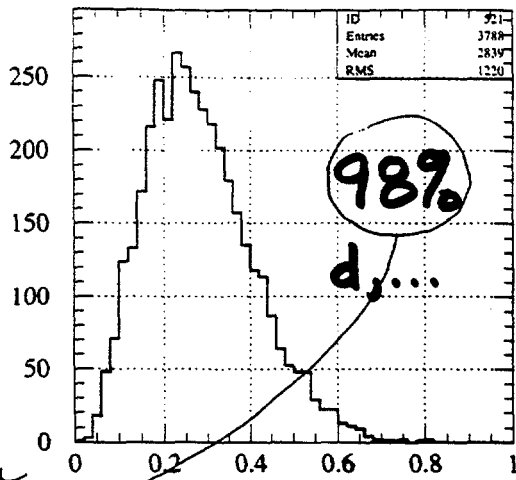
Fig. 4

$W^- \rightarrow e^- \bar{u}$

98/04/25 21.58

beam a

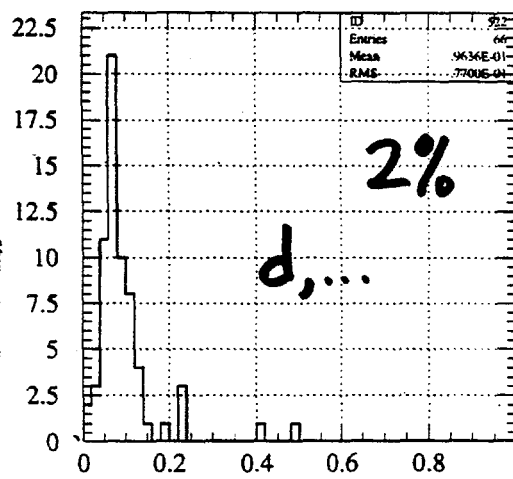
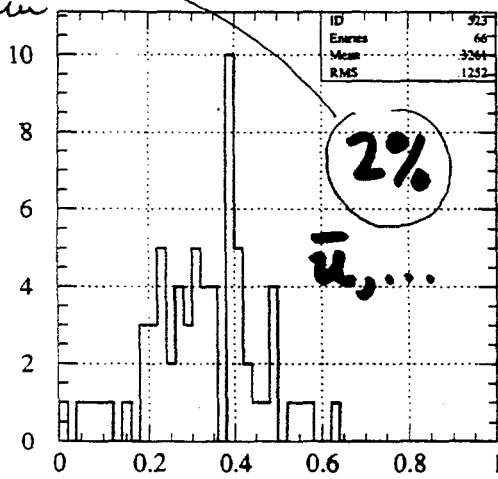
beam b



parton composition of beam

$x q$ for e^- and q p_z pos

$x qbar$ for e^- and $qbar$ p_z neg



$x qbar$ for e^- and $qbar$ p_z pos

$x q$ for e^- and q p_z neg

$\langle A_L \rangle \sim -0.3 \quad \times \quad \langle A_L \rangle \sim 0$

(endcap EMC)

$1 < \eta_e < 2$

$\Rightarrow A_L$ is directly related to $\frac{\Delta d}{d}$ (beam a) & $\frac{\Delta \bar{u}}{\bar{u}}$ (beam b)

(Fig. 5)

Measurement of Anti-Quark Polarization at PHENIX

Naohito Saito

Radiation Laboratory

RIKEN (The Institute of Physical and Chemical Research)

Saitama 351-0198, Japan

(<http://www.rhic.bnl.gov/phenix/WWW/publish/saito/>)

The measurement of the anti-quark polarization and its flavor decomposition is crucial in the study of the spin structure of the nucleon. The deep inelastic scattering of polarized lepton off polarized nucleon target is not sensitive to those, because photon couples only to electric charge squared. Because of this, the current study of the flavor structure of the quark/anti-quark polarization has to assume flavor SU(3) symmetry.

The parity violating asymmetry A_L for W production in polarized pp collision is very sensitive not only to helicity structure of the anti-quarks in the proton but also to the flavor structure of them. The asymmetry for W^+ production can be written as:

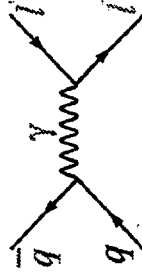
$$A_L^{W^+} = \frac{\Delta u(x_a, M_W^2) \bar{d}(x_b, M_W^2) - \Delta \bar{d}(x_a, M_W^2) u(x_b, M_W^2)}{u(x_a, M_W^2) \bar{d}(x_b, M_W^2) + \bar{d}(x_a, M_W^2) u(x_b, M_W^2)}$$

For W^- production, the u and d should be exchanged. Obviously the asymmetry is just the linear combination of the quark and anti-quark polarization. Furthermore, the flavor in the reaction is almost fixed. Thus flavor decomposition is possible.

In the PHENIX detector at RHIC, the production of W can be identified with the lepton with high transverse momentum such as $p_T > 20$ GeV/c. With this experimental cut in the PHENIX Muon Arm, we expect about 5,000 events for each of W^+ and W^- productions with the integrated luminosity of 800 pb⁻¹. Reconstruction of partonic level kinematics is one of the key issues in the hadronic collisions. Using the correlation between muon momentum and x carried by the parton due to the decay angle distribution in $V-A$ reaction, it is possible to extract the polarization as a function of x . The high momentum resolution expected from the detailed simulation and good muon identification proven in the beam test at KEK of the PHENIX detector system, will help this reconstruction very much.

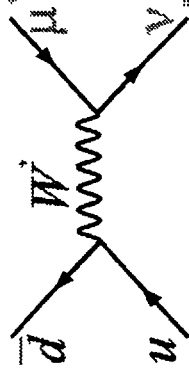
Anti-quark Helicity Distribution

- Drell-Yan Production of lepton pairs
 - maximal parton level asymmetry: $a_{LL} = -1$
 - possible severe background from semi-leptonic decays of open charm productions $\sum_i e_i^2 [\Delta q_i(x_a) \Delta \bar{q}_i(x_b) + (x_a \leftrightarrow x_b)]$



$$A_{LL} = - \frac{\sum_i e_i^2 [q_i(x_a) \bar{q}_i(x_b) + (x_a \leftrightarrow x_b)]}{\sum_i e_i^2 [q_i(x_a) \bar{q}_i(x_b) + (x_a \leftrightarrow x_b)]}$$

- W production
 - helicity of quarks definitely defined via V-A nature
 - flavor almost fixed: flavor analysis possible
 - PHENIX-Muon Arms, EMCal important



$$A_L^{W^+} = \frac{\Delta u(x_a, M_W^2) \bar{d}(x_b, M_W^2) - \Delta \bar{d}(x_a, M_W^2) u(x_b, M_W^2)}{u(x_a, M_W^2) \bar{d}(x_b, M_W^2) + \bar{d}(x_a, M_W^2) u(x_b, M_W^2)}$$

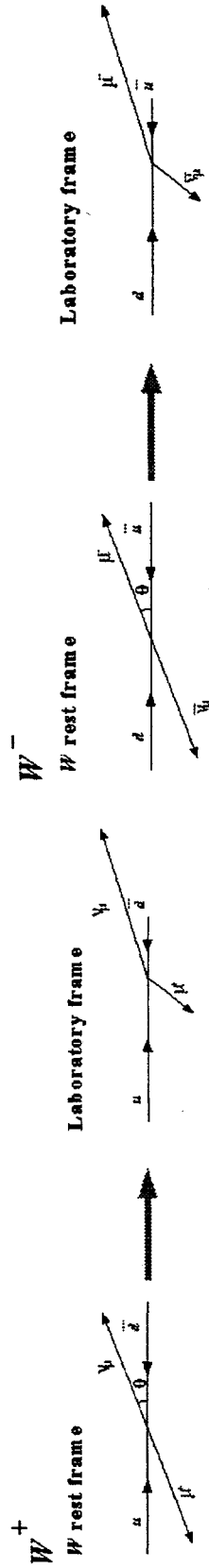
Naohito Saito, RIKEN

W yield with 800 pb⁻¹

PYTHIA w/ GRV94LO checked against CDF data

	W ⁻	W ⁺
acceptance for muon w/ $p_T > 20 \text{ GeV}/c$	14%	4%
yield (both muon arms)	5100	5600
ΔA_L (statistical only)	2%	2%
rapidity average	0.78 ± 0.34	0.71 ± 0.41
background from Z-decay	1095(21.5%)	984(17.6%)

Acceptance difference between W⁻ and W⁺



Naohito Saito, RIKEN

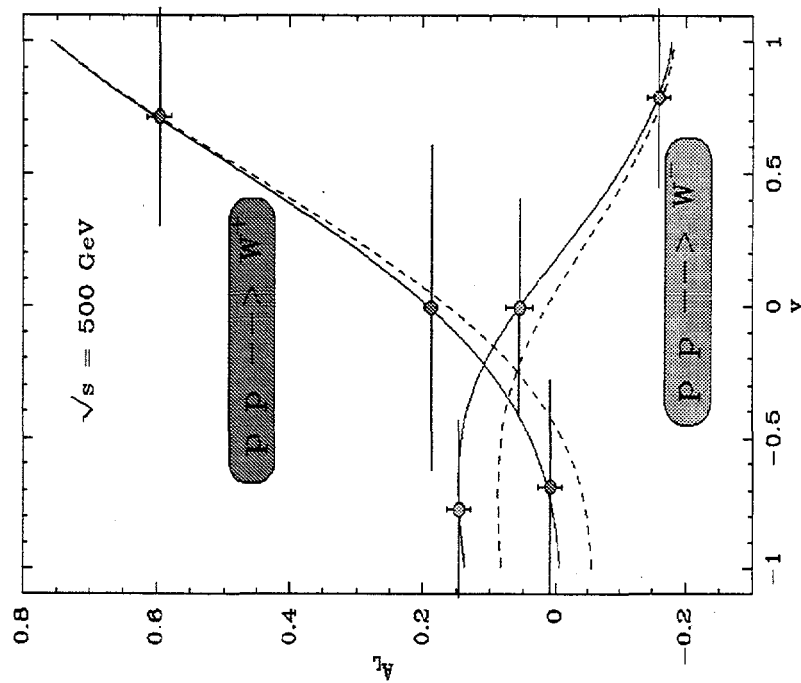
Prediction and Projected Error

• C. Bouchery, J. Soffer Published in Nucl.Phys.B445:341-379,1995

Prediction for the
parity violating
asymmetry A_L as a
function of y^W

solid line: soft gluon

dashed line: hard gluon

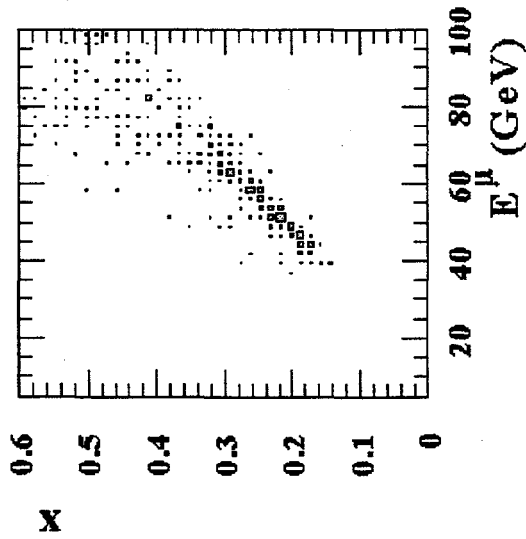


Naohito Saito, RIKEN

Parton Level Kinematics

- Decay ν cannot be detected: x -determination hard
- but good correlation x vs E^μ : V-A requires $(1+\cos\theta)^2$

$$P_\mu = \frac{\sqrt{s}}{4} [(1+\cos\theta)x_u + (1-\cos\theta)x_{\bar{d}}] M_W = \sqrt{x_u x_{\bar{d}} s}$$

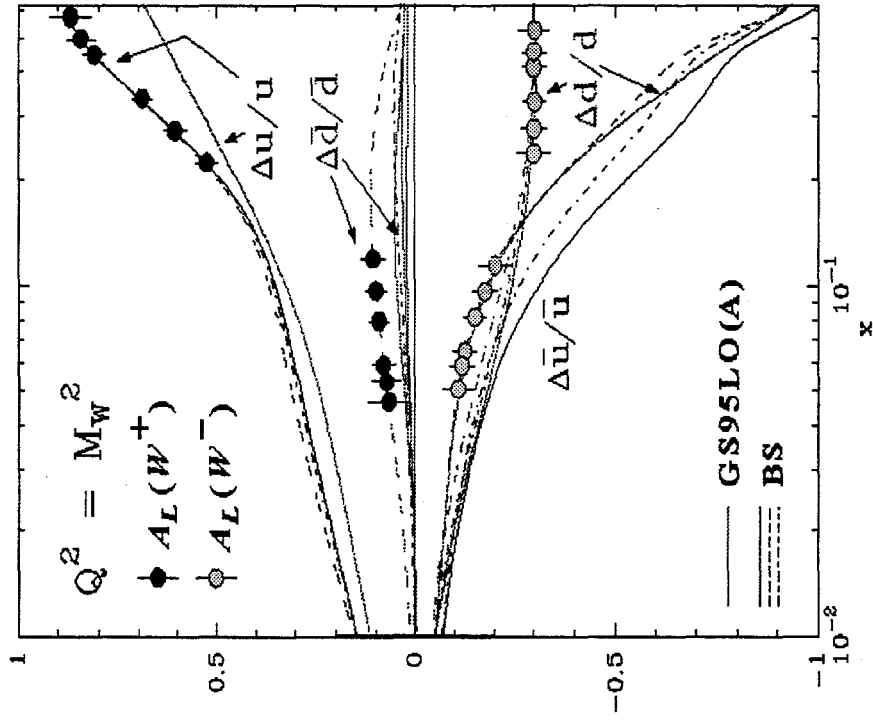


p^μ region	x -average W^+
$34 < p^\mu < 50 \text{ GeV}/c$	0.22 ± 0.08
$50 < p^\mu < 60 \text{ GeV}/c$	0.27 ± 0.08
$60 < p^\mu < 70 \text{ GeV}/c$	0.33 ± 0.09
$70 < p^\mu < 80 \text{ GeV}/c$	0.44 ± 0.11
$80 < p^\mu < 95 \text{ GeV}/c$	0.49 ± 0.10
$95 < p^\mu < 120 \text{ GeV}/c$	0.56 ± 0.11

Naohito Saito, RIKEN

Sensitivity Goal - statistical limit

- Anti-quark polarization measured with A_L^W
- More systematic studies are underway
 - background from π/K decays
 - background from Z^0 decays



Naohito Saito, RIKEN

Sensitivity to New Physics in Parity Violating Asymmetries at RHIC

Jean-Marc Virey¹

Centre de Physique Théorique
CNRS Luminy, Case 907
13288 Marseille cedex 09, France

We have presented the sensitivity of the RHIC Spin experiment to some new physics contributions, from the analysis of the Parity Violating (PV) asymmetry $A_{LL}^{PV} (\equiv d\sigma^{--} - d\sigma^{++} / d\sigma^{--} + d\sigma^{++})$ defined for jet production ($d\sigma \equiv d\sigma_{1-jet}$).

In the first part, we have recalled the sensitivity to the presence of some new quark-quark Contact Interactions (CI). Such CI could represent some effects of quark compositeness. At RHIC, with the conventional parameters of the experiment, we will be sensitive to some energy scales of $\Lambda \sim 3-4 TeV$, if PV is maximal. It appears that the RHIC is perfectly competitive with the TEVATRON for the discovery of CI, however, we have to note that the integrated luminosity is a key parameter for the polarized analysis. The study of A_{LL}^{PV} could give some unique informations on the chiral structure of the new interaction.

The second part was devoted to a review of the different theoretical motivations for the presence of a "leptophobic" Z' of relatively low mass, that we briefly report now :
1) Leptophobia corresponds to some new interactions belonging to the "pure" quark sector. 2) Leptophobic Z' appears naturally in several models derived from string theory. Within these models, the absence of Z' leptonic couplings appears in several ways : from the classification of the fermions in the different representations of the gauge group, or from kinetic mixing between two abelian gauge groups which produces a mixing between the charges of the fermions under these two $U(1)$ factors. 3) Some theoretically consistent leptophobic Z' bosons have been constructed also for non-supersymmetric models. 4) In the framework of supersymmetric models with an additional abelian gauge factor $U(1)'$, it has been shown that the Z' boson could appear with a relatively low mass ($M_Z \leq M_{Z'} \leq 1 TeV$) and with a mixing angle with the Z close to zero. In addition, these classes of models have several appealing features for soft supersymmetry breaking and for cosmology. 4) The present experimental constraints on these models are rather weak. Several classes of models are absolutely unconstrained. 5) All these theoretically motivated models exhibit, in general, some PV couplings to up and down quarks, which could induce some interesting effects on A_{LL}^{PV} measured in $p-p$ or/and $n-n$ collisions at RHIC. The main results are presented in the following transparencies.

The last section concerned the measurement of A_{LL}^{PV} in $p-n$ collisions, which could detect the presence of a new charged boson W' unconstrained by present experimental data.

¹email: virey@cpt.univ-mrs.fr

3. Properties for u_P / A_{LL}^{PV} in $p-p$ collisions

In general, the leptophobic Z' violates Parity in the up quark sector!

- "Flipped $SU(5)$ " : Maximal PV!

$$C_L^{u'} = \pm \frac{1}{2} \quad C_R^{u'} = 0 \quad (\Rightarrow \text{Left})$$

- "3-kinetic" : $C_R^{u'} = -2 C_L^{u'} = \frac{1}{3}$ (\Rightarrow Right)

- The constraint of all the "classes" of models is:

$$C_L^{u'} \neq C_R^{u'}$$

ie: axial couplings ($C_L^{u'} = -C_R^{u'}$) authorized \Rightarrow No effect on A_{LL}^{PV} !

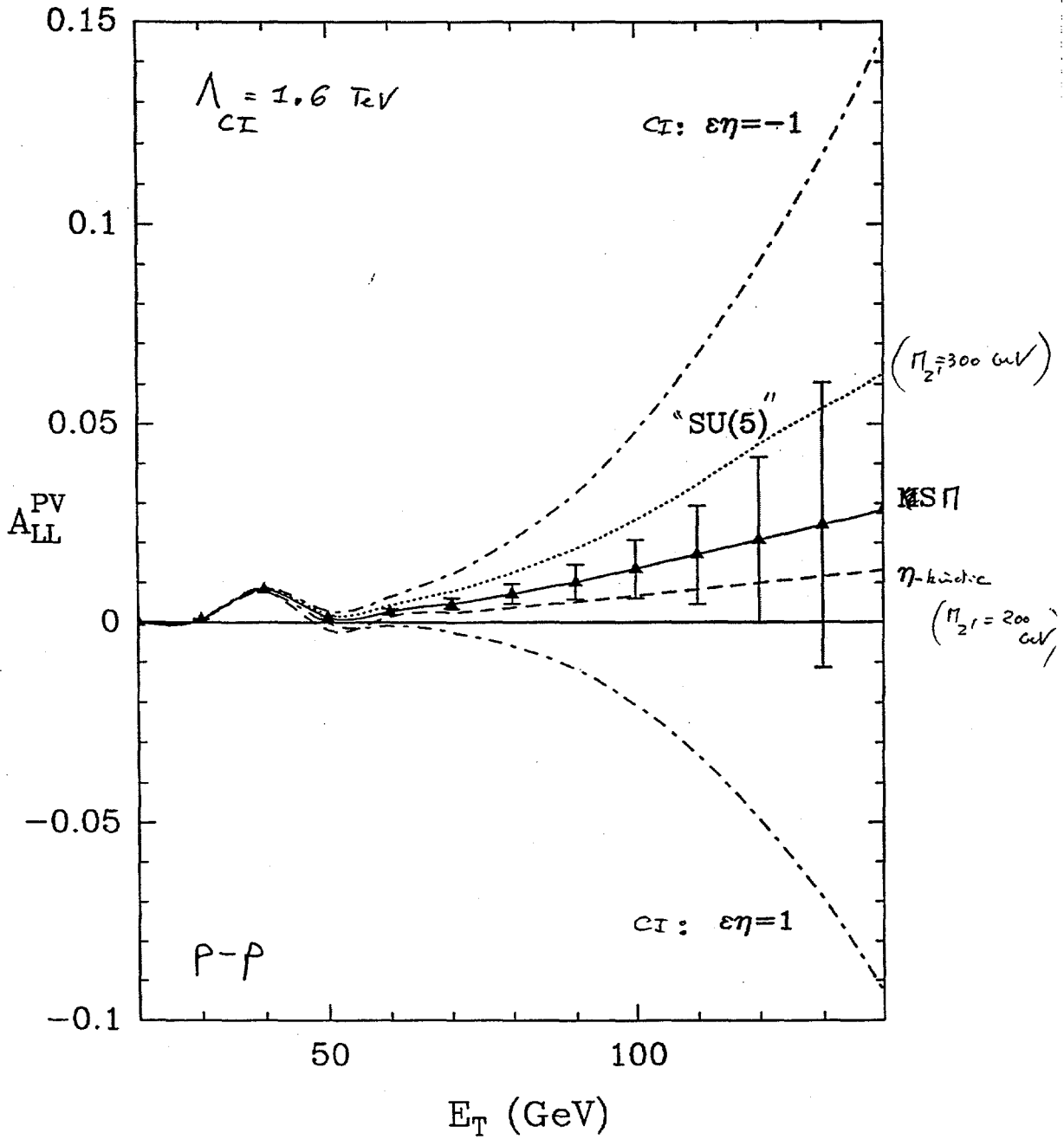
Except this case, for $M_{Z'} \lesssim 300 - 400$ GeV,

these models could be detected at RHIC

from A_{LL}^{PV} in $p-p$ collisions!

error bars: $\sqrt{s} = 500 \text{ GeV}$
 $L = 800 \text{ pb}^{-1}$
 $\Delta E_T = 10 \text{ GeV}$
 $\Delta y = 1$

$$\frac{\Delta \Gamma_{\text{systematic}}}{\Gamma} = 10\%$$



3°] Properties for down / A_{LL}^{PV} in $n-n$ collisions

Isospin symmetry $\Rightarrow A_{LL}^{PV} (n-n)$ tests d

What could we expect from these Z' ?

\rightarrow Models with Parity Conservation (for d)

(\Rightarrow No effect on $A_{LL}^{PV} (n-n)$)

• "flipped $SU(5)$ " and " η -kinetic" are PC : $C_L^d = \pm C_R^d$

• PC for d is a general property of the minimal 2 doublets Higgs model

$$h_u Q u^c H_u + h_d Q d^c H_d + h_e L e^c H_d \in \frac{Z'_Y}{W}$$

$$\text{Leptophobia} \equiv Q'(L) = 0 = Q'(e^c)$$

$$\Rightarrow Q'(H_d) = 0 \Rightarrow Q'(Q) + Q'(d^c) = 0$$

$$\Rightarrow C_L^{d'} = C_R^{d'} \quad \text{i.e. Vectorial couplings}$$

Δ $Q'(f)$: change of g under $U(1)$
 $C_L^{d'} = Q'(f)$
 $C_R^{d'} = -Q'(f^c)$

→ Non-Minimal Higgs Models

- 3 Higgs doublets (Georgi-Glashow)
 Higgs et al.
- 2 Higgs doublets + d mass terms (in W) from
 higher dimensional operators: (Cvetič et al)
 Natural in string models (Faraggi PLB 377 (96)
 43)

They do not impose PC for d, conversely

we often have: $C_L^{d'} \neq C_R^{d'}$

(i.e. PV for d except for the axial case)

- Interesting model: "Minor Z" (Caravaggio & Ross
 PLB 346 (95) 159)

$$\frac{C_L^q}{C_R^q} = \frac{C_R^{q'}}{C_L^{q'}} \Rightarrow \begin{cases} C_R^{u'} \approx -2 C_L^{u'} \\ C_R^{d'} \approx -5 C_L^{d'} \end{cases}$$

We expect strong PV for d in this model!

No curves for $A_{LL}^{PV}(n,n)$, Sorry! (Available soon.)

Conclusions: • $A_{LL}^{PV}(n,n)$ is sensitive to NP if PV/a.

- It could constraint the scalar sector of the new theory!

4) Experimental Constraints

• Direct:

Come from $\nabla_{\text{set}}^{\text{unpol}}$

$$\text{U(1)}_2 : \text{forbids for } K = \frac{g_{Z'}}{g_2} = 1: \quad 100 < M_{Z'} < 250 \quad \text{GeV}$$

$$\Delta \emptyset : \quad \text{"} \quad \text{"} \quad \text{"} \quad 365 < M_{Z'} < 615$$

CMF : no - constraints

→ limits obtained for SM-like Z' (i.e. same coupling)

→ limits highly model dependent

→ Disappear for $K \lesssim 0.95$

need
 $K \lesssim 0.9$ for b τ
 high masses. Some
 irrelevant for RHIC.

(Re : $K_{\text{GUT}} \sim 0.7$!)

"g-kinetic" absolutely unconstrained (and for take

→ Large uncertainties (exp. + th.) for $\nabla_{\text{set}}^{\text{unpol}}$!

• Indirect

from Z-pole (LEP/SLC) + low energy PV $\rightarrow \sigma_{Z-Z'} \lesssim \frac{10^{-2}}{10^{-3}}$

In leptophobic Z' models, in general, $\sigma_{Z-Z'}$ is naturally ~ 0

• conclusion:

Low mass leptophobic Z' are not in contradiction with present experiments

III W' at RHIC

(P. Tan & SMV PL B404 (97)
302

A_{LL}^{PV} is sensitive to a W' in $p-n$ collisions

(result from Isospin symmetry)

→ SM effects: pp: $Z-g \sim 70\%$ $W-g \sim 30\%$
pn: $Z-g \sim 2\%$ $W-g \sim 98\% !!$

→ W_R from LRM

Limits on M_{W_R} are highly model dependant.

Relevant parameters: (Langacker & UmaSankar PRB40 (89))

V_{CKM}^R , γ_R , $K = \frac{g_R}{g_2}$, ξ, ω (CP phases), σ_{W-W_R}

Case the weakest constraint: $V_{CKM}^R \sim 1$, γ_R heavy Dirac
(natural! less (!))

A_{LL}^{PV} in $p-n$ collisions is sensitive

to this model if $M_{W_R} \lesssim 400 \text{ GeV}$

($K \approx 0.9$)

Spin Physics with Jets at STAR

Geary Eppley (for the STAR Collaboration)
Rice University, Houston TX 77005

The spin physics program from jet detection at STAR is presented in order of increasing luminosity requirements, hence by year. (1) In year 1 it will be technically feasible, given one transversely polarized beam and collisions, for STAR to measure A_T with the baseline detector. In excess of 10k low p_T (> 15 GeV) jet events can be accumulated in several days at low luminosity. A measurement of A_T consistent with zero will place a limit on higher twist effects that could complicate the subsequent measurements of A_{LL} . (2) In year 2, A_{LL} can be measured from an inclusive low p_T jet sample giving an indication of the magnitude of ΔG in the neighborhood of $x = 0.1$. Since the observable A_{LL} is quadratic in ΔG , this result will not determine the sign of ΔG . (3) In year 2 and beyond, a high statistics dijet sample, $> 10M$ events, can be used to determine A_{LL} as a function of x partons for $0.05 < x < 0.25$. Cuts are imposed on the sample to insure that the jets represent the partons from the hard scattering: no third jet, p_T balance, back-to-back in ϕ . Assuming a sign for ΔG or using the sign determined by the direct photon analysis, $\Delta G(x)$ may be extracted from the data subject to uncertainties in the production processes and in the polarized quark distributions. (4) Given integrated luminosity of 800 pb^{-1} per year, it should be possible to measure A_{pv} from a high p_T (> 45 GeV) inclusive jet sample as described in the subsequent 5 pages. (For motivation see the previous talk by J.M. Virey.) Page 1 shows the \hat{p}_T distribution for an event sample passing a level 0 trigger using the electromagnetic calorimeter. At the level 3 trigger were track information from the TPC is available, jets are reconstructed and an event sample is selected with $p_T^j > 45$ GeV, see page 2. The calculation of the standard model (SM) A_{pv} expected in this sample is shown on pages 3 and 4. The last figure (p. 5) shows the departure from SM A_{pv} as a function of $M_{Z'}$ for $\hat{p}_T = 60, 80, \text{ and } 100$ GeV. For $M_{Z'} = 600$ GeV, the observed A_{pv} increases 30% therefore a measurement to $< 10\%$ uncertainty is required to look for this effect. As pointed out by Virey, current limits from $p\bar{p}$ colliders assume SM couplings for new Z' . Since this coupling is not determined by theory, there is a substantial window of opportunity at RHIC to search for these effects. (5) The third fundamental leading twist partonic structure function $h_1(x)$ may be determined from A_{TT} measured in high p_T dijet events.

Parity-violating spin asymmetries

- pp scattering at $\sqrt{s} = 500$ GeV
- polarized protons
- inclusive jet production
- Parity-violating asymmetry

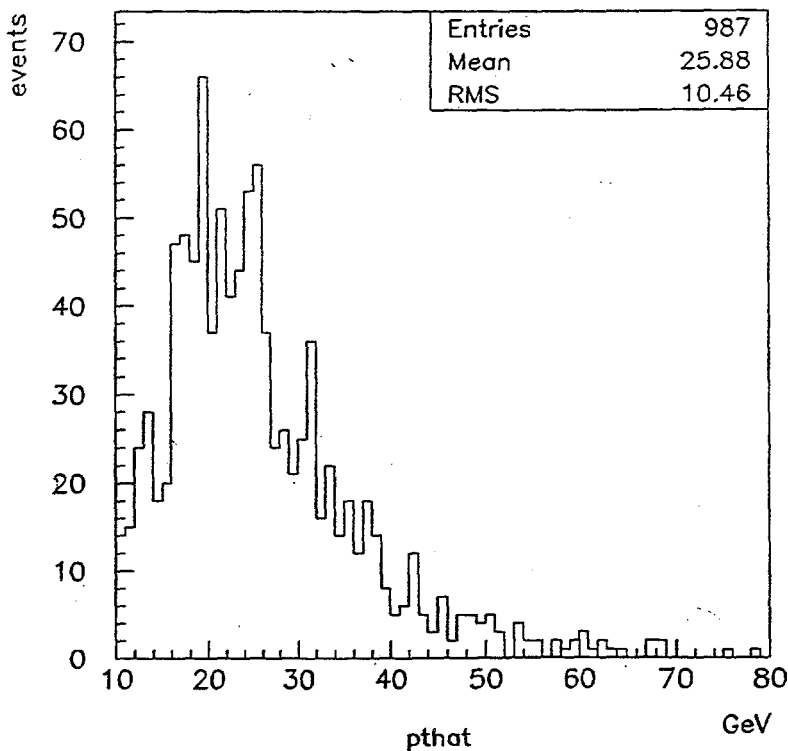
$$A_{LL}^{PV} = \frac{d\sigma_{--} - d\sigma_{++}}{d\sigma_{--} + d\sigma_{++}}$$

- Largest effect: t-channel, same flavor, interference between g and Z

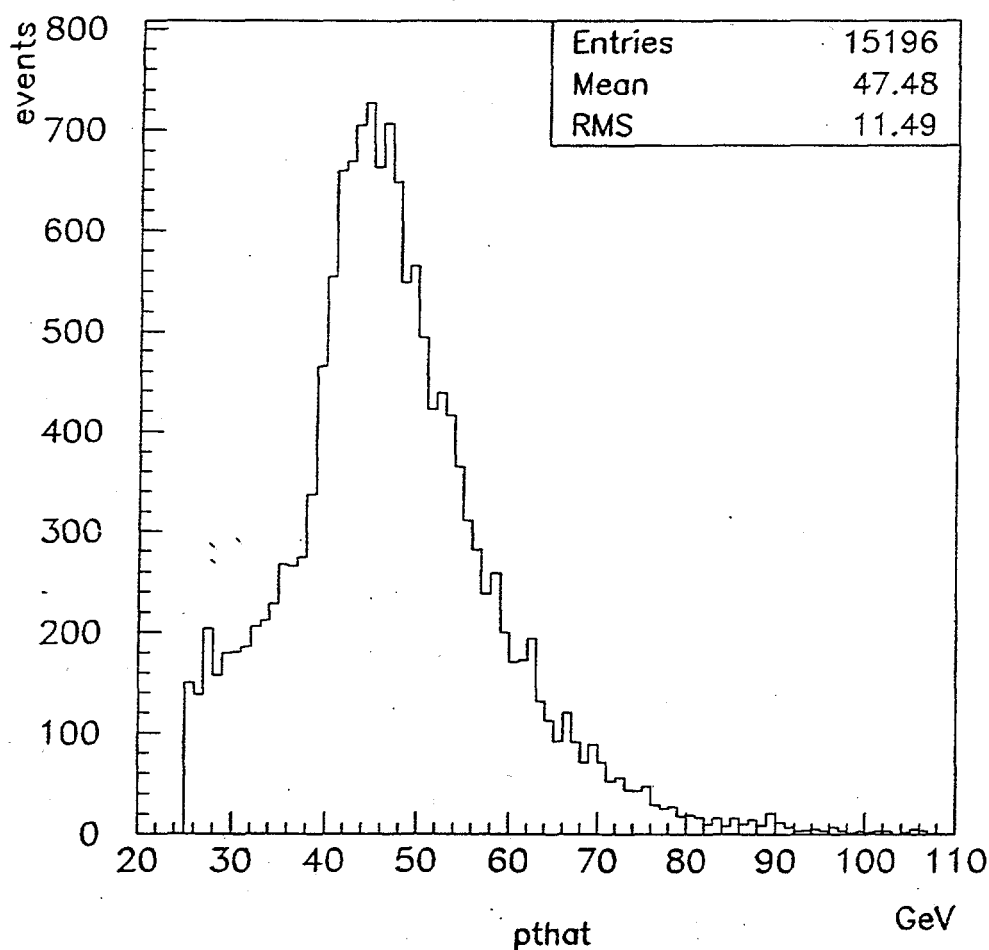
BNL
4-28-98

GEARY EPPLEY
RICE UNIVERSITY

STAR



Select events
passing a level 0
trigger tower
.8x.8 in EM
calorimeter



select events with a jet, $R = .7$
 $\bar{E}_T > 45 \text{ GeV}$ $|\eta| < 0.8$

the trigger is 50% efficient but
there is 33% dead time

$$800 \text{ pb}^{-1} : ++ + - - + - -$$

$$16 \text{ nb} \times 800 \text{ pb}^{-1} \times \frac{33\%}{\text{trigger}} = 4 \text{ M events}$$

2 M for A_{PV}

$$A_{PV}(\hat{P}_T) :$$

$\hat{P}_T = (\text{GeV})$	A_{PV}
35	.0007
45	.0018
55	.004
65	.007
75	.012
85	.019
95	.026
105	.036

$$A_{PV}(E_T^+ > 45 \text{ GeV}) = 0.003 \pm 0.001 \pm 0.0006 \text{ (sys)}$$

systematic error :

- 10% P and L
- 12% threshold uncertainty
- 4% jet energy scale
- 3% neutral hadrons
- 15% PDF's

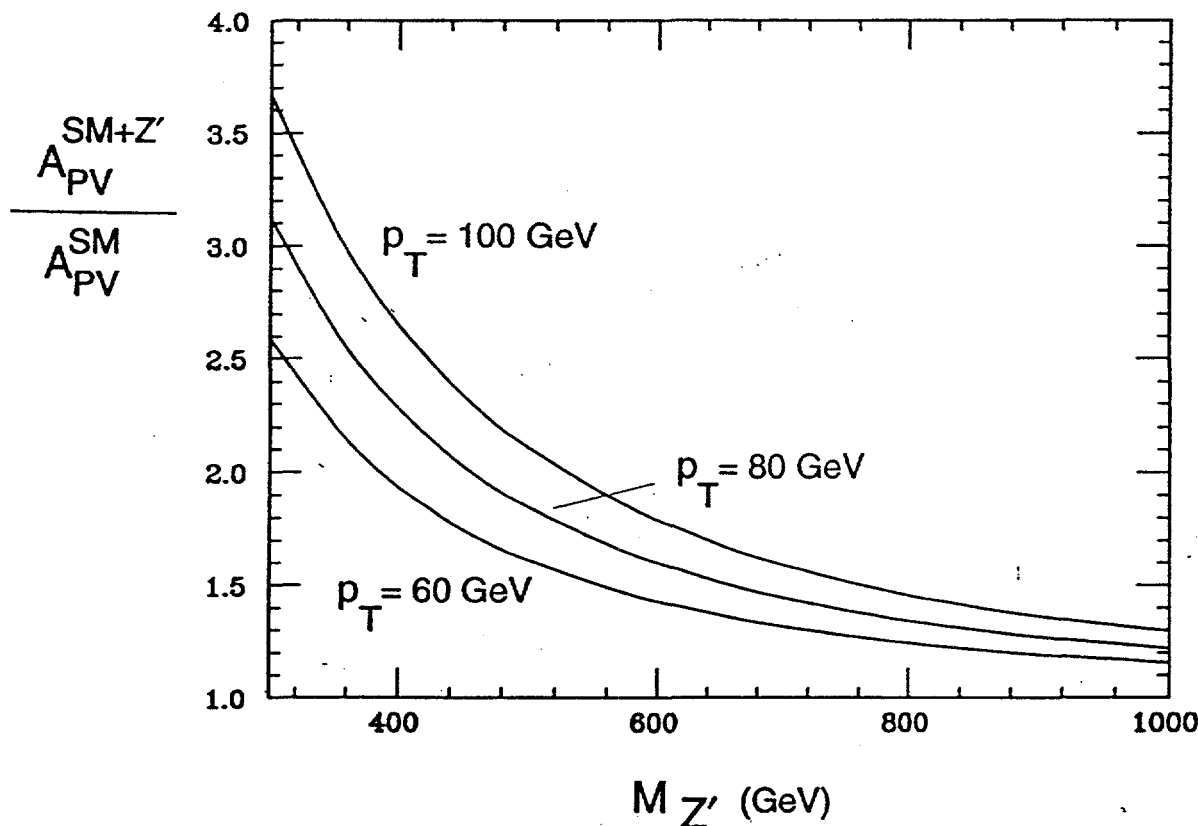
Leptophobic Z'

[Lopez-Nanopoulos, hep-ph/9605359]

- Leptophobia is *natural* in flipped SU(5)

$$10 = \left\{ \begin{pmatrix} u_L \\ d_L \end{pmatrix}, d_R, \nu_R \right\}; \quad \bar{5} = \left\{ \begin{pmatrix} e_L \\ \nu_L \end{pmatrix}, u_R \right\}; \quad 1 = e_R$$

Leptons (L) uncharged $\Rightarrow Z'$ must not "see" $\bar{5}$
 Z' may "see" 10: several quarks (no leptons)



For 600 GeV leptophobic Z' , just above current Fermilab reach:

$$A_{PV} = 0.004 \quad \text{in standard model} = 0.003$$

Need at least a 10% measurement to see this.

Could large CP -violation be detected in polarized proton collisions at RHIC?

V. L. Rykov¹

Wayne State University, Detroit, MI 48201, USA

The measurable asymmetries which could be an indication of CP - and/or T -violation in charged current leptonproduction by polarized protons are discussed.

Summary

What is discussed?

- The single- and double-spin leptonproduction asymmetries and their relative sensitivities to CP -odd terms of the phenomenological charged current lagrangian.
- Crude estimates for spurious " T -odd-like" asymmetries due to initial and final state interactions and the possible ways to distinguish them from the true CP -violating effects.

What is not discussed?

- The nature of CP -violating phenomenological terms (Higgs, Leptoquarks, Supersymmetry, ...).
- The (model dependent) limits to CP -odd asymmetries at the energy scale of W^\pm/Z^0 mass, arising from low energy searches for CP - and T -violation.
- The dilution of asymmetries due to (strong/loose?) correlations of quarks' and antiquarks' polarizations to the polarizations of colliding protons.

Conclusion

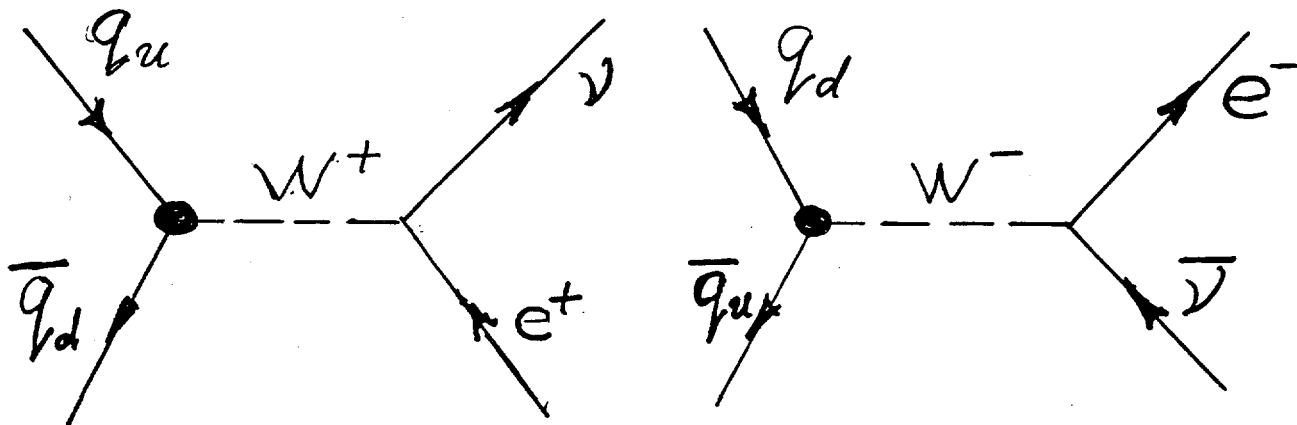
- (i) The measurement of T -odd correlations on the order of at least $\sim 10^{-2}$ is possible in polarized proton collisions at RHIC.
- (ii) The observation of nonzero T -odd correlations in $W^\pm \rightarrow e(\mu)\nu$ mode would be a strong indication of CP - and/or T -violation at about the weak coupling scale.

Issues to address in more details

- (i) RHIC sensitivity to the broken CP - and/or T -symmetries in both quark and lepton coupling sectors, including also hadron decay modes of W^\pm (and probably even Z^0 ?) bosons.
- (ii) Separation of "true" T -odd correlation from the "spurious" asymmetries.
- (iii) Systematic errors due to the experimental tolerances (spin alignment, etc)
- (iv) Predictions of various models as well as the limitations to CP - and/or T -violating asymmetries at RHIC energies, arising from the earlier accomplished experiments.
- (v) Search for other CP - and T -violating processes that might be potentially interesting for Spin Physics Program at RHIC.
- (vi) ... (???)

¹ Phone: (313)-577-2781; fax: (313)-577-0711; e-mail: rykov@physics.wayne.edu

If free polarized quarks could be collided at RHIC



Disclaimer: There is (almost?) no hope to measure at RHIC CP -violating asymmetries due to CP -odd phase in CKM-matrix.

T -odd correlations in $q\bar{q}$ C.M. system:

$$k \cdot [\zeta_q \times p] ; \quad k \cdot [\zeta_q \times p] ; \quad k \cdot [\zeta_q \times \zeta_{\bar{q}}].$$

p is momentum of quark ($p \equiv p_q$);

k is momentum of lepton ($k \equiv k_\nu$ or $k \equiv k_{e^-}$);

ζ_q is polarization of quark;

$\zeta_{\bar{q}}$ is polarization of antiquark.

At least one quark has to be transversely polarized.

Phenomenological interaction lagrangian:

(*G. L. Kane, G. A. Ladinsky, and C. P. Yuan, Phys.Rev. D45 (1992) 124*)

$$L = \frac{g}{\sqrt{2}} \{ [W_{\mu}^{-} \bar{q}_d \gamma^{\mu} (f_1^L P_- + f_1^R P_+) q_u + \text{h.c.}] - \frac{1}{M_W} [\partial_{\nu} W_{\mu}^{-} \bar{q}_d \sigma^{\mu\nu} (f_2^L P_- + f_2^R P_+) q_u + \text{h.c.}] + \frac{1}{M_W} [\partial^{\mu} W_{\mu}^{-} \bar{q}_d (f_3^L P_- + f_3^R P_+) q_u + \text{h.c.}] \}$$

where $P_{\pm} = \frac{1}{2}(1 \pm \gamma_5)$, $i\sigma^{\mu\nu} = -\frac{1}{2}(\gamma^{\mu}\gamma^{\nu} - \gamma^{\nu}\gamma^{\mu})$.

Using other notations,

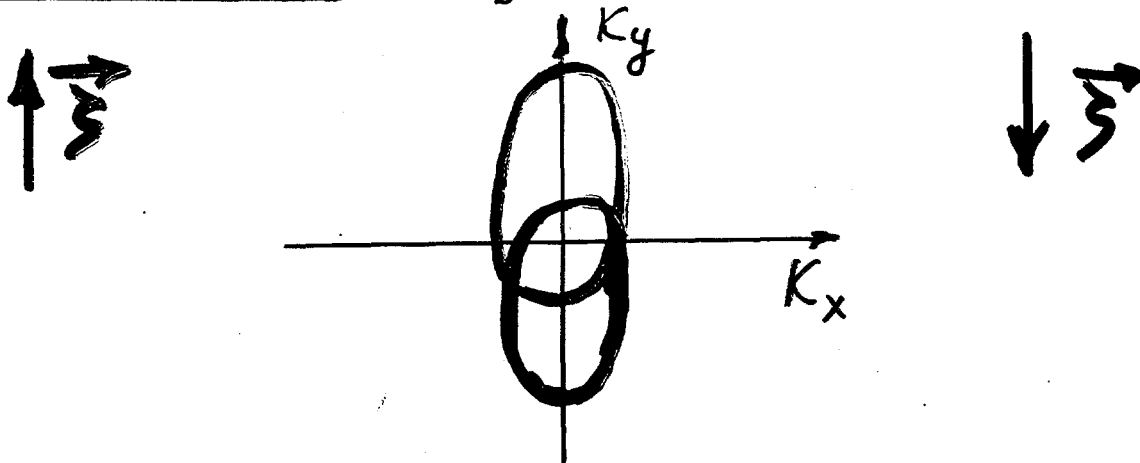
$$L = \frac{g'}{\sqrt{2}} \{ [W_{\mu}^{-} \bar{q}_d \gamma^{\mu} (1 - \eta \gamma_5) q_u + \text{h.c.}] + \dots \}$$

***CP*- and *T*-symmetries are broken if**

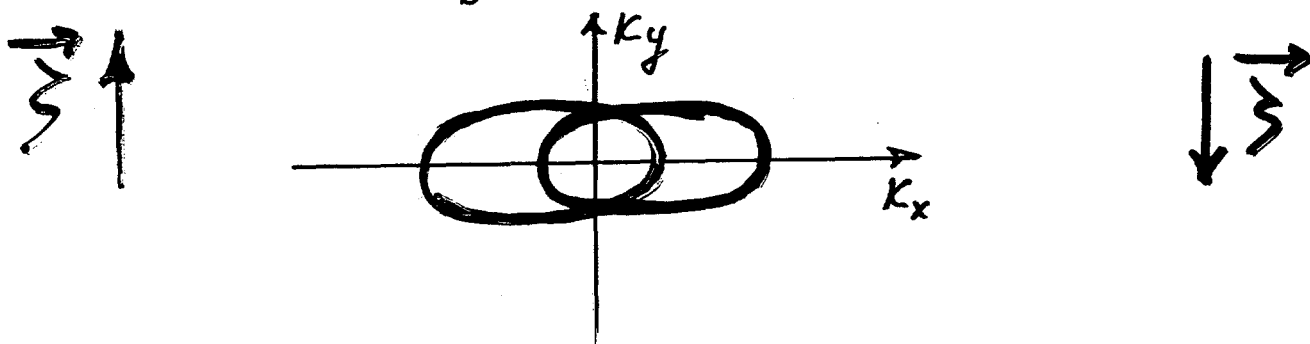
$$\text{Im}\{\eta\} \neq 0.$$

Single-spin asymmetries:

T-even (but P-odd): $A \propto \frac{M_q}{S} (\mathbf{k} \cdot \zeta)$



T-odd: $A \propto \text{Im}\{\eta\} \frac{M_q}{S^{3/2}} \mathbf{k} \cdot [\zeta \times \mathbf{p}]$



Small double-spin asymmetries:

T-even: $A \propto \frac{M_q^2}{S^2} (\zeta_q \cdot \mathbf{k})(\zeta_{\bar{q}} \cdot \mathbf{k})$

T-odd:

Both quarks transversely polarized:

$$A \propto \text{Im}\{\eta\} \frac{M_q^2}{S^{3/2}} \mathbf{k} \cdot [\zeta_q \times \zeta_{\bar{q}}]$$

One quark longitudinally polarized:

$$A \propto \text{Im}\{\eta\} \frac{M_q}{S} \mathbf{k} \cdot [\zeta_q \times \zeta_{\bar{q}}]$$

$$(1 - |\eta|^2) (\vec{\xi}_1 \cdot \vec{\xi}_2)$$

(Potentially) **Large double-spin asymmetries:**

Parallel spins

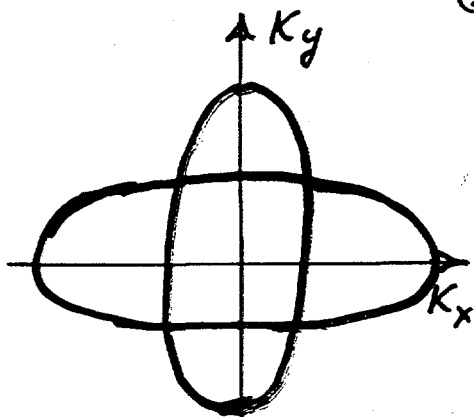


T-even:

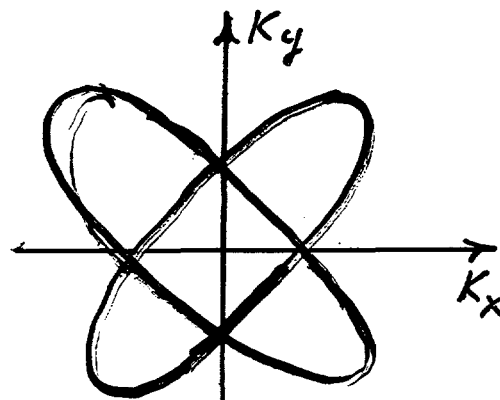
$$A \propto (1 - |\eta|^2) (\zeta_q \cdot k) (\zeta_{\bar{q}} \cdot k) / S$$



Perpendicular spins



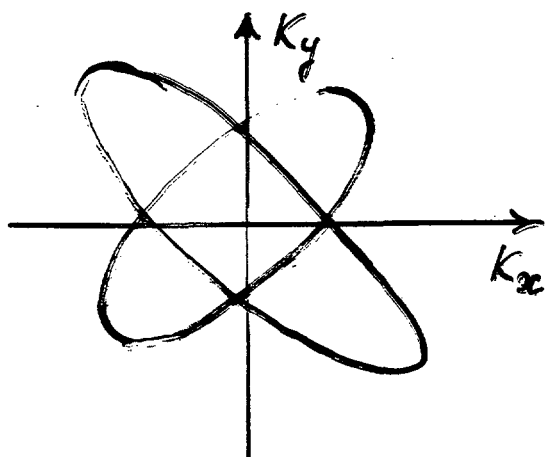
$$\pm \cos 2\varphi$$



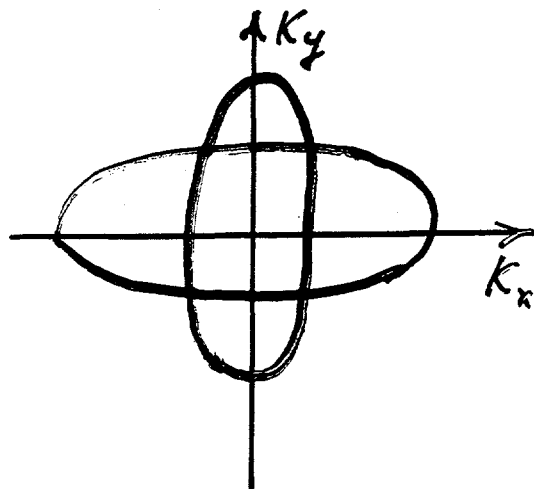
$$\pm \sin 2\varphi$$

T-odd:

$$A \propto \pm \text{Im}\{\eta\} \{ k \cdot [\zeta_q \times p] (\zeta_{\bar{q}} \cdot k) + k \cdot [\zeta_{\bar{q}} \times p] (\zeta_q \cdot k) \} / S^{3/2}$$

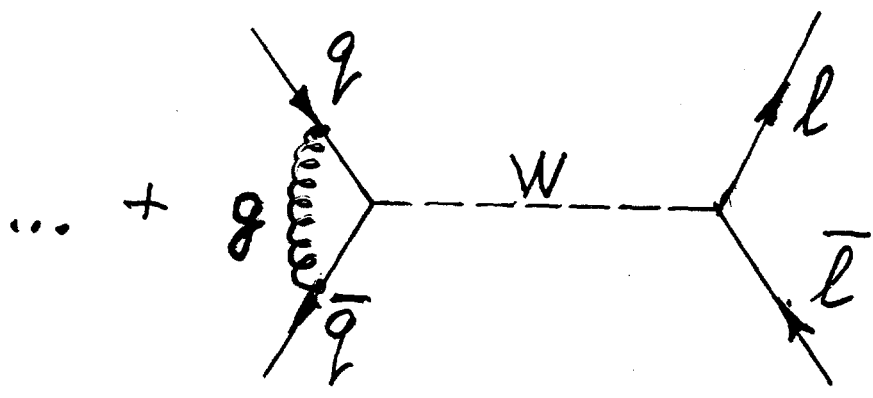


$$\pm \sin 2\varphi$$



$$\pm \cos 2\varphi$$

Spurious asymmetries

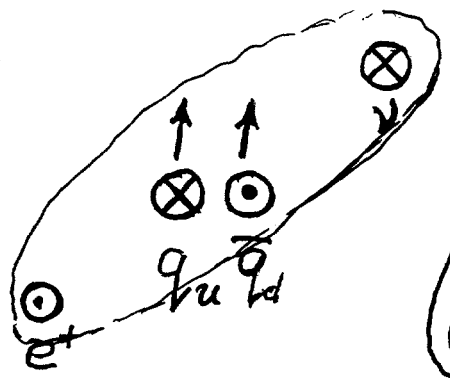


$$A_s \sim \alpha_s \frac{M_q}{\sqrt{s}} \lesssim 10^{-2} \text{ for } u, d, s, c, b$$

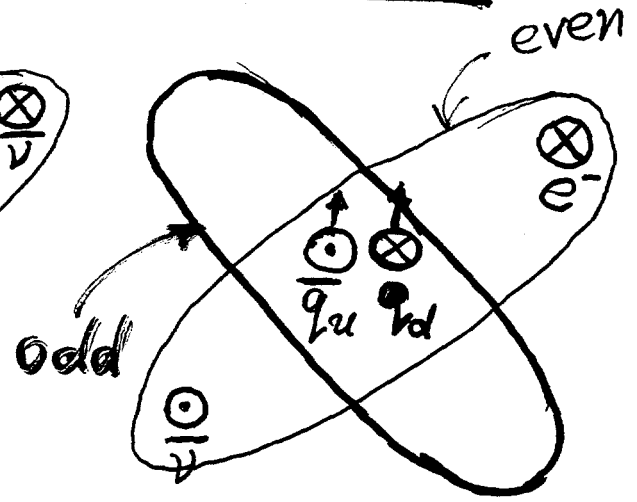
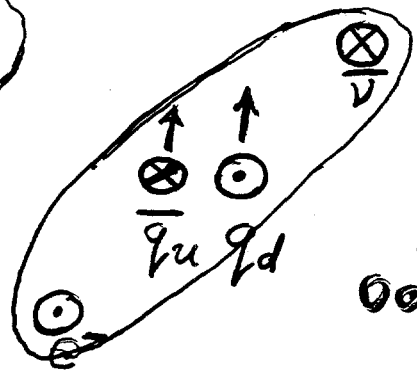
Is there any difference between "true" and "fake" asymmetry?

C

CP



$$+ \sin 2\phi$$



$$+ \sin 2\phi \quad \text{T-even}$$

$$- \sin 2\phi \quad \text{T-odd}$$

The Usefulness of Positivity in Spin Physics.

Jacques SOFFER¹

Centre de Physique Théorique

CNRS Luminy Case 907

13288 Marseille Cedex 09 France

We will emphasize the relevance of *positivity* in spin physics, which puts non-trivial model independent constraints on spin observables. These positivity conditions are based on the positivity properties of density matrix or Schwarz inequalities for transition matrix elements in processes involving several particles carrying a non-zero spin. We will illustrate this important point by means of several examples chosen in different areas of particle physics.

First we consider longitudinally and transversely polarized nucleon-nucleon total cross sections, which involve three observables σ_{tot} , $\Delta\sigma_T$ and $\Delta\sigma_L$. Positivity leads to the following non-trivial inequality among them, $|\Delta\sigma_T| \leq \sigma_{tot} + \Delta\sigma_L/2$, fulfilled by low energy data. In polarized Deep-Inelastic scattering (DIS), we recall the positivity bound on the A_2 asymmetry, namely $|A_2| \leq \sqrt{R}$, where R is the usual ratio σ_L/σ_T . Given the small value of R , A_2 is expected to be not very large and, indeed, recent data from E143 at SLAC and SMC at CERN, do satisfy this condition. Next let us turn to some considerations on the gluon distributions (GD). In addition to the two familiar GD, $G(x)$ and $\Delta G(x)$, off-shell gluons generate a longitudinal GD, denoted by $G_L(x)$ and a transverse GD, denoted by $\Delta G_T(x)$. Positivity provides an upper bound on $\Delta G_T(x)$ in complete analogy with the previous case, which can be turned into a lower bound for $G_L(x)$. Another interesting case is that of a two-body exclusive reaction with spin-1/2 particles, i.e. $NN \rightarrow NN$, $p\bar{p} \rightarrow \Lambda\bar{\Lambda}$, etc... One can prove the existence of many quadratic relations among the spin observables and when some of them are not measured, one gets non-trivial inequalities. As an example, in $p\bar{p} \rightarrow \Lambda\bar{\Lambda}$ from the existing data on A_{LL} one can exclude a large value for D_{NN} at large angles. Returning to inclusive production, if we consider a reaction of the type $spin1/2 + spinless \rightarrow spin1/2 + anything$, which is described in terms of seven spin observables, one can derive several positivity conditions. Finally, the positivity properties of the *forward* quark-nucleon elastic amplitude led to a non-trivial bound for the quark chiral-odd distribution $h_1^q(x, Q^2)$, namely, $2|h_1^q(x, Q^2)| \leq q(x, Q^2) + \Delta q(x, Q^2)$, which is not affected by QCD corrections. This positivity bound can be generalized to the case of *off-forward* parton distributions and lead to new interesting constraints, very useful in the small x -region.

¹E-MAIL: SOFFER@CPT.UNIV-MRS.FR

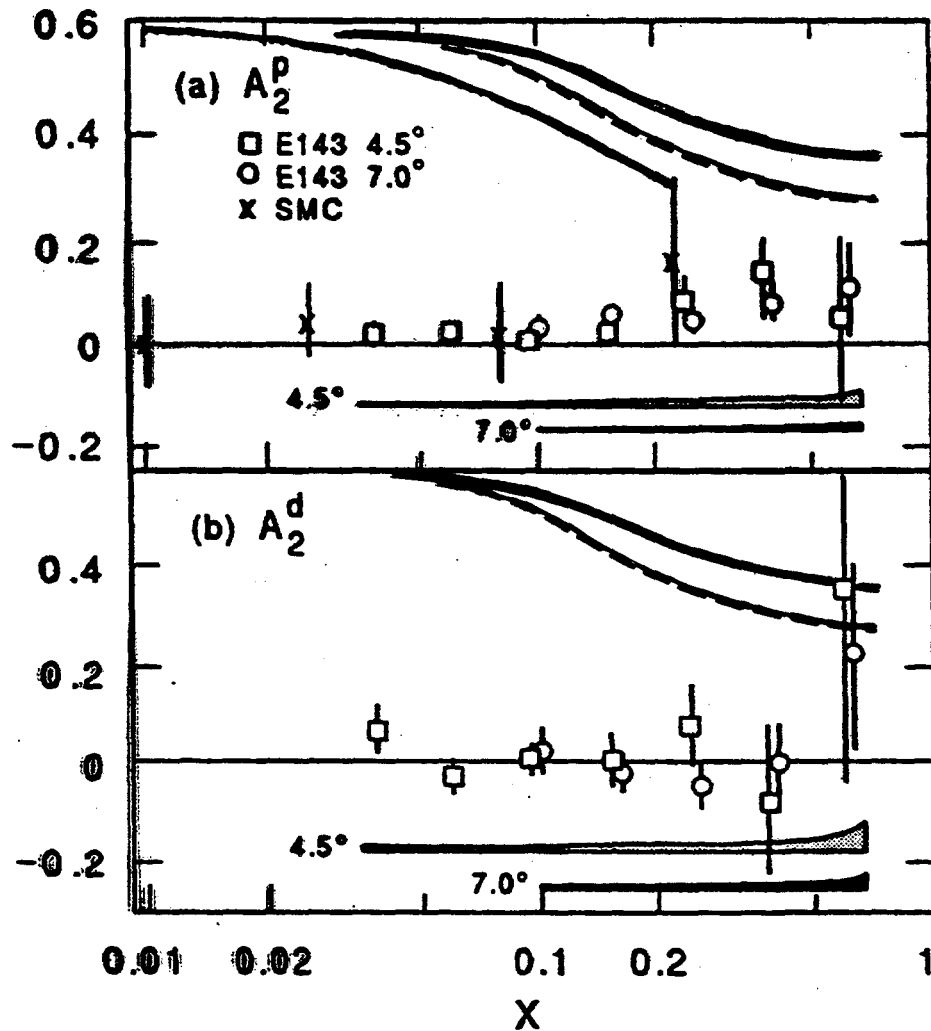


FIG. 1. Measurements for (a) A_2^p and (b) A_2^d from E143 (two data sets) and SMC as a function of x . Systematic errors are indicated by bands. The curves show the \sqrt{R} [22] positivity constraints. The solid, dashed, and dotted curves correspond to the 4.5° E143, 7.0° E143, and SMC kinematics, respectively. Overlapping data have been shifted slightly in x to make errors clearly visible.

$$|A_2| \leq \sqrt{R}$$

3. LONGITUDINAL GLUON DISTRIBUTION

(J.S. AND O. TERYAEV, PHYS. LETT. B419 (1998) 400)

IN ADDITION TO THE TWO FAMILIAR GLUON DISTRIBUTIONS $G(x)$ AND $\Delta G(x)$, OFF-SHELL GLUONS GENERATE A LONGITUDINAL G.D. AND A TRANSVERSE G.D.

CONSIDER THE LIGHT-CONE GLUON MATRIX DENSITY

$$\int \frac{dz}{2\pi} e^{izx} \langle p, s | A^j(0) A^{\sigma}(z) | p, s \rangle$$

$$\sim \frac{1}{2} \left(\frac{e^j e^{\sigma}}{1T} + \frac{e^{\sigma} e^j}{2T} \right) G(x) + \frac{i}{2} \left(\frac{e^j e^{\sigma}}{1T} - \frac{e^{\sigma} e^j}{2T} \right) \Delta G(x)$$

$$+ \frac{i}{2} \left(\frac{e^j e^{\sigma}}{1T} - \frac{e^{\sigma} e^j}{L} \right) \Delta G_T(x) + \frac{e^j e^{\sigma}}{L} G_L(x)$$

↑
ANALOGOUS TO g_2 FOR QUARKS

FOR THE TWIST-TWO PART OF $\Delta G_T(x)$ WE HAVE A W-W "TYPE" RELATION (J.S. AND O. TERYAEV, PRD56 (1997) R1353)

$$\Delta G_T(x) = \int_x^1 \frac{\Delta G(z)}{z} dz$$

A SIMPLE ANALOGY BETWEEN $\gamma^* p \rightarrow \gamma^* p$

AND $G p \rightarrow G p$ LEADS TO THE FOLLOWING POSITIVITY CONSTRAINT

$$|\Delta G_T(x)| \leq \sqrt{\frac{1}{2} G(x) G_L(x)}$$

IF WE CONSIDER THAT $G(x)$ AND $\Delta G_T(x)$ ARE KNOWN WE CAN TURN THIS INEQUALITY INTO A LOWER BOUND FOR $G_L(x)$

$$G_L(x) \geq 2\lambda(x) G(x) \quad \lambda(x) = \left(\frac{\Delta G_T(x)}{G(x)} \right)^2$$

IN TWIST-TWO APPROXIMATION FOR $x \sim 0.1$, $z \sim 0.01$

$\Rightarrow G_L(x) \geq 0.3$ BUT LARGER FOR SMALLER x .

3. LONGITUDINAL GLUON DISTRIBUTION

(J.S. AND O. TERYAEV, PHYS. LETT. B419 (1998) 400)

IN ADDITION TO THE TWO FAMILIAR GLUON DISTRIBUTIONS $G(x)$ AND $\Delta G(x)$, OFF-SHELL GLUONS GENERATE A LONGITUDINAL G.D. AND A TRANSVERSE G.D.

CONSIDER THE LIGHT-CONE GLUON MATRIX DENSITY

$$\int \frac{dz}{2\pi} e^{izx} \langle \phi, S | A^S(0) A^S(2n) | \phi, S \rangle$$

$$\sim \frac{1}{2} \left(e_{IT}^S e_{IT}^S + e_{2T}^S e_{2T}^S \right) G(x) + \frac{i}{2} \left(e_{IT}^S e_{IT}^S - e_{2T}^S e_{2T}^S \right) \Delta G(x)$$

$$+ \frac{i}{2} \left(e_{IT}^S e_L^S - e_L^S e_{IT}^S \right) \Delta G_T(x) + e_L^S e_L^S G_L(x)$$

↑
ANALOGOUS TO \int_2 FOR QUARKS

FOR THE TWIST-TWO PART OF $\Delta G_T(x)$ WE HAVE A W-W "TYPE" RELATION (J.S. AND O. TERYAEV, PRD 56 (1997) R1353)

$$\Delta G_T(x) = \int_x^1 \frac{\Delta G(z)}{z} dz$$

A SIMPLE ANALOGY BETWEEN $\gamma^* \phi \rightarrow \gamma^* \phi$ AND $G \phi \rightarrow G \phi$ LEADS TO THE FOLLOWING POSITIVITY CONSTRAINT

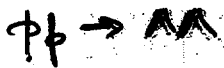
$$|\Delta G_T(x)| \leq \sqrt{\frac{1}{2} G(x) G_L(x)}$$

IF WE CONSIDER THAT $G(x)$ AND $\Delta G_T(x)$ ARE KNOWN WE CAN TURN THIS INEQUALITY INTO A LOWER BOUND FOR $G_L(x)$

$$G_L(x) \geq 2\lambda(x) G(x) \quad \lambda(x) = \left(\frac{\Delta G_T(x)}{G(x)} \right)^2$$

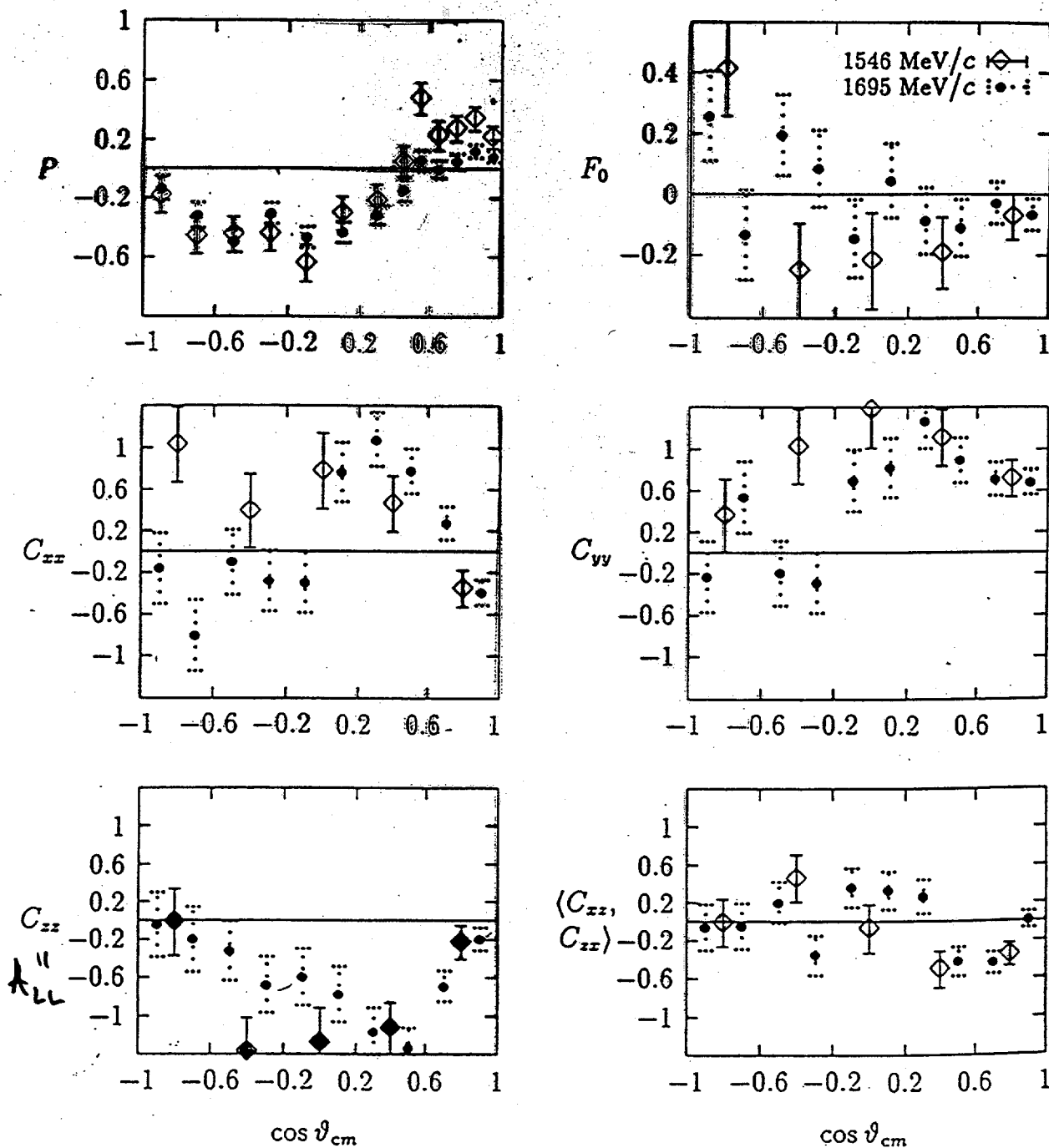
IN TWIST-TWO APPROXIMATION FOR $x \sim 0.1$, $z \sim 0.01$

$\Rightarrow G_L(x) \geq 0.3$ BUT LARGER FOR SMALLER x



$$A_{LL}^2 + \sum_{MN} \lambda_{MN}^2 \leq 1$$

J.-M. Richard / Physics Letters B 369 (1996) 358-361



1. Polarisation P , spin-singlet fraction F_0 , and spin-correlation coefficients C_{ij} for the reaction $\bar{p}p \rightarrow \bar{\Lambda}\Lambda$ at 1446 (open squares) and 1695 MeV/c (black dots). Data are from Ref. [2].

5. POSITIVITY CONSTRAINTS FOR $pp \rightarrow \Lambda X$
 (M.G. DONCEL and A. MENJEE, PHYS. LETT. 84 (1972) 83)

LET'S CONSIDER THREE TRANSVERSE SPIN OBSERVABLES

P_Λ Λ POLARIZATION

A_N ANALYZING POWER (OR LEFT-RIGHT ASYM.)

D_{NN} DEPOLARIZATION PARAMETER

POSITIVITY YIELDS THE FOLLOWING CONSTRAINTS WHICH MUST BE SATISFIED FOR ANY KINEMATIC POINT $(\sqrt{s}, p_T, \sqrt{s})$

$$\textcircled{1} \quad 1 + D_{NN} \geq |P_\Lambda + A_N|$$

$$\textcircled{2} \quad 1 - D_{NN} \geq |P_\Lambda - A_N|$$

GIVEN D_{NN} ONE CAN FIND THE ALLOWED REGION IN THE PLANE P_Λ, A_N (AND VICE VERSA)

SEE GRAPHS FOR THREE VALUES $D_{NN} = 0, 1/3, 1/2$
 FOR $D_{NN} < 0$ SAME REGION BUT MUST EXCHANGE P_Λ AND A_N . IF $D_{NN} \rightarrow 1 \Rightarrow P_\Lambda$ AND $A_N \rightarrow 0$

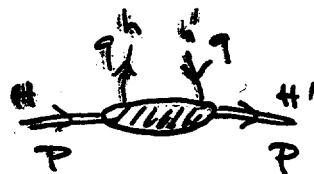
E704 SATISFIES POSITIVITY

FOR EXAMPLE AT $p_T \sim 1.6 \text{ GeV}/c$

$D_{NN} \sim 1/3$ AND THEY HAVE $A_N \sim -10\%$, $P_\Lambda \sim -30\%$

6. POSITIVITY CONSTRAINTS FOR FORWARD PARTON DISTRIBUTIONS

LET'S CONSIDER THE THREE FORWARD QUARK DISTRIBUTIONS



$$q(x), \Delta q(x), h_1^q(x)$$

WHICH CAN BE RELATED TO THE FORWARD QUARK-NUCLEON ELASTIC AMPLITUDE

$$q_{h'}(q) + N_H(P) \rightarrow q_h(q) + N_{H'}(P)$$

h_1^q CORRESPONDS TO $H=h'=+1/2, H'=h=-1/2$

LET'S USE THE MATRIX ELEMENTS

$$a_x^{H,h}(P,q) = \langle N_H(P) | 0 | q_h(q), x \rangle$$

ONE CAN SHOW THAT

$$q_+(x) \equiv \frac{1}{2} (q(x) + \Delta q(x))$$

$$= \frac{1}{2} \sum_x (|a_x^{+,+}|^2 + |a_x^{-,-}|^2)$$

$$h_1^q(x) = \frac{1}{2} \sum_x [(a_x^{+,+})^* (a_x^{-,-}) + (a_x^{+,+}) (a_x^{-,-})^*]$$

SCHWARZ INEQUALITY LEADS IMMEDIATELY TO

$$2|h_1^q(x)| < q(x) + \Delta q(x)$$

(J.S. PHYS. REV. LETT. 74 (1995) 1292)

STRONGER THAN THE TRIVIAL ONE $|h_1^q(x)| \leq q(x)$

THIS SIMPLE RESULT IS NOT AFFECTED BY QCD CORRECTIONS UP TO NLO

(W. VOGELSANG, PHYS. REV. D 57 (1998) 1886 ;

C. BOURRELY, J.S., O. TERYAEV, PHYS. LETT. B 420 (1998) 375)

Transversity and polarized Drell-Yan at RHIC

W. Vogelsang

Theory Division, CERN, CH-1211 Geneva 23, Switzerland

The transversity densities $\Delta_{Tq}(x, Q^2)$ are the only completely unknown twist-2 parton distribution functions of the nucleon. In a transversely polarized nucleon they count the number of quarks with spin parallel to the nucleon spin minus the number of quarks with anti-aligned spin. In field theory the transversity distributions are defined in terms of expectation values of chirally-odd operators between nucleon states, which is the reason why they cannot be measured in inclusive DIS. The most promising hard process allowed by this chirality selection rule seems to be Drell-Yan dimuon production, and exactly this reaction will be utilized for attempting a first measurement of the $\Delta_{Tq}(x, Q^2)$ at RHIC via the transverse double spin asymmetry $A_{TT} = d\Delta_{T\sigma}/d\sigma$. In perturbative QCD, A_{TT} can be expressed in terms of unpolarized parton distributions, the yet unknown transversity densities, and the relevant partonic cross sections. Although the latter have been known to NLO accuracy in the strong coupling for several years by now, consistent NLO calculations of A_{TT} for Drell-Yan became possible only recently, when the two-loop transversity splitting functions became available.

The unpolarized, longitudinally and transversely polarized quark distributions ($q, \Delta q, \Delta_{Tq}$) of the nucleon are expected to obey an inequality derived by Soffer:

$$2|\Delta_{Tq}(x, Q^2)| \leq q(x, Q^2) + \Delta q(x, Q^2),$$

which can be used to constrain the Δ_{Tq} when trying to make predictions for RHIC. We will first show numerically that Soffer's inequality is preserved under NLO QCD evolution to $Q^2 > Q_0^2$ once it is satisfied at the input scale Q_0 . Our aim will then be to estimate, within LO and NLO, upper bounds on A_{TT} for the Drell-Yan process at RHIC. To do so, we will assume the validity of Soffer's inequality, which seems reasonable and is corroborated by our finding that NLO evolution preserves the inequality. The maximal asymmetry A_{TT} can then be estimated by further assuming *saturation* of the Soffer bound.

For further details of the work presented here, see: O. Martin, A. Schäfer, M. Stratmann, W. Vogelsang, Soffer's inequality and the transversely polarized Drell-Yan process at next-to-leading order, Phys. Rev. **D57** (1998) 3084.

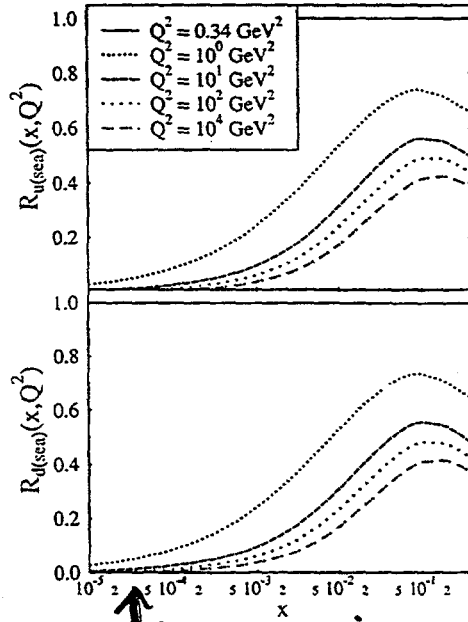
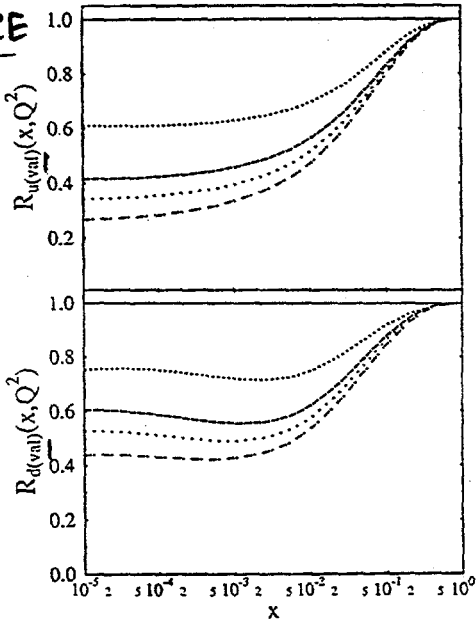
"Radiative Parton Model"

assume

$$\Delta_T q \equiv \frac{1}{2} [q + \Delta q] \text{ at } Q = \mu \approx 0.6 \text{ GeV}$$

Then:

VALENCE



Martin,
Schäfer,
Stratmann,
u.v.

[MS]

SI remains intact!

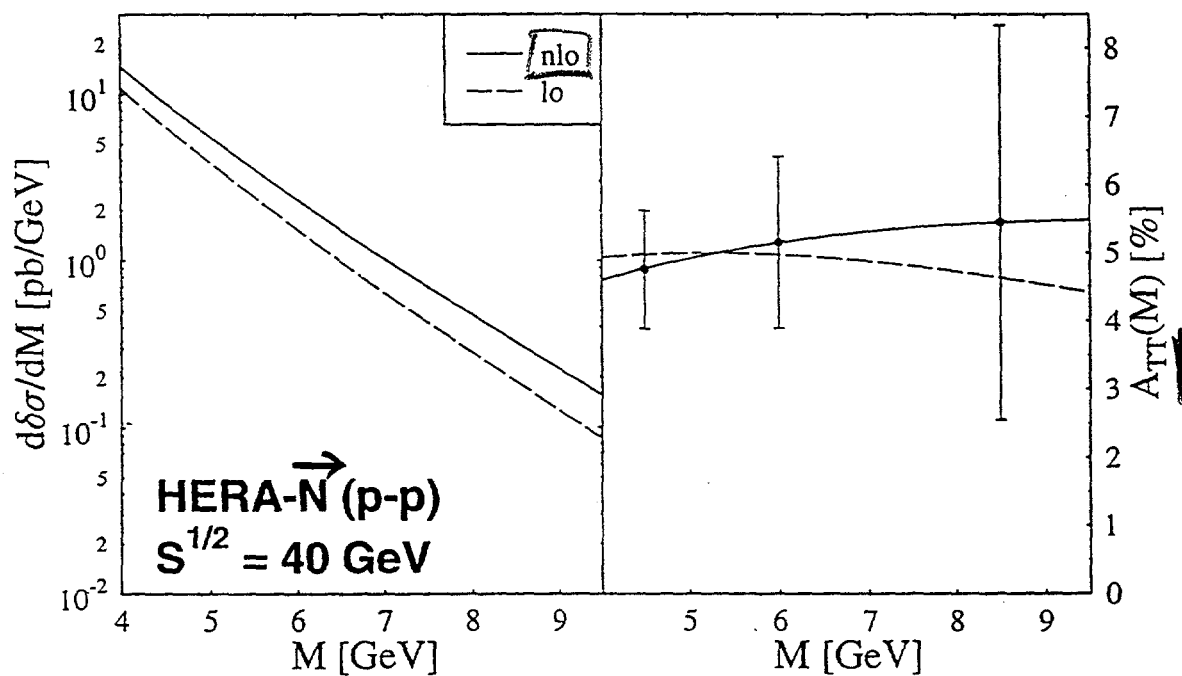
↑ Suppression at small x!

$$R_q \equiv \frac{|\Delta_T q(x, Q^2)|}{\frac{1}{2} (q(x, Q^2) + \Delta q(x, Q^2))}$$

(→ good constraint for NLO input densities)

$$\Delta_T q(x, \mu^2) \equiv \frac{1}{2} [q(x, \mu^2) + \Delta q(x, \mu^2)]$$

⇒ "upper bounds" on A_{TT}
(within radiative PM)



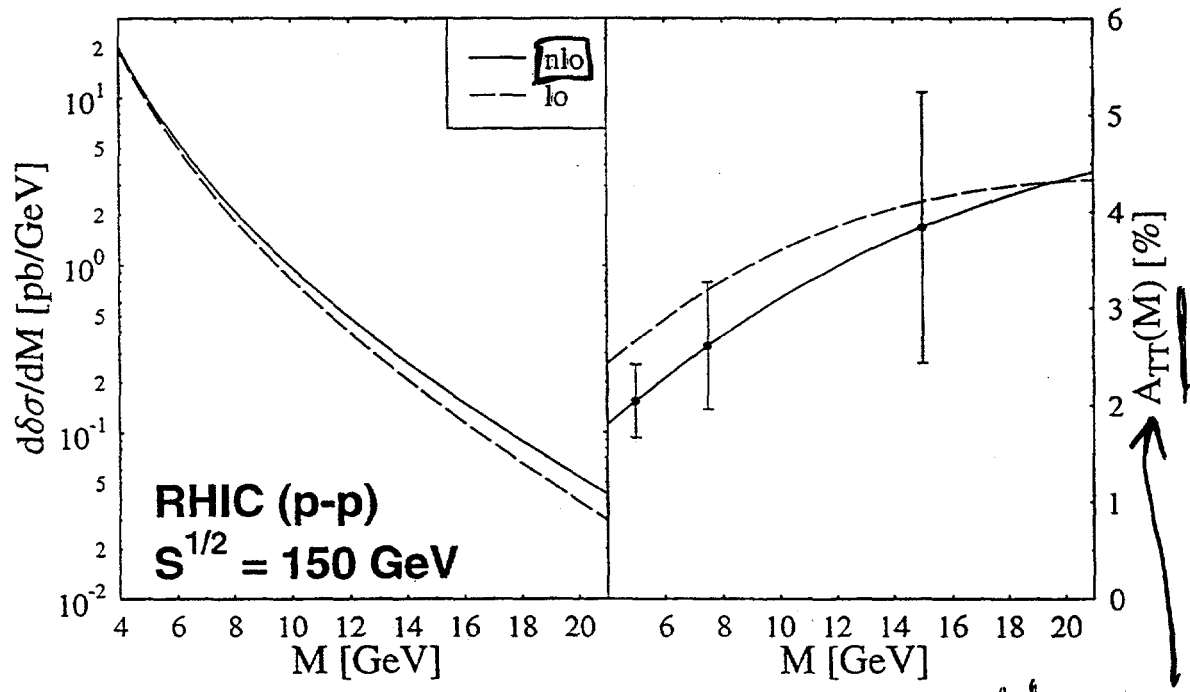
Martin,
Schäfer,
Stratmann,
W.V.

errors for $\mathcal{L} = 240 \text{ Pb}^{-1}$

$\sim \cos(2\phi)$

FOR $\Delta_T \neq 0$: INTEGRATE

$$\left[\int_{-\pi/4}^{\pi/4} - \int_{\pi/4}^{3\pi/4} + \int_{3\pi/4}^{5\pi/4} - \int_{5\pi/4}^{7\pi/4} \right] d\phi$$

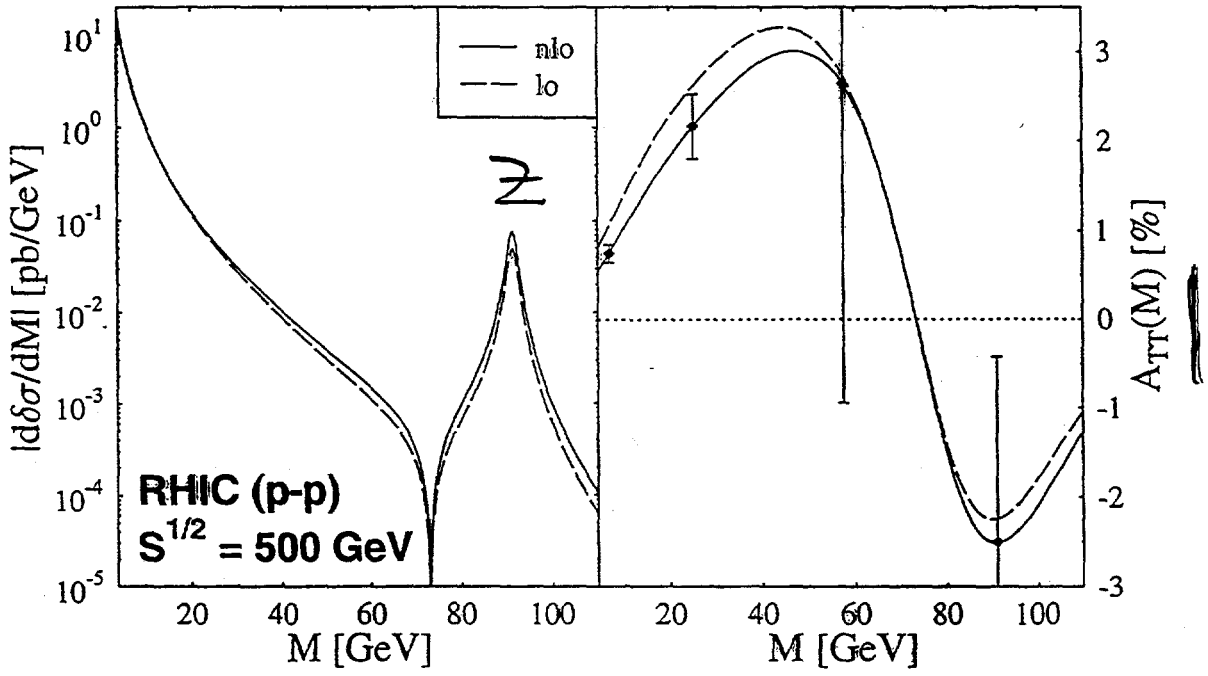


MARTIN, SCHÄFER, STRATMANN W.V.

$\mathcal{L} = 240 \text{ pb}^{-1}$

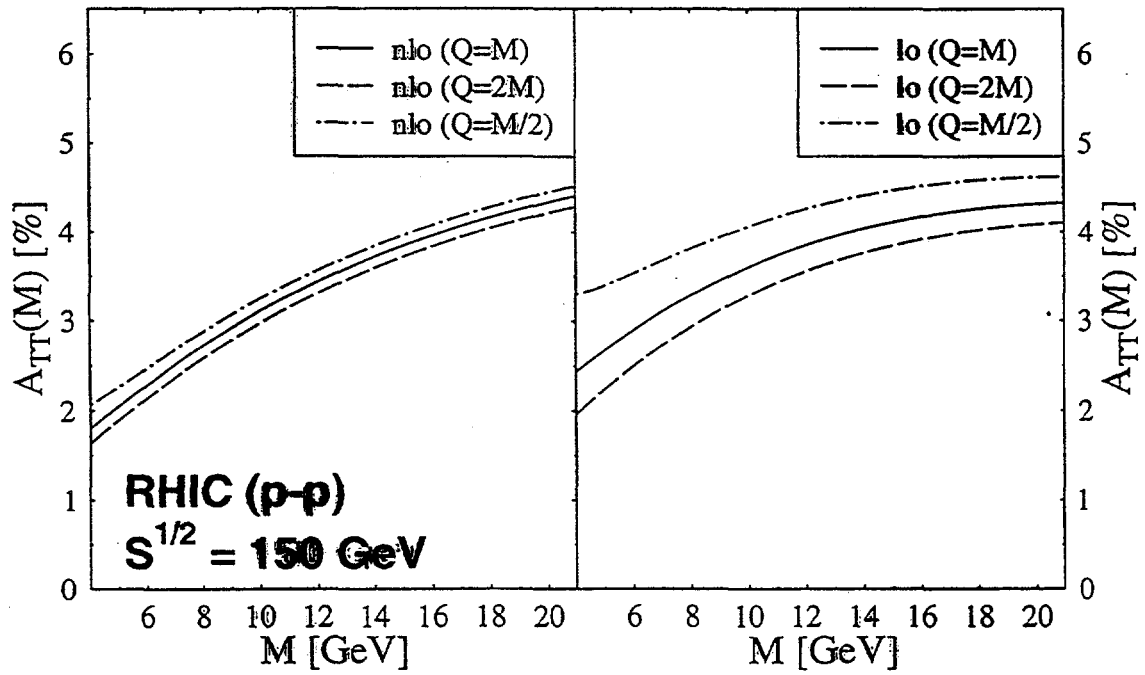
WOULD BE SMALL & NEG. FOR $\Delta_T = \Delta_T q$ at μ

→ NLO CORRECTIONS NON-NEGLECTIBLE



$\mathcal{L} = 800 \text{ pb}^{-1}$

Scale dependence: LO/NLO



Studies of transversity distributions at RHIC

S. Hino, M. Hirai, S. Kumano, and M. Miyama

Department of Physics

Saga University

Saga 840-8502

JAPAN

ABSTRACT

We explain our studies on transversity distributions. First, Q^2 evolution for the transversity distributions is discussed. It is given by a single integrodifferential equation without coupling to the gluon distribution. Dividing the variables x and Q^2 into small steps, we solve the integrodifferential equation by the Euler method in the variable Q^2 and by the Simpson method in the variable x . We provide a FORTRAN program for the Q^2 evolution and devolution of the transversity distribution $\Delta_T q$. Using the program, we show the LO and NLO evolution results of the valence-quark distribution $\Delta_T u_v + \Delta_T d_v$ and the singlet distribution $\sum_i (\Delta_T q_i + \Delta_T \bar{q}_i)$. Because the evolution results are very different from the longitudinal ones, the measurement of the transversity distributions could be an important test of perturbative QCD. Next, we consider a flavor asymmetry distribution $\Delta_T \bar{u} - \Delta_T \bar{d}$. There is a finite contribution to $\Delta_T \bar{u} - \Delta_T \bar{d}$ in perturbative QCD; however, it is rather a small effect. If a significant amount of the flavor asymmetry is found by future experiments, it is likely due to a nonperturbative mechanism. Using a theoretical model, in particular the Pauli blocking model, for explaining the unpolarized asymmetry $\bar{u} - \bar{d}$, we show the flavor asymmetric transversity distribution $\Delta_T \bar{u}(x) - \Delta_T \bar{d}(x)$. Then, we discuss its Q^2 dependence and its effects on the spin asymmetries at RHIC.

Studies of transversity distributions at RHIC

S. Hino, M. Hirai, S. Kumano, M. Miyama

Department of Physics
Saga University

Email: kumanos@cc.saga-u.ac.jp

<http://www.cc.saga-u.ac.jp/saga-u/riko/physics/quantum1/structure.html>

References

- Phys. Rev. D56 (1997) 2504.
- Comput. Phys. Commun. 108 (1998) 38.
- hep-ph/9712410, in press.
- research in progress.

April 29, 1998
RHIC-Spin, BNL

for transversity distributions

“nonsinglet type”

$$\frac{\partial}{\partial(\ln Q^2)} \Delta_{Tq}(x, Q^2) = \frac{\alpha_s}{2\pi} \int_x^1 \frac{dy}{y} \Delta_{TP}\left(\frac{x}{y}\right) \Delta_{Tq}(y, Q^2)$$

Numerical solution

x \longrightarrow divided into $2N_x$ steps

$t = \ln Q^2$ \longrightarrow divided into N_t steps

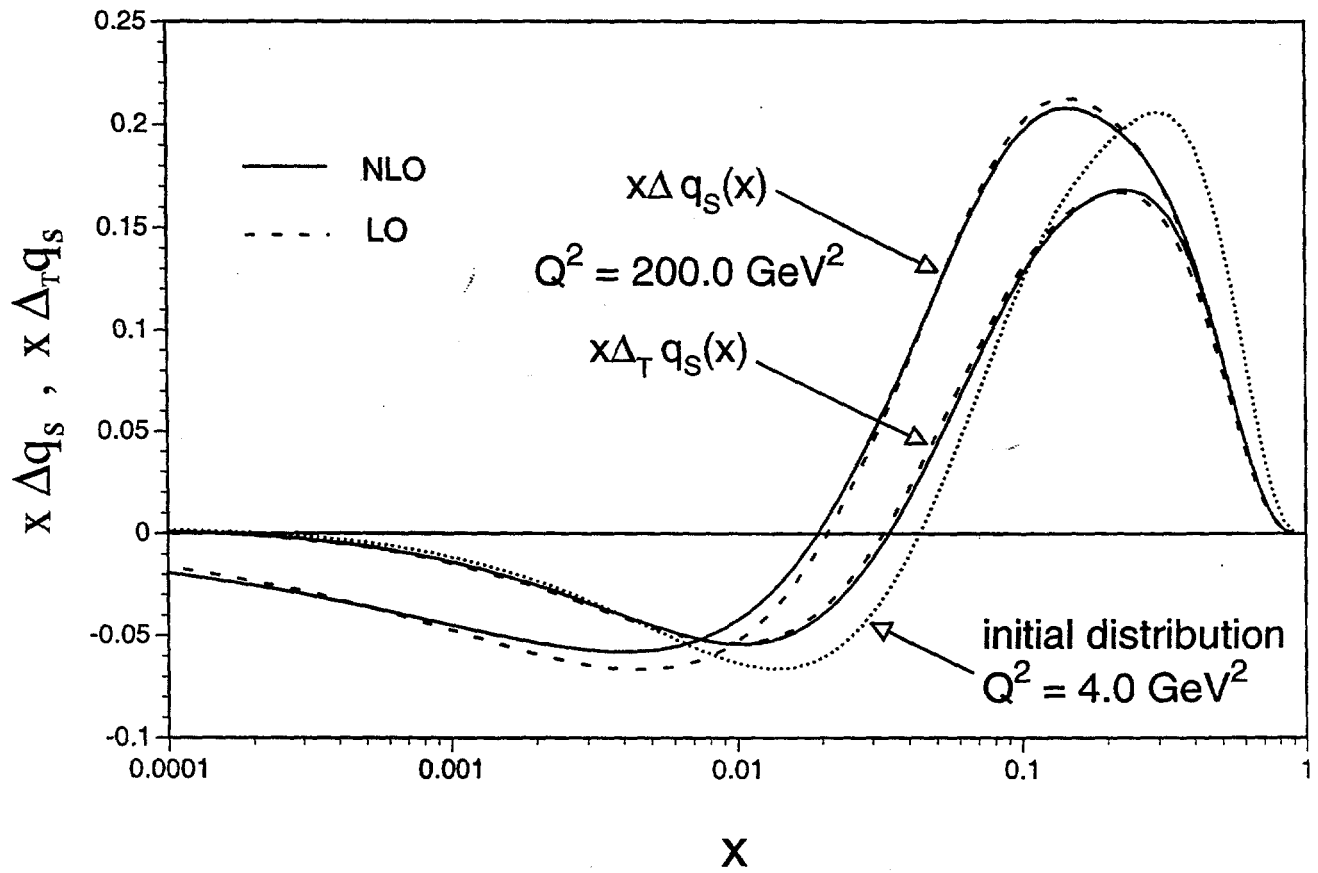
$$\frac{\partial}{\partial t} f(x, t) \Rightarrow \frac{f(x_i, t_{j+1}) - f(x_i, t_j)}{\delta t}$$

$$\int dz f(z) \Rightarrow \sum_{k=2,4,\dots}^{2N_x} \frac{\delta z}{3} [f(z_{k-1}) + 4f(z_k) + f(z_{k+1})]$$

see hep-ph/9712410

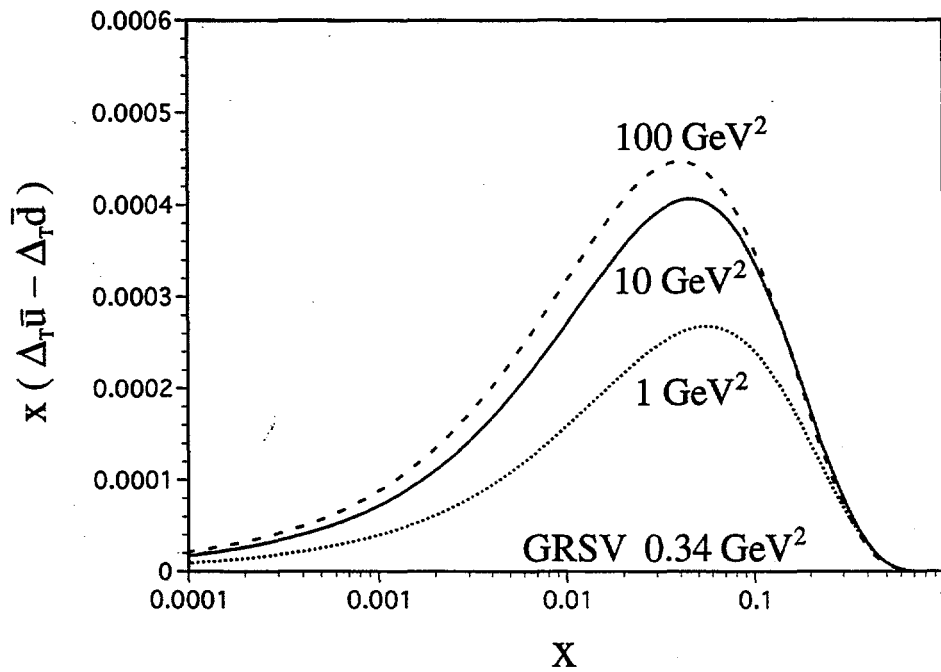
**Our evolution program could be
obtained upon email request.**

Q^2 evolution of longitudinally polarized and transversity distributions

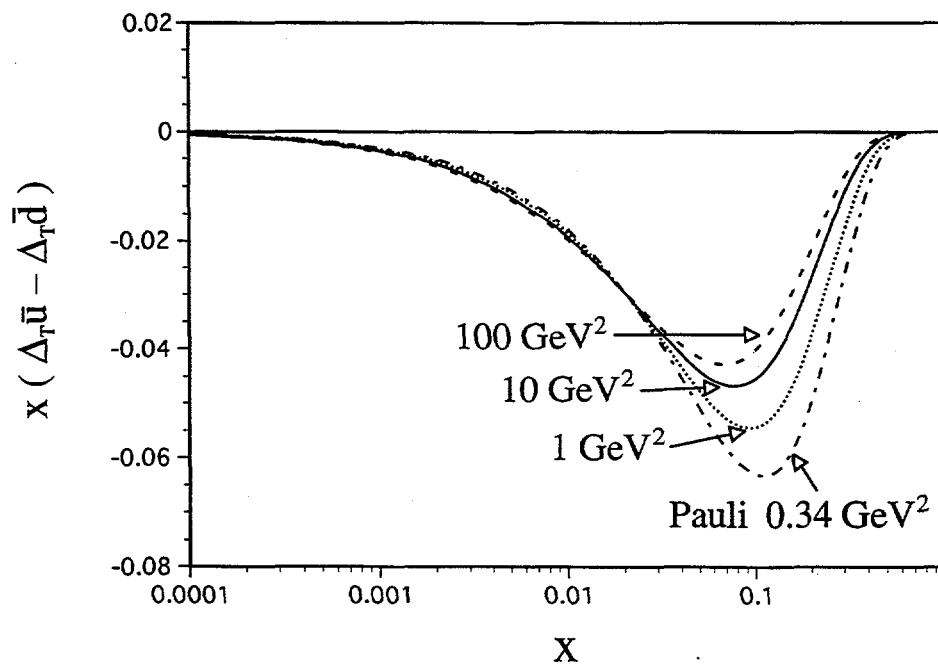


Q^2 dependence of $\Delta_T \bar{u} - \Delta_T \bar{d}$

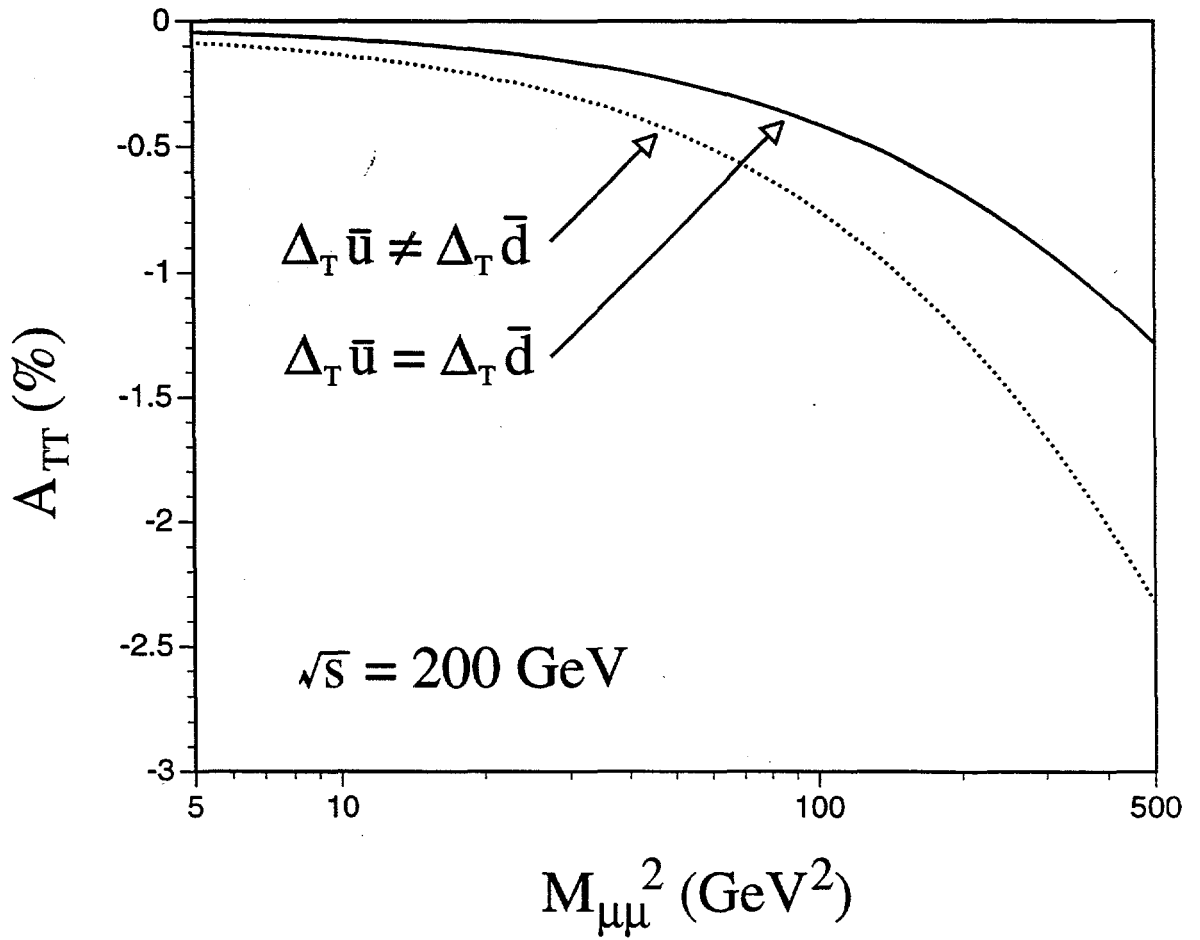
initial $(\Delta_T \bar{u} - \Delta_T \bar{d})_{GRSV} = 0$ at $Q^2 = 0.34 \text{ GeV}^2$



initial $(\Delta_T \bar{u} - \Delta_T \bar{d})_{Pauli} \neq 0$ at $Q^2 = 0.34 \text{ GeV}^2$



Transverse spin asymmetry



RHIC
Workshop
'98

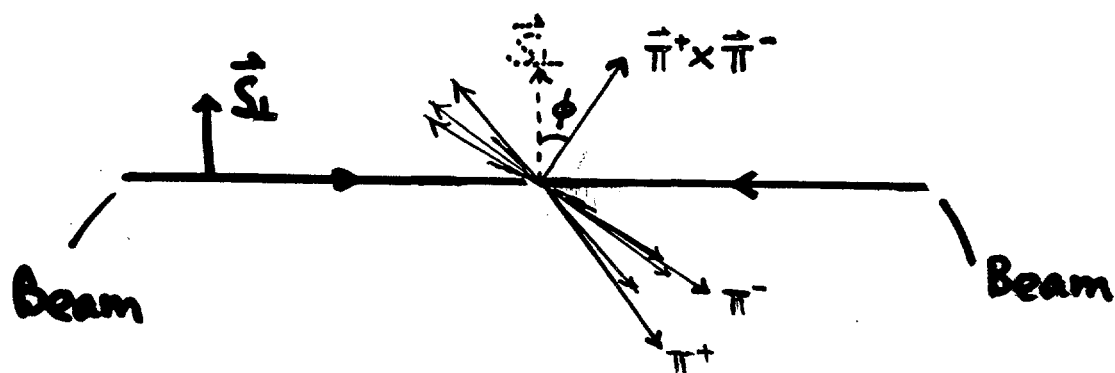
**PROBING THE NUCLEON'S TRANSVERSITY
VIA TWO-PION PRODUCTION AT RHIC**

Jian Tang

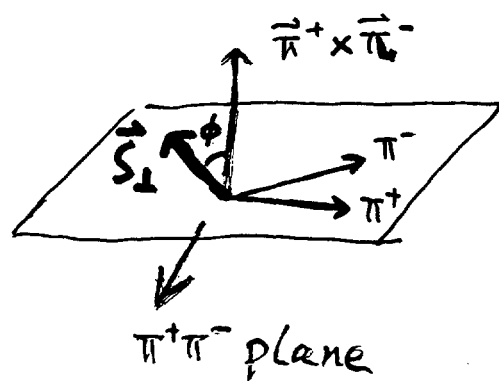
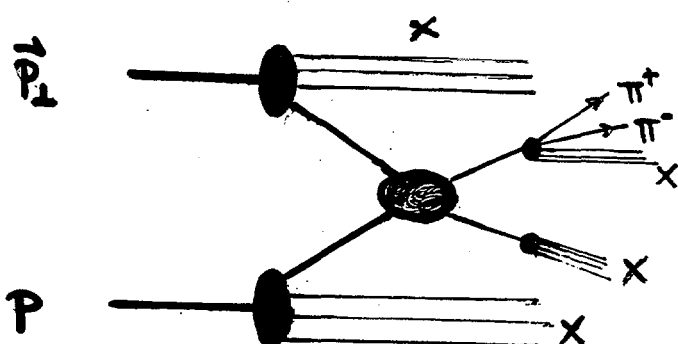
MIT

Collaborators: R. L. Jaffe, Xuemin Jin

The result



At partonic level



observable:

$$\vec{\pi}^+ \times \vec{\pi}^- \cdot \vec{S}_\perp$$

Nucleon's
polarization

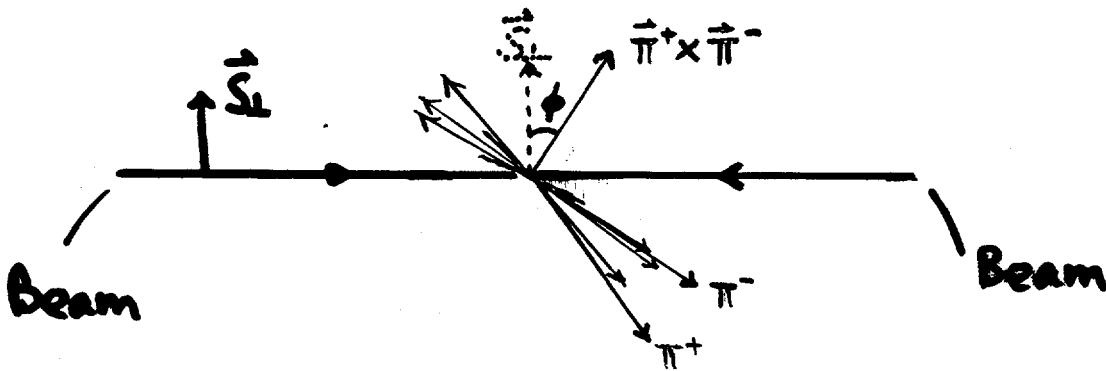
$$\propto \cos \phi$$

collins
angle

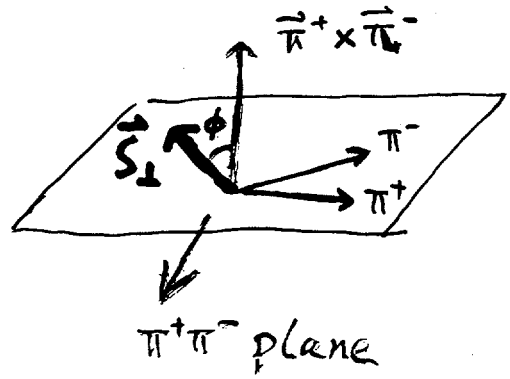
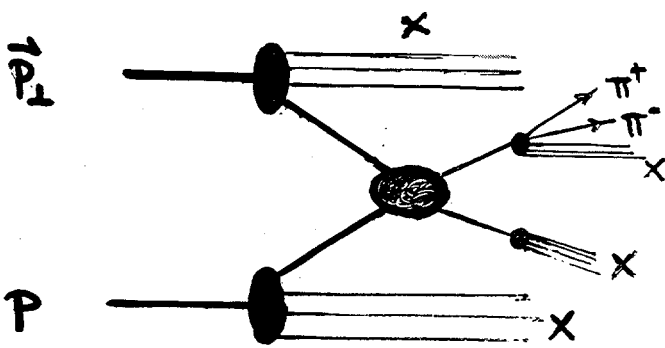
Pion momentum

The result

$$\vec{P}_\perp P \rightarrow \pi^+ \pi^- X$$



At partonic level



observable:

$$\vec{\pi}^+ \times \vec{\pi}^- \cdot \vec{S}_\perp$$

Nucleon's polarization

$$\propto \cos \phi$$

Pion momentum

collins angle

An asymmetry

$$A_{\perp T} \equiv \frac{d\sigma_{\perp} - d\sigma_{\parallel}}{d\sigma_{\perp} + d\sigma_{\parallel}}$$

FSI phases

Collins angle $\propto \frac{\hat{\sigma}^+ \hat{\sigma}^-}{\hat{\pi}^+ \hat{\pi}^-} \hat{S}_{\perp}$

$$= -\frac{\sqrt{6}}{4} \pi \sin \delta_0 \sin \delta_1 \sin(\delta_0 - \delta_1) \cos \phi$$

$$\times \frac{\delta \hat{\sigma}_{\perp}^a}{\hat{\sigma}_{\perp}^a} \frac{\sum_a \delta \hat{\sigma}_{\perp}^a}{\sum_a \hat{\sigma}^a (\sin^2 \delta_0 \hat{\sigma}_0^a + \sin^2 \delta_1 \hat{\sigma}_1^a)}$$

Hard
process
asymmetry

$\hat{A}_{\perp T}$
for
 $g\bar{g} \rightarrow g\bar{g}$,
which is
dominant
here.

$\delta \hat{\sigma}^a$: Transversity

$\delta \hat{\sigma}_{\perp}^a$: unknown interference
fragmentation function

$\hat{\sigma}^a$: unpolarized quark distribution

$\hat{\sigma}_0^a$: "0" fragmentation function

$\hat{\sigma}_1^a$: "1" fragmentation

Suppressed dependences

$$\delta \hat{\sigma} \rightarrow \delta \hat{\sigma}(x, Q^2), \quad \delta \hat{\sigma}_{\perp}^a \rightarrow \delta \hat{\sigma}_{\perp}^a(z, Q^2, m^2)$$

$$\hat{\sigma} \rightarrow \hat{\sigma}(x, Q^2), \quad \hat{\sigma}_0^a, \hat{\sigma}_1^a \rightarrow \hat{\sigma}_0^a(z, Q^2), \hat{\sigma}_1^a(z, Q^2)$$

$$\delta_{0,1} \rightarrow \delta_{0,1}(m^2)$$

Advantages:

- Twist 2
- Abundant pions
- Crucial FSI are known (δ_0, δ_1)

An asymmetry

$$A_{\perp T} \equiv \frac{d\sigma_{\perp} - d\sigma_{\parallel}}{d\sigma_{\perp} + d\sigma_{\parallel}} \quad \text{FSI phases} \quad \text{Collins angle} \propto \frac{\hat{\sigma}_{\perp} - \hat{\sigma}_{\parallel}}{\hat{\sigma}_{\perp} + \hat{\sigma}_{\parallel}}$$

$$= -\frac{\sqrt{6}}{4}\pi \sin\delta_0 \sin\delta_1 \sin(\delta_0 - \delta_1) \cos\phi$$

$$\times \frac{\delta\hat{\sigma}_{\perp}}{\hat{\sigma}_{\perp}} \frac{\delta\hat{\sigma}_{\parallel}}{\hat{\sigma}_{\parallel}} \frac{\sum \delta f^a \delta \hat{g}_z^a}{\sum f^a (\sin^2\delta_0 \hat{g}_0^a + \sin^2\delta_1 \hat{g}_1^a)}$$

Hard
process
asymmetry

$\hat{A}_{\perp T}$
for
 $g g \rightarrow g g$,
which is
dominant
here.

δf^a : Transversity

$\delta \hat{g}_z^a$: unknown interference
fragmentation function

f^a : unpolarized quark distribution

\hat{g}_0^a : "0" fragmentation function

\hat{g}_1^a : "1" fragmentation \checkmark

Suppressed dependences

$$\delta f \rightarrow \delta f(x, Q^2), \quad \delta \hat{g}_z^a \rightarrow \delta \hat{g}_z^a(z, Q^2, m^2)$$

$$f \rightarrow f(x, Q^2), \quad \hat{g}_0, \hat{g}_1 \rightarrow \hat{g}_0(z, Q^2), \hat{g}_1(z, Q^2)$$

$$\delta_{0,1} \rightarrow \delta_{0,1}(m^2)$$

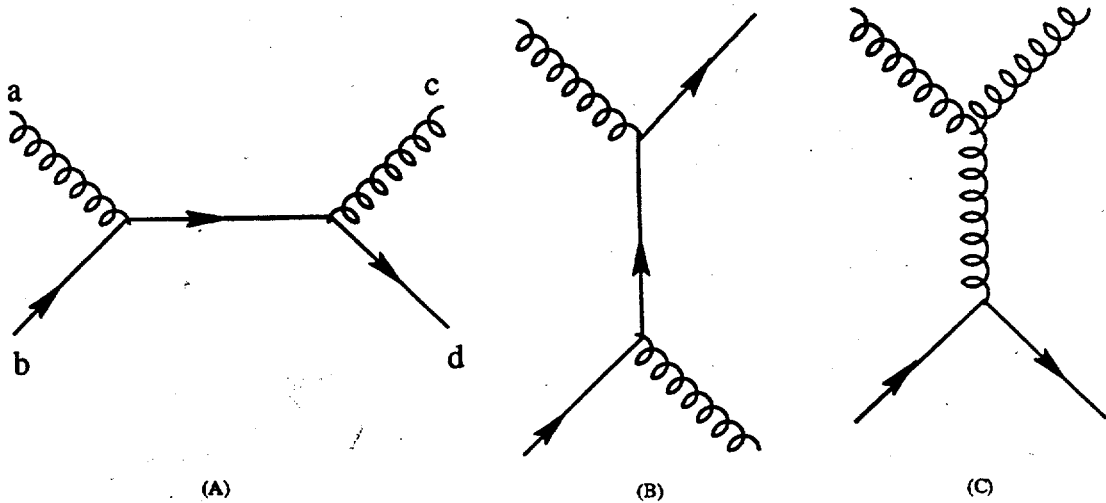
Advantages:

- Twist 2
- Abundant pions
- Crucial FSI are known (δ_0
 δ_1)

Parton process	Spin Average	Transversity Dependent
$ab \rightarrow cd$	Cross Section $-\sigma_{ab}^{cd}$	Cross Section $-\delta\sigma_{ab}^{cd}$
$qg \rightarrow qg$	$\frac{s^2 + \hat{u}^2}{\hat{t}^2} - \frac{4s^2 + \hat{u}^2}{9s\hat{u}}$	$\frac{s\hat{u}}{\hat{t}^2} - \frac{4}{9}$
$\bar{q}g \rightarrow \bar{q}g$	$\frac{s^2 + \hat{u}^2}{\hat{t}^2} - \frac{4s^2 + \hat{u}^2}{9s\hat{u}}$	$\frac{s\hat{u}}{\hat{t}^2} - \frac{4}{9}$
$qq \rightarrow qq$	$\frac{4}{9} \left(\frac{s^2 + \hat{u}^2}{\hat{t}^2} + \frac{s^2 + \hat{t}^2}{\hat{u}^2} \right) - \frac{8s^2}{27\hat{u}\hat{t}}$	$\frac{4s}{27\hat{t}} - \frac{4s\hat{u}}{9\hat{t}^2}$
$qq' \rightarrow qq'$	$\frac{4s^2 + \hat{u}^2}{9}$	$-\frac{4s\hat{u}}{9\hat{t}^2}$
$q\bar{q} \rightarrow q\bar{q}$	$\frac{4s^2 + \hat{u}^2}{9} + \frac{\hat{u}^2 + \hat{t}^2}{s^2} - \frac{8\hat{u}^2}{27s\hat{t}}$	$\frac{8\hat{u}}{27\hat{t}} - \frac{4s\hat{u}}{9\hat{t}^2}$
$q\bar{q}' \rightarrow q\bar{q}'$	$\frac{4s^2 + \hat{u}^2}{9}$	$-\frac{4s\hat{u}}{9\hat{t}^2}$

Where Each Entries multiplies factor $\pi\alpha_s^2/\hat{s}^2$

For example, $qg \rightarrow qg$



The dominance of $gg \rightarrow gg$ over other processes:

- From Hard cross section

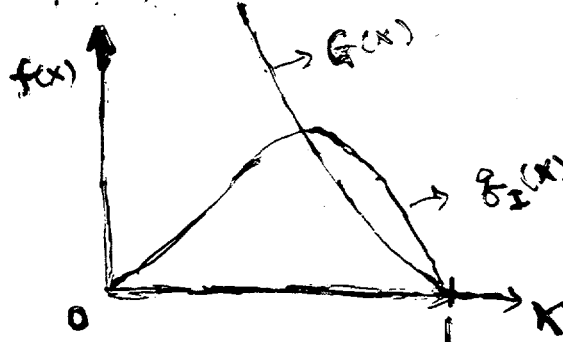
$$\hat{\sigma}_{2T}(gg \rightarrow gg) \sim -\frac{2}{5}$$

$$\hat{\sigma}_{1T}(gg \rightarrow gg) \sim \frac{2}{11}$$

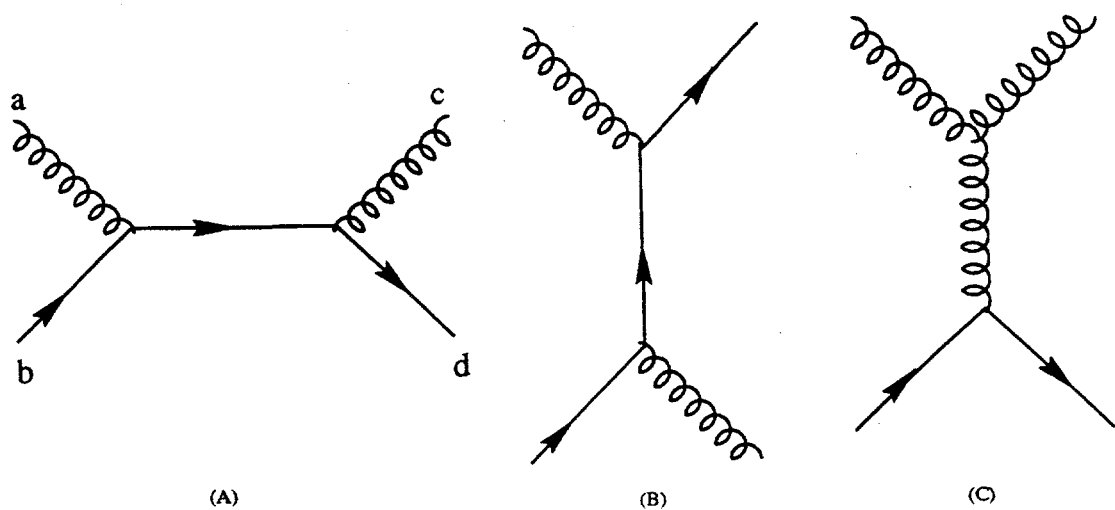
$$\text{at } \theta_{cm} = \frac{\pi}{2}$$

- From distribution

gluon dominates at small x



For example, $qg \rightarrow qg$



The dominance of $gg \rightarrow gg$ over other processes:

- From Hard cross section

$$\hat{\sigma}_{\text{LT}}(gg \rightarrow gg) \sim -\frac{2}{5}$$

$$\hat{\sigma}_{\text{LT}}(qg \rightarrow qg) \sim \frac{2}{11}$$

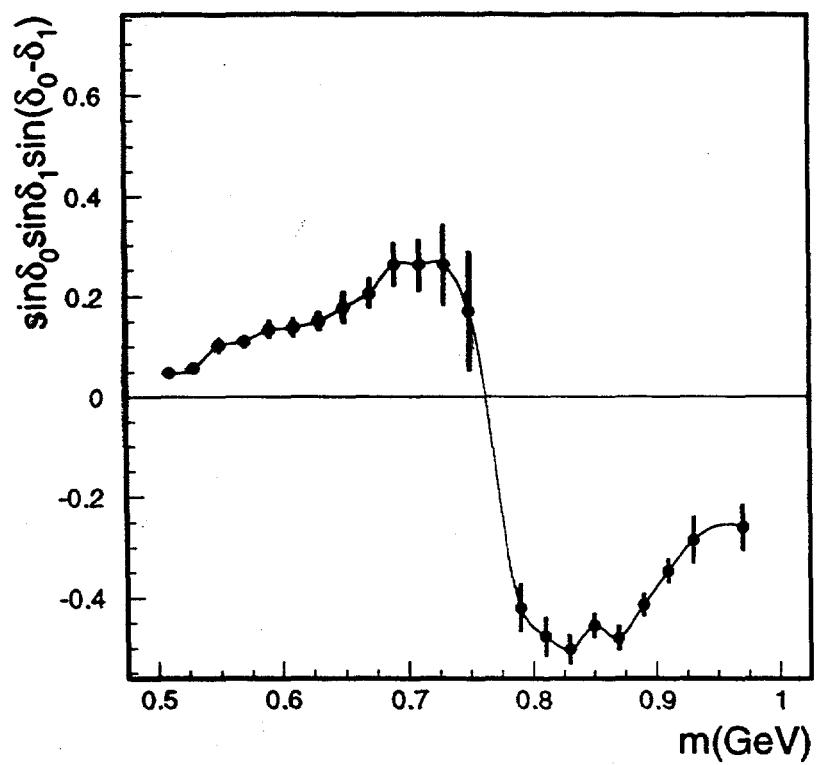
$$\text{at } \theta_{\text{cm}} = \frac{\pi}{2}$$

- From distribution

gluon dominate at small x



— *Figure of merit*



Data from P. Estabrooks and A. D. Martin, Nucl. Phys. **B79**, 301 (1974)

Polarized Λ -Baryon Production in pp

D. de Florian

Theoretical Physics Division, CERN, CH-1211 Geneva 23, Switzerland

In this talk, I analyze the possibility of obtaining polarized Λ fragmentation functions from single polarized processes at RHIC.

Working within the framework of the radiative parton model, our starting point has been a fit to unpolarized data for Λ production taken in e^+e^- annihilation, yielding a set of realistic unpolarized fragmentation functions for the Λ . Taking into account the sparse LEP data on the polarization of Λ 's produced on the Z -resonance, we were able to set up three distinct "toy scenarios" for the spin-dependent Λ fragmentation functions, to be used for predictions for future experiments. We emphasize that our proposed sets can by no means cover all the allowed possibilities for the polarized fragmentation functions, the main reason being that the LEP data are only sensitive to the valence part of the polarized fragmentation functions. Thus, there are still big uncertainties related to the "unfavoured" quark and gluon fragmentation functions, making further measurements in other processes indispensable.

Under these premises, we have studied Λ production in semi-inclusive deep-inelastic scattering. Turning to spin transfer asymmetries sensitive to the longitudinal polarization of the produced Λ 's, we have considered both $\bar{e}p \rightarrow \bar{\Lambda}X$ and $ep \rightarrow \bar{\Lambda}X$ scattering. It turns out that in the first case SIDIS measurements at HERA (with spin-rotators in front of the H1 and ZEUS detectors) and at HERMES should be particularly well suited to yield further information on the ΔD_f^Λ : differences between the asymmetries obtained when using different sets of ΔD_f^Λ are usually larger than the expected statistical errors. In contrast to this, having a polarized proton target (or beam) does not appear beneficial as far as Λ production is concerned.

Then, we have also studied the production of longitudinally polarized Λ -baryons in single-spin $pp \rightarrow \bar{\Lambda}X$ collisions at RHIC and HERA- \bar{N} as a means of determining the spin-dependent Λ fragmentation functions. It is shown that a measurement of the rapidity distribution of the Λ 's would provide an excellent way of clearly discriminating between the suggested sets of polarized Λ fragmentation functions. We also addressed the main theoretical uncertainties, which appear to be well under control.

As a final point, we have also done the analysis for the case of transversely polarized proton and Λ , a twist two observable which depends on both transverse parton distributions and transverse fragmentation functions. If Soffer's inequality is assumed to be saturated for both distributions at a very low scale, large asymmetries are expected for this process.

POLARIZED FRAGMENTATION FUNCTIONS

- ONLY LEP data at the mass of the Z

Unpolarized $e^+e^- \rightarrow \bar{\Lambda} X$ parity violating process
(3)

measure

$$A^{\Lambda} \propto \frac{g_3^{\Lambda}}{F_1^{\Lambda}} \quad g_3^{\Lambda} \propto \Delta D_q - \Delta D_{\bar{q}} \quad \text{non-singlet (valence dist)}$$

ONLY FIX $\sum e_q^2 (\Delta D_q - \Delta D_{\bar{q}})$ at $Q^2 = M_Z^2$

new assumptions

gluon distribution $\Delta D_g(\mu^2) = 0$
unflavored distributions $\Delta \hat{D}_{\bar{u}}^{\Lambda} = \Delta \hat{D}_{\bar{d}}^{\Lambda} = \dots = 0$

+ 3 Scenarios for $\Delta D_u, \Delta D_d, \Delta D_s$

- SCENARIO 1 ('naive NRQM'): $\Delta D_s^{\Lambda}(\mu^2) = z^{\alpha} D_s^{\Lambda}(\mu^2) \quad \Delta D_u(\mu^2) = \Delta D_d(\mu^2) = 0$
- SCENARIO 2 ('Burkardt-Jaffe like') $\Delta D_s^{\Lambda}(\mu^2) = z^{\alpha} D_s^{\Lambda}(\mu^2)$
 $\Delta D_u^{\Lambda}(\mu^2) = \Delta D_d^{\Lambda}(\mu^2) = -0.2 \Delta D_s^{\Lambda}(\mu^2)$
- SCENARIO 3 ('EXTREME BREAKING') $\Delta D_s^{\Lambda}(\mu^2) = \Delta D_u^{\Lambda}(\mu^2) = \Delta D_d^{\Lambda}(\mu^2) = z^{\alpha} D_s^{\Lambda}(\mu^2)$

- none of them can be eliminated yet $\left. \begin{array}{l} \text{unflavored dist.} \\ \text{breaking of SU(3) in} \\ \text{unpolarized F.F.} \end{array} \right\}$
- they provide a way to compute other observables and to study sensitivity to pol. F.F.

PP collisions (only @ LO) (LONGITUDINALLY POLARIZED)

$P\bar{P}_2 \rightarrow \bar{\Lambda}_2 X$ (to obtain $\Delta D_u^{\Lambda}, \Delta D_d^{\Lambda}$)

$\frac{d\Delta\sigma}{d\eta} \stackrel{P\bar{P}_2 \rightarrow \bar{\Lambda}_2 X}{=} \frac{d\sigma}{d\eta}^{P\bar{P}_2 \rightarrow \bar{\Lambda}_2 X} - \frac{d\sigma}{d\eta}^{P\bar{P}_2 \rightarrow \Lambda_2 X}$ $\eta > 0$ direction of \bar{P}

$= \int_{P_T^{min}} dP_T \sum_{FF' \rightarrow iX} \int dx_1 dx_2 dt f^P(x_1, M^2) \Delta F^{iP}(x_2, M^2) \Delta D_{i(P_T)}^{\Lambda} \frac{d\Delta\sigma^{FF' \rightarrow iX}}{d\eta}$

• P_T^{min} such that $z > 0.05$

ENSURES :

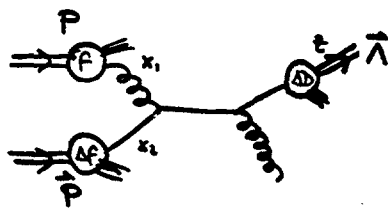
- APPLICABILITY OF PERT. QCD $M \sim P_T$
- " " FRAG. FUNCTIONS
- LARGER ASYMMETRIES $\frac{\Delta D}{D} \sim 20\%$

• two extreme kinematical regions

i) $\eta < 0$ small x_2 , so $\frac{\Delta F}{F}$ very small $\Rightarrow A \rightarrow 0$

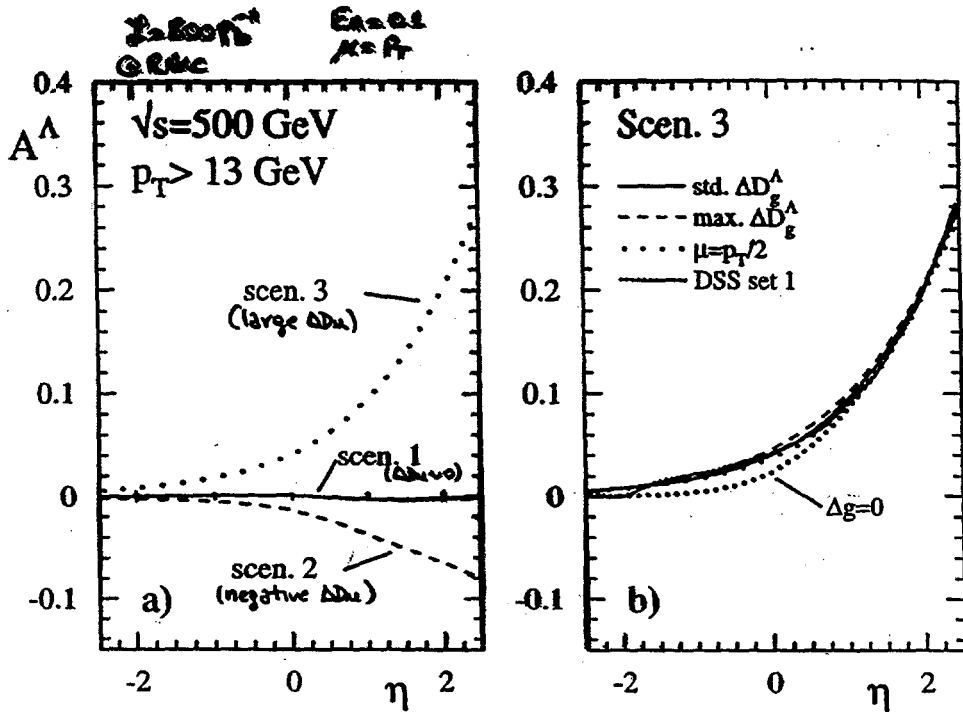
ii) $\eta > 0$ x_2 in the valence region, so larger $\frac{\Delta F}{F}$
 (ADVANTAGE WITH RESPECT TO 'DOUBLE ASYMMETRIES' \Rightarrow and small x_2 (sea and unpol. gluons))

Process dominated by



$g \bar{q}_v \rightarrow \bar{q} g$
 $(x_1) (x_2) \quad (z) \quad (z')$

$\Delta D_u^{\Lambda}, \Delta D_d^{\Lambda}$ (KNOWN \sim)
 $\Delta D_u^{\Lambda}, \Delta D_d^{\Lambda}$



• SOURCES OF UNCERTAINTY

- scale dependence : important because of LO (and $\alpha_s^2(\mu^2)$)

$\mu = \frac{p_T}{2}$ } large changes in $\Delta\sigma$ and σ
 $2p_T$ } — but cancel in the asymmetry

- Dependence on Δg { GRSV std.
DSS set 1 — very small
- " " Δg { GRSV std.
 $\Delta g = 0$ " "

- Dependence on ΔD_g^{Λ} { std. $\Delta D_g^{\Lambda}(0.3 \text{ GeV}^2) = 0$
max. $\Delta D_g^{\Lambda}(0.3 \text{ GeV}^2) = D_g^{\Lambda}(0.3 \text{ GeV}^2)$
— negligible

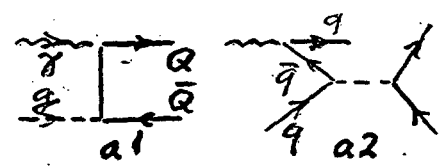
• SIMILAR SITUATION FOR $\sqrt{s} = 200 \text{ GeV}$ and $p_T > 8 \text{ GeV}$ ($Z = 240 \text{ Pb}^+$)

EXCELLENT PROSPECTS FOR MEASURING ΔD_u^{Λ} and ΔD_d^{Λ}

POLARIZED PHOTOPR. OF HEAVY Q (OPEN)

Leading order (α_s)

(a1) Born

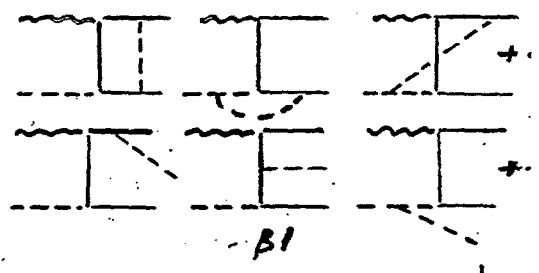


(a2) Resolved γ via
 $q\bar{q} \rightarrow Q\bar{Q}$
 γ str. fn $\Delta F_{q/\gamma}$

$q\bar{q} \rightarrow Q\bar{Q}$
 $\Delta F_{q/\gamma}$ known only thro.

NLO (α_s^2)

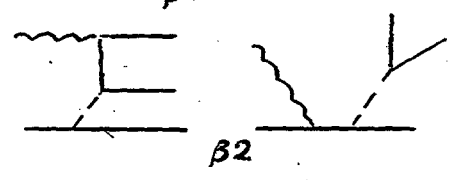
(B1) Loops & Brems
HARDEST part due
to $m_Q \neq 0$.



Results for this.

(B2) Subpr.

$\gamma q \rightarrow Q\bar{Q}q$
no loops
Prelim. results: small



Req. (a2): Using theoret. $\Delta F_{q/\gamma}$ $\Delta F_{q/\gamma}$
contribtns small in \overline{MS} & phys. scales.

Hassan & Pittkin

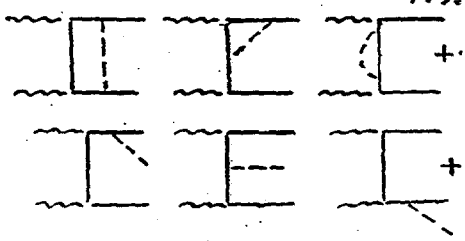
NOTE

Abelian part of (B1) provides HOC to

Kamal-Hereb. - C
Phys. Rev. D51, 4801
199.

$\gamma\gamma \rightarrow Q\bar{Q}$

This of interest in itself
in Higgs search when
 $m_H < 2m_V$



pp Collisions : transverse polarization

- UNKNOWN $\Delta_T M$ $\Delta_T d$ (information from Drell-Yan)
 $\Delta_T D_M^{\wedge}$ $\Delta_T D_d^{\wedge}$

BUT A NICE LEADING TWIST (2) TRANSVERSE OBSERVABLE (LARGE ASYM?)

- ESTIMATIONS USING SOFFER'S INEQUALITY FOR BOTH $\Delta_T q$ and $\Delta_T D$

$$|\Delta_T q| \leq \frac{1}{2} (q + \Delta_2 q)$$

$$q: \text{GRV} \\ \Delta_2 q: \text{GRSV}$$

$$|\Delta_T D| \leq \frac{1}{2} (D + \Delta_2 D)$$

assuming saturation at a very small scale $Q_0^2 \sim 0.3 \text{ GeV}^2 \Rightarrow$
 \Rightarrow inequality valid at any scale $Q^2 > Q_0^2$

- in the saturation limit D dominates \Rightarrow smaller differences between SCENARIOS
- even without imposing saturation one could expect asymmetries similar to LONGITUDINAL CASE

Advantage with respect to $p_T^{\uparrow} p_T^{\uparrow}$

here dominates

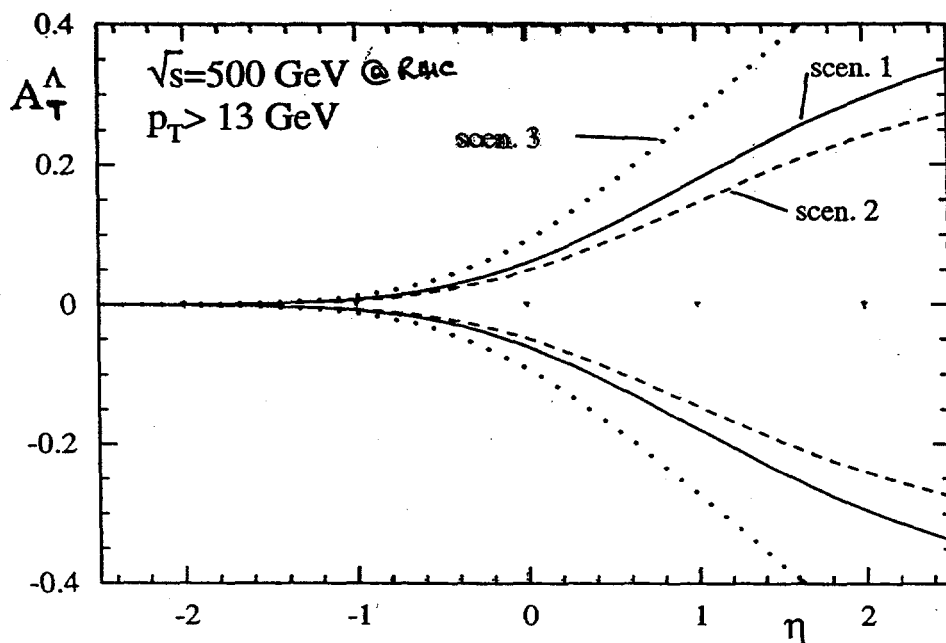
$g q_T^{\uparrow} \rightarrow g q_T^{\uparrow}$ large part. asym.
 (crossing to $p_T^{\uparrow} p_T^{\uparrow}$ would mean $q_T^{\uparrow} q_T^{\uparrow} \rightarrow gg$)

in $p_T^{\uparrow} p_T^{\uparrow} \Rightarrow q_T^{\uparrow} q_T^{\uparrow} \rightarrow q q$ small part. asym

$$\mu = p_T$$

$$P \vec{P}_T \rightarrow \vec{\Lambda}_T X$$

\hat{S}_P and \hat{S}_{Λ_T} have the same angle with respect to the scattering plane



• IF ΔD KNOWN \Rightarrow GOOD CHECK FOR 'DOUBLE' SOFFER'S INEQUALITY

photos

Single Spin Asymmetries and Higher Twist

George Sterman, *Institute for Theoretical Physics, SUNY Stony Brook*

Single spin asymmetries in single-particle inclusive cross sections have been observed at moderately large transverse momenta [1]. Nevertheless, they must vanish as $1/p_T$ at high energies. This may be seen directly from QCD factorization theorems, taking into account all possible twist-2 parton distributions. For these cross sections, we are therefore led to a twist-3 analysis. The relevant factorization theorem in this case is [2, 3]

$$\begin{aligned} \Delta\sigma_{A+B\rightarrow\pi}(\vec{s}_T) &= \sum_{abc} \phi_{a/A}^{(3)}(x_1, x_2, \vec{s}_T) \otimes \phi_{b/B}(x') \otimes \hat{\sigma}_{a+b\rightarrow c}(\vec{s}_T) \otimes D_{c\rightarrow\pi}(z) \\ &+ \sum_{abc} \delta q_{a/A}(x, \vec{s}_T) \left\{ \otimes \phi_{b/B}(x') \otimes \hat{\sigma}'_{a+b\rightarrow c}(\vec{s}_T) \otimes D_{c\rightarrow\pi}^{(3)}(z, z') \right. \\ &\quad \left. + \otimes \phi_{b/B}^{(3)}(x'_1, x'_2) \otimes \hat{\sigma}''_{a+b\rightarrow c}(\vec{s}_T) \otimes D_{c\rightarrow\pi}(z) \right\}. \end{aligned}$$

$\phi_{a/A}^{(3)}(x'_1, x'_2, s_T)$ represents the possible twist-3 spin-dependent parton distributions, while $\delta q_{a/A}$ is the spin-dependent, chiral-odd, twist-2 transversity distribution [4], which must be paired in this case with a twist-3 chiral-odd fragmentation function $D^{(3)}$ or spin-independent parton distribution $\phi^{(3)}$, as shown.

For a number of reasons, we have suggested [3] that the dominant contribution to the asymmetry at large transverse momentum is associated with the matrix element

$$\begin{aligned} T_{F_a}^{(V)}(x_1, x_2, s_T) &= \int \frac{dy_1^- dy_2^-}{4\pi} e^{ix_1 P^+ y_1^- + i(x_2 - x_1) P^+ y_2^-} \\ &\quad \times \langle P, \vec{s}_T | \bar{\psi}_a(0) \gamma_+ [e^{s_T \sigma n \bar{n}} F_{\sigma+}(y_2^-)] \psi_a(y_1^-) | P, \vec{s}_T \rangle, \end{aligned}$$

which couples gluon and quark degrees of freedom in the nucleon. The computed spin asymmetry for pion production [5] is proportional to a derivative of $T_F^{(V)}$, which enhances the cross section in the large- x_F region, where substantial effects are seen at moderate p_T [1]. The form of the leading-order calculation suggests that the twist-3 cross section will remain observable at RHIC energies, and predicts explicit dependences on kinematic variables that can be tested, perhaps with the Brahm's detector [6].

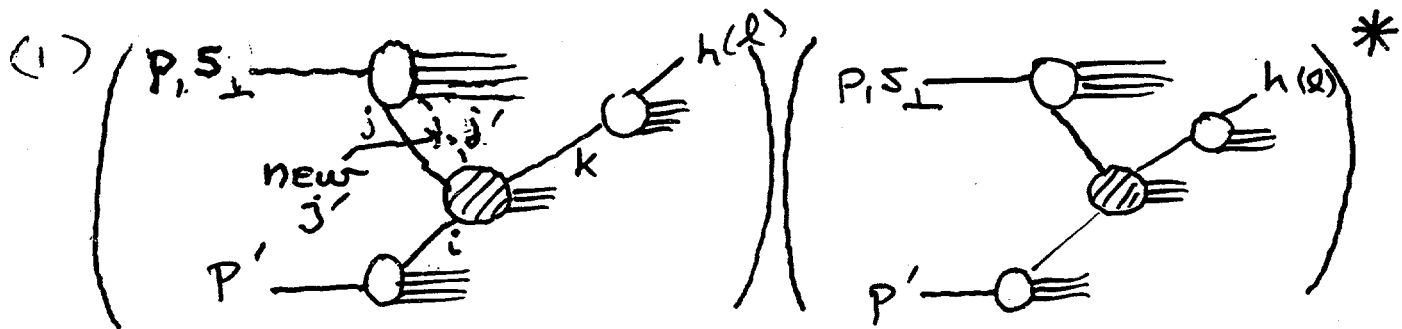
References

- [1] D.L. Adams et al., Phys. Lett. B261, 201 (1991); B264, 462 (1991); A. Bravar et al., Phys. Rev. Lett. 77, 2626 (1996).
- [2] A.V. Efremov and O.V. Teryaev, Phys. Lett. 150B, 383 (1985); Yad. Fiz. 36, 950 (1982); 39, 1517, (1984) [Sov. J. Nucl. Phys. 36, 557 (1982); 39, 962 (1984)].
- [3] J.W. Qiu and G. Sterman, Phys. Rev. Lett. 67, 2264 (1991); Nucl. Phys. B378, 52 (1992).
- [4] J. Ralston and D.E. Soper, Nucl. Phys. B152, 109 (1979); R.L. Jaffe and X. Ji, Phys. Rev. Lett. 67, 552 (1991); Phys. Lett. B284, 137 (1992).
- [5] J.W. Qiu and G. Sterman, in preparation.
- [6] Flemming Videbaek, presentation at this workshop.

'MINIMAL APPROACH'

2. (Spin-Dependent) Factorization at $\mathcal{O}(1/Q)$ (what we need)

8



Interference $\rightarrow \Delta\sigma(P, P', l, S_\perp)$
 new $\sim \dots$ costs $1/Q \sim 1/l_\perp$

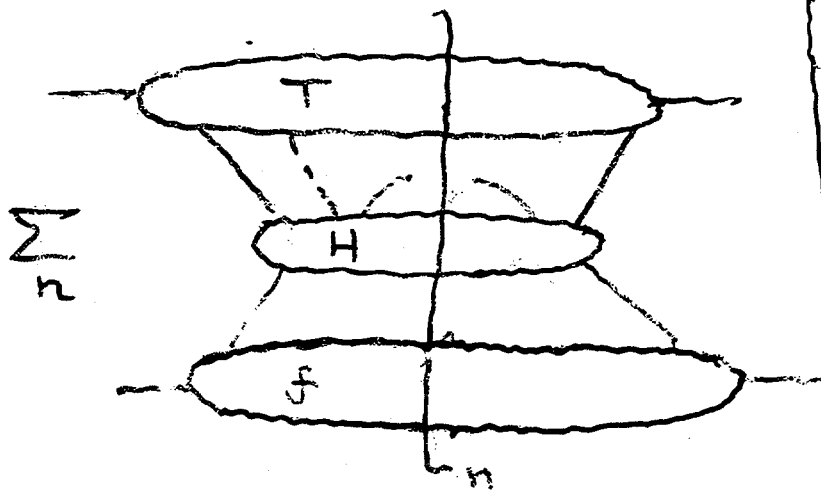
$$(2) \quad \omega \frac{d\Delta\sigma_\perp}{d^3p} = \sum_{i(jj')k} \int \frac{dx_i}{x_i} f_{i/p}(x_i) \int \frac{dz}{z} P_{ijk}$$

$$* \int dx_j dx_{j'} T_{(jj')/p}(x_j, x_{j'})$$

$$* H_{i(jj')k}(x_i, x_j, x_{j'}, x_k, l)$$

$$j, j' = q, D = i(\partial + igA), F$$

(3)



work in DIS:
 Vainshtein, Shuryak
 Ellis, Formanski
 Petronzio
 Jaffe, Soldate

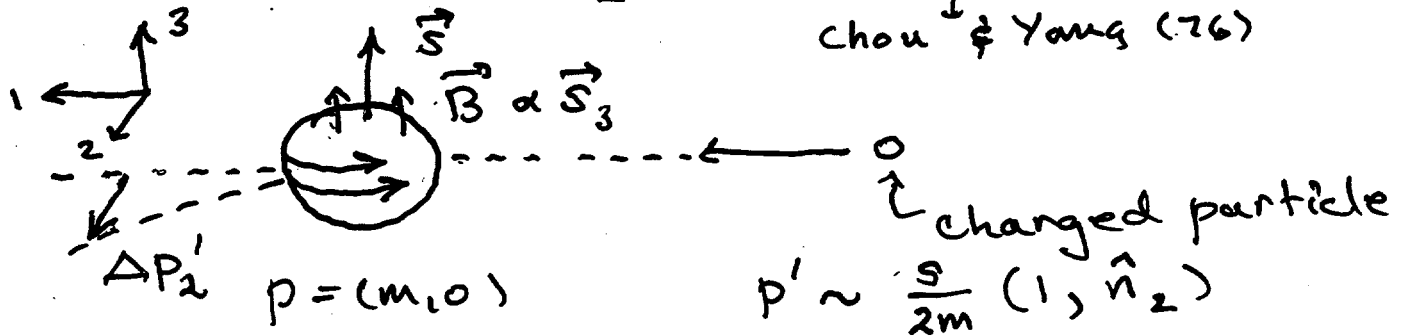
What are we looking at in $T_F^{(v)}$?

- Rotating Matter Currents?

Classical (Abelian) Analogy
rest frame of (p, \vec{s})

Liang & Meng (90)

Chou & Yang (76)



$$\dot{p}'_2 = e (\vec{v}' \times \vec{B})_2$$

$$= -e v_1 B_3$$

$$= e v_1 F_{21}$$

cm frame $(m, 0) \rightarrow n$
 $(1, \hat{n}_2) \rightarrow \bar{n}$

$$\dot{p}'_2 = e n^\alpha \bar{F}_{2\rho} \epsilon^{\sigma\nu\lambda\sigma} n_\nu \bar{n}_\lambda \delta_\sigma$$

$$\Delta p_i = \int dy \dot{p}_i$$

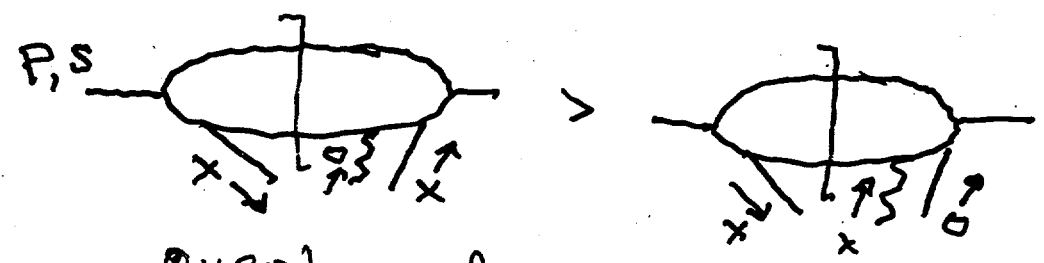
But recall $T_F^{(v)}$ a quantum correlation

\Rightarrow new information on parton/parton correlations

We believe $\frac{dT_F^{(v)}}{dx}$ term dominates

(1) Because we expect

$$T_F^{(v)}(x, x) > T_D^{(v, A)}(x, 0)$$



Overlap of states that differ by soft gluon emission > 'soft quark emission'!

(2) Because if

$$T_F^{(v)}(x, x) = A(1-x)^N$$

$$\frac{d}{dx} T_F^{(v)}(x, x) = AN(1-x)^{N-1} \gg T_F^{(v)}$$

So: in more complicated processes it may make sense to only look at $\frac{d}{dx}$ terms for large x_F, x_T

But: $\frac{d}{dx} \leftrightarrow \frac{d}{dk_T} \leftrightarrow \langle \bar{\psi} F \psi \rangle$ ('soft') $(x_F \rightarrow 1)$
or $\langle F \cdot F \rangle$ $(x_F \approx 0)$? (10)

3. Results

SPIN ASYMMETRY:

$$\begin{aligned}
 E_\ell \frac{d^3 \Delta \sigma(\vec{s}_T)}{d^3 \ell} &= \frac{\alpha_s^2}{S} \sum_{a,c} \int_{z_{\min}}^1 \frac{dz}{z^2} D_{c \rightarrow \pi}(z) \\
 &\times \int_{x_{\min}}^1 \frac{dx}{x} \frac{1}{xS + U/z} \int \frac{dx'}{x'} \delta \left(x' - \frac{-xT/z}{xS + U/z} \right) \\
 &\times \sqrt{4\pi\alpha_s} \left(\frac{\epsilon^{lsr\bar{n}\bar{n}}}{z(-\hat{u})} \right) \\
 &\times \left[-x \frac{\partial}{\partial x} T_{F_a}^{(V)}(x, x) \right] \left[\Delta \hat{\sigma}_{ag \rightarrow c} G(x') + \Delta \hat{\sigma}_{aq \rightarrow c} \sum_q q(x') \right]
 \end{aligned}$$

OUR FAVORITE MATRIX ELEMENT:

$$T_{F_a}^{(V)}(x, x) = \int \frac{dy^-}{4\pi} e^{ixP^+y^-} \langle P, \vec{s}_T | \bar{\psi}_a(0) \gamma_+ \left[\int dy_2^- \epsilon^{sr\bar{o}\bar{n}\bar{n}} F_{\sigma+}(y_2^-) \right] \psi_a(y^-) | P, \vec{s}_T \rangle$$

COMPARE TO:

$$q_a(x) = \int \frac{dy^-}{4\pi} e^{ixP^+y^-} \langle P | \bar{\psi}_a(0) \gamma_+ \psi_a(y^-) | P \rangle$$

MODEL:

$$T_{F_a}^{(V)}(x, x) \equiv \kappa_a \lambda q_a(x)$$

$$\kappa_u = +1 \quad \text{and} \quad \frac{\kappa_u}{\kappa_d} = -1 \quad (\text{proton})$$

only for
'large' x !

viz

A. Schafer
et al

PL B321, 121
(94)

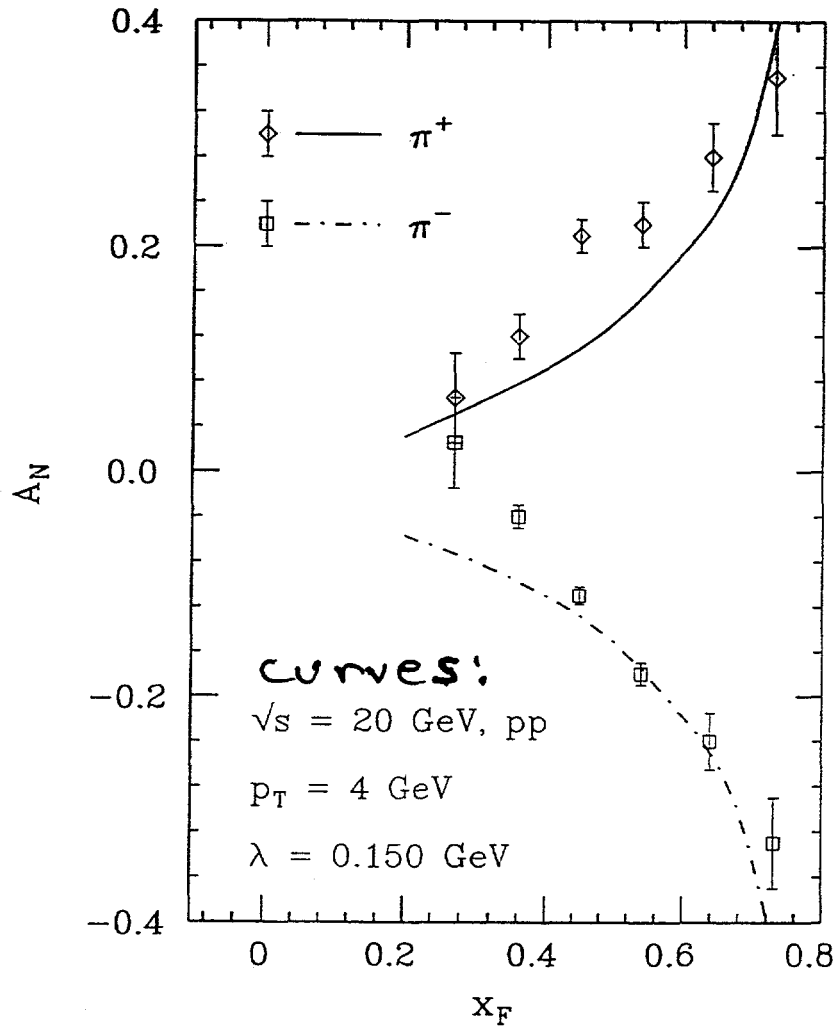
qq SHORT DISTANCE FUNCTION:

note relative size

$$\begin{aligned} \Delta \hat{\sigma}_{ag \rightarrow c} = & \delta_{ac} \left\{ 2 \left(1 - \frac{\hat{s}\hat{u}}{\hat{t}^2} \right) \left[\frac{9}{16} + \frac{1}{8} \left(1 + \frac{\hat{u}}{\hat{t}} \right) \right] \right. \\ & + \frac{4}{9} \left(\frac{-\hat{u}}{\hat{s}} + \frac{\hat{s}}{-\hat{u}} \right) \left[\frac{63}{128} - \frac{1}{64} \left(1 + \frac{\hat{u}}{\hat{t}} \right) \right] \\ & + \left(\frac{\hat{s}}{\hat{t}} + \frac{\hat{u}}{\hat{t}} \right) \left[\frac{9}{16} + \frac{1}{8} \left(1 + \frac{\hat{u}}{\hat{t}} \right) \right] \\ & \left. + \left[\frac{9}{32} \left(\frac{-\hat{u}}{\hat{s}} - \frac{\hat{s}}{-\hat{u}} \right) \right] + \left[\frac{9}{16} \left(\frac{\hat{s}}{\hat{t}} - \frac{\hat{u}}{\hat{t}} \right) \right] \right\} \end{aligned}$$

qq, q \bar{q} SHORT DISTANCE FUNCTIONS:

$$\begin{aligned} \Delta \hat{\sigma}_{ab \rightarrow c} = & \delta_{ac} \delta_{bq} \frac{4}{9} \left(\frac{\hat{s}^2 + \hat{u}^2}{\hat{t}^2} \right) \left[\frac{21}{64} + \frac{1}{8} \left(1 + \frac{\hat{u}}{\hat{t}} \right) \right] \\ & + \delta_{ac} \delta_{b\bar{q}} \frac{4}{9} \left(\frac{\hat{s}^2 + \hat{u}^2}{\hat{t}^2} \right) \left[-\frac{51}{64} + \frac{1}{8} \left(1 + \frac{\hat{u}}{\hat{t}} \right) \right] \\ & + \delta_{bc} \frac{4}{9} \left(\frac{\hat{s}^2 + \hat{t}^2}{\hat{u}^2} \right) \left[\frac{21}{64} - \frac{51}{64} \left(1 + \frac{\hat{u}}{\hat{t}} \right) \right] \\ & + \delta_{ab} \delta_{bc} \frac{-8}{27} \left(\frac{\hat{s}^2}{\hat{u}\hat{t}} \right) \left[\frac{10}{8} + \frac{1}{8} \left(1 + \frac{\hat{u}}{\hat{t}} \right) \right] \\ & + \delta_{a\bar{b}} \frac{4}{9} \left(\frac{\hat{t}^2 + \hat{u}^2}{\hat{s}^2} \right) \left[\frac{1}{8} - \frac{51}{64} \left(1 + \frac{\hat{u}}{\hat{t}} \right) \right] \end{aligned}$$



data at $\lesssim 1.5 \text{ GeV}$

Possibilities for spin measurements in BRAHMS.

Flemming Videbæk

Physics Department, BNL

The Broad Range Hadron Magnetic Spectrometer (BRAHMS) experiment at RHIC is one of the four approved Heavy Ion experiments at RHIC. The primary goal is to measure semi-inclusive spectra for identified charged hadron over a wide range of rapidity and transverse momenta p_t . The spectrometer consists of two moveable arms, one at mid-rapidity and one in the forward region. The latter is of potential interest to the RHIC spin program. It consists, as depicted in the first slide, of 4 dipole magnets with a total maximum bending field of 9.6 Tm, tracking stations, and time-of-flight and Cherenov detectors for particle identification. For more details see ref 1¹. The detector is placed in the 2 O'clock area. Here the proton beam can only be polarized transversely. In the preceding contribution² to the spin workshop the possibility of learning about higher order twist effects by measuring the transverse spin asymmetry $A_N = (N^+ - N^-) / (N^+ + N^-)$ vs. X_f and p_t is described.

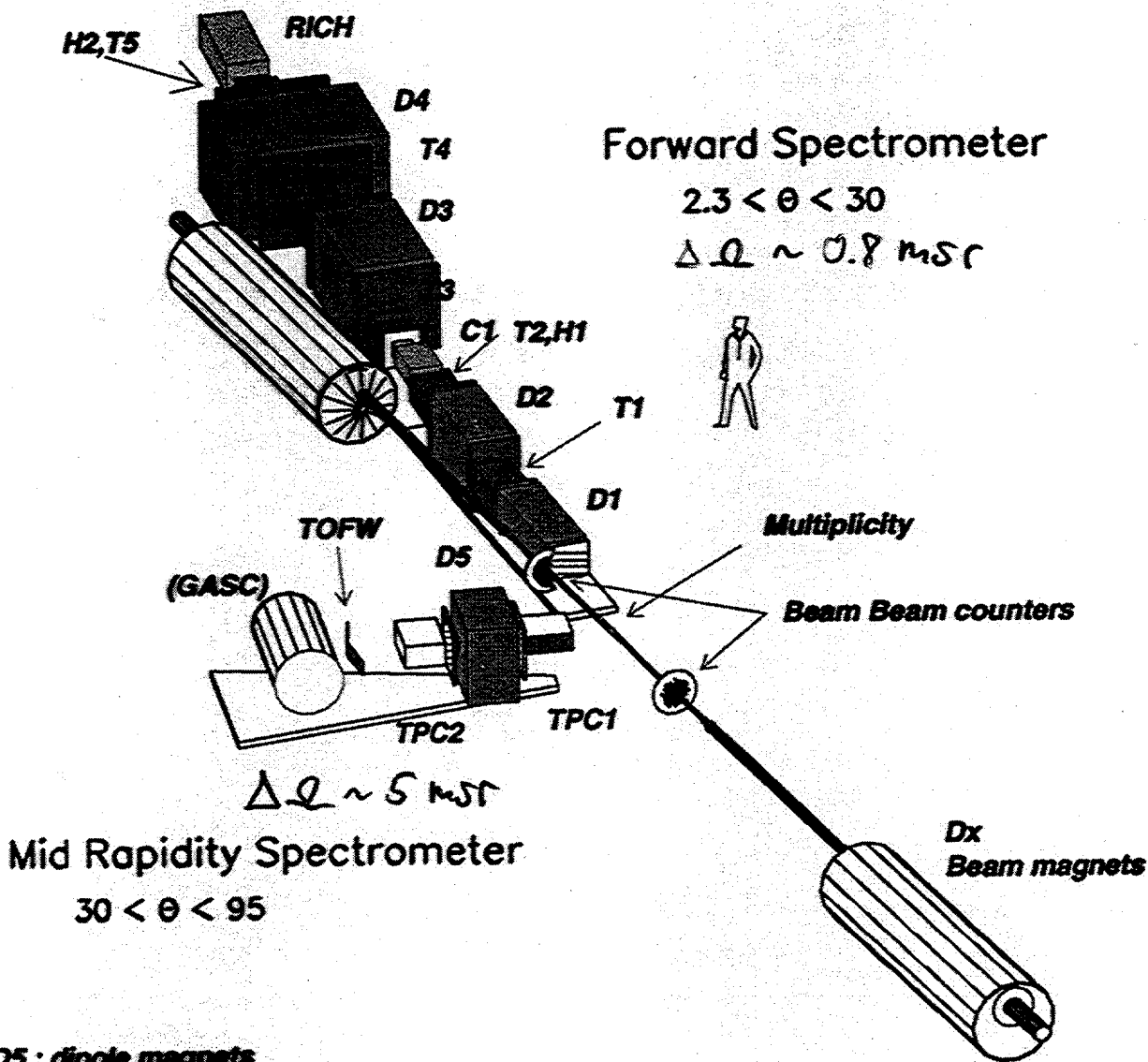
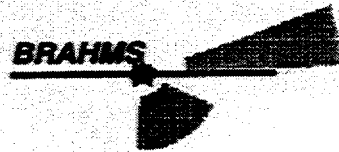
The acceptance over all angles and magnetic settings are shown in the second figure for the 100 GeV/c p on 100 GeV/c p. The hatched areas indicated where good PID is possible. This region has a too low a X_f to be interesting for non-zero measurements of A_N . It is though possible to operate the spectrometer by moving the front section in such a way that an acceptance region for $.2 < X_f < .7$ can be reached. This is shown in the 3 figure. One characteristic feature is that p_t change with X_f .

Based on the model estimates asymmetries of about 2-5% can be expected in this region of phase space. Thus to get a measurement with a statistical accuracy of about 1% about 10,000 counts are needed per been of each polarization state. The un-polarized cross sections were obtained from a Pythia calculation using standard parameters. Based on this, it is estimated that a fairly complete measurement can be achieved in about 1 month of RHIC running.

The last slide summarizes the investigation, and some issues that have to be resolved for this measurement to take place.

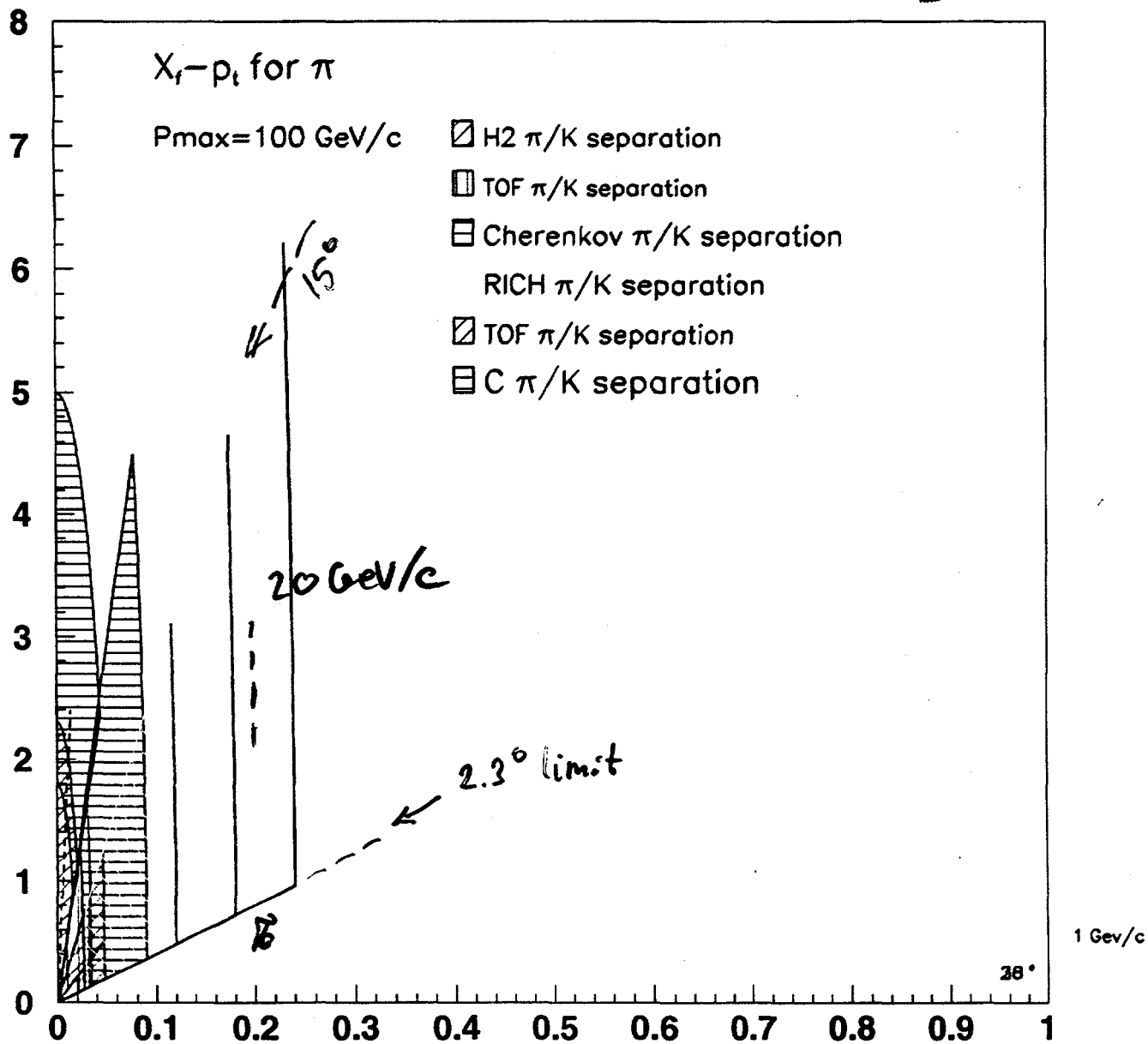
¹ See e.g. The BRAHMS experiment at RHIC F.Videbaek, RHIC summer study 1995. The BRAHMS Conceptual Design report available on the web via the BRAHMS home page <http://rsgi01.rhic.bnl.gov/export1/brahms/WWW/brahms.html>

² G.Sterman, these proceedings.



D1,D2,D3,D4,D5 : dipole magnets
T1,T2,T3,T4,T5, TPC1 TPC2: tracking detectors
H1,H2,TOFW : Time-of-flight detectors
RICH, GASC : Cherenkov detectors

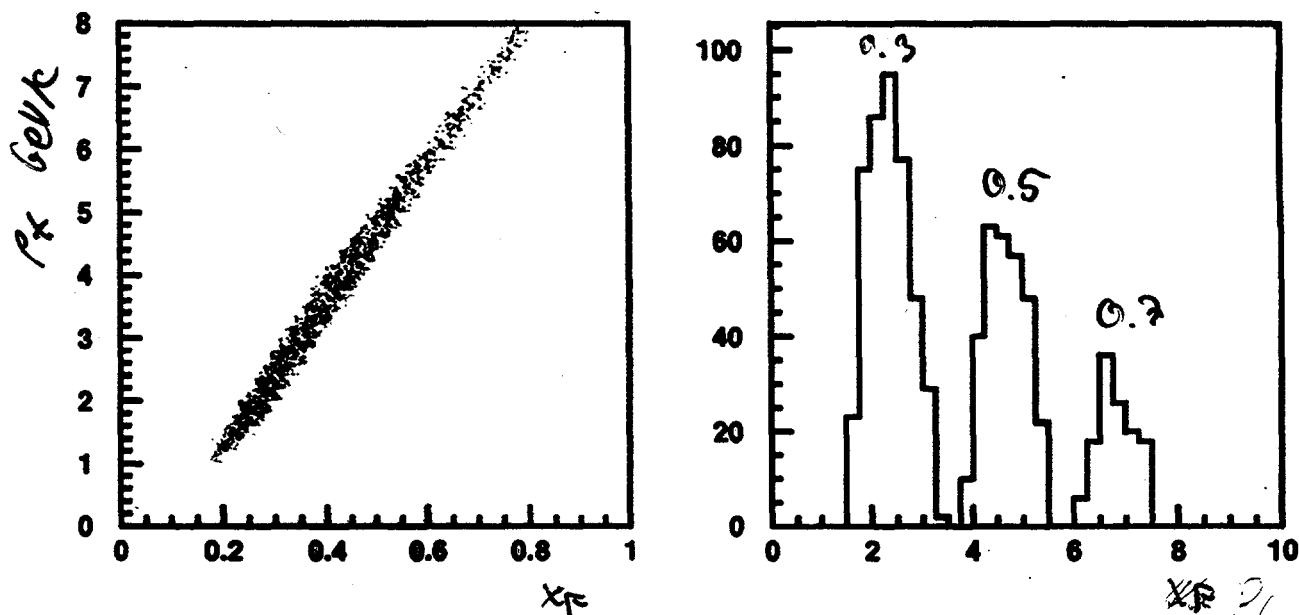
Default/Standard Configuration:



Requirement: Good P.I.D.
 $\delta p/p \lesssim 1\%$

Kinematic coverage for high momentum pp running

100 t 600



- Kinematic region accessible for one setting .
- Field 2.4Tm per magnet
- Line of sight through system (front system moved relative to back)
- $\delta p/p$ about 5%

Rate estimates in pp for BRAHMS

To get an idea for this Lund (i.e. Pythia) was used at 100+100 GeV/c. The total population is given as a 2-dimensional distribution in X_f vs. p_t and shown in the figure below.

This calculation was used to estimate the overall rate at $X_f=0.5$ and $p_t=5$ GeV/c. It is

$$d^2n/dp_t dx_F \sim 2.0 \cdot 10^{-5}$$

What luminosity is needed to get 1000 counts. The inelastic cross section σ_{pp} is 45 mb at $\sqrt{s} = 200$.

$$N(1000) = d^2n/dp_t dx_F \sigma_{pp} \Delta p_t \Delta x_F L$$

$$\Rightarrow L = 10^2 \text{ nb}^{-1}$$

RHIC delivers at $10^{31} \text{ cm}^{-2}\text{sec}^{-1}$; this is a modest estimate for the 2 O'clock area, but probably realistic in the first year of running.

Thus 1000 count can be achieved in about 3 hours of running. To get a good measurement at an expected asymmetry of 0.05 with an accuracy of 0.01, 20,000 count for up-down is needed i.e. approximately 60 hours.

G. Sterman, J. Qiu's model
 predicts $A_N \sim 2\%$ at $x_F = 0.3$
 $\sim 5\%$ at $x_F = 0.5$

Outlook

- The BRAHMS Detector has acceptance and capabilities for a measurement of the transverse spin-asymmetry for $X_f = 0.3, 0.5$ and $P_t = 3-5 \text{ GeV}/c$ in pp at $100+100 \text{ GeV}/c$.
- It could take place at >2000
 - Beams available
 - Additional A/C power at 2 O'clock
 - trigger upgrades needed
- It is presently not part of the BRAHMS physics program to carry out this measurements. It needs some additional effort == people.
 - preparations
 - 1 mo. Running
 - Analysis

Bounds on Helicity Amplitudes at low Momentum Transfer

N. H. BUTTIMORE

*University of Dublin, Trinity College
Dublin 2, Ireland*

In the context of electromagnetic hadronic interference for elastic scattering, a study of bounds on helicity amplitudes provides important information related to the evaluation of polarization and the understanding of spin-dependent reactions.

Notation for spin- $\frac{1}{2}$ spin- $\frac{1}{2}$ non-identical particle elastic reactions, proton-spin- $\frac{1}{2}$ ion collisions for example, is introduced by exhibiting the high s Born approximation Coulomb helicity amplitudes with Pauli form factor normalization $F_2(0) = \mu - 1$. The rôle played by single-flip and double-flip amplitudes in the asymmetry maximum near the interference region is similar to that for identical particle elastic scattering.

In the case of pp collisions, the asymmetry maximum is sensitive to the forward imaginary part of $\phi_2 = \langle ++ | \phi | -- \rangle$ which may be bounded up to 6 GeV energies by the known transverse spin-polarized total cross section difference $\Delta\sigma_T = \sigma_{\uparrow\downarrow} - \sigma_{\uparrow\uparrow}$. The maximum is more sensitive to the ratio of the helicity single-flip amplitude to the averaged *imaginary* non-flip amplitude $r_5 = (2m/\sqrt{-t}) \phi_5 / \text{Im}(\phi_1 + \phi_3)$, imaginary values of which, according to a wide range of models incorporating—in various forms—the Pomeron, quarks, gluons and instantons, all have magnitude less than 20%. Several studies of the limited high energy elastic data in the interference region reveal that $\text{Im}r_5 \approx 0.2 \pm 0.3$ with something similar for proton carbon collisions.

Rigorous bounds on the helicity ratio for spin-0 spin- $\frac{1}{2}$ collisions based on partial wave unitarity unfortunately merely indicate that the flip nonflip ratio $|\text{Im}r| \leq 2.3$, at the high energies of interest. A positivity analysis of the absorptive element of the differential cross section in higher spin elastic cases also leads to a comparable bound on the helicity flip nonflip ratio, where the helicity-dependent hadronic slope parameters are supposed not to depart too greatly from the prominent t variation associated with the slope parameter b of the dominant spin-averaged amplitude.

This study is supported in part by funds from the International Collaboration Programme IC/97/061 of Forbairt, the Science and Technology Agency in Ireland.

IMPORTANCE OF HELICITY FLIP AMPLITUDES

For the elastic scattering of non-identical particles, $NN' \rightarrow NN'$, of spin $\frac{1}{2}$ the one photon exchange asymptotic amplitudes

$$\begin{aligned} \varphi_1(++;++) & \quad \frac{ds}{t} F_1 F_1' & \quad \varphi_3(+--;+-) \\ \varphi_2(++;--) & \quad \frac{ds}{4mm'} F_2 F_2' & \quad - \varphi_4(+--; -+) \\ \varphi_5(++;+-) & \quad \frac{-ds}{2m'\sqrt{-t}} F_1 F_2' & \quad - \varphi_6(++; -+) \\ & & \quad (m \leftrightarrow m', F \leftrightarrow F') \end{aligned}$$

are significant near interference, t_c .

Isospin invariance indicates $\varphi_5 = -\varphi_6$ for $u \rightarrow u$ but $e \rightarrow e$ breaks this, so $\varphi_5^{\prime\prime} \neq -\varphi_6^{\prime\prime}$ here.

In terms of helicity amplitudes, asymmetry

$$\frac{k^2 s}{\pi} A_N \frac{d\sigma}{dt} = \mathcal{I}_m \left[(\varphi_1 + \varphi_3)^* \varphi_5 - (\varphi_2 - \varphi_4)^* \varphi_6 \right]$$

is studied for polarization evaluation.
(B. Gotsman, Leader, Phys. Rev. D18, 694, 1978)

Identical particles, so $\phi_5 = -\phi_6$

and near interference, $t_e = 8\pi\alpha/\sigma_{tot}$

$$\frac{m}{\sqrt{-t}} A_N = \frac{(2g_m r_s - k_p) \frac{t_e}{t} + (2\rho g_m r_s - 2\text{Re} r_s)}{1 + (t_e/t + \rho + \delta)^2}$$

(Kopeliovich and Lapidus) Bethe phase δ ,

where the possible presence of the normalized single-flip / nonflip ratio at high energies

$$r_s = \frac{m}{\sqrt{-t}} \frac{\phi_5}{g_m \phi_+}, \quad \phi_+ = \frac{1}{2}(\phi_1 + \phi_3)$$

is of concern for proton polarimetry.

RIKEN BNL Summer Workshop 1997

studied the hadron spin-flip question.

Bounds on ϕ_5 are reviewed and

examined, in addition to bounds on ϕ_+ , ϕ_2 .

Coefficient of t_c/t in A_N relates to the maximum asymmetry at interference.

$$2 \operatorname{Im} \tau_5 - K_p - \frac{1}{2} K_p \operatorname{Im} \tau_2 \quad (\text{VI Blois})$$

is more accurate and includes a term involving the transverse-spin total cross section difference $\Delta \sigma_{\text{tot}}^T$, where

$$\tau_2 = \frac{\phi_2}{\operatorname{Im} \phi_+} \quad \text{and} \quad \operatorname{Im} \tau_2 \Big|_{t=0} = - \frac{\Delta \sigma_{\text{tot}}^T}{\sigma_{\text{tot}}}$$

The difference $\Delta \sigma_{\text{tot}}^T$ drops from

6 mb at 2 GeV/c to 0.5 mb at 6 GeV/c

It would be vital to confirm this continuing decrease at higher energies.

An improvement on the bound for $\operatorname{Im} \phi_2$

$$|\operatorname{Im} \tau_2(s, 0)| < 1\% \quad \text{is desirable.}$$

Hadronic Flip / Nonflip

$|\tau_s|$

M O D E L S	Landshoff $\frac{1}{2} \mu_p - 1 - \mu_n $	0.06
	Berger, (data > 3 GeV) Irring, Sorensen	$\left\{ \begin{array}{l} 0.09 \\ 0.03 \end{array} \right.$
	R parameter, 45 GeV pp	0.07 ± 0.04
	B.Z. Kopeliovich, 2 gluon	0.10
	Goloskokov, $q^2 \text{TP}$	$\sim 0.20, -\tau = .3$
S	Anselmino, Forte	~ 0.1
D A T A	T.L. Trueman, $9m^2$ s	0.2 ± 0.3
	AKcharin, B, Penzo (150-300) "	0.08 ± 0.18
	E704 (200 GeV/c only) "	0.15 ± 0.30
	Kopeliovich (pC, 200) $9m^2$	0.22 ± 0.26

Hadronic Double-flip / Nonflip

$$\left. \begin{array}{l} \sigma_{tot}^{\uparrow\uparrow} / \sigma_{tot}^{\uparrow\downarrow} \\ (A. Martin) \end{array} \right\} \begin{array}{l} 3/4 \rightarrow 4/3 \text{ ISR} \\ 1/2 \rightarrow 2 \text{ Sp}\bar{p}S \end{array}$$

BOUND ON HELICITY FLIP AMPLITUDE

For spin 0 - spin $\frac{1}{2}$ elastic collisions described by non flip $F_{++}(s,t)$ and flip $F_{+-}(s,t)$ amplitudes, the forward ratio is bounded

$$\frac{m}{\sqrt{-t}} \left| \frac{\text{Im } F_{+-}}{\text{Im } F_{++}} \right|_{t=0} \leq \frac{3m}{2} \sqrt{b} \left(\frac{16\pi}{15} \frac{b \sigma_{el}}{\sigma_{tot}^2} \right)^{\frac{1}{6}}$$

$$\text{or, } |\text{Im } \mathcal{V}| \leq 0.87 m \sqrt{b}$$

where $2b$ is approximately the $\frac{d\sigma}{dt}$ slope

and

$$b = \frac{d}{dt} \ln \text{Im } F_{++} \Big|_{t=0} \approx \frac{\sigma_{tot}^2}{32\pi \sigma_{el}}$$

D. P. Hodgkinson, Phys. Lett. 39B, 640 (1972).

Over the range $\sqrt{s} \in [50, 500]$, the slope $2b \in [14.0, 15.5]$, and for proton mass m ,

$$|\text{Im } \mathcal{V}| \leq 2.3,$$

significantly greater than the critical value 0.9

HIGHER SPIN BOUNDS

Bound on $\text{Im } \phi_s(++;+-)$ from

$$\begin{aligned} \frac{d\sigma^A}{dt} &= \sum_i \left(\text{Im } \phi_i \right)^2 \\ &= \sum_n (2n+1) c_n P_n(\cos\theta) \end{aligned}$$

Mahoux (1976) BLS Phys Rep. 59(80)164

$$c_n \geq 0 \Rightarrow$$

$$d\sigma^A/dt(t=0) \geq d\sigma^A/dt(t<0)$$

$$\left(\text{Im } \phi_s \right)^2 / |t| \leq \frac{1}{2} \left(b + \zeta_L^2 b_- + \frac{1}{2} \zeta_T^2 b_2 \right)$$

$$|\text{Im } \Gamma_s| \lesssim 2.3$$

S. M. Roy has improved bound

PL 70B (1977) 213.

Mennessier, Roy, Singh N.C. 50A, 443 (1979)

CONCLUSIONS

1. Confirm $\text{Im} \phi_2(s, 0) \propto \Delta \sigma_T$ is small
2. Many models indicate $\text{Im} T_5 \approx 0.1$ suggesting CNI polarimetry at 10%
3. Rigorous bounds $\Rightarrow |\text{Im} T_5| < 2.5$ mainly for spin 0 - spin $\frac{1}{2}$ collisions
4. Higher spin bounds leading to similar conclusions are available with additional assumptions.
5. Important to confirm that $\rho = \frac{\text{Re} T_4}{\text{Im} T_4}$ agrees with analytic expectations
6. Measurements at small angles with polarized protons give considerable information on the helicity amplitudes of elastic scattering.

The Odderon and spin-dependence of elastic proton-proton scattering.

T.L.Trueman, BNL

April 29, 1998

Spin-dependence of high energy proton-proton elastic scattering provides a new and sensitive tool to search for the Odderon. The reason for this is that the asymptotic phase of the scattering amplitude is closely tied to the C of the exchanged system; thus, in leading order, if the Pomeron and Odderon have the same asymptotic behaviour, up to logs, then they are out of phase by 90° . Spin dependent asymmetries depend on various real and imaginary parts of products of amplitudes and so the Odderon can dominate some asymmetries to which the Pomeron cannot contribute: thus, for example the purely hadronic piece of A_N , (Fig.1) which vanishes as $t \rightarrow 0$, is zero for purely $C = +1$ exchange; a deviation from zero would be a strong indicator that a Pomeron is present. (If the two parts differ in their asymptotic behaviour by powers of $\ln(s/s_0)$ there will be $\pi/\ln(s/s_0)$ corrections to this and most of the other comments made in this talk. For this reason, it will be important to measure the asymmetries over as wide a range of s as possible.) At the same time, in the CNI region the purely $C = +1$ spin-flip Pomeron piece is what stands in the way of using this process as a polarimeter. (Fig.2,3,4). The basic properties of the Odderon and the phase argument are given in Fig. 4 and 5.

Fig.6 lists all the measurable asymmetries using polarized beams, without final polarization measurements. A_{NN} gives a CNI-type peak if the Odderon contributes to the double spin-flip amplitude ϕ_2^O (Fig.7). If the Pomeron also couples to ϕ_2^P there will be a purely hadronic (non-enhanced) piece which will have a distinctly different shape. It may very well be possible to extract both of these pieces from measuring A_{NN} if they are not too small (Fig.8). Similar arguments can be applied to the other asymmetries. A_{SS} is basically the same as A_{NN} at small t , so additional information requires longitudinally polarized protons as well. If this is possible then complete information about the asymptotic amplitudes ϕ_-, ϕ_2 and ϕ_5 , both the $C = +1$ and $C = -1$ pieces, should be attainable. (Fig.9) The last column shows the expected dominant contributions to the purely hadronic piece of the asymmetry, based on the minimum number of Odderons and spin-flips in the combination. Of course, this will need to be checked.

A final comment: in order to use CNI in elastic $p - p$ scattering for polarimetry it is necessary to know the ratio ϕ_5^P/ϕ_+^P ; see A_N in the Table in Fig.9. If the expectation for the dominant amplitudes for each of the asymmetries is valid, and if A_{SS} or A_{LL} is large enough to make a reliable measurement, then one can use, in addition, the measurement (or limit) on A_{SL} to determine (or bound) this ratio, *independent of P* . Thus elastic $p - p$ scattering may turn out to be useful as a self-calibrating polarimeter for RHIC.

Workshop on Spin Dependence of
Elastic proton-proton scattering
at RHIC Energy

(Summer 1997 - sponsored by
RIKEN BNL Research Center)

Leader
Buttmore
Soffer
Kopelovich
Trueman
+ others

Instigated by problem of
Polarimetry at RHIC:
CNI

Hadronic Spin-flip Contribution to AN

Parametrize hadronic spin-flip:

$$\phi_5^h = \tau \sqrt{-t/m^2} (\phi_1^h + \phi_3^h) / 2$$

For $s \gg m^2$, $t \ll m^2$:

ϕ_2^h, ϕ_4^h negligible

$$A_N \frac{d\sigma}{dt} = \frac{\alpha \sigma_{tot}}{2m\sqrt{-t}} \{(\mu - 1) - 2\text{Re}(\tau)\} + 2\text{Im}(\tau) \frac{\sqrt{-t}}{m} \frac{d\sigma}{dt}$$

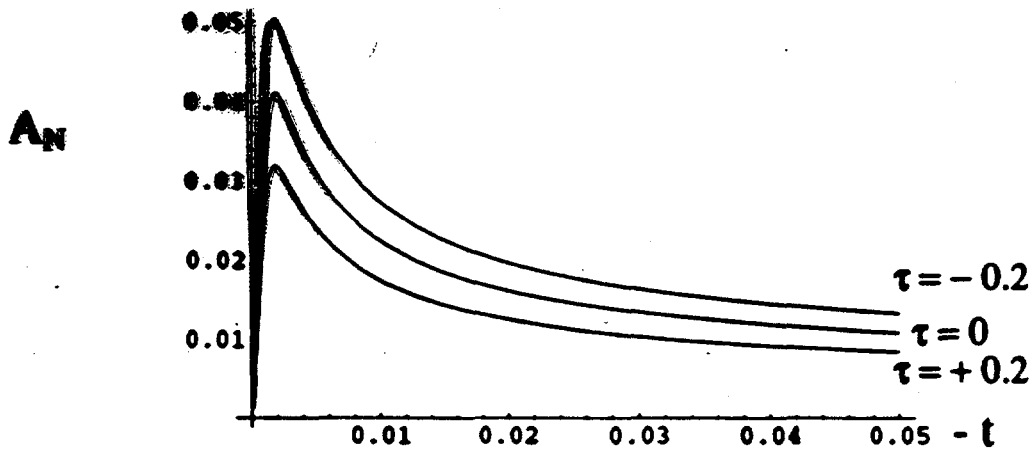
Define τ^* as best limit on $\text{Re}(\tau)$:

$$|\text{Re}(\tau)| \leq \tau^*$$

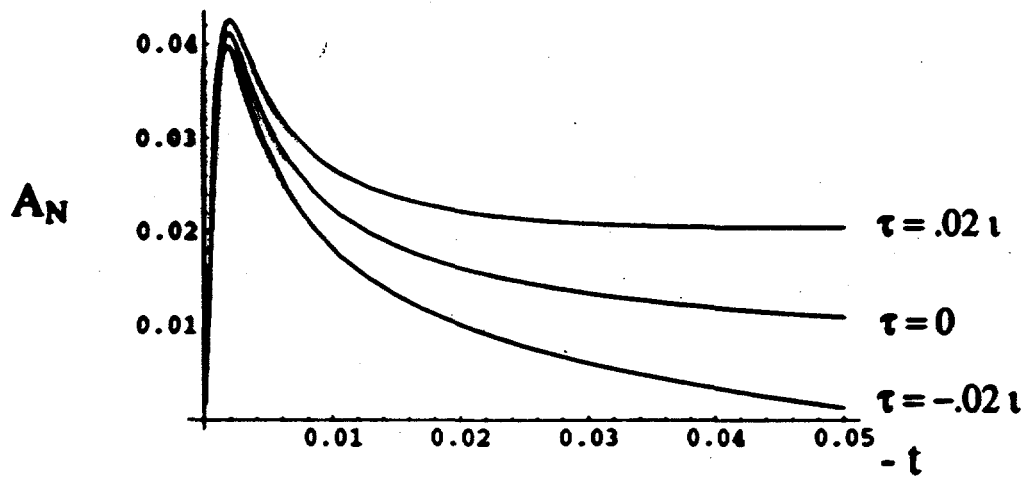
Precision of measurement of P limited by:

$$\frac{\Delta P}{P} \geq \frac{2\tau^*}{(\mu - 1)}$$

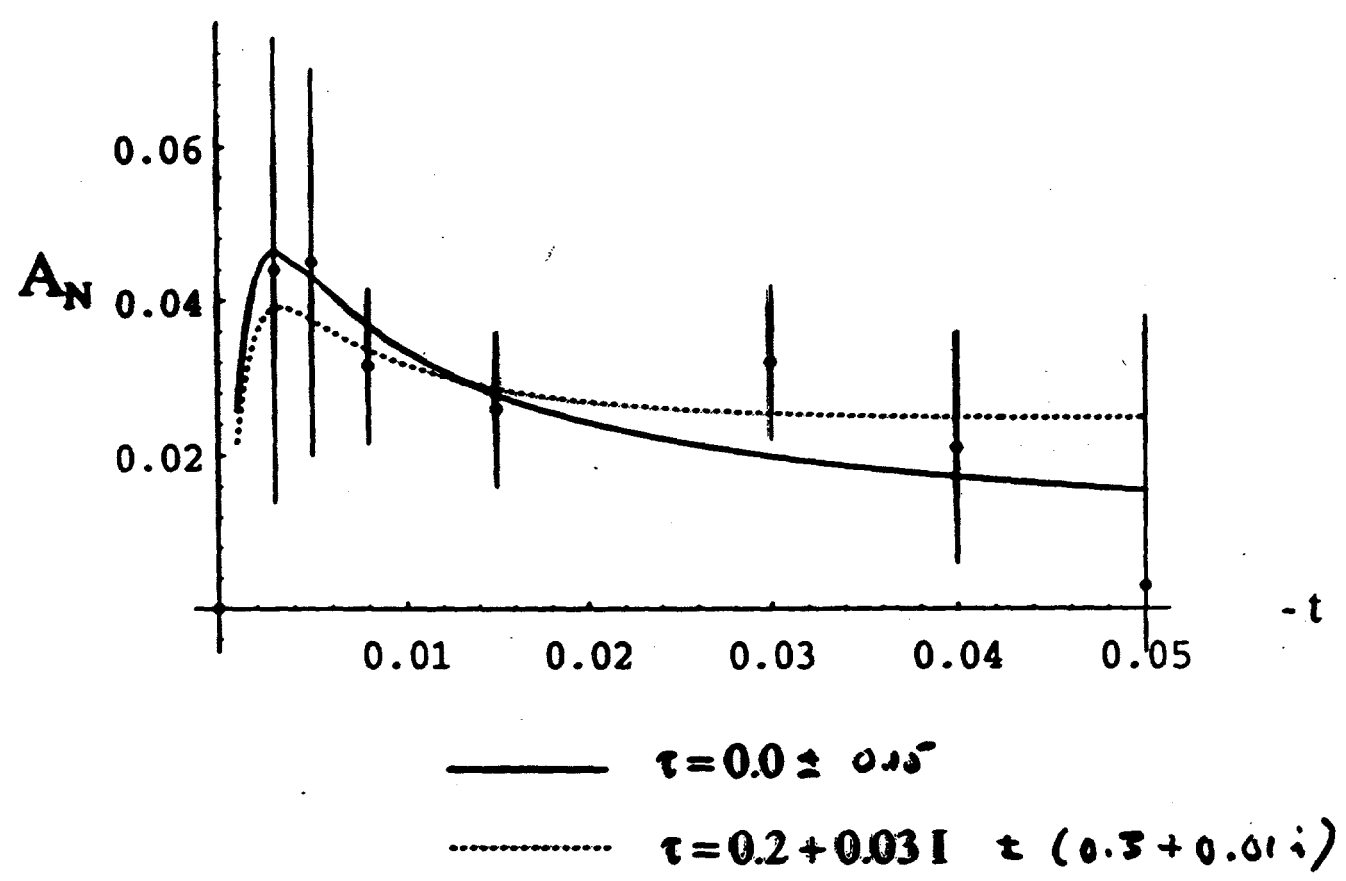
Analyzing power at RHIC for various in-phase spin-flip amplitudes



Analyzing power for various out-of-phase spin-flip amplitudes



Best fits to 704 data with and without $\text{Im}(\tau) = 0$



The Odderon

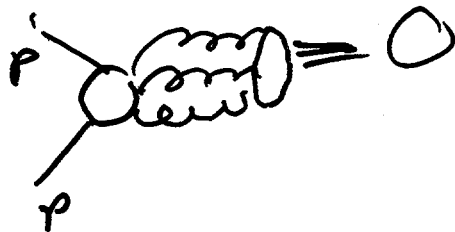
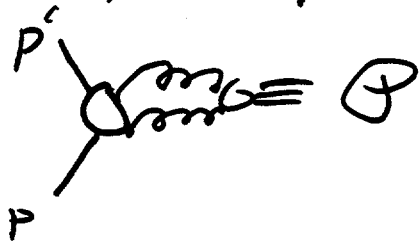
the $C = -1$ partner of the Pomeron

- arbitrary relative phase of ϕ_1 and ϕ_3^-
- coupling to $\phi_1 + \phi_3$ gives

$$\sigma_{PP} - \sigma_{\bar{P}P} \rightarrow 0 \quad \text{as } s \rightarrow \infty$$

and possible large corrections to
 ρ and $\bar{\rho}$

originated with Lukaszuk & Nicolescu (1978),
Leader et al, Lipatov et al



- limit on coupling to $(\phi_1 + \phi_3)$ (Black et al)
 $< 20\%$. Nothing known of
coupling to ϕ_2, ϕ_3^-

Phase of scattering amplitudes

Theorem of Van Hove - based on real analyticity of scattering amplitudes

$$\text{If } f(-s) = \eta f(s) \quad , \quad \eta = \pm 1$$

$$\text{and } f(s) \sim s^\alpha \text{ as } s \rightarrow \infty$$

$$\text{then phase of } f \text{ is } e^{i\pi\alpha/2}, \quad \eta = +1$$

$$e^{-i\pi\alpha/2}, \quad \eta = -1$$

so spinless amp. with $C=+1$ Pomeron is
pure imaginary (with calculable $1/\log s$ real part)
(importance of measuring s -dependence)

For pp need C and crossing:

$$M_{\lambda_3 \lambda_4 \lambda_1 \lambda_2}(s, t) = \eta_C \overline{M_{\lambda_3 \lambda_4 \lambda_1 \lambda_2}(s, t)}$$

$$\overline{M_{\lambda_3 \lambda_4 \lambda_1 \lambda_2}(s, t)} = M_{\lambda_3 - \lambda_2, \lambda_1, -\lambda_4}(s, t)$$

$$\text{so } \phi_1 + \phi_3 = \phi_4, \quad \phi_2, \quad \phi_5 \text{ imaginary}$$

$$\phi_1 - \phi_3 = \phi_4 \text{ real as } s \rightarrow \infty$$

for $C=+1$

Measurable quantities

$$\sigma_{\text{tot}} = \frac{4\pi}{s} \text{Im}(\phi_1(s, 0) + \phi_3(s, 0))$$

$$\Delta\sigma_T = -\frac{8\pi}{s} \text{Im} \phi_2(s, 0)$$

$$\frac{d\sigma}{dt} = \frac{2\pi}{s^2} (|\phi_1|^2 + |\phi_2|^2 + |\phi_3|^2 + |\phi_4|^2 + 4|\phi_5|^2)$$

$$\Rightarrow A_N \frac{d\sigma}{dt} = -\frac{4\pi}{s^2} \text{Im}(\phi_5^* (\phi_1 + \phi_2 + \phi_3 - \phi_4))$$

$$A_{NN} \frac{d\sigma}{dt} = \frac{4\pi}{s^2} \left\{ 2|\phi_5|^2 + \text{Re}(\phi_1^* \phi_2 - \phi_3^* \phi_4) \right\}$$

$$A_{LL} \frac{d\sigma}{dt} = \frac{2\pi}{s^2} \left\{ |\phi_1|^2 + |\phi_2|^2 - |\phi_3|^2 - |\phi_4|^2 \right\}$$

$$= \frac{2\pi}{s^2} \left\{ \text{Re} \phi_1^* \phi_2 + |\phi_2|^2 - |\phi_4|^2 \right\}$$

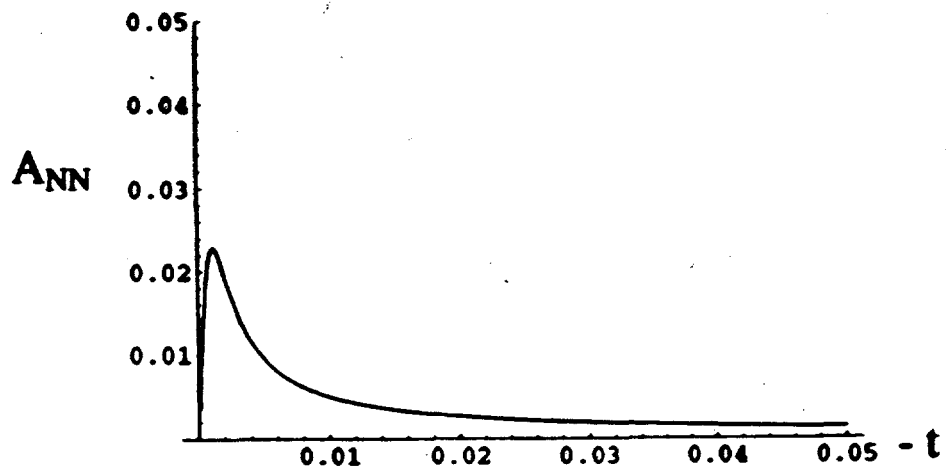
$$A_{SS} \frac{d\sigma}{dt} = \frac{4\pi}{s^2} \text{Re}(\phi_1^* \phi_2 + \phi_3^* \phi_4)$$

$$A_{SL} \frac{d\sigma}{dt} = \frac{4\pi}{s^2} \text{Re}(\phi_5^* (\phi_1 + \phi_2 - \phi_3 + \phi_4))$$

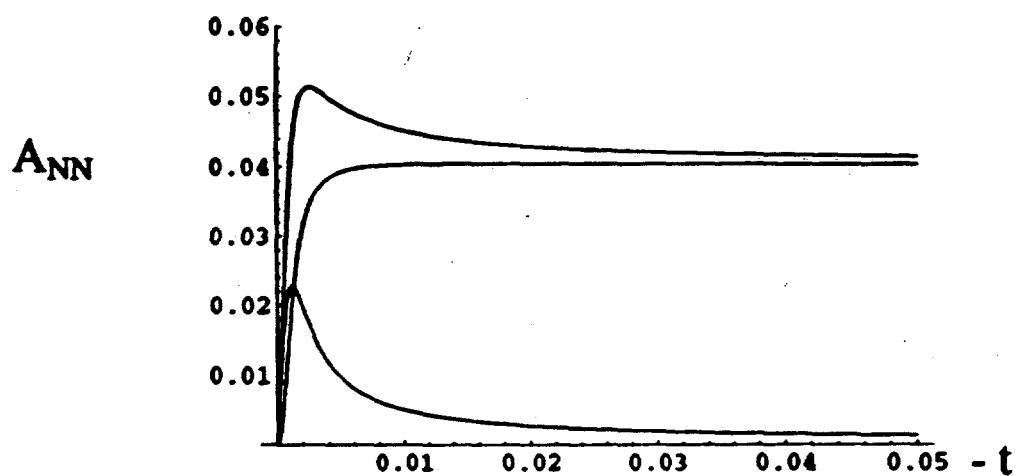
$$\Delta\sigma_L = \frac{4\pi}{s} \text{Im}(\phi_1 - \phi_3)$$

cf. e.g. Buttimore, Gotsman
& Leader (1978)

Enhanced A_{NN} for $r_2 = .02 I$,
where $\phi_2 = r_2 \phi_1$.



Comparison of A_{NN} for various values of r_2 :
.02 I (lower), .02 (middle), .02 + .02 I (upper).



AsymmetryCNI EnhancedDominant? ($\Delta S \neq \text{odd}$) A_N ϕ_+^P, ϕ_5^P $\phi_+^P \phi_5^0 (1, 1)$ A_{NN} ϕ_2^0 $\phi_+^P \phi_2^P (2, 0)$ A_{SS} ϕ_2^0 $\phi_+^P \phi_2^P (2, 0)$ A_{SL} ϕ_-^P $\phi_5^P \phi_-^0 (1, 1)$ $\propto \phi_5^P \phi_2^P (3, 0)$ A_{LL} ϕ_-^P $\phi_+^P \phi_-^0 (0, 1)$

and

 $\sigma_{tot} : \phi_+^P$ $\Delta\sigma_T : \phi_2^P$ $\Delta\sigma_L : \phi_-^0$

Experiment to Measure Total Cross Sections, Differential Cross Sections and Polarization Effects in pp Elastic Scattering at RHIC

Wlodek Guryn *

Brookhaven National Laboratory, Upton NY 11973, USA

Abstract

We are describing an experiment to study proton-proton (pp) elastic scattering experiment at the Relativistic Heavy Ion Collider (RHIC.) Using both polarized and unpolarized beams, the experiment will study pp elastic scattering from $\sqrt{s} = 50$ GeV to $\sqrt{s} = 500$ GeV in two kinematical regions. In the Coulomb Nuclear Interference (CNI) region, $0.0005 < |t| < 0.12$ (GeV/c)², we will measure and study the s dependence of the total and elastic cross sections, σ_{tot} and σ_{el} ; the ratio of the real to the imaginary part of the forward elastic scattering amplitude, ρ ; and the nuclear slope parameter of the pp elastic scattering, b . In the medium $|t|$ -region, $|t| \leq 1.5$ (GeV/c)², we plan to study the evolution of the dip structure with s , as observed at ISR in the differential elastic cross section, $d\sigma_{el}/dt$, and the s and $|t|$ dependence of b . With the polarized beams the following can be measured: the difference in the total cross sections as function of initial transverse spin states $\Delta\sigma_T$, the analyzing power, A_N , and the transverse spin correlation parameter A_{NN} . The behavior of the analyzing power A_N at RHIC energies in the dip region of $d\sigma_{el}/dt$, where a pronounced structure was found at fixed-target experiments will be studied. The relation of pp elastic scattering to the beam polarization measurement at RHIC is also discussed.

Paper presented by Wlodek Guryn for R7 collaboration

*This manuscript has been authored under contract number DE-AC02-76CH0-0016 with the U.S. Department of Energy.

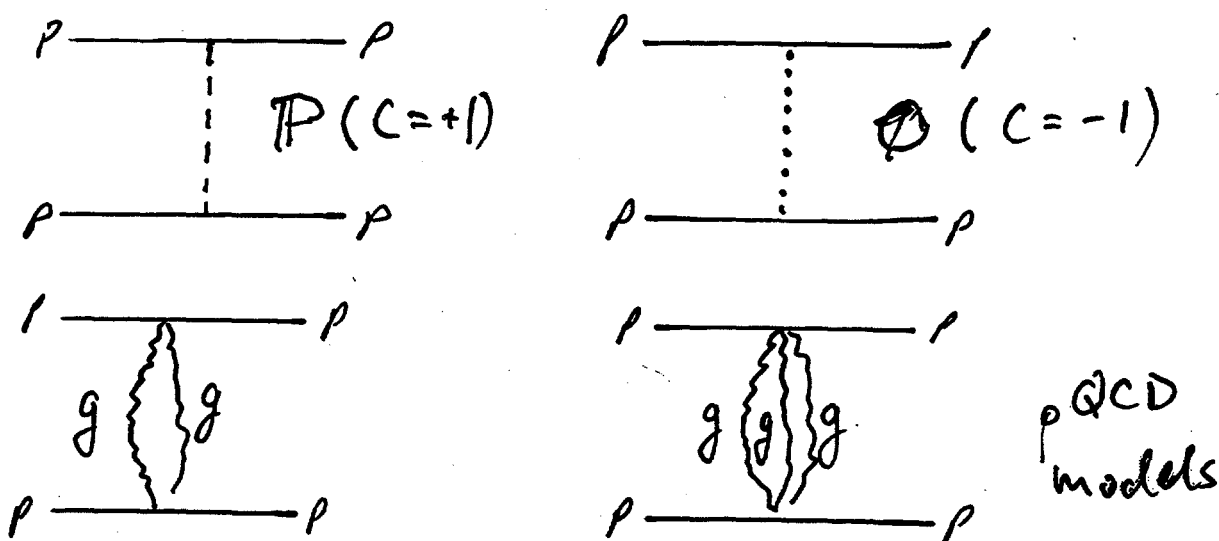
Studying total and elastic cross sections played a crucial role in particle and nuclear physics, in particular, pp and $p\bar{p}$ experiments extend to the highest s . **Elastic scattering has been measured at every accelerator, for every cms energy available.**

Spin related cross sections have been measured at fixed target energies up to $p_{\text{lab}} = 300 \text{ GeV}/c$.

Elastic scattering at high energies is dominated by exchange of **Pomeron** and **Odderon**, the Pomeron's partner with negative C-parity.

The properties of the **Pomeron**, vacuum quantum numbers, are quite well known but more studies are needed to determine it's structure, especially it's unknown **spin properties**.

Even-though there are very strong theoretical reasons for it, the existence of the Odderon has not been established experimentally.



The information gained in elastic scattering tests two areas of particle interactions:

1. **In the region of small four momentum transferred - $|\mathbf{t}|$, one tests in a model independent way, general analytical properties of scattering amplitudes: analyticity, unitarity and crossing symmetry, σ_{tot} , ρ .**
2. **In the diffractive region, with four momenta transferred $|\mathbf{t}| < 1.5 \text{ GeV}^2$, one studies the dynamics of long range strong interactions. Hence, addressing one of the main, unsolved problems in particle physics: confinement and non-perturbative QCD. Namely, being able to derive from the QCD Lagrangian fundamental equations when the strong interaction α_s is large, and thus preventing a perturbative expansion.**

In this "data-driven" field, having more experimental results is important. Additional observable like polarization, will give access to one more degree of freedom, spin.

SPIN EFFECTS in ELASTIC SCATTERING

For the unpolarized beams, it is assumed real and imaginary parts have the same $|t|$ dependence and that spin effects are negligible.

However, it has been observed experimentally that there is a correlation between the position of the dip and the single spin asymmetry A_N crossing zero at the same $|t|$ value. The spin-flip amplitude contributes to filling of the dip.

$$A_N = \frac{2 \operatorname{Im} f_{++} f_{+-}^*}{|f_{++}|^2 + |f_{+-}|^2}$$

This experiment will test the Odderon hypothesis by:

1. Measuring the region of the first diffractive minimum and comparison with data from $S p \bar{p} S$ collider, UA4 experiment
2. Measuring spin asymmetries A_N , A_{NN} and A_{LL} at moderate values of $|t|$. *

** An interesting suggestion was made at this workshop by L. Trueman: Odderon could contribute to spin related asymmetries in pp elastic scattering.*

RHIC Operation

- More than one p_{beam} . It is very likely that RHIC will have at least 100 GeV/c and 250 GeV/c proton beams, which will allow us to take data at two \sqrt{s} points.
- 5000 evts/ 10^{-4} GeV²/c² bin $\Rightarrow \int Ldt \approx 2 \times 10^{33} \text{ cm}^{-2}$. The effective luminosity in our IR is $5 \times 10^{28} \text{ cm}^{-2}\text{sec}^{-1}$. Two short (few days) running periods separated by one year are preferable.
- In the **dip region** we can run with the standard tune and all data we need can be taken while other experiments are running. No dedicated run conditions are required. At luminosity $4 \times 10^{30} \text{ cm}^{-2}\text{sec}^{-1}$, 200 hrs data on tape to acquire 1000 evts/0.02 GeV²/c² bin.

Tune	Roman pot position	L_{eff}	-t range (GeV/c)**2	Comment
Standard	20 m	--	0.02 - 1.5	NO special hardware
Standard	57 m	20 m	0.008 - 0.2	NO special hardware
Special	72 m	37 m	0.004 - 0.12	PS NO warm-cold
Special	144 m	87 m	0.0004 - 0.03	PS Warm-Cold

We shall study systematically pp elastic scattering in

$$50 < \sqrt{s} < 500 \text{ GeV}$$

with polarized and/or unpolarized beams in the four-momentum transferred $-t$ sub-divided into two kinematic ranges:

1. Day one of proton running, in the diffractive region, with no special running conditions required

$$0.006 < -t < 1.5 \text{ (GeV/c)}^2$$

DAY

- evolution of dip structure observed at the ISR in $d\sigma_e/dt$;
- s and t dependence of the nuclear slope, b ;
- s dependence of σ_{tot} .

ONE
(STANDARD
TUNE)

2. Coulomb Nuclear Interference (CNI) region:

$$0.0004 < -t < 0.12 \text{ (GeV/c)}^2$$

- s dependence of σ_{tot} and $d\sigma_e/dt$;
- ratio of real to imaginary part of the forward scattering amplitude, ρ ;

With well understood and straight-forward upgrades of the setup the following could be studied:

1. Measurement of the elastic scattering in the CNI region will allow precise determination of ρ , σ_{tot} and their spin dependence, ϕ_s spin flip hadronic amplitude. (Machine modifications are required.)
2. Large -t region will test pQCD calculations. Same detectors, but a magnet in the IR for momentum measurement will be needed.

With no modification to the setup the following can be studied:

1. **Single diffraction dissociation**, can be studied by appropriate design of the veto system and a an additional trigger condition.
2. **Elastic scattering of $pd, p^{\uparrow}d, dd$** , can be measured. Some of those measurements have been done at the ISR, with very nice results confirming extended Glauber model. **I think that understanding of those reactions might be very important to the HI program at RHIC. Need to study dynamical range and trigger.**

Status and Plans

1. Experiment has scientific approval.
2. Since the approval time our work concentrated on:
 - Optimization of the experiment;
 - Interaction with the accelerator group;
 - Design of critical parts: Roman pots, detectors;
 - Design of inelastic veto is ongoing.
3. Our goal is to be ready in the spring of 2001 when the RHIC spin program is expected to run in full capacity.
4. We are working on the TDR with a goal of finishing it by the end of the summer.

In order to achieve these goals need to do R&D during the next twelve months.

Start building components of the experiment in FY 2000.

We have a lot of work to do: MORE collaborators are welcome!

Feasibility of DIS (Polarized e-p Collider) at RHIC

G. Igo, UCLA & T. Sloan, Lancaster U.

The Relativistic Heavy Ion Collider (RHIC) with polarized proton and He³ beams and with heavy ion beams could support a program of deep inelastic scattering experiments if a low energy beam (~2 GeV) of electrons circulated in RHIC. These experiments, which would have a similar center of mass energy to the highest energy fixed target experiments, would allow precision measurements of the polarized proton and neutron structure functions down to Bjorken x of 10^{-3} and permit a precision test of the Bjorken Sum Rule (BjSR) [1]. Collisions of 50 GeV/nucleon polarized protons and He-3 ions with 2 GeV polarized electrons (60 circulating bunches of 10^{11} polarized electrons produced by a SLAC-type [3] polarized electron source) would allow the BjSR integrals to be determined to a statistical precision of 1.4% and 0.8% at Q^2 of 2 and 8 GeV² respectively for runs of luminosity of 1000 pb⁻¹ for each of e-p and e-He³ collisions. The BjSR is a deeply fundamental sum rule which, if broken, would imply serious consequences for QCD [5]. The current world data agrees with the BjSR at the level of 10% due to all sources of error [3,4]. Higher precision measurements would provide a more stringent test of QCD. Such an experiment at RHIC would complement those proposed at HERA [6], which would have a much wider Q^2 and higher energy range and hence probe different physics.

The addition of the option of e-p, He³ collisions to RHIC's arsenal would provide a nice way to measure the absolute polarization of these hadron beams by measuring the elastic scattering asymmetry A_{nn} and by measuring the electron beam polarization with high precision in Moller scattering.

1. J. D. Bjorken, Phys. Rev. **148** (1966) 1467, *ibid* **D1** (1970) 1376.
2. R. Alley et al., Nucl. Instrum. Methods **A365** (1995) 1.
3. B. Adeva et al., submitted to Physical Review D, May 1998.
4. K. Abe et al., Phys. Lett. **B405** (1997) 180.
5. R. P. Feynman, Photon Hadron Interactions (Benjamin Press, 1972).
6. *Future Physics at HERA*, [www\(http://www.desy.de/~heraws96\)](http://www.desy.de/~heraws96).

FEASIBILITY OF DIS (POLARIZED e-p COLLIDER) AT RHIC

G. IGO, UCLA & T. SLOANE, LANCASTER U.

HISTORY

SPIN 1/2 \uparrow nucleon = $\circlearrowleft \begin{matrix} \uparrow \\ \downarrow \\ \uparrow \end{matrix} \circlearrowright$ i.e. $\Delta\Sigma = \Delta u + \Delta d = 1$

$$\Delta u = \int_0^1 u^{\uparrow}(x) - u^{\downarrow}(x) dx$$

$$\Delta d = \int_0^1 d^{\uparrow}(x) - d^{\downarrow}(x) dx$$

STRUCTURE FUNCTION

$$g_1(x) = 1/2 \sum e_i^2 (q_i(x) \uparrow - q_i(x) \downarrow)$$

MEASURED IN POLARIZED DIS.

$$A = \frac{d\sigma^{\uparrow\downarrow} - d\sigma^{\uparrow\uparrow}}{d\sigma^{\uparrow\downarrow} + d\sigma^{\uparrow\uparrow}} = (a g_1(x, Q^2) + b g_2(x, Q^2))$$

KINEMATIC FACTORS: b small for $\uparrow\uparrow$ - a small(ish) for $\uparrow \leftarrow$

ALTERNATIVE NOTATION

VIRTUAL PHOTON ASYMMETRIES $A_1 = \frac{\sigma_{1/2} - \sigma_{3/2}}{\sigma_{1/2} + \sigma_{3/2}} ; A_2 = \sigma_{TL} / \sigma_T$

$$A_1 = g_1 / F_1 \text{ (approx)}$$

MEASURE

$$A_m = \frac{N^{\uparrow\downarrow} - N^{\uparrow\uparrow}}{N^{\uparrow\downarrow} + N^{\uparrow\uparrow}} = P_B P_T f D A_1 \quad (\underline{D \propto y})$$

FEASIBILITY OF DIS (POLARIZED e-p COLLIDER) AT RHIC

G. IGO, UCLA & T. SLOANE, LANCASTER U.

HISTORY

SPIN 1/2 \uparrow nucleon = $\left(\uparrow \downarrow \uparrow \right)$ i.e. $\Delta\Sigma = \Delta u + \Delta d = 1$

$$\Delta u = \int_0^1 u^{\uparrow}(x) - u^{\downarrow}(x) dx$$

$$\Delta d = \int_0^1 d^{\uparrow}(x) - d^{\downarrow}(x) dx$$

STRUCTURE FUNCTION $g_1(x) = 1/2 \sum e_i^2 (q_i(x) \uparrow - q_i(x) \downarrow)$

MEASURED IN POLARIZED DIS.

$$A = \frac{d\sigma^{\uparrow\downarrow} - d\sigma^{\uparrow\uparrow}}{d\sigma^{\uparrow\downarrow} + d\sigma^{\uparrow\uparrow}} = (a g_1(x, Q^2) + b g_2(x, Q^2))$$

KINEMATIC FACTORS: b small for $\uparrow\uparrow$ - a small(ish) for $\uparrow \leftarrow$

ALTERNATIVE NOTATION

VIRTUAL PHOTON ASYMMETRIES $A_1 = \frac{\sigma_{1/2} - \sigma_{3/2}}{\sigma_{1/2} + \sigma_{3/2}} ; A_2 = \sigma_{TL} / \sigma_T$

$$A_1 = g_1 / F_1 \text{ (approx)}$$

MEASURE

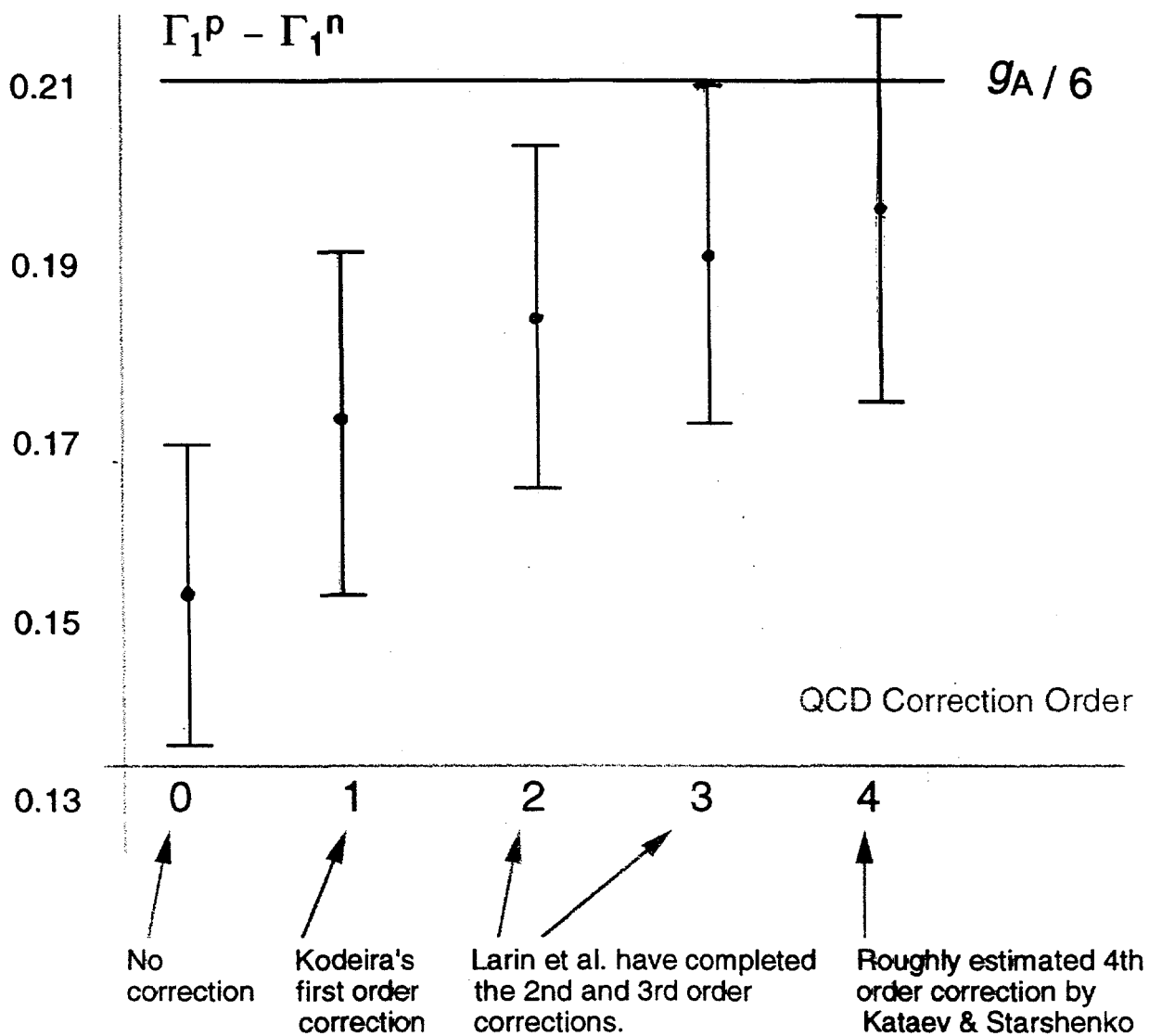
$$A_m = \frac{N^{\uparrow\downarrow} - N^{\uparrow\uparrow}}{N^{\uparrow\downarrow} + N^{\uparrow\uparrow}} = P_B P_T f D A_1 \quad (D \propto y)$$

E142 $\Gamma_1^n = -0.022 \pm 0.011$ ←

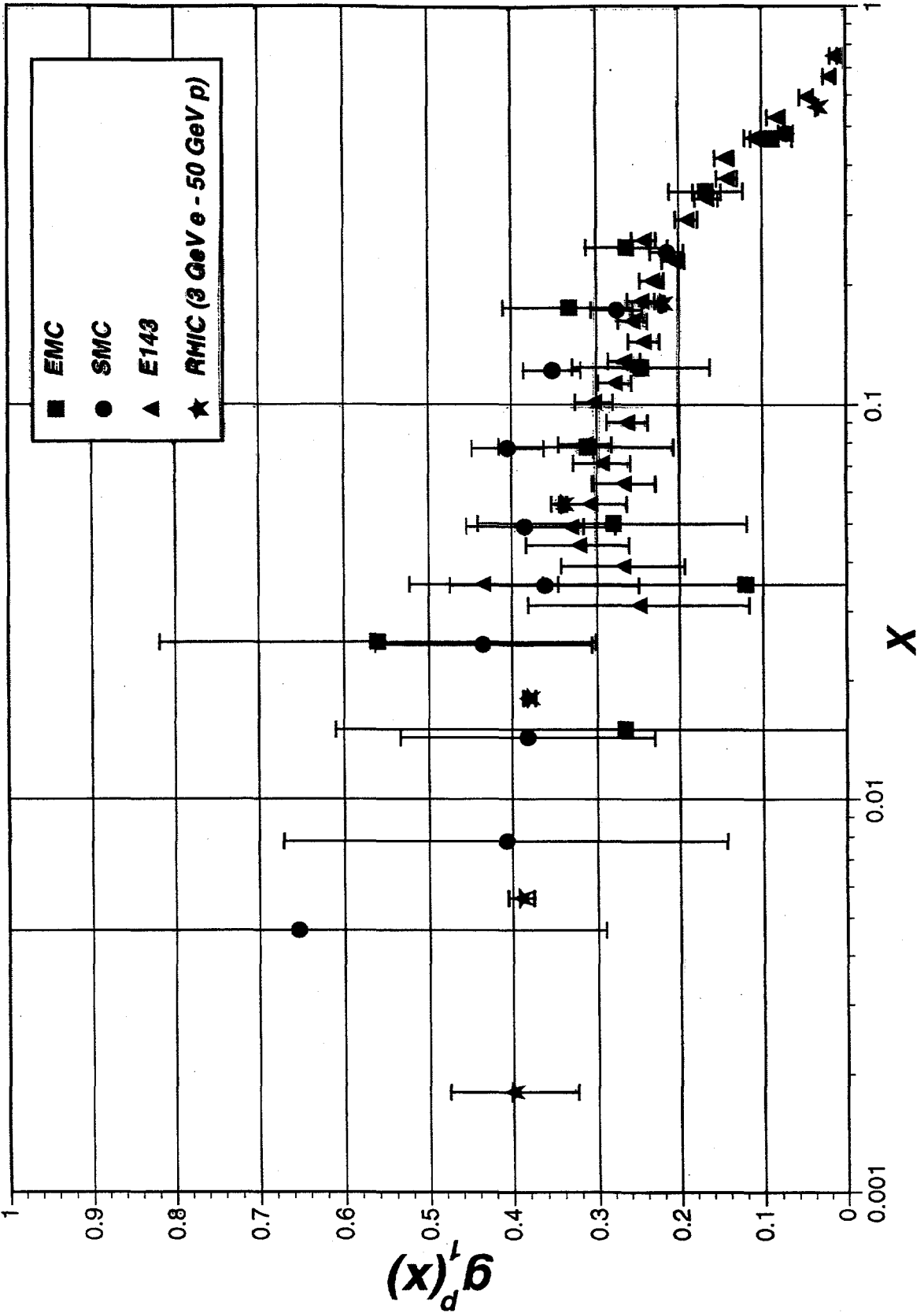
E143 $\Gamma_1^p = 0.129 \pm 0.010$ ← measured values

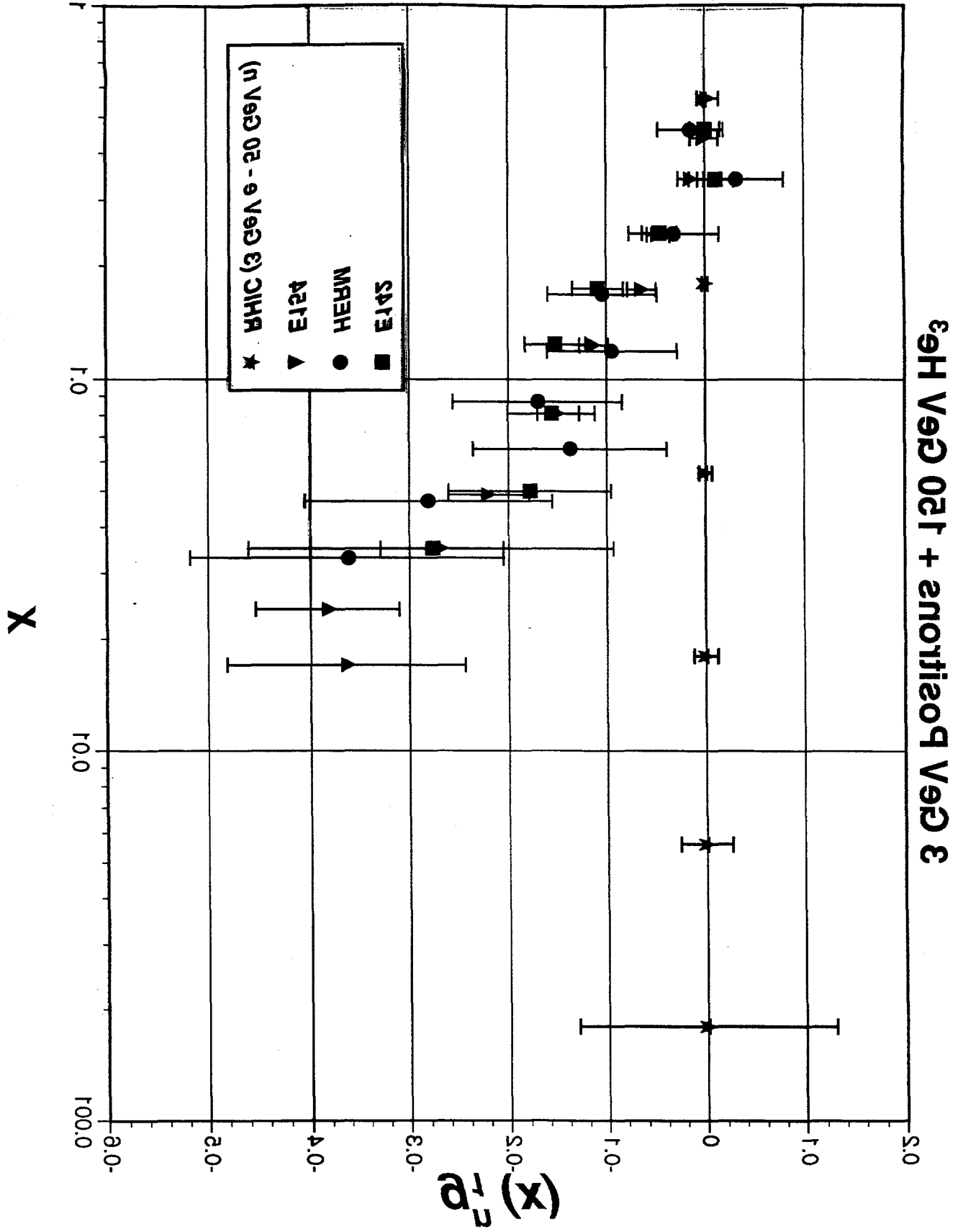
ie. $\Gamma_1^p - \Gamma_1^n = 0.151 \pm 0.015$ ←

EXPECT $g_A/6 \times \text{QCD Rad. Corr.} = 0.21 \times \text{QCD Corr.}$
 calculate the QCD corrections to different orders.



Proton Spin Structure Function $g_1^p(x)$





$$\frac{\Gamma_1^p - \Gamma_1^n}{\Gamma_1^p + \Gamma_1^n}$$

Nucleon energy	25 GeV	50 GeV	100 GeV
Gamma 1 p at $qsq=2$	+-.0013	.0023	.0037
Gamma 1 n at $qsq=2$	+-.0018	.0031	.0050
Bj sum rule at $qsq=2$	+-.0022	.0039	.0062
% accuracy on Bj SR	1.1	2.0	3.1
Gamma 1 p at $qsq=8$	+-.00081	.0015	.0025
Gamma 1 n at $qsq=8$	+-.0011	.0020	.0035
Bj sum rule at $qsq=8$	+-.0014	.0025	.0043
% accuracy on Bj SR	0.7	1.3	2.2
(taking gamma 1 p - gamma 1 n = 0.2)			

WORLD DATA % accuracy on Bj SR
 vs $3\frac{1}{2}\%$ STAT.
 $\pm 7\%$ SYST.

Summary

- Rich program at RHIC energies
complementary to HERA program

✓ By SR

Important improvement in
both statistical and systematic
errors is possible.

✓ variable \vec{p}_{proton} energy

✓ Polarized He^3 crucial

- Heat load on RHIC

- STAR & PHENIX DETECTORS

Participant List

RHIC Spin Workshop — April 27-29, 1998

Gerry Bunce, Yousef Makdisi, N Saito,

Mike Tannenbaum, Larry Trueman and Aki Yokosawa — Organizers

Igor G. Alekseev
ITEP
B. Cheremushkinskaya 25
Moscow 117259
Russia
alekseev@vitep5.itep.ru

Chris E. Allgower
Argonne National Laboratory
344 Artist Lake Drive
Middle Island, NY 11953
cea@hep.anl.gov

Vladimir A. Anferov
University of Michigan
Physics Department
Ann Arbor, MI 48109-1120
anferov@umich.edu

Robin Appel
University of Pittsburgh
P.O. Box 5
Upton, NY 11973
appel@bnl.gov

Samuel H. Aronson
Brookhaven National Laboratory
Physics Dept., Bldg. 510C
Upton, NY 11973-5000
aronson@bnl.gov

Mei Bai
Brookhaven National Laboratory
AGS, Bldg. 911B
Upton, NY 11973-5000
bai@bnl.gov

Kenneth N. Barish
UCLA
Dept. of Physics & Astronomy
405 Hilgard Ave.
Los Angeles, CA 90095
barish@physics.ucla.edu

Sergei Bashinsky
MIT
Center for Theor. Phys., 6-411A
77 Massachusetts Ave.
Cambridge, MA 02139
sergie@mit.edu

Leslie C. Bland
IUCF
Indiana University
2401 Milo B. Sampson Lane
Bloomington, IN 47408
bland@iucf.indiana.edu

Melynda Brooks
Los Alamos National Laboratory
MS H846, Group P-25
Los Alamos, NM 87545
mbrooks@lanl.gov

Gerry Bunce
Brookhaven National Laboratory
AGS, Bldg. 911A
Upton, NY 11973-5000
bunce@bnl.gov

Nigel Buttimore
University of Dublin
Hamilton Building
Dublin 2, Ireland
nhb@maths.tcd.ie

Robert E. Chrien
Brookhaven National Laboratory
Physics Department, 510A
Upton, NY 11973-5000
chrien@bnl.gov

Andreas P. Contogouris
University of Athens
Nuclear & Particle Physics
Panepistimiopolis-Ilisia
15771 Athens, Greece
acontog@atlas.uoa.gr

Ernest C. Courant
Brookhaven National Laboratory
Building 1005
Upton, NY 11973-5000
courant@bnl.gov

Daniel de Florian
CERN, TH Division
CH-1211 Geneva 23
Switzerland
daniel.deflorian@cern.ch

Albert de Roeck
DESY
Notkestrasse 85
D-22603 Hamburg
Germany
deroeck@mail.desy.de

Abhay L. Deshpande
Yale University
Physics Department
P.O. Box 666
New Haven, CT 06620-8211
abhay.deshpande@yale.edu

Lidia Didenko
Brookhaven National Laboratory
Physics Dept., Bldg. 510A
Upton, NY 11973-5000
didenko@bnl.gov

Yuji Goto
RIKEN BNL Research Center
Brookhaven National Laboratory
Bldg. 902C
Upton, NY 11973-5000
goto@bnl.gov

Michael Harrison
Brookhaven National Laboratory
RHIC, Bldg. 1005
Upton, NY 11973-5000
harrison@bnl.gov

Haixin Huang
Brookhaven National Laboratory
AGS, Bldg. 911B
Upton, NY 11973-5000
huang@bnl.gov

George Igo
UCLA
Department of Physics
1273 Leona Drive
Beverly Hills, CA 90210
igo@physics.ucla.edu

Basim Kamal
Brookhaven National Laboratory
Physics Department, Bldg. 510A
Upton, NY 11973-5000
kamal@bnl.gov

Tom Kirk
Brookhaven National Laboratory
Bldg. 510
Upton, NY 11973-5000
tkirk@bnl.gov

Geary Eppley
Rice University
Bonner Laboratory, MS315
6100 Main St.
Houston, TX 77005
eppley@physics.rice.edu

Wlodek Guryn
Brookhaven National Laboratory
Physics Department, Bldg. 510A
Upton, NY 11973-5000
gurun@bnl.gov

Naoki Hayashi
RIKEN BNL Research Center
Brookhaven National Laboratory
Bldg. 902C
Upton, NY 11973-5000
hayashi@bnl.gov

Huan Z. Huang
UCLA
Department of Physics
Los Angeles, CA 90095
huang@physics.ucla.edu

Kenichi Imai
Kyoto University and RIKEN
Department of Physics
Kyoto 606 Japan
imai@ne.scphys.kyoto-u.ac.jp

Vadim P. Kanavets
ITEP
B. Cheremushkinskaya 25
Moscow 117259
Russia
kanavets@vitep5.itep.ru

Steve Kuhlmann
Argonne National Laboratory
Bldg. 362, Rm E281
9700 S. Cass Avenue
Argonne, IL 60439
stk@hep.anl.gov

Douglas E. Fields
University of New Mexico
Dept. of Phys. & Astromomy
800 Yale NE
Albuquerque, NM 87131
fields@lanl.gov

Timothy J. Hallman
Brookhaven National Laboratory
Physics Department, Bldg. 510A
Upton, NY 11973-5000
hallman@bnl.gov

Steve Hepplemann
Penn State University
Physics Department
104 Davey Lab
University Park, PA 16802
heppel@phys.psu.edu

Takashi Ichihara
RIKEN BNL Research Center
Bldg. 510
Upton, NY 11973-5000
ichihara@bnl.gov

Robert L. Jaffe
MIT
Department of Physics
Cambridge, MA 02139
jaffe@mitlms.mit.edu

David M. Kaway
Yale University
Department of Physics
260 Whitney Avenue
New Haven, CT 06520
kaway@hepmail.physics.yale.edu

Shunzo Kumano
Saga University
Department of Physics
Saga 840-8502
Japan
kumano@cc.saga-u.ac.jp

T.D. Lee
RIKEN BNL Research Center
Brookhaven National Laboratory
Bldg. 510A
Upton, NY 11973-5000
tdl@cuphyb.phys.columbia.edu

Thomas J. LeCompte
Argonne National Laboratory
HEP, 362-F233
9700 S. Cass Avenue
Argonne, IL 60439
lecompte@anl.gov

Andreas Lehrach
Forschungszentrum Juelich
Institut für Kernphysik
Postfach 1913
52425 Juelich, Germany
a.lehrach@fz-juelich.de

Robert Lourie
SUNY/Stony Brook
Renaissance Technologies Corp.
600 Route 25A
Setauket, NY 11733
lourie@wallst.physics.sunysb.edu

Derek Lowenstein
Brookhaven National Laboratory
AGS, Bldg. 911
Upton, NY 11973-5000
lowenstein@bnl.gov

Alfredo U. Luccio
Brookhaven National Laboratory
AGS, Bldg. 911B
Upton, NY 11973-5000
luccio@bnldag.ags.bnl.gov

Leon Madansky
Johns Hopkins University
Physics Department
34th & Charles Streets
Baltimore, MD 21218
lm@jhup.pha.jhu.edu

Yousef I. Makdisi
Brookhaven National Laboratory
RHIC Project, Bldg. 1005-4
Upton, NY 11973-5000
makdisi@bnl.gov

Akio Ogawa
PSU/BNL
Physics Dept.- Rm 1-179
Upton, NY 11973-5000
akio@bnl.gov

Nasahiro Okamura
RIKEN BNL Research Center
Bldg. 911B
Upton, NY 11973-5000
okamura@bnl.gov

Frank E. Paige
Brookhaven National Laboratory
Physics Dept., Bldg. 510A
Upton, NY 11973-5000
paige@bnl.gov

Yuri Panebratsev
JINR, LHE
Dubna, Moscow Region
Russia
panebrat@sunhe.jinr.ru

Aldo Penzo
INFN
Univ. di Trieste
Via A. Valerio 2,
Trieste, Italy
penzo@vxcern.cern.ch

Gordon P. Ramsey
Loyola University Chicago
Physics Department
6525 N. Sheridan
Chicago, IL 60626
gpr@hep.anl.gov

Stepan Razin
JINR, LHE
Dubna, Moscow Region
Russia
razin@sunhe.jinr.ru

Thomas Roser
Brookhaven National Laboratory
AGS Dept., Bldg. 911B
Upton, NY 11973-5000
roser@bnl.gov

Adam Rusek
Brookhaven National Laboratory
Physics Dept., Bldg. 510A
Upton, NY 11973-5000
rusek@bnl.gov

Vladimir L. Rykov
Wayne State University
Physics and Astronomy
666 W. Hancock
Detroit, MI 48201
rykov@rhic.physics.wayne.edu

Naohito Saito
RIKEN BNL Research Center
Brookhaven National Laboratory
Bldg. 510C
Upton, NY 11973-5000
saito@bnl.gov

Andrew M. Sandorfi
Brookhaven National Laboratory
Physics Department, Bldg. 510A
Upton, NY 11973-5000
sandorfi@bnl.gov

Toshi-Aki Shibata
Tokyo Inst. of Technology
Department of Physics
2-12-1 Okayama, Meguro
Tokyo 1528851 Japan
shibata@nucl.phys.titech.ac.jp

Dennis Sivers
Portland Physics Inst.
4730 SW Macadam Ave.
Portland, OR 97201
DenSivers@Delphi.com

Jacques Soffer
Centre de Phys. Theor., CNRS
Luminy Case 907
F-13288 Marseille
Cedex 09 France
soffer@cpt.univ-mrs.fr

Harold Spinka
Argonne National Laboratory
9700 S. Cass Avenue
Argonne, IL 60439-4815
hms@hep.anl.gov

Axel Steinmetz
Yale University
P.O. Box 571
Upton, NY 11973-0571
axels@bnl.gov

Ed Stephenson
Indiana University
Cyclotron Facility
2401 Milo B. Sampson Lane
Bloomington, IN 47408
stephens@iucf.indiana.edu

George Sterman
SUNY/Stony Brook
ITP
Stony Brook, NY 11794
sterman@insti.physics.sunysb.edu

Christof Struck
Frankfurt University
J.W. Goethe-Univ.
August-Euler-Str. 6
60846 Frankfurt, Germany
struck@bnl.gov

Michael J. Syphers
Brookhaven National Laboratory
AGS, Bldg. 911B
Upton, NY 11973-5000
msyphers@bnl.gov

Chunmei Tang
SUNY/Stony Brook
Physics Department
Stony Brook, NY 11794-3800
chunmei@mathlab.sunysb.edu

Jian Tang
MIT
Dept. of Physics, 6-402
Cambridge, MA 02139
jtang@ctpa03.mit.edu

Michael J. Tannenbaum
Brookhaven National Laboratory
Physics Dept., Bldg. 510C
Upton, NY 11973-5000
mjt@bnl.gov

Timothy L. Thomas
University of New Mexico
Dept. of Physics & Astronomy
Albuquerque, NM 87131
thomas@phys.unm.edu

Michael Tokarev
JINR
Dubna, Moscow Region
141890 Russia
tokarev@sunhe.jinr.ru

Larry Trueman
Brookhaven National Laboratory
Physics Dept., Bldg. 510A
Upton, NY 11973-5000
trueman@bnl.gov

Kathleen R. Turner
Brookhaven National Laboratory
Physics Dept., Bldg. 510A
Upton, NY 11973-5000
kathy@bnl.gov

Dave Underwood
Argonne National Laboratory
9700 S. Cass Avenue
Argonne, IL 60439-4815
dgu@hep.anl.gov

Fleming Videbaek
Brookhaven National Laboratory
Physics Dept., Bldg. 510C
Upton, NY 11973-5000
videbaek@hi2.hirg.bnl.gov

Steven E. Vigdor
Indiana University
Department of Physics
Bloomington, IN 47405
vigdor@iucf.indiana.edu

Jean-Marc Virey
Centre de Physique Theorique
CNRS Luminy Case 907
13288 Marseille
Cedex 9 France
virey@cpt.univ-mrs.fr

Werner Vogelsang
CERN, TH Division
CH-1211 Geneva 23
Switzerland
werner.vogelsang@cern.ch

Yasushi Watanabe
Brookhaven National Laboratory
RIKEN BNL Research Center
Bldg. 510C
Upton, NY 11973-5000
watanabe@bnl.gov

Erich Willen
Brookhaven National Laboratory
RHIC, Bldg. 902
Upton, NY 11973-5000
willen@bnl.gov

Scott W. Wissink
Indiana University
Cyclotron Facility
2401 Milo B. Sampson Lane
Bloomington, IN 47408
wissink@iucf.indiana.edu

Guanghua Xu
Univ. of California, Riverside
P-25 MS H846
Los Alamos National Laboratory
Los Alamos, NM 87545
gxu@p2hp2.lanl.gov

Peter Yamin
Brookhaven National Laboratory
Bldg. 510F
Upton, NY 11973-5000
yamin@bnl.gov

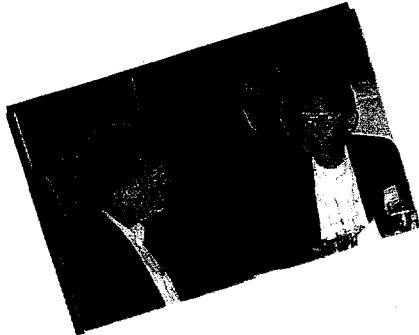
Minoru Yanokura
RIKEN
Planning Office
Wako-shi, Saitama 351-01
Japan
yanokura@postman.riken.go.jp

Pablo P. Yepes
Rice University
MS 315
6100 Main Street
Houston, TX 77005
yepes@physics.rice.edu

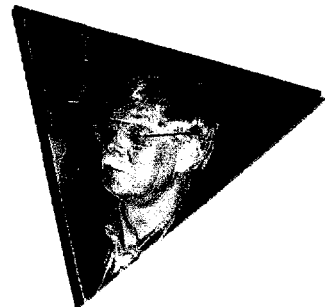
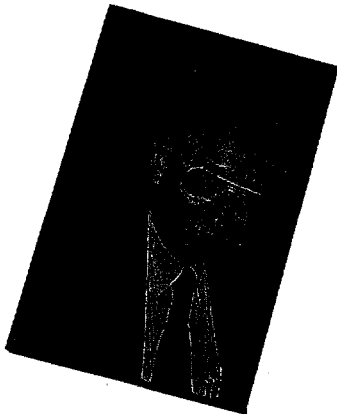
Aki Yokosawa
Argonne National Laboratory
Department of Physics
Argonne, IL 60439
AY@hep.anl.gov

Anatoli Zelinski
TRIUMF
4004 Wesbrook Mall
Vancouver B.C.
Canada





An Evening at







RIKEN BNL Center Symposium/Workshops

Title: **Fermion Frontiers in Vector Lattice Gauge Theories**
Organizer: R. Mawhinney and S. Ohta
Dates: May 6-9, 1998

Title: **High Density Matter in AGS, SPS and RHIC Collisions**
Organizer: K. Kinder-Geiger and Y. Pang
Dates: July 11, 1998

Title: **Quarkonium Production in Relativistic Nuclear Collisions**
Organizers: D. Kharzeev
Dates: Sept. 28 - Oct. 2, 1998

Title: **Quantum Fields In & Out of Equilibrium**
Organizers: D. Boyanovsky, H. de Vega, R. Pisarski
Dates: Oct. 26-30, 1998

Title: **QCD Vacuum and Phase Transitions**
Organizer: E. Shuryak
Dates: Nov. 4-7, 1998

For information please contact:

Ms. Pamela Esposito
RIKEN BNL Research Center
Building 510A, Brookhaven National Laboratory
Upton, NY 11973, USA
Phone: (516)344-3097 Fax: (516)344-4067
E-Mail: rikenbnl@bnl.gov
Homepage: <http://penguin.phy.bnl.gov/www/riken.html>



RIKEN BNL RESEARCH CENTER

RHIC SPIN PHYSICS

APRIL 27 - 29, 1998



Li Keran

Copyright©CCASTA

*Nuclei as heavy as bulls
Through collision
Generate new states of matter.
T. D. Lee*

Organizers:

Gerry Bunce
Yousef Makdisi
Naohito Saito
Mike Tannenbaum
Larry Trueman
Aki Yokosawa

BNL/RIKEN BNL Research Center
Brookhaven National Laboratory
RIKEN and Brookhaven National Laboratory
Brookhaven National Laboratory
BNL/RIKEN BNL Research Center
Argonne National Laboratory